UNIVERSIDAD DE OVIEDO

Departamento de Química Física y Analítica

Programa de Doctorado de Análisis Químico, Bioquímico y Estructural y Modelización Computacional

NANOVESÍCULAS DE TAMAÑO CONTROLADO PARA APLICACIONES BIOTECNOLÓGICAS Y BIOANALÍTICAS

TESIS DOCTORAL

PABLO GARCÍA MANRIQUE

Oviedo, 2019

UNIVERSITY OF OVIEDO

Departament of Physical and Analytical Chemistry

Ph.D. program: Chemical, Biochemical and Structural Analysis and Computational Modelling

SIZE CONTROLLED NANOVESICLES FOR BIOTECHNOLOGICAL AND BIOANALYTICAL APPLICATIONS

Ph.D. THESIS

PABLO GARCÍA MANRIQUE

Oviedo, 2019

Universidad de Oviedo
Universidá d'Uviéu
University of Oviedo

RESUMEN DEL CONTENIDO DE TESIS DOCTORAL

1.- Título de la Tesis	
Español/Otro Idioma: **"Nanovesículas de tamaño controlado para aplicaciones biotecnológicas y bioanalíticas"**	Inglés: **"Size controlled nanovesicles for biotechnological and bioanalytical applications"**

2.- Autor	
Nombre: **Pablo García Manrique**	DNI/Pasaporte/NIE: **-Q**
Programa de Doctorado: **Análisis químico, bioquímico y estructural, y modelización computacional**	
Órgano responsable: **Departamento de Química Física y Analítica, Facultad de Química**	

RESUMEN (en español)

Las nanovesículas, un tipo particular de coloides orgánicos, está generando un interés creciente en el ámbito de la biotecnología, y particularmente en el campo del bioanálisis. La versatilidad de sus características morfológicas y funcionales hace de ellas un biomaterial muy interesante para vehículo de liberación de fármacos, marca de inmunoensayos, o como sistema biomiético de membranas o vesículas extracelulares. Sin embargo, estas nuevas aplicaciones imponen una serie de requisitos sobre los métodos de preparación que suponen un reto tecnológico y han generado un campo de investigación muy activo. El control sobre el tamaño de partícula y su monodispersidad son características esenciales que se deben controlar mediante la mejora de los métodos actuales y la propuesta de nuevas tecnologías diseñadas para tal fin. En este escenario científico-tecnológico se enmarca la presente Tesis Doctoral. El objetivo general es desarrollar métodos eficaces de síntesis con tamaño controlado. Con las vesículas obtenidas se han mimetizado exosomas (vesículas extracelulares) con el fin de investigar su uso como standard analítico en inmunoensayos. Estas vesículas están despertando un gran interés en el campo de la salud como nuevos biomarcadores, y son necesarias nuevas aproximaciones para poner a punto métodos de análisis.

Tras una introducción sobre las generalidades de las nanovesículas, el **quinto capítulo** de la tesis presenta una profunda revisión del estado del arte del concepto de exosoma artificial, así como la revisión crítica de las diferentes aproximaciones metodológicas para su producción y una nueva clasificación de estos nuevos biomateriales en función de los mismos. Además, se han expuesto los usos biotecnológicos de dichas partículas, como son la distribución y liberación controlada de fármacos, su papel en diagnóstico, y su posible empleo en el desarrollo y estudio de métodos bioanalíticos. Para ello, es necesario procesos adaptados para la preparación de exosomas puramente artificiales mediante técnicas nano-biotecnológicas. Esta temática es precisamente sobre la que versa el trabajo experimental expuesto en los siguientes capítulos.

El **sexto capítulo** presenta el desarrollo de un modelo matemático multivariante de Diseño de Experimentos y su aplicación al estudio de un método clásico de preparación de nanovesículas, como es la inyección de etanol. Con dicho estudio se pretende controlar los parámetros para la obtención de partículas con propiedades morfológicas deseadas y controladas. Para llevar a cabo el trabajo se han escogido dos formulaciones clásicas: una de liposoma y otra de niosoma. Además, se ha realizado un estudio de parámetros adicionales como la estabilidad coloidal y la eficacia de encapsulación de compuestos de diferente naturaleza química.

En el **séptimo capítulo** se ha abordado la producción de niosomas de tamaño controlado y monodispersos mediante un dispositivo de microfluídica a temperatura controlada. El sistema ha sido diseñado para su acoplamiento sobre un microscopio invertido con el fin de observar

los fenómenos de interfase acaecidos en su interior (como por ejemplo fenómenos de difusión molecular en flujo laminar). Además, se ha estudiado el efecto de parámetros metodológicos, poniendo especial énfasis en la temperatura. También se han tenido en cuenta otros parámetros como la longitud de la cadena hidrocarbonada del tensioactivo. Este sistema miniaturizado es idóneo para etapas de optimización de formulaciones y para la evaluación de la eficacia de encapsulación de las mismas, especialmente en los casos en que se disponga de poco volumen de reactivos.

En el **octavo capítulo** se estudia la mejora de la encapsulación de compuestos hidrófilos mediante el empleo de disoluciones acuosas con poli-oles (glicerol y polietilenglicol), y el efecto de éstas sobre el tamaño de vesícula. Por otra parte, se evalúa el impacto sobre dichos parámetros que puede tener el peso molecular de los compuestos encapsulados. Este estudio se ha llevado a cabo con el empleo de una formulación basada en una mezcla de surfactantes no iónicos en presencia y ausencia de dodecanol como estabilizante de membrana.

Finalmente, en el **noveno capítulo** se parte de los modelos obtenidos para niosomas en etapas anteriores, y han sido empleados para obtener partículas de tamaño y monodispersidad similar a exosomas naturales. Además, mediante la funcionalización superficial de los mismos con estreptavidina y posteriormente con péptidos biotinilados recombinantes de tetraspaninas (principal marcador molecular de exosomas), se han desarrollado exosomas artificiales. Dichos exosomas han sido testados mediante immunoensayos de tipo ELISA como un posible nuevo estándar analítico para el desarrollo y/o mejora de métodos bioanalítcos basados en el reconocimiento molecular para la determinación de vesículas extracelulares, como son los exosomas.

RESUMEN (en Inglés)

Nanovesicles, a particular type of organic colloids, is generating a growing interest in the field of biotechnology, and particularly in the field of bioanalysis. The versatility of its morphological and functional characteristics makes them a very promising biomaterial. Some of these aplications are as drug delivery vehicle, multilabel system for immnunoassays or biomietic membrane or extracellular vesicles. However, these new applications impose a series of requirements on preparation methods that carry along a technological challenge and have triggered a very active field of research. Control over the particle size and its monodispersity are essential characteristics that must be controlled by improving current methods and proposing new technologies designed for such purpose. Withing this framework, the general objective of this Doctoral Thesis is the development of efficient methods for controlled size syntesis. The nanovesicles obtained have been used to mimic exosomes (extracelular vesicles) with the aim of investigating their use as analytical standard at immunoassays. These nanovesicles are attracting high interest as novel biomarkers at the biomedical field, and novel approaches are necessary in order to develop analytical methods.

After an introduction about the general concepts of nanovesicles, the **fifth chapter** presents a deep review of the state of the art of the artificial exosome concept, as well as the critical evaluation of the different approaches for its production. A systematic classification of these new biomaterials was carried out, with the aim of providing some reference guides for standardization the field. In addition, the biotechnological application of these particles has been discussed. This includes the distribution and controlled release of drugs, their role in diagnosis, and their possible use in the development of bioanalytical methods. For that purpose, novel methods are required for the preparation of fully artificial exosomes by using nano-biotechnological techniques. This topic is the core of the experimental work presented in the following chapters.

The **sixth chapter** includes de development of a mathematical model of Design of Experiments (DoE) for nanovesicles preparation by the ethanol injection method (EIM.) The objective of the study is to control the parameters for obtaining particles with controlled morphological properties. For the DoE set up, two classical formulations have been chosen: one representative of liposomes and the other of niosomes,. In addition, a study of additional parameters such as colloidal stability and the encapsulation efficiency of compounds with different chemical nature has been carried out.

In the **seventh chapter**, the production of controllable-size and monodispersed niosomes has been approached by means of a microfluidic device at controlled temperature. This system was designed in a way to be coupled to an inverted microscope. This allowed to visualize the interphase phenomena occurring inside (such as molecular diffusion in laminar flow). In addition, the effect of methodological parameters has been studied, with special emphasis on temperature. Other parameters such as the length of the surfactant alkyl chain have also been taken into account. This miniaturized system is ideal for formulations optimization and for the evaluation of their encapsulation efficiencies. It is especially useful when small volume of reagents is available.

In the **eighth chapter** the enhacement of hydrophilic compounds encapsulation is studied through the use of aqueous solutions with polyols (glycerol and polyethylene glycol), and their effect of these over vesicle size. On the other hand, the effect of cargo molecular weight over these parameters has been evaluated. This study has been carried out with the use of a formulation based on a mixture of non-ionic surfactants in the presence and absence of dodecanol as a membrane stabilizer.

Finally, in the **nineth chapter** the models obtained for niosomes in previous stages have been used to obtain particles with an average size and monodispersity similar to that of natural exosomes. In addition, by surface functionalization first with streptavidin and in a second step with recombinant biotinylated tetraspanin peptides (classical molecular biomarkers of exosomes), fully artificial exosomes have been developed. These particles have been tested by ELISA immunoassays as a potential new analytical standard for the development and/or enhacement of bioanalytical methods based on molecular recognition for the determination of extracellular vesicles, such as exosomes.

SR. PRESIDENTE DE LA COMISIÓN ACADÉMICA DEL PROGRAMA DE DOCTORADO EN ANÁLISIS QUÍMICO, BIOQUÍMICO Y ESTRUCTURAL, Y MODELIZACIÓN COMPUTACIONAL

Índice de contenidos

Índice de Figuras

Índice de Tablas

Lista de Abreviaturas

A

AA Ácido ascórbico

AFM Acronimo anglosajón para *atomic force microscopy*

ANOVA Acronimo anglosajón para *analysis of the variance*

ATMPs Acronimo anglosajón para *advanced therapy medicinal products*

a.u. Acronimo anglosajón para *arbitrary units*

B

B12 Vitamina B12, conocida también como cobalamina

BBS Acrónimo anglosajón para *borate buffer saline*

BCA Acrónimo anglosajón para *bicinchoninic acid*

BirA Acrónimo anglosajón para *biotin ligase A*

BSA Acrónimo anglosajón para *bovine serum albumin*

BS Acrónimo anglosajón para *backscattering*

C

CRY2 Acronimo anglosajón para *cryptochrome 2*

CPP Acrónimo anglosajón para *critical packing parameter*

CD9/63/81 Tetraspanina 9/63/81

D

DBCO Acrónimo anglosajón para *dibenzocyclooctyne*

Dc Dodecanol

DCs Acrónimo anglosajón para *dendritic cells*

DF Acrónimo anglosajón para *degrees of freedom*

DLS Acrónimo anglosajón para *dynamic light scattering*

DoE Acrónimo anglosajón para *design of experiments*

DOGS-NTA Acrónimo anglosajón para *1,2-dioleoyl-sn-glycero-3-[(N-(5-amino-1-carboxypentyl)iminodiacetic acid)succinyl]*

DSC Acrónimo anglosajón para *differential scanning calorimetry*

E

EBSSNs

ECL Acrónimo anglosajón para *enhanced chemiluminescence*

EDC 1-etil-3-(3-dimetilaminopropil)carbodiimida

EE Eficacia de encapsulación

EGFR Acrónimo anglosajón para epidermal growth factor receptor

EIM Acrónimo anglosajon para *ethanol injection method*

ELISA Acrónimo anglosajón para *enzyme-linked immunosorbent assay*

EXPLORs Acrónimo anglosajón para *exosomes for protein loading via optically reversible protein–protein interactions*

EVs Acrónimo anglosajón para *extracellular vesicles*

F

FRR Acrónimo inglés para *flow rate ratio*

G

Gly Glicerol, aunque también se refiere a una disolución agua:glicerol 60:40 v/v

H

HEK293 Acrónimo anglosajón para *human embryonic kidney cell line 293*

HER2 Acrónimo anglosajón para *human epidermal growth factor receptor 2*

hFC Acrónimo anglosajón para *high-resolution flow cytometry*

HLA Acrónimo anglosajón para *human leukocyte antigen*

HLB Acrónimo anglosajón para *hydrophilic-lipophilic balance*

HPLC Acrónimo anglosajón para *high performance liquid chromatography*

HR Acrónimo anglosajón para *high resolution*

HRP Acrónimo anglosajón para *Horseradish peroxidase*

I

IDO Acrónimo anglosajón para *indoleamine 2,3-dioxygenase*

L

LEL Acrónimo anglosajón para *large extracelular loop*

LUV Acrónimo anglosajón para *large unilamelar vesicles*

LUV-TRAIL Acronimo anglosajón para vesículas sintéticas recuviertas de TRAIL

M

miRNA Acrónimo anglosajón para micro *interference ribonucleic acid*

MFLs Acrónimo anglosajón para *membrane fusogenic liposomes*

MLVs Acrónimo anglosajón para *multilamelar vesicles*

MS Acrónimo anglosajón para *mean of squares*

MSCs Acrónimo anglosajón para *mesenchymal stem cells*

MQ Acrónimo anglosajón para *Mili-Q water*, agua ultrapura o de Tipo I

MVBs Acrónimo anglosajón para *multivesicular bodies*

MW Acrónimo anglosajón para *molecular weigth*

MWCO Acrónimo anglosajón para *molecular weigth cut-off*

N

(sulfo)NHS Sulfo N-hyidroxyisulfosuccinimida

Nio niosomas

Nio_Str Niosomas con streptavidina conjugada en superficie

NLCs Acronimo anglosajón para *nanostructured lipid carriers*

NPMs Nanopartículas metálicas

NTA Acrónimo anglosajón para *nanoparticle tracking analysis*

NVs Nanovesículas

O

O/A relación de volúmenes de fase orgánica/acuosa

OVA Acrónimo anglosajón para *chicken egg ovalbumin*

P

PB Acronimo anglosajón para *phosphate buffer*

P-B Plackett-Burman

PBS Acrónimo anglosajón para *phosphate buffer saline*

PC Acronimo anglosajón para *Phosphatidylcholine*

PDI Acrónimo anglosajón para *polydispersity index*

PEG Poly(Ethylene) glicol, aunque también se refiere a una disolución de polietilengligol-400 55:45 v/v.

R

RB Rodamina B

RM acrónimo anglosajón para *reference material*

RNA Acronimo anglosajón para *ribonucleic acid*

RT acrónimo anglosajón para *room temperature*

RP-HPLC Acrónimo anglosajón para *Reverse-Phase High Perfomance Liquid Chromatography*

S

SDS-PAGE Acronimo anglosajón para sodium dodecyl sulfate polyacrylamide gel electrophoresis

SEC Acrónimo anglosajón para *size exclusion chromatography*

siRNA Acronimo anglosajón para *small interference ribonucleic acid*

Sp80 Span® 80, o monooleato de sorbitano

SPIONs Acronimo anglosajón para *superparamagnetic iron oxide nanoparticles*

SS Acrónimo anglosajón para *sum of squares*

Str Estreptavidina

SUV Acrónimo anglosajón para *small unilamelar vesicles*

T

TAMEL Acronimo anglosajón para *targeted and molecular extracelular vesicles loading*

TEM Acrónimo anglosajón para *transmission electron microscopy*

TFH Acrónimo anglosajón para *thin film hydration method*

TFR Acrónimo anglosajón para *total flow rate*

TMB 3,3',5,5'-Tetrametilbenzidina

tRPS Acrónimo anglosajón para *tunable resistive pulse sensing*

Tw80 Tween® 80, o monooleato de polioxietilen(20)sorbitano

U

UC Ultracentrifugación

Uv/vis Ultravioleta/visible

V

VE Vesículas extracelulares

v/v Relación de volúmenes

w/v Relación peso/volumen

Símbolos y unidades

λ Longitud de onda

ζ Potencial zeta

A Amplitud de sonicación (%)

C Concentración de compuestos de membrana

F Fischer's ratio (u.a.)

I Fuerza iónica (mM)

$\mathbf{N_E}$ Rotación del matraz en evaporación (rpm)

$\mathbf{N_S}$ Velocidad de agitación durante la inyección (rpm)

P p-valor (u.a.)

$\mathbf{Q_T}$ Flujo volumétrico (mL)

$\mathbf{Q_V}$ Flujo de inyección (mL)

Re Número de Reynolds

t Tiempo de sonicación (min)

T Temperatura

$\mathbf{T_c}$ Temperatura de transición *gel-líquido* cristalino

$\mathbf{T_E}$ Temperatura de evaporación (°C)

$\mathbf{T_I}$ Temperatura de inyección (°C**)**

$\mathbf{V_0}$ Volumen muerto

1. Introducción

Capítulo 1. Introducción

En la actualidad existen numerosos productos basados en coloides orgánicos como elemento funcional:[1] limpiadores cosméticos basados en soluciones micelares, cremas y alimentos con vesículas para la administración y liberación controlada de principios activos, nuevas formas de administración de fármacos basadas en vehículos moleculares, detergentes con aromas encapsulados en partículas orgánicas, o aceites lubricantes con aditivos para la mejora de sus propiedades. A su vez, los coloides orgánicos también forman parte de procesos químicos, como son la fabricación de nanomateriales[2] y los métodos bioanalíticos.[3]

Un tipo particular de coloide orgánico cuyo espectro de aplicaciones es elevado, y en expansión, son los sistemas vesiculares o nanovesículas (NVs): partículas generalmente de unos pocos nanómetros a unas pocas de micras, con una estructura molecular basada en una bicapa de compuestos anfifílicos[4] que encierra en su interior una cavidad acuosa. Esta estructura ofrece la capacidad de incorporar tanto compuestos de naturaleza hidrofílica como de carácter hidrofóbico.[5] La bicapa ofrece una gran versatilidad, ya que puede presentarse en diversos tamaños y grado de lamelaridad, lo que les confiere multitud de aplicaciones en los campos de la medicina,[6] cosmética,[7] alimentación,[8] medioamiente[9] y de la química, especialmente la química analítica.[3]

Por otra parte, la naturaleza química de dichos compuestos, permite su asociación a macromoléculas[10] (como enzimas, anticuerpos, ácidos nucleicos, polisacáridos, etc.) o su fijación a superficies[11] o nanomateriales inorgánicos, tales como nanopartículas metálicas.[12] Las NVs fueron desarrolladas inicialmente para el campo de la cosmética, siendo posteriormente expandido su uso a otros sectores tecnológicos.

Sin embargo, es en el campo de la biomedicina donde han encontrado mayor aceptación y auge, siendo numerosas las formulaciones aprobadas y comercializadas para uso terapéutico humano y animal,[13] habiendo sido *Doxil/Caelyx®* el primer fármaco basado en liposomas (en el mercado desde 1995). Por otra parte, es el campo donde existe mayor diversidad de tipos de vesículas empleadas.

Este elevado interés clínico ha llevado al desarrollo de nanovesículas con propiedades mejoradas, como una mayor estabilidad coloidal, distribución

organotrópica, o liberación inteligente del componente encapsulado.[14] Estas características funcionales se consiguen mediante la incorporación de elementos activos como son polímeros hidrófilos (ej. Poli(Etilenglicol)),[15] anticuerpos[16] o ligandos de receptores de membrana,[17] o la cuidadosa selección del tipo de lípidos empleados[18] así como la incorporación de nanopartículas metálicas (NPMs) que ejercen de *interruptores* de la liberación.[19]

En el campo de la biomedicina este tipo de partículas no sólo han sido empleados como vehículos moleculares de por sí, sino que han sido empleados para la mejora y aumento de propiedades de sistemas vesiculares naturales como son los exosomas.[20,21] Éstos son un sub-tipo de vesículas extracelulares (VE) secretadas por cualquier célula, y con un papel muy importante en comunicación celular, así como en procesos fisio-patológicos.[22] Este rol les ha puesto en el foco de atención de nuevas aplicaciones terapéuticas y de diagnóstico.[23] Y a su vez, éstos han servido de inspiración para el desarrollo de nuevos agentes teranósticos,[24] denominados exosomas artificiales. Este tema será abordado con mayor profundidad en capitulos siguientes.

Por último y no menos importante, el sector químico se ha beneficiado de estas partículas. En concreto, la química analítica y el sector de los biosensores especialmente, han explorado su uso en el desarrollo y mejora analítica de varios métodos.[25,32] El campo de los immunoensayos es un claro ejemplo, y numerosos trabajos sobre su uso como sistema de amplificación de señal pueden encontrarse en la literatura,[26] tanto en formatos tradicionales como ensayos ELISA,[27] en test immunocromatográficos,[28] o en sistema de flujo.[29] La amplificación de señal puede también producirse no por la vesícula en sí, si no que ésta puede adquirir un rol de soporte[30] y potenciación de fenómenos espectroscópicos como es la fluorescencia mejorada por metales.[31] A su vez, nanovesículas como los liposomas pueden ser empleados como elemento de reconocimiento,[32] como por ejemplo de lipasas (enzimas implicadas en procesos de inflamación). Este reconocimiento puede ser empleado para su detección, y mediante una correcta transducción, su cuantificación en fluidos biológicos mediante test rápidos.[33]

La semejanza estructural y química de estos biomateriales con las vesículas naturales (como los exosomas), han inspirado su empleo como herramientas de estudio de los mismos.[34] Para ello, es necesario su producción con características morfológicas lo más parecidas posibles, especialmente de tamaño y monodispersidad, ya que son

parámetros importantes en el bioanálisis de las VE. Por otra parte, su modificación biotecnológica para incroporar moléculas bioactivas de diversa naturaleza química en el interior o en superficie, hace necesario la adaptación o diseño de procesos adaptados a tal fín, con la idea de producir estructuras biomiméticas de una forma adecuada y asequible. Si bien los liposomas han destacado en estas aplicaciones, este campo en auge, ofrece elevadas posibilidades para los niosomas también, y su empleo en bioanalítica de exosomas está ofreciendo los primeros resultados.[35]

La efectividad de los sistemas vesiculares en sus aplicacione está íntimamente ligada a una propiedad esencial como es el tamaño promedio de partículas y a otro parámetro relacionado como es la monodispersidad de tamaño (cuán grande es la diversidad de tamaños de partícula en una suspensión).[36]

Su empleo como vehículos de distribución y liberación de fármacos, se asocia a un tamaño inferior a 150-200 nm para no ser reconocidos por el sistema monocítico nuclear,[37] y como consecuencia ser eliminados de la circulación (proceso de aclaramiento plasmático). Por ello, se reduce su tiempo de vida útil, requiriéndose mayores dosis, lo que puede conllevar efectos secundarios asociados a su transporte no específico.

Debe existir un compromiso, ya que a mayor tamaño mayor es la carga de principio activo que pueden portar. Sin embargo, un tamaño pequeño (≤150 nm) les confiere una capacidad intrínseca para permear por la red de capilares que nutren los tumores, ya que el tamaño de las fenestraciones vasculares permite un filtrado no selectivo de las vesículas al espacio intersticial.[38] Pero por otro lado, deben poseer un tamaño mínimo que evite su aclaramiento plasmático a nivel renal (≥10-15 nm). De este modo, este compromiso de tamaño permite una distribución del fármaco con características pseudo-dirigidas. En relación con la distribución de biocompuestos, otro aspecto importante es la incorporación celular, es decir, su paso al interior de las mismas. Este proceso se sabe que es dependiente de la forma que presenta la partícula, pero también del tamaño de la misma.[39]

Puesto que ha quedado evidenciado la importancia de tamaño promedio de partícula, se puede llegar a la conclusión que una homogeneidad en el mismo es igual de importante. Una distribución de tamaño monodispersa, asegura un comportamiento homogéneo de la población de partículas, lo que permite observar

respuestas diferenciadas atribuidas al material, y en cierta forma predecible. En otros casos, como es su papel como marca en immunoensayos, es una característica casi más importante que el propio tamaño. Puesto que a mayor tamaño, mayor es su superficie, la capacidad de portar más elementos de reconocimiento aumenta en proporción, lo que tiene importantes repercusiones sobre las características analíticas como puede ser el límite de detección. Distribuciones de tamaños amplias introducen heterogeneidad en el comportamiento de las partículas en cuanto a capacidades de reconocimiento y generación de señal, ya que pueden producirse impedimentos estéricos que reduzcan la señal analítica y generen un aumento en el límite de detección, siendo contrario a la finalidad de su empleo en esta aplicación, como es una amplificación de la señal analítica.

Por todo esto, estrategias de producción de partículas con control de tamaño y de su monodispersidad son esenciales para sus aplicaciones bioanalíticas. En este escenario socio-tecnológico se enmarca la presente Tesis Doctoral. El objetivo general de la misma, será el estudio de metodologías de preparación de sistemas vesiculares (liposomas y niosomas), con especial énfasis en la producción controlada de tamaño de partícula, para su uso en aplicaciones biotecnológicas, fundamentalmente bioanalíticas.

Referencias bibliográficas

[1] Willen Norden (editor) (2011). Colloids and interfaces in Life Sciences and Bionanotechnologies, segunda edición, CRC Press, Taylor & Francis Group, New York, USA.

[2] De S., Kundu R., Biswas A. (2012). Synthesis of gold nanoparticles in niosomes. *Journal of Colloids and Interface Science*, 386:9-15.

[3] Gómez-Hens A., Fernández-Romero J.M. (2005). The role of liposomes in analytical process. *Trends in Analytical Chemistry*, 24:9-19.

[4] Chen I.A., Walde P. (2010). From self-assembled vesicles to protocells. C*old Spring Harbor Perspectives in Biology*, 2:a002170.

[5] Damera D.P., Krishna Venuganti V.V., Nag A. (2018). Deciphering the role of bilayer of a noisome towards controlling the entrapment and release of dyes. *Chemistry Select*, 3:3930-3938.

[6] Caddeo C., Diez Sales O, Valentia D., Ruiz Saurí A., Fadda A.M., Manconi M. (2013). Inhibition of skin inflammation in mice by diclofenac in vesicular carriers: Liposomes, ethosomes and PEVs. *Int. J. Pharm*., 443:128-136.

[7] Hamid Reza Ahmadi Ashtiani H.R., Bishe P., Lashgari N.-A., Nilforoushzadeh M.A., Zare S. (2016). Liposomes in cosmetics. *Journal of Skin and Stem Cell*, 3(3):e65815.

[8] Gutiérrez G., Matos M., Barrero P., Pando D., Iglesias O., Pazos C. (2016). Iron-entrapped niosomes and their potential application for yogurt fortification. *Food Science and Technology*, 74:550-556.

[9] Gatt S., Bercovier H., Barenholz Y. Use of liposomes for combating oil spills and their potential application to bioreclamation. In: On-site bioreclamation: processes for xenobiotic and hydrocaron treatment, editado por Hinchee R.E. and Olfenbuttel R.F. 1991, Battelle Press, USA.

[10] Eroğlu İ., İbrahim M. (2019). Liposome-Ligand Conjugates: A Review on the Current State of Art. *Journal of drug targeting*, in press.

[11] Anbumozhi Angayarkanni S., Kampf N., Klein J. (2019). Surface interactions between boundary layers of poly(ethylene oxide)-liposome complexes: lubrication, bridging and selective ligation. *Langmuir*, in press.

[12] Al-Jamal W.T. and Kostarelos K. (2007). Liposome–nanoparticle hybrids for multimodal diagnostic and therapeutic applications. *Nanomedicine*, 2(1):85-98.

[13] Carugo D., Bottaro E., Owen J., Stride E., and Nastruzzi C. (2016). Liposome production by microfluidics: potential and limiting factors. Sci. Rep., 19(6):25876.

[14] Lombardo D., Calandra P., Barreca D., Magazù S., Kiselev M.A. (2016). Soft interaction in liposome nanocarriers for therapeutic drug delivery. *Nanomaterials*, 6(7):125.

[15] Ishida T., Ichihara M., Wang X.Y., Yamamoto K., Kimura J., Majima E., Kiwada H. (2006). Injection of PEGylated liposomes in rats elicits PEG-specific IgM, which is responsible for rapid elimination of a second dose of PEGylated liposomes. *J. Control Release.*, 112(1):15-25.

[16] Lukyanov A.N., Elbayoumi T.A., Chakilam A.R., Torchilin V.P. (2004). Tumor-targeted liposomes: doxorubicin-loaded long-circulating liposomes modified with anti-cancer antibody. *J. Control Release*, 100(1):135-144.

[17] Sihorkar V., Vyas S.P. (2001). Potential of polysaccharide anchored liposomes in drug delivery, targeting and immunization. *J. Pharm. Pharm. Sci*, 4(2):138-158.

[18] Kunisawa J. , Masuda T., Katayama K., Yoshikawa T., Tsutsumi Y., Akashi M., Mayumi T., Nakagawa S. (2005). Fusogenic liposome delivers encapsulated nanoparticles for cytosolic controlled gene release. *J. Control Release.,* 105(3):344-353.

[19] Kumar Rengan A., Banerjee R., Srivastava R. (2012). Thermosensitive gold-liposome hybrid nanostructures for photothermal therapy of cancer. Comunicación oral. 12th IEEE International Conference on Nanotechnology (IEEE-NANO). 20-23 Agosto, Birmingham, Reino Unido.

[20] Lee J., Lee H., Goh U., Kim J., Jeong M., Lee J., Park J.H.. (2016). Cellular engineering with membrane fusogenic liposomes to produce functionalized extracellular vesicles. *ACS Applied Materials and Interfaces*, 8(11):6790-6795.

[21] Sato Y.T., Umezaki K., Sawada S., Mukai S., Sasaki Y., Harada N., Shiku H., Akiyoshi K. (2016). Engineering hybrid exosomes by membrane fusion with liposomes. *Sci. Rep.*, 6:21933.

[22] Yáñez-Mó M., Siljander P.R., Andreu Z., Zavec A.B., Borràs F.E., Buzas E.I., Buzas K., Casal E., Cappello F., Carvalho J., Colás E., Cordeiro-da Silva A., Fais S., Falcon-Perez J.M., Ghobrial I.M., Giebel B., Gimona M., Graner M., Gursel I., Gursel M., Heegaard N.H., Hendrix A., Kierulf P., Kokubun K., Kosanovic M., Kralj-Iglic V., Krämer-Albers E.M., Laitinen S., Lässer C., Lener T., Ligeti E., Linē A., Lipps G., Llorente A., Lötvall J., Manček-Keber M., Marcilla A., Mittelbrunn M., Nazarenko I., Nolte-'t Hoen E.N., Nyman T.A., O'Driscoll L., Olivan M., Oliveira C., Pállinger É., Del Portillo H.A., Reventós J., Rigau M., Rohde E., Sammar M., Sánchez-Madrid F., Santarém N., Schallmoser K., Ostenfeld M.S., Stoorvogel W., Stukelj R., Van der Grein S.G., Vasconcelos M.H., Wauben M.H., De Wever O. (2015). Biological properties of extracellular vesicles and their physiological functions. *Journal of Extracellular Vesicles*, 14(4):27066.

[23] Cappello, F., Logozzi, M., Campanella, C., Bavisotto, C. C., Marcilla, A., Properzi, F., Fais, S. (2017). Exosome levels in human body fluids: a tumor marker by themselves?. *European Journal of Pharmaceutical Sciences*, 96:93-98.

[24] Jung K.O., Jo H., Yu J.H., Gambhir S.S., Pratx G. (2018). Development and MPI tracking of novel hypoxia-targeted theranostic exosomas. *Biomaterials*, 177:139-148.

[25] Liu Q., Boyd B.J. (2013) Liposomes in biosensors. *Analyst*, 138:391-409.

[26] Lee M., Durst R.A., Wong R.B. (1998). Development of flow-injection liposome immunoanalysis (FILIA) for imazethapyr. *Talanta*, 46:851-859.

[27] Lin B., Liu D., Yan J., Qiao Z., Zhong Y., Yan J., Zhu Z., Ji T., Yang C.J. (2016). Enzyme-encapsulated liposome-linked immunosorbent assay enabling sensitive personal glucose meter readout for portable detection of disease biomarkers. *ACS Applied Material & Interfaces*, 8:6890-7.

[28] Edwards K.A., Korff R., Baeumner A.J. (2017). Liposome-Enhanced Lateral-Flow Assays for Clinical Analyses. *Methods in Molecular Biology*., 1571:407-434

[29] Ho J.A., Wu L.-C. , Huang M.R., Lin Y.-J., Baeumner A.J., Durst R.A. (2007) Application of Ganglioside-Sensitized Liposomes in a Flow Injection Immunoanalytical System for the Determination of Cholera Toxin. *Analytical Chemistry*, 79:246-250.

[30] Olguín Y., Villalobos P., Carrascosa L.G., Young M., Valdez E., Lechuga L., Galindo R. (2013). Detection of flagellin by interaction with human recombinant TLR5 immobilized in liposomes. *Anal. Bioanal. Chem.*, 405(4):1267-1281.

[31] Shweta Pawar S., Bhattacharya A., Nag A. (2019). Metal-Enhanced Fluorescence Study in Aqueous Medium by Coupling Gold Nanoparticles and Fluorophores Using a Bilayer Vesicle Platform. *ACS Omega*, 4(3):5983-5990.

[32] Mazur F., Bally M., Städler B., Chandrawati R. (2017). Liposomes and lipid bilayers in biosensors. *Advanced in Colloids and Interface Science*, 249:88-99.

[33] Chapman R., Lin Y., Burnapp M., Bentham A., Hillier D., Zabron A., Khan S., Tyreman M., Stevens M.M. (2015). Multivalent nanoparticles networks enable point-of-care detection of human phospholipase-A2 in serum. *ACS Nano*, 9:256-73.

[34] Lane R. E., Korbie D., Anderson W., Vaidyanathan R., Trau, M. (2015). Analysis of exosome purification methods using a model liposome system and tunable-resistive pulse sensing. *Sci. Rep.*, 5:7639.

[35] Lozano-Andrés E., Libregts S.F., Toribio V., Royo F., Morales S., López-Martín S., Valés-Gómez M., Reyburn H.T., Falcón-Pérez J.M., Wauben M.H., Soto M., Yáñez-Mó M. (2019). Tetraspanin-decorated extracellular vesicle-mimetics as a novel adaptable reference material. *Journal of Extracellular Vesicles*, 8(1):1573052.

[36] Danaei M., Dehghankhold M., Ataei S., Davarani Hasanzadeh F., Javanmard R., Dokhani A., Khorasani S., Mozafari M.R. (2018). Impact of particle size and polidespersity index on the clinical applications oflipidic nanocarrier systems. *Pharmaceutics*, 10(57):1-17.

[37] Kraft J.C., Freeling, J.P., Wang Z., Ho R.J. (2014). Emerging research and clinical development trends of liposome and lipid nanoparticle drug delivery systems. *J. Pharm. Sci.*, 103:29-52.

[38] Blasi P., Giovagnoli S., Schoubben A., Ricci M., Rossi C. (2007). Solid lipid nanoparticles for targeted brain drug delivery. *Adv. Drug. Deliv. Rev.*, 59:454-477.

[39] Andar A.U., Hood R.R., Vreenland W.N., DeVoe D.L., Swaan P.W. (2014). Microfluidic preparation of liposomes to determine particle size influence on cellular uptake mechanism. *Pharmaceutical Research*, 31:401-413.

2. Objetivos/Objetives

Capítulo 2. Objetivos

La presente Tesis Doctoral se ha centrado en el estudio de metodologías de preparación de sistemas vesiculares (liposomas y niosomas), con especial énfasis en la producción controlada de tamaño de partícula, para su uso en aplicaciones bioanalíticas. En concreto, se emplearán para el desarrollo de un modelo mimético de exosomas para su empleo como estándar analítico. Este objetivo general se ha divido en cuatro objetivos específicos, que se exponen a continuación:

- Estudio de la influencia de parámetros de operación sobre las características morfológicas finales de vesículas, tanto niosomas como liposomas, preparadas mediante una técnica comúnmente utilizadas como es la inyección con etanol.

- Desarrollo y puesta a punto de un dispositivo de microfluídica con control de temperatura para la preparación de sistemas vesiculares, lo que permitirá el uso de pequeños volúmenes de muestra.

- Estudio de la influencia de las variables medio de hidratación y compuesto a encapsular, en la caracterización final de vesículas preparadas con el método de hidratación de la película fina.

- Diseño y producción de sistemas vesiculares para la producción de un analito modelo: partículas biomiméticas de exosomas, denominados Exosomas Artificiales, y su aplicación en bioanálisis**.**

Chapter 2. Objetives

The main objective of this Ph.D. Thesis is the study of methodologies for the preparation of vesicular systems (liposomes and niosomes), with special emphasis on the controlled production of particle size for their use in bioanalytical applications. Specifically, they will be used for the development of a mimetic model of exosomes for their use as an analytical standard. This main objective has been divided into the following specific objectives:

- Study of operating parameters influence over the final morphological characteristics of vesicles, niosomes and liposomes, prepared by a commonly used technique such as ethanol injection method.

- Development and optimization of a microfluidic device with temperature control for the preparation of vesicular systems, which will allow the use of small sample volumes.

- Study of the influence of the variables hydration solution and encapsulated compound, over the final characterization of vesicles prepared by the thin film hydration method

- Design and preparation of vesicular systems for the production of a model analyte: exosomes biomimetic particles, called Artificial Exosomes, and their application for bioanalysis.

3. Consideraciones básicas

Capítulo 3. Consideraciones básicas

3.1. Sistemas vesiculares: generalidades

Las vesículas son un tipo de coloide orgánico artificial, formado por la agregación supramolecular de moléculas anfifílicas que se disponen en una organización de bicapa, que puede ser unilamelar o multilamelar.[1] Ésta, separa una cavidad acuosa interior de la solución en la que se encuentran. La naturaleza química y la disposición y tamaño de la misma establecen los tipos de vesículas artificiales que se pueden encontrar en la literatura. La **Figura 3.1** representa esta diversidad química y morfológica que se pueden encontrar en este tipo de sistemas.

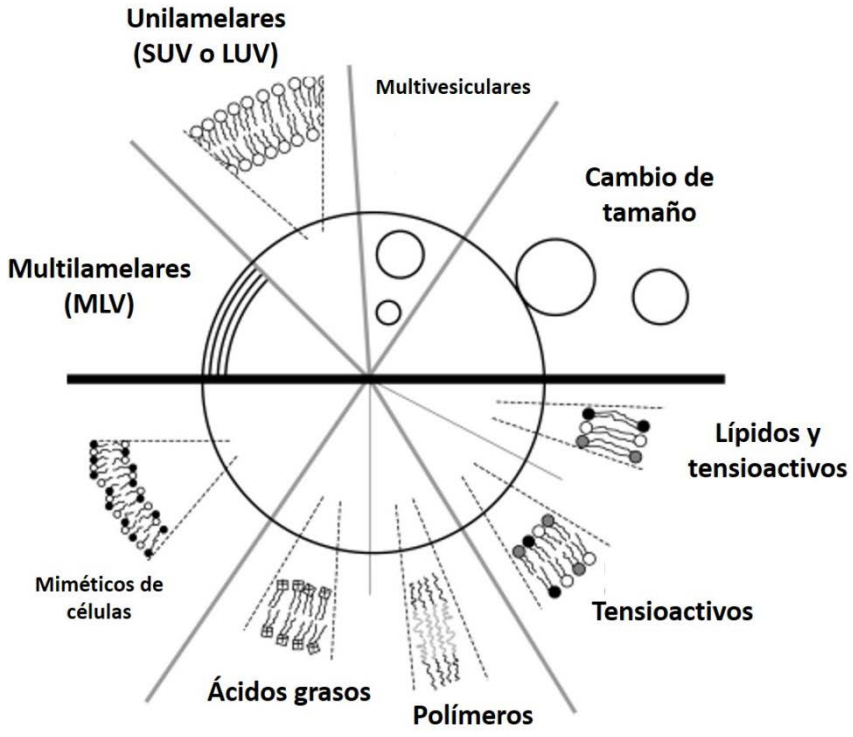

Figura 3.1. *Diversidad química y morfológica de las vesículas artificiales creadas por autoensamblaje de moléculas anfifílicas. Figura adaptada de la referencia 1. SUV: small unilamelar vesicles; LUV: large unilamelar vesicles; MLV: multilamelar vesicles.*

3.1.1. Moléculas anfifílicas

La estructura en bicapa responde al comportamiento físico-químico de ciertos tipos de moléculas anfifílicas, ya que no todas son capaces de agregarse en este tipo de

estructura supramolecular.[2] La característica por la que pueden o no formar bicapa se comentará más adelante.

Para entender primero el proceso de agregación, es necesario considerar previamente la físico-química básica de las moléculas anfifílicas. Como su propio nombre indica, se trata de moléculas con un comportamiento simultáneo hidrofílico e hidrofóbico, derivado de poseer en su estructura una región polar y otra apolar, denominadas de forma general cabeza y cola respectivamente (ver **Figura 3.2**).[3] Esta última, puede estar presente en una, dos, o varias repeticiones, siendo a su vez iguales o diferentes entre sí en cuanto a longitud o grado de saturación como se ha indicado en la sección anterior.

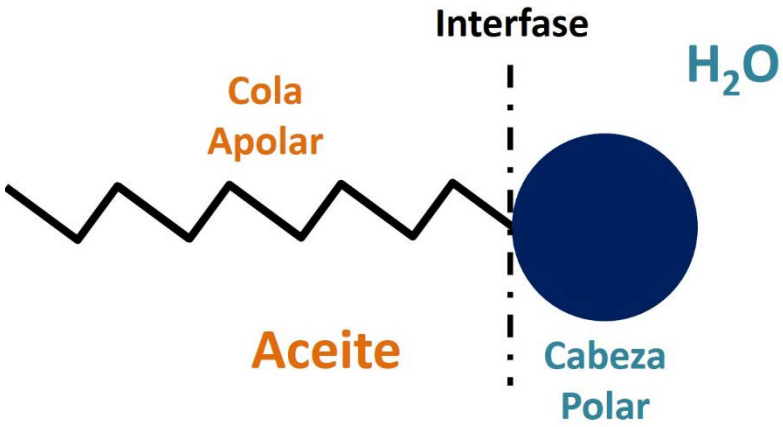

Figura 3.2. *Estructura típica de una molécula anfifílica, en la que se señalan sus dos porciones principales: la cabeza polar y la cola apolar, entre las cuales se establece la interfase cuando son puestas en disolución acuosa.*

La red de moléculas de agua que se establece gracias a los puentes de hidrógeno de las mismas se ve interrumpida por la existencia de esas porciones apolares de las moléculas anfifílicas en disolución, en contraposición a las interacciones positivas que establecen las cabezas polares (debido a esto, se habla entonces de la existencia de un balance de fuerzas que no se encuentra en equilibrio).[4] Este hecho establece pues una interfase en este tipo de moléculas, con una consecuente entropía negativa que tiende a minimizarse por la agregación de las mismas en un intento de reducir la exposición de dicha interfase. La existencia de fuerzas de repulsión entre las cabezas polares hace que no se produzca una separación total de fases, sino que se las moléculas agreguen en estructuras de orden superior.

Esta agregación es un fenómeno cooperativo, donde una concentración de moléculas cercana a un punto concreto favorece la incorporación al estado agregado.

Este punto se conoce generalmente como *concentración crítica de agregación o CCA*, que en el caso de la formación de micelas recibe el nombre de *concentración micelar crítica o CMC*, valor de extremada importancia en la predicción de fenómenos de interfase en disoluciones acuosas de tensioactivos.

En este punto de agregación inicial, la geometría de las moléculas juega un papel importante para la formación final de una bicapa u otra estructura como puede ser una micela. La proporción entre ambas porciones de la molécula es un valor crítico, y su valor se mide por un parámetro denominado *balance hidrofílico-lipofílico*, conocido por su acrónimo anglosajón como HBL.

El parámetro de empaquetamiento del tecton[5,*1] o CPP (siglas en ingles de *Critical Packing Parameter*) es la expresión geométrica del valor HBL, y se define como la relación entre el volumen de la porción hidrofílica (v) y el producto entre el área interfacial (a) y la longitud de la cadena hidrofóbica (l) como muestra la ecuación 1 **(Ecuación 1)** y se muestra gráficamente en la **Figura 3.3**.**A.**

$$cpp = \frac{v}{al} \qquad \textit{Ecuación 1}$$

Determinados valores de este parámetro sirven para predecir la estructura que pueden formar las moléculas.[6] De acuerdo a este parámetro, valores próximo a 1 darán como resultado bicapas, mientras que a medida que se reduce hasta 1/3 se formarán cilindros y esferas (micelas) respectivamente (**Figura 3.3**.**B**)**.** Esto es debido a las implicaciones geométricas que conllevan estos valores, y al radio de curvatura que permiten, produciéndose por consiguiente las diversas estructuras mencionadas. Esta agregación de una forma u otra es la consecuencia final del intento de reducir la energía libre de la interfaz por unidad de volumen. Esta agregación se ve aún más forzada cuando la parte apolar es rígida (aporta comportamiento nemático, con orientaciones moleculares preferenciales) como en el caso de los lípidos, y otro tipo de interacciones moleculares secundarias (interacciones dipolares y π-π) que colaboran en la estabilidad del agregado. Debido a esto, estructuras como la bicapa son muy estables.

*1 Término general para referirse a la porción apolar de la molécula anfifílica que actúa como monómero de la estructura.

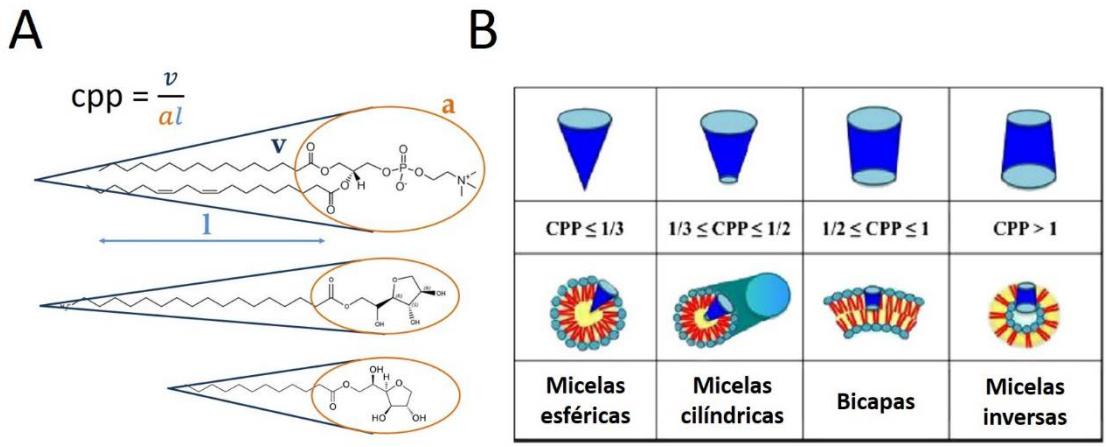

Figura 3.3. *(**A**) Representación gráfica del concepto del parámetro de empaquetamiento crítico o CPP sobre un fosfolípido (superior) y dos surfactantes no iónicos como son el Span® 60 y Span® 20 (medio e inferior respectivamente) que difieren únicamente en longitud de cadena apolar. (**B**) Implicaciones geométricas de los valores de CPP sobre la morfología del agregado de compuestos anfifílicos, figura adaptada de la referencia 6.*

La formación de una vesícula se puede dividir en dos etapas: la formación de una micela plana, y su posterior crecimiento como bicapa hasta cerrarse en forma de vesícula (**Figura 3.4**).[7] A su vez, la primera etapa se divide en una fase de nucleación (formación del agregado primigenio), y una fase de crecimiento del agregado por fusión entre agregados, pero también por la incorporación a los mismos de moléculas anfifílicas en disolución.[1] Estos procesos de nucleación y crecimiento ocurren en el orden de microsegundos y nanosegundos respectivamente. Inicialmente, este modelo fue propuesto para el método de preparación de vesículas mediante detergentes,[8] pero su corroboración experimental ha hecho que se extienda a casi todos los métodos que ocurren con una mezcla de disolventes polares y apolares.[9] Recientemente, un modelo de dispositivo microfluídico especial ha demostrado mediante crio-capturas la existencia de las bicapas discoidales.[10]

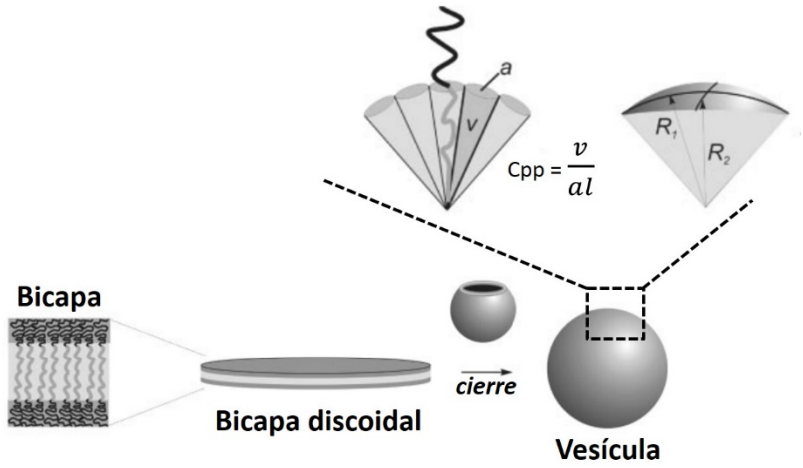

Figura 3.4. *Factores que condicionan la curvatura de la bicapa, como el parámetro de empaquetado crítico que deriva de la forma de las moléculas anfifílicas, y como éste afecta al radio de curvatura R durante la etapa de crecimiento de la bicapa discoidal. Figura compuesta y adapta de la referencia 7.*

La planicidad de la micela proviene de esa disposición preferencial de las moléculas que se ha comentado anteriormente, y es la consecuencia del proceso de un reordenamiento molecular que tiene lugar también como resultado de la interacción con el medio acuoso en el que se encuentran.[11] Brevemente, estos reordenamientos ocurren mediante interacciones cabeza-cabeza en la parte externa de la micela, cola-cola en la porción interior, y a consecuencia de ambos, la creación de canales de paso del agua (ver **Figura 3.5**).[12] Como resultado final, se forma la micela plana en forma de disco cuyo extremo es la parte activa donde se incorporan nuevas moléculas en disolución que permanecen individualizadas, y por donde se fusionan las micelas como segundo mecanismo de crecimiento.

Cuando la elasticidad de la bicapa es reducida, la tensión superficial aumenta, lo que provoca el aumento del módulo de *bending* y de la energía responsable del cierre de la bicapa para formar la vesícula. Cuando el tamaño de la micela es tal que el módulo de *bending* supera la tensión lineal, ésta se cierra espontáneamente en forma de esfera.[13]

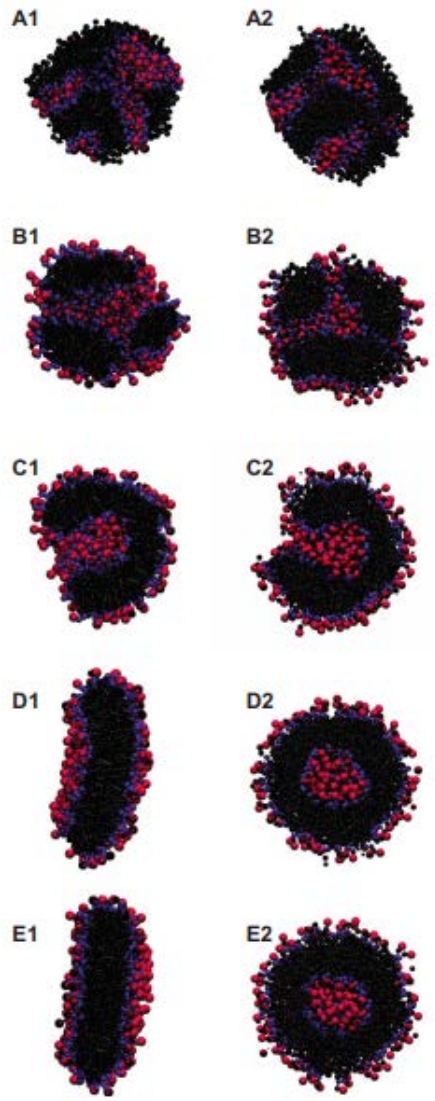

***Figura 3.5**. Simulación informática del remodelado que sufre la micela inicial de moléculas anfifílicas durante su auto-ensamblado en bicapas para formar vesículas. Estos cambios en la estructura de la micela se producen como fruto de interacciones cabeza-cabeza en la superficie y cola-cola en el interior al interactuar las moléculas con las de agua de la fase contínua. Este reordenamiento lleva a la creación de poros por los que circula el agua (B1 y B2), y este paso de disolvente acaba por reordenar la estructura hasta formar un disco plano (D1). En rojo se representan las moléculas de agua, mientras que en azul la cabeza polar y en negro la cola apolar. Figura tomada de la referencia 11.*

Un aspecto importante en esta etapa es el papel de la propia formulación de las vesículas. Como se ha visto es importante la contribución geométrica de las moléculas[14] y las interacciones entre ellas. La formulación pues, introduce cambios en la fluidez de la bicapa y la posibilidad de la existencia de asimetría en la misma, que favorece la curvatura.[15] Por ejemplo, se ha observado que longitudes de cadena reducidas (C_{12}) generan bicapas más fluidas que longitudes mayores (C_{18}) incluso en presencia de colesterol como aditivo de membrana,[16] cuya presencia suele asociarse a menor fluidez y por ende, una menor tasa de liberación pasiva de compuestos

encapsulados. Esa presencia de colesterol inhibe la transición *gel-líquido* de los compuestos de membrana,[17] y por lo tanto permite alcanzar rápidamente valores de módulos de bending que induzcan el cierre de la bicapa con prontitud, por lo que las vesículas formadas son pequeñas al reducirse la etapa de crecimiento.

El proceso de autoensamblaje requiere de energía como se comentó anteriormente, y esa energía generalmente se aporta en forma de calor. Ese calor debe ser por una parte el necesario para sobrepasar ligeramente la temperatura de transición *gel-líquido* (T_m) y así permitir el cierre de las vesículas. La temperatura provoca estados más relajados en el reordenamiento molecular (una reducción en el valor del módulo de compresión superficial C_s^{-1}),[18] y una disminución de las interacciones inter-moleculares. Así pues, el tamaño final de la vesícula dependerá de los parámetros de tasa de crecimiento de las bicapas planas y la tasa de cierre en vesículas de las mismas. Esto se integra en uno de los modelos de formación más aceptados, el denominado *modelo de la cinética en no equilibrio.*[19] En este modelo, ambos parámetros se ven influenciados por la temperatura como se ha explicado anteriormente. Cabe destacar, que las moléculas de disolvente empleado para dispersar los compuestos anfifílicos estabilizan los bordes activos de las membranas planas, por lo que contribuyen en ese crecimiento. De forma similar, las moléculas de detergentes empleadas en ciertos métodos cumplen la misma función.[20]

Por otra parte, pueden producirse subdominios como son las balsas lipídicas (reordenamientos de lípidos que se caracterizan por un mayor grado de empaquetamiento y por ende, una reducida fluidez).[2] También se han descrito la existencia de micro-dominios en estados fluidos.[21] Es comprensible pues que esto modifique las energías involucradas en el cierre de la vesícula y en la duración de la etapa de crecimiento. Así mismo, la incorporación de heterogeneidad en la formulación y la posibilidad de reordenamientos intra-moleculares de los compuestos anfifílicos con cadenas no rígidas, es la base de la existencia de vesículas estables y altamente deformables como son los transfersomas.[22]

Como conclusión de esta sección, se puede afirmar que parámetros como la concentración de componentes de bicapa, estructura y composición molecular, así como homogeneidad o heterogeneidad en la composición son parámetros de la formulación con un claro efecto en la morfología final de la vesícula. Por otra parte, aspectos como la temperatura, composición del medio acuoso o aporte de

componentes libres durante la formación de las vesículas son aspectos metodológicos que también poseen impacto sobre las características de las vesículas. Este hecho conforma la base del control del proceso e introduce la posibilidad de obtener sistemas vesiculares con características deseadas. Para ello, el estudio de procesos y el diseño de los mismos teniendo en cuenta estos aspectos son un campo de estudio que permite la ampliación del empleo de estos biomateriales en innovadoras aplicaciones.

3.1.2 Clasificación de los sistemas vesiculares

Los tipos de moléculas anfifílicas que han sido empleadas en formulaciones para la preparación de sistemas vesiculares son numerosos, y con naturaleza química muy diversa: fosfolípidos (neutros o cargados), esfingolípidos, copolímeros, ácidos grasos, surfactantes no iónicos y/o de amonio cuaternario, o incluso mezclas de dos o más de estos tipos de compuestos.

Estos compuestos representan la unidad básica de las bicapas que forman, y frecuentemente son denominados *componentes de membrana.* Adicionalmente en muchas formulaciones vesiculares es necesario la adición de un aditivo de membrana, con el fin de ofrecer mayor estabilidad y rigidez a la membrana vesicular, o para introducir modificaciones químicas que permitan nuevas características empleadas para ciertas aplicaciones.

El tipo de compuesto utilizado en la formulación de la membrana vesicular da nombre a los diversos tipos químicos de vesículas que existen, y que de manera resumida se exponen a continuación.

Liposomas

Descubiertos por Bangham y colaboradores hace 50 años,[23] inicialmente estaban compuestos por lípidos de origen natural, aunque en la actualidad muchos de ellos se encuentran formulados con lípidos sintéticos, muchos de ellos con modificaciones de la cabeza polar con la finalidad de introducir nuevas propiedades (al emplearse generalmente en pequeñas cantidades, se pueden considerar como aditivos).[24]

Sin lugar a dudas se trata del tipo de vesícula más empleado y sobre el que existe un mayor número de publicaciones tanto experimentales como de revisión. Parte de esta popularidad se debe a las ventajas que poseen, como son un alto grado de bio-compatibilidad, su capacidad de portar tanto moléculas hidrófilas como hidrófobas en

su interior o bicapa respectivamente y su carácter biodegradable.[25] Han sido formulados tanto con composiciones muy sencillas[26] como con composiciones miméticas de la composición natural de membranas biológicas,[27] y la recreación de dominios de membrana han sido descritas con éxito.[28] Fosfatidilcolina, fosfatidilserina, fosfatidiletanolamina, esfingomielina, y colesterol son algunos de los tipos de lípidos naturales más comunes en liposomas.

Sin embargo, poseen una clara desventaja como es una reducida estabilidad en suspensiones acuosas, donde los fenómenos de hidrólisis degradan los lípidos y reducen la vida útil de los liposomas. Esta característica fue la fuerza impulsora para explorar otros compuestos a la hora de preparar vesículas.

Niosomas

La primera alternativa a los lípidos surgió en el uso de los tensioactivos no iónicos (compuestos química- y estructuralmente análogos a los lípidos,) en el campo de la cosmética.[29] Los ternsioactivos no iónicos poseen unas claras ventajas como son su elevada estabilidad físico-química, elevada diversidad química, bajo coste y fácil derivatización para introducir nuevas posibilidad químicas y físicas en las bicapas.[30]

Los surfactantes no iónicos son compuestos sintéticos que pueden prepararse a partir de aminoácidos, ácidos grasos, amidas, ésteres alquílicos y éteres alquílicos de surfactantes.[6] Estos últimos pueden crearse con azúcares, óxidos de etileno o repeticiones de moléculas de glicerol. Sin embargo, no todos los surfactantes son idóneos para la formación de vesículas. Los surfactantes más comúnmente utilizados para la formulación de niosomas son los comercializados con el nombre de Span®, Tween® y Brij®, ésteres de sorbitan y ácidos grasos, de poli-oxietilen sorbitan y ácidos grasos, y éteres de cadenas alquiladas y repeticiones de poli-oxietilen respectivmente (**Figura 3.6**).

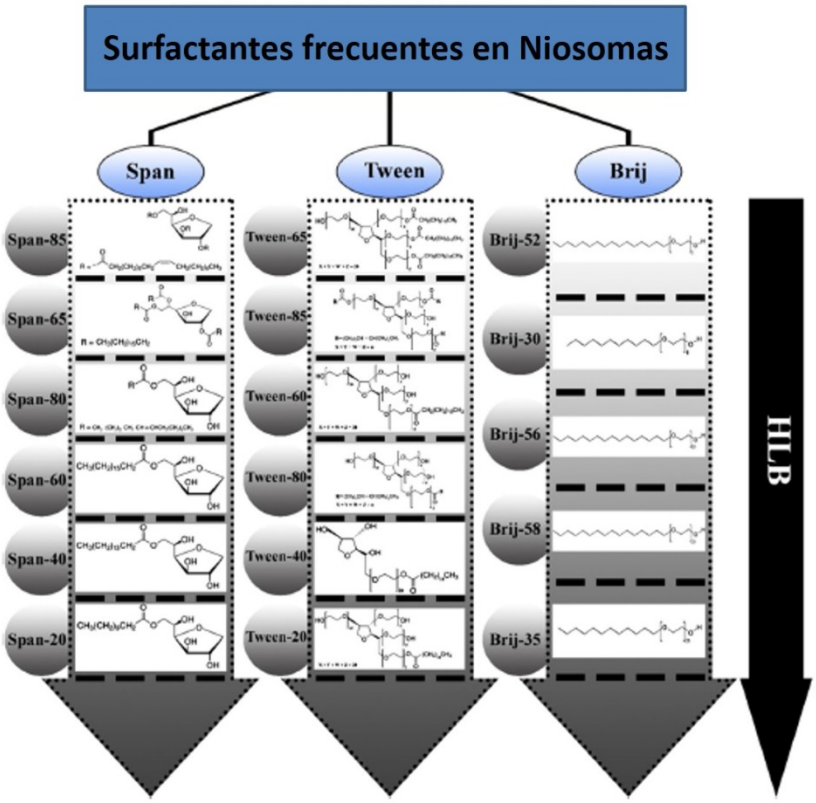

Figura 3.6. *Surfactantes no iónicos más frecuentes en formulaciones de niosomas. Se representan de arriba abajo en función del valor creciente de HBL, que surge de la diferente longitud de cadena apolar que poseen los miembros de una misma familia de surfactante. Figura tomada de la referencia 114.*

Un parámetro que sirve como predictor de su idoneidad para la formulación de niosomas es el HLB (acrónimo anglosajón de Balance Hidrofílico-Lipofílico) y que representa una estimación de las proporciones de ambas porciones químicas en el anfífilo. La **Tabla 3.1** resume los principales usos de los tensioactivos según su HLB. Como puede comprobarse, valores entre 4-8 son los adecuados para la formulación de niosomas, siendo necesario incorporar en las formulaciones aditivos de membrana para valores cercanos a 10. Esta adición compensa el exceso de peso que posee la porción hidrofílica de la molécula, e interacciones con el colesterol y entre moléculas del mismo permiten establecer bicapas estables.[31]

Estas formulaciones pueden manejarse como las de los liposomas, por lo que los mismos tipos morfológicos de vesículas pueden obtenerse, ya que los métodos de preparación empleados son los mismos en ambos tipos de vesículas.

Tabla 3.1. *Usos de los surfactantes no iónico en función de su valor HLB.*

Valor de HLB	Aplicación general
1-3	Antiespumantes
3-6	Emulsiones agua en aceite
7-9	Agentes humectantes y dispersantes
8-18	Emulsiones aceite en agua
13-15	Detergencia
15-18	Solubilización

Transfersomas

Los dos tipos de formulaciones anteriores se caracterizan por la rigidez de la bicapa que se produce por el empaquetamiento de las moléculas gracias a las fuertes interacciones inter-moleculares. Esta rigidez puede llegar a ser una desventaja en ciertas vía de administración como puede ser la vía tópica, ya que provoca la incapacidad para llegar a capas profundas de la piel y pasar al torrente sanguíneo.[32]

Para evitar este inconveniente, se propusieron formulaciones que contenían a la vez ambos tipos de componentes de membrana: lípidos y surfactantes, denominados *Transfersomas* por su principal uso transdérmico.[33] En este caso, el surfactante no iónico adquiere un papel muy importante, ya que es el encargado de producir la elasticidad de la bicapa. Para ello, se suelen emplear compuestos como Tween® 80 y Span® 80, con altos valores de HLB (≥15), que rompen la cohesión molecular de los lípidos, permitiendo un mayor radio de curvatura y elasticidad de membrana.[34] Otro compuesto que actúa de forma similar y es frecuentemente empleado es el colato de sodio.

Esfingosomas

Otro tipo de vesículas con base lipídica son los *esfingosomas*, nombre recibido en alusión al tipo de lípido empleado en su formulación: los esfingolípidos.[35] El empleo de estos lípidos tiene su origen en la búsqueda de una mayor estabilidad por ausencia de fenómenos de oxidación en fase acuosa.[36] Como estabilizante de membrana para la formación de una bicapa estable y con buenos valores de eficacia de encapsulación se suele emplear colesterol.[37]

Ufasomas

Otro tipo de vesículas con base mixta lipídica y de surfactantes son los *ufasomas,*[38] vesículas formuladas a base de ácidos grasos insaturados (oleico y linoleico) e insaturados (octanoico y decanoico). De nuevo, su composición y propiedades de membrana los hacen buenos candidatos para la preparación de vehículos de administración de biocompuestos por vía tópica.[39]

Etosomas

Este tipo de vesículas recuerda a los transfersomas, ya que poseen de nuevo una base lipídica y otro componente encargado de modular la elasticidad mediante relajación molecular de la bicapa. En este caso, esa función es llevada a cabo por moléculas de alcoholes como el etanol e isopropanol en elevadas proporciones.[40] De forma análoga a los casos anteriores, son de gran utilidad en la administración tópica.[41]

Quatsomas

Existe otra familia de surfactantes no iónicos capaces de formar vesículas únicamente en presencia de esteroles, y son los surfactantes de amonio cuaternario (que dan nombre al tipo vesicular).[42] Estos compuestos son de reducido coste, y fácilmente disponibles en calidad farmacéutica, además presentan una característica adicional como es un carácter antimicrobiano.[43]

Polimersomas

Por último, se han empleado copolimeros en la formulación de vesículas denominadas polimersomas.[44] Estos copolimeros tienen un peso molecular alto, y existen diversos tipos que facilitan la versatilidad química de este tipo de vesículas.[45] Idealmente, los polímeros deben estar formados por bloques hidrofóbicos con temperaturas de transición cristalina bajas. Un ejemplo son los polímeros peptídicos sintetizados por la polimerización anionica de N-carboxianhidros.[46] Estas vesículas han sido funcionalizadas por la incorporación de proteínas funcionales en su estructura de bicapa,[47] y representan un tipo vesicular con elevado potencial tanto en estudios de biología básica como aplicada.

3.1.2.1. El papel de los aditivos en las formulaciones

Mejora de la estabilidad coloidal

Existen dos mecanismos básicos que permiten a un coloide mantenerse en suspensión de forma individual:[48] que existan impedimentos estéricos (físicos) que impidan aproximarse y coalescer dos partículas adyacentes, o que dicho impedimento se deba a la repulsión por poseer ambas una carga del mismo signo, es decir, una repulsión electroestática.

Uno de las moléculas más empleadas para fines estéricos es el polímero hidrofílico poli(etilenglicol) o PEG.[49] Su incorporación post-preparación o la incorporación en forma de lípido modificado aumenta considerablemente la vida de la vesícula, ya que no solo aporta el citado impedimento estérico, si no que les hace "invisibles" al sistema monocitico-nuclear.[50]

Compuestos con carga negativa como dicetilfosfato y ácido fosfatídico, o con carga positiva como estearilamina y cloruro de cetilpiridinio, son empleados frecuentemente[6] para aportar carga superficial neutra diferente de cero (parámetro medido por el potencial ζ). Esta carga, ayuda a mantener la estabilidad coloidal mediante repulsiones electrostáticas, siendo ±30 mV un valor de ζ lo suficiente grande como para asegurar dicha estabilidad.[51]

Propiedades nuevas, tales como fluorescencia

En la actualidad, existen numerosos lípidos sintéticos comerciales conjugados a fluoróforos orgánicos como la rodamina o NBD.[52] La existencia tanto de fosfolípidos como de esteroles, como el colesterol, modificados con este tipo de marcadores permite la preparación de casi cualquier tipo de vesícula capaz de ser monitorizada mediante fluorescencia molecular. Por otro lado, existen otro tipo de fluoróforos capaces de incorporarse a bicapas, por lo que pueden ser añadidos *a posteriori*, y marcar las vesículas para fines tanto analíticos como biomédicos. Un ejemplo de este tipo de marcadores es la carbocianina lipofílica $DilC_{18.}$

Mejora de la penetrabilidad dérmica

La mejora de la penetrabilidad dérmica de las vesículas ha sido explorada también con la incorporación en las formulaciones de aditivos como el ácido oleico y linoleico.[53]

A pesar de existir vesículas formuladas con ellos como son los ufasomas, en este caso la proporción en la que se añaden hace que sean clasificados como aditivos.

Incorporación de puntos de unión a otras biomoléculas

Los lípidos y los esteroles son fácilmente modificables de forma química para introducir nuevos grupos funcionales que permitan ser empleados en reacciones de bioconjugación de moléculas o a superficies.[54] Son numerosos los ejemplos de su uso para tal fin con liposomas y niosomas.[55-57] Estos compuestos presentan un elevado coste, aunque pueden ser preparados en el laboratorio,[30] pero su empleo en relaciones molares pequeñas respecto a los componentes mayoritarios permite su empleo con facilidad y de una forma económicamente viable.

3.1.2.2 Principales aplicaciones de los tipos de sistemas vesiculares

Como se ha citado en la introducción, los sistemas vesiculares poseen un amplio espectro de aplicaciones. A modo de ejemplo de esta versatilidad, la **Tabla 3.2** resume dichas aplicaciones por tipo de sector tecnológico y tipo de sistema vesicular empleado.

Tabla 3.2. *Ejemplos de aplicaciones biotecnológicas de los diversos tipos de sistemas vesiculares según sector industrial y tipo de NVs.*

Sector Industrial	Tipo de nanovesícula	Aplicación	Ref.
Farmaceútico	*Liposomas*	Solubilización de compuetos hidrofóbicos, sensibles a la luz y al pH, y su posterior distribución y liberación controlada por diferentes vías de administración (oral, nasal, ocular, tópica y parenteral)	58, 33
	Niosomas		40, 45
	Transfersomas		59
	Etosomas		
	Polimersomas	Incoporación de nanopartículas metálicas para el desarrollo de agentes de contraste en diagnóstico por imagen	60
	Esfingosomas		
	Ufasomas	Modificación de vesículas extracelulares teranósticas	61, 62
	Quatsomas		
Cosmético	*Liposomas*	Encapsulación de compuestos con reducida biodisponibilidad y sensibilidad ambiental	63,64
	Niosomas		
Alimentario	*Liposomas*	Encapsulación de compuestos con reducida biodisponibilidad y sensibilidad ambiental	65,127
	Niosomas		
Ambiental	*Liposomas*	Bio-remediación de vertidos de combustibles fósiles	66
Textil	*Liposomas*	Fabricación y tinción del tejido	67
Químicio (Bioanalítico)	*Liposomas*	Amplificación de señal en immunoensayos y biosensores	68, 69 70, 71
		Reconocimiento específico de biomoleculas	72
		Fase estacionaria en Cromatografía Electrocinética Capilar	73
		Nanocristalizadores para estudios de Difracción de Rx (DRX)	74
		Soporte de macromoléculas de membrana para estudios por DRX	75
	Niosomas	Síntesis de nanopartículas metálicas	76, 77
		Desarrollo de estándares analíticos	122

3.1.3. Tipos morfológicos de vesículas

Como se comentaba al principio de esta sección, existen diversos tipos morfológicos de vesículas en cuanto a tamaño, grado de lamelaridad, y número de cavidades acuosas internas (partículas multivesícula). Existe una dependencia del tipo de vesícula con el método de preparación, que deriva de los procesos de formación de vesícula que ocurren durante su preparación. En la **Figura 3.7** se representa la diversidad de tipos morfológicos vesiculares y su relación con el método de formación.

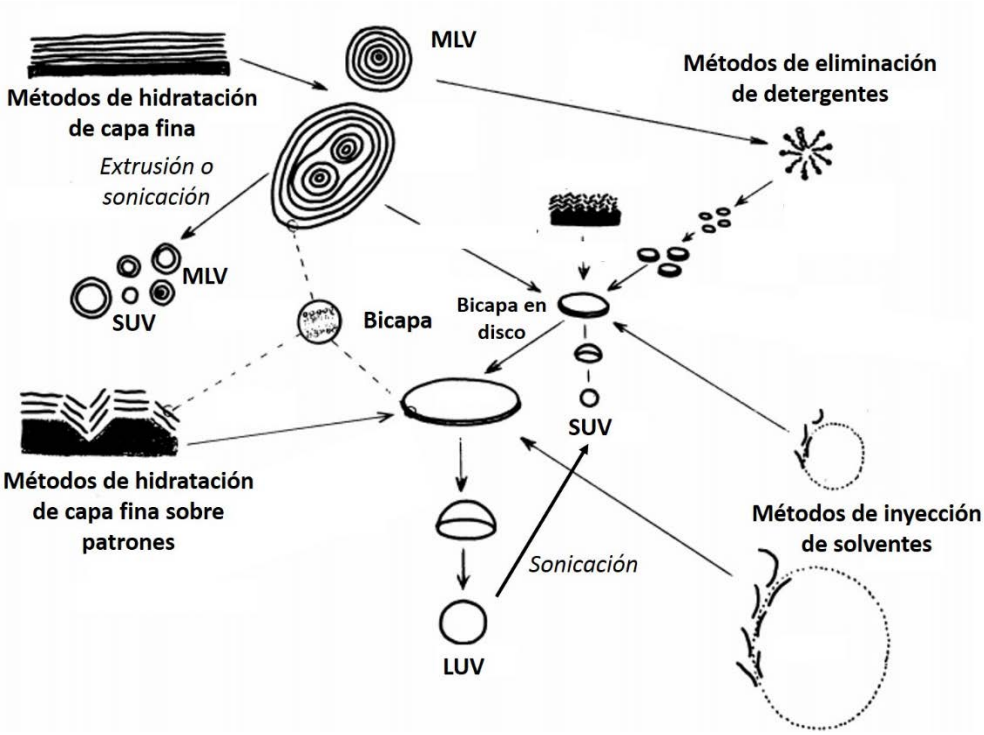

Figura 3.7. *Diversidad morfológica de las vesículas, y su relación con los métodos de preparación. Figura adaptada de la referencia 9.*

Por un lado tenemos vesículas unilamelares (una única bicapa separa el medio acuoso de la cavidad interior), que se dividen de acuerdo en el tamaño en pequeñas (conocidas como SUVs, *Small Unilamelar Vesicles*), o grandes (conocidad como LUVs, Large Unilamer Vesicles). Estos tipos se relacionan con métodos de cambio de polaridad del medio, como la inyección de disolventes, y con métodos que implican hidratación de películas finas mediante descargas eléctricas o flujos de fase acuosa en microcanales respectivamente. Estos métodos se comentan en la sección 3.2.

Por otro lado, existen vesículas con más de una bicapa, y éstas se encuentran de forma concéntrica como si fuesen las capas de una cebolla (vesículas multamelares o

MLV). Generalmente presentan un tamaño grande, aproximadamente entorno a media micra, y este tipo morfológico se asocia al método de hidratación de capa fina, donde la película se hidrata de forma progresiva liberando bicapas que geman de la película hasta cerrarse en vesículas.

En ocasiones, y dependiendo de las condiciones de la hidratación se ha visto la generación de multivesículas (vesículas con más de una cavidad acuosa en su interior, o vesículas que contiene a su vez vesículas en su interior). Este tipo morfológico se ha observado también en métodos de hidratación directa o en tecnología de Proniosomas.

Por otro lado, existen metodologías para reducir el tamaño o cambiar el tipo morfológico, como son la extrusión[78] y la sonicación.[79] En el primero, el paso por una membrana de tamaño de poro reducido hace que las vesículas se rompan en fragmentos que se cierran en nuevas vesículas con un tamaño similar al del poro. En el segundo, la aplicación de ultrasonidos en las suspensiones crea fenómenos de cavitación con igual resultado que la extrusión. En este caso, el tamaño final va en función de la amplitud de la frecuencia de los ultrasonidos.

3.2. Métodos de preparación de vesículas

Desde el descubrimiento de los liposomas hace 50 años, se han descrito numerosos métodos de preparación de vesículas aplicables a casi todas las formulaciones comentadas en la sección 3.1.2., y éstos han sido revisados en la literatura,[80] encontrándose incluso revisiones monográficas sobre tipos particulares de métodos.[81]

Es importante remarcar que no existe un método mejor que otro, o particularmente idóneo para un tipo específico de formulaciones, pero ciertos aspectos han de tenerse en cuenta a la hora de seleccionarlo. Posiblemente lo más importante a la hora de la selección del método de preparación sea la aplicación final para la que se desean preparar las vesículas. Como se ha comentado en la sección 3.1.3. existen diversos tipos morfológicos de vesículas que se encuentran íntimamente ligados a los métodos de preparación y a los principios que rigen el autoensablaje. Estos métodos influencian de manera importante las características finales de las partículas,[82] como son el tamaño, el grado de lamelaridad, y la eficacia de encapsulación, todas ellas características a controlar en el desarrollo de una aplicación biotecnológica.

A continuación se hace una breve descripción de los métodos de preparación encontrados en la literatura. Se han agrupado en base al principio general en el que se sustentan.

3.2.1. Métodos que implican cambio de polaridad en el medio

Los métodos que se describen a continuación tienen en común el empleo de un disolvente orgánico en el que se disuelven los componentes de la bicapa y los aditivos. Posteriormente esta fase es dispersada en una fase acuosa cuya proporción en la mezcla final es muy superior, lo que provoca el cambio de polaridad del medio en el que se encuentran las moléculas anfifílicas.

Inyección de etanol

En este método, los componentes de membrana son disueltos en etanol, y esta disolución es dispersada en el seno de una disolución acuosa con agitación constante, mediante un sistema continuo de bombeo (generalmente una bomba de jeringa).[83] La fase acuosa se mantiene a una temperatura superior a la de transición T_c del sistema (formulación), y tras finalizar la fase de dispersión el disolvente es eliminado mediante evaporación a vacío. Como ventajas posee la baja toxicidad del etanol, la sencillez de los dispositivos involucrados y la facilidad de escalado a nivel industrial. Dependiendo de la polaridad del compuesto a encapsular, éste se incorpora en la fase orgánica o acuosa si es apolar o polar respectivamente. Método frecuentemente empleado para la preparación de SUVs.

Inyección de éter

Conceptualmente es idéntico al anterior, pero se emplea como disolvente dietil éter, que no es miscible con la fase acuosa, y la temperatura de la fase acuosa se ajusta para estar por encima del punto de ebullición del disolvente. Debido a esto, no es recomendable para la encapsulación de compuestos termolábiles, y generalmente requiere de etapas adicionales para la reducción del tamaño promedio de partículas, ya que por lo general produce LUVs.[84]

Evaporación de fase reversa

Similar al anterior, los componentes de membrana se disuelven en un disolvente no miscible en agua, pero previo a la evaporación del mismo, la mezcla se somete a agitación mecánica para formar una emulsión, donde las gotas harán de molde para la

formación de las vesículas en la etapa de eliminación del disolvente.[85] Únicamente se emplea en la encapsulación de compuestos apolares, ya que la encapsulación pasiva de compuestos hidrófilos no es compatible.

Existe una variedad, donde se evapora el primer disolvente tras la disolución de los compuestos de membrana, y se forma una capa fina que se re-disuelve en un segundo disolvente que se mezcla con la fase acuosa, y se procede como en la versión anterior.[86] En ambos casos, se forman LUVs y MLVs, por lo que se requieren etapas de post-procesado para reducir el tamaño o cambiar el tipo de vesícula.

Eliminación de detergentes

En este método los componentes de membrana se disuelven en una solución micelar de detergentes, que posteriormente se somete a un proceso de eliminación de los mimos (por ejemplo por diálisis), lo que fuerza la formación de las vesículas.[87]

Hidratación de capa fina

Este método es el más antiguo, con el que se descubrieron los liposomas. Se parte de una disolución orgánica que contiene los componentes de membrana y que mediante rotavapor es desecada para forma una película final en las paredes del matraz. Esta capa fina es hidratada por la fase acuosa a temperatura adecuada a la Tc del sistema, y una fuerza mecánica en forma de agitación o ultrasonidos asiste en la homogenización e hidratación. Debido a este proceso, MLVs es el producto mayoritario, por lo que se requieren de etapas siguientes para obtener SUVs. Es adecuada a todo tipo de compuestos, polares y apolares, e incluso para la encapsulación de NPMs.[12]

3.2.2. Métodos directos

Sonicación directa

La disolución de los componentes de membrana se realiza directamente en fase acuosa, que es sonicada directamente a temperatura elevada, hasta la homogenización y formación de vesículas.[88]

Método de calentado de disoluciones

En este método, los componentes se disuelven en fase acuosa directamente en presencia o ausencia de poliol (3%v/v), sometida posteriormente a altas temperatura y

a agitación contínua a medida que se reduce la temperatura.[89] En ocasiones, los diferentes componentes de membrana son disueltos por separado y puesto en común en la etapa de agitación.[90]

Método del burbujeo

Se trata de otro método directo en el que los componentes en disolución acuosa se someten a calentamiento directo en presencia de un flujo burbujeante de N_2, que da lugar a una suspensión de LUVs.[91]

Microfluidización

Flujos acuosos conteniéndolos compuestos de membrana son propulsados a alta velocidad y presión por canales de reducidas dimensionas hacia una cámara donde interacciones entre ellos en un espacio confinado, produciéndose la mezcla y formación de las vesículas,[92] que poseen un tamaño uniforme, unilamelaridad y reducido tamaño.

Proniosomas

Este método implica el recubrimiento de partículas solubles (tipo cristales de azúcares) por los surfactantes no iónicos, por lo que es exclusivo de niosomas.[93] Los complejos formados en estado seco son posteriormente hidratados en el momento de la encapsulación y de uso, por lo que este método permite tener lotes pre-preparados que pueden almacenarse y transportarse con facilidad.

3.2.3. Métodos de nueva generación

Esta categoría de métodos engloba técnicas no convencionales desarrolladas fundamentalmente en los últimos 15 años, y que se clasifican en dos grandes bloques:

3.2.3.1. Métodos basados en fluidos supercríticos

Este conjunto de métodos se basa en el empleo de fluidos supercríticos[2*] para la formación de vesículas[94] en un proceso que se caracteriza por: (i) reducción del estrés mecánico y de la temperatura a la que se someten las vesículas, por lo que mejora la posible degradación de lípidos y compuestos termolábiles, (ii) una reducción en el

[2*] Compuestos que se encuentran a una presión y temperatura superiores a su punto crítico, lo que provoca un comportamiento híbrido entre líquido y gas, por lo que puede difundir como un gas y disolver sustancias como un líquido.

consumo de disolventes orgánicos y de la toxicidad residual de su uso, (iii) facilidad del proceso que se lleva a cabo en una única etapa, y (iv) esterilidad de la producción inherente al empleo de fluidos supercríticos).[95]

El fluido más empleado es CO_2, por ser inerte, no tóxico, barato y no inflamable. Este gas se mezcla con el disolvente que contiene los componentes de membrana a una alta temperatura y presión. Esta mezcla se inyecta sobre la fase acuosa, y en ese contacto se forman las vesículas mientras se evapora el disolvente al burbujear el gas. Existen números ejemplos del empleo de estas técnicas para producir niosomas[96] y liposomas.[97]

3.2.3.2. Métodos basados en microcanales (microfluídica)

Las ventajas que aportan los microcanales en dispositivos de microfluídica han hecho que este conjunto de técnicas haya ganado mucha importancia en la preparación de vesículas para bio-aplicaciones.98 De forma resumida, estas características son: (i) manipulación precisa de los flujos, lo que permite un control elevado sobre los procesos de mezcla de reactivos, (ii) Mezclado rápido y homogéneo, (iii) temperatura homogénea y de rápido intercambio frio/calor, (iv) reducción del consumo de reactivos, (v) producción de pequeños lotes para procesos de optimización, (vi) rapidez en la obtención de partículas, (vii) capacidad de observar la formación *in situ* de las partículas, (viii) oportunidad de integrar *on line* etapas de post-procesado y/o caracterización, (ix) fácil escalado mediante combinación en paralelo de varis dispositivos.

Existe gran diversidad de técnicas microfluidicas[99,100] ampliamente descritas en excelentes revisiones bibliográficas. A continuación se hace un breve resumen de los mismos, en función del mecanismo de acción del dispositivo microfluídico.

Electroformación

Aunque descrita a nivel macroscópico inicialmente,[101] la electroformación en microcanales fue descrita por Kuribayashi *et al.* en 2006,[102] y consiste en la aplicación de corriente alterna en el interior de microcanales con fase acuosa sobre los que previamente se ha depositado una capa fina de lípidos por evaporación de una solución orgánica con los mismos. Se podría asemejar al método de hidratación de capa fina, pero en este caso la fuerza eléctrica sustituye a la agitación mecánica o

ultrasonidos. Este método suele generar vesícular unilamelares gigantes (más de una micra).

Mejoras de este método han ido encaminadas al uso de micro-patrones sobre los electrodos, para conseguir un mayor control de la hidratación de la capa fina depositada sobre ellos, y así, controlar el tamaño de partícula generada.[103]

Hidratación directa de capas lipídicas

Similar al anterior, en este método es el flujo de la fase acuosa a través del canal la fuerza que desprende las bicapas de la capa fina previamente depositada,[104] por lo que se consiguen vesículas MLVs y altamente polidispersas.

Micro-extrusión

En esta técnica, se deposita una capa fina sobre una membrana de nitruro de silicio con un tamaño de poro nanométrico (≤ 300 nm), y es impulsada por un flujo de fase acuosa para atravesando la membrana, fragmentarse y general pequeñas vesículas de tamaño controlado y monodisperso.[105]

Enfoque hidrodinámico de fluidos

Aunque recuerda a la inyección de disolvente, esta técnica no es comparable con el método convencional. En este caso, un flujo de disolvente orgánico que contiene los precursores de membrana es enfocado por dos flujos adyacentes de fase acuosa.[106] Este enfoque provoca la reducción del diámetro del flujo orgánico, y gracias a ello, el completo mezclado de ambas corrientes se produce por difusión molecular únicamente, al encontrarse en un régimen de flujo laminar debido a los bajos valores de Reynolds que se obtienen al trabajar en la microescala.

De esta forma, controlando los flujos y su relación,[107] se puede controlar la extensión y eficacia del mezclado por su efecto sobre el tiempoo necesario para alcanzar la total mezcla al igual que se puede llevar a cabo el proceso en canales de longitud variable, con o sin elementos que favorezca la total mezcla adicional.[108] El enfoque puede llevarse a cabo bidimensional o tridimensionalmente.[109]

Propulsión de gotas o burbujas

Esta sofisticada técnica recuerda a soplar por el aro de formación de pompas de jabón como sus autores describen.[110] Una bicapa se establece entre dos compartimentos

acuosos, y el empleo de micro pulsos de aire o fluido sobre la misma efectúa su deformación hasta formar una vesícula que emerge de la bicapa cuando ésta se deforma en exceso y se fragmenta.

Empleo de emulsiones dobles W/O/W como micropatrones

En este caso, micro-elmulsiones dobles son creadas en microcanales[111] o mediante emulsificación con membranas,[112] para su posterior empleo como patrones en la creación de vesículas a partir de componentes de membrana disueltos en la fase orgánica (generalmente un disolvente no miscible en agua). La eliminación de dicho disolvente por evaporación fuerza la creación de bicapas en la interfaz O/W, que se acaban convirtiendo en vesículas.

3.3. Procesos asociados al uno biotecnológicoy bioanalítico de los sistemas vesiculares

Como se ha comentado en la introducción, la versatilidad que ofrecen estos sistemas vesiculares deriva de su capacidad para encapsular moléculas tanto hidrofílifcas como hidrofóbicas, y de la posibilidad de crear estructuras complejas con otras biomoléculas, y así sumar propiedades hasta crear auténticos biomateriales multi-funcionales (**Figura 3.8**). En este apartado se explican brevemente los procesos de asociación a otras moléculas (encapsulación y bioconjugación) y el conjunto de procesos que implican la separación de los elementos que no han interactuado con las vesículas de las nuevas estructuras generadas (purificación).

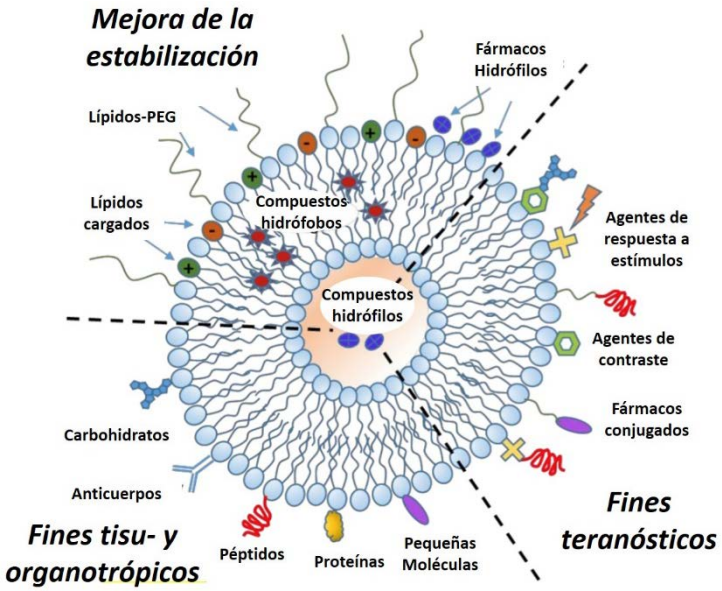

Figura 3.8. *Diferentes estrategias de mejora de las propiedades básicas de las vesículas artificiales, basadas en la incorporación de biomoléculas bioactivas, para el desarrollo de biomateriales multifuncionales. Figura adaptada de la referencia 14.*

3.3.1. Encapsulación

La encapsulación se define como la incorporación de moléculas al interior acuoso de la vesícula o a la bicapa, en función de la polaridad de las mismas. Este proceso puede ser pasivo o activo, en función del momento en el que se incorporan las moléculas a la vesícula.[113] En el primer caso, pasivo, éstas se incorporan durante la formación de las vesículas añadiéndose dichas moléculas, o bien junto a los componentes de membrana en la fase orgánica, o bien disueltas en la fase acuosa. Este es el mecanismo que se ha empleado en la presente Tesis Doctoral.

En el segundo de los casos el proceso es activo puesto que se realiza una vez se han creado las vesículas, por lo que es necesario mecanismos físico-químicos que incorporen las moléculas a dichas estructuras. Estos mecanismos se basan en la creación de gradientes transmembrana, bien sean de pH o iónicos.[114]

La eficacia de encapsulación depende en gran medida de la naturaleza química de la especie a encapsular. Compuestos hidrofílicos suelen ofrecer eficacias de encapsulación inferiores, especialmente por encapsulación pasiva. Este hecho suele ir asociado a una elevada tasa de fuga por permeación através de las bicapas, a pesar de la existencia de aditivos como el colesterol, cuya presencia suele reducir este fenómeno.[31]

Por otro lado, la composición de la bicapa condiciona la incorporación de moléculas en la misma, y el peso molecular del compuesto a encapsular suele ser un parámetro crucial.[115] Recordemos que las interacciones moleculares en la bicapa es parte de la estabilidad de la misma, por lo que la llegada de nueva moléculas puede desestabilizar el sistema. Por último, el método de preparación de vesículas puede jugar un papel importante,[116] especialmente para la encapsulación pasiva ya que como se ha mencionado, los mecanismos de formación de las vesículas son complejos y altamente influenciables por variables metodológicas.

3.3.2. Bioconjugación

La bioconjugación es un proceso químico por el que se unen dos elementos, donde al menos uno de ellos es una biomolécula.[117] Esta unión puede ser de diversa naturaleza: de afinidad molecular, de coordinación o mediante enlace covalente. Como se comentaba en la sección de aditivos de membrana, existen numerosos lípidos y surfactantes modificados con diversos grupos funcionales que permiten establecer los citados tipos de unión (**Figura 3.9**). A modo de ejemplo de esta diversidad, la figura 10 muestra el elevado número de grupos funcionales que se pueden emplear con vesículas.

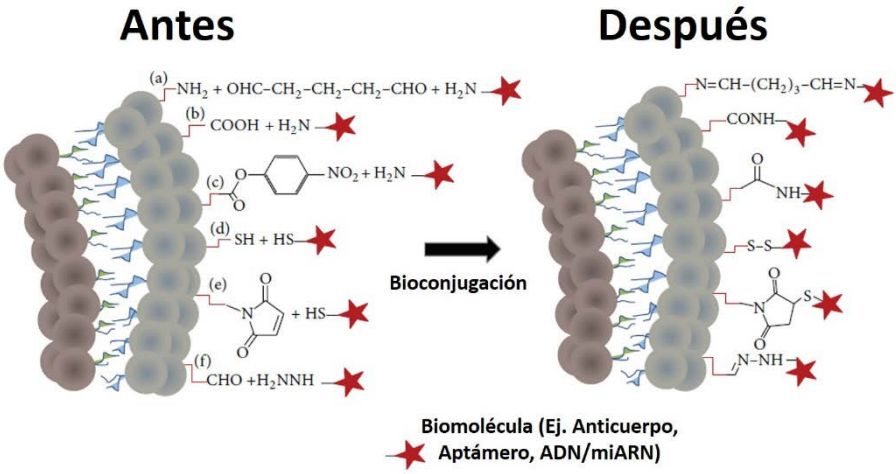

Figura 3.9. *Esquema ilustrativo de los grupos funcionales involurados en las principales estrategias de conjugación basadas en el establecimiento de un enlace químico entre la superficie de una vesícula y una biomolécula. (a) Entrecruzamiento de aminas primarias mediante glutaraldehido, (b) enlace amida entre un carboxilo y una amina primaria, (c) enlace amida mediante reacción de para-nitrofenilcarbonil con una amina primaria, (d) puente disulfuro, (e) enlace tioester mediante reacción con maleimidetiol, y (f) enlace hidrazona. Figura adaptada de la referencia 118.*

Las diversas estrategias de bioconjugación de vesículas han sido revisadas[118]. Debido a esto, únicamente se comentarán aquellas estrategias que han sido empleadas en la presente Tesis Doctoral.

Bioconjugación por afinidad: interacción Biotina-Estreptavidina

Esta estrategia emplea la elevada afinidad que existe entre la biotina y la estreptavidina/avidina/neutravidina, la mayor constante de afinidad descrita en la naturaleza[119]. Este método es muy popular, ya que existen formas recombinantes de estas proteínas con un precio muy reducido, y por otro lado se pueden encontrar kits comerciales de biotinilización que permite marcar con esta molécula casi cualquier otra biomolécula.[120] Para ello, estos kits emplean muchas de las reacciones que se muestran el **Figura 3.9**.

En la bibliografía se pueden encontrar ejemplos de bioconjugación de moléculas de estreptavidina sobre la superficie de vesículas, y su posterior conjugación con elementos biotinilados, como por ejemplo anticuerpos[121] o proteínas recombinantes.[122] La elevada constante de afinidad hace este proceso pasivo (únicamente hay que poner ambos elementos en común disolución, **Figura 3.10**.**A**) rápido, eficaz y muy sencillo.

Bioconjugación por enlace covalente tipo amida mediante el método de la Carbodiimida

Este método se basa en el establecimiento de un enlace covalente de tipo amida entre una amina primaria y un grupo carboxilo activado.[123] Esta activación está llevada a cabo por molécula que reacciona con este grupo a pH ácido, como son las *carbodiimidas* (EDC). Esta activación es estabilizada por moléculas de N-hidroxisuccinimida (NHS), que sustituye a la *carbodiimida* de forma estable, ya que ésta tiende a hidrolizarse del –COOH en medio acuoso. Posteriormente, el éster al entrar en contacto con la amina primaria forma un enlace de tipo amida, cuya eficacia de establecimiento es mejor a pH neutro. El proceso se recoge en la **Figura 3.10.B**.

Puesto que muchas macromoléculas poseen ambos grupos funcionales, este proceso se lleva a cabo por etapas, eliminando el exceso de EDC/NHS mediante alguna de las técnicas que se comentan en el siguiente apartado. Esto a su vez favorece que se pueda ajustar el pH de cada etapa para maximizar la conjugación. Esta estrategia se ha empleado tanto en liposomas[124] como en niosomas.[125] Para evitar

reacciones cruzas e interacciones inespecíficas, los ésteres que quedan libres pueden ser bloqueados con una amina primaria como puede ser la hidroxilamina o la glicina.[126]

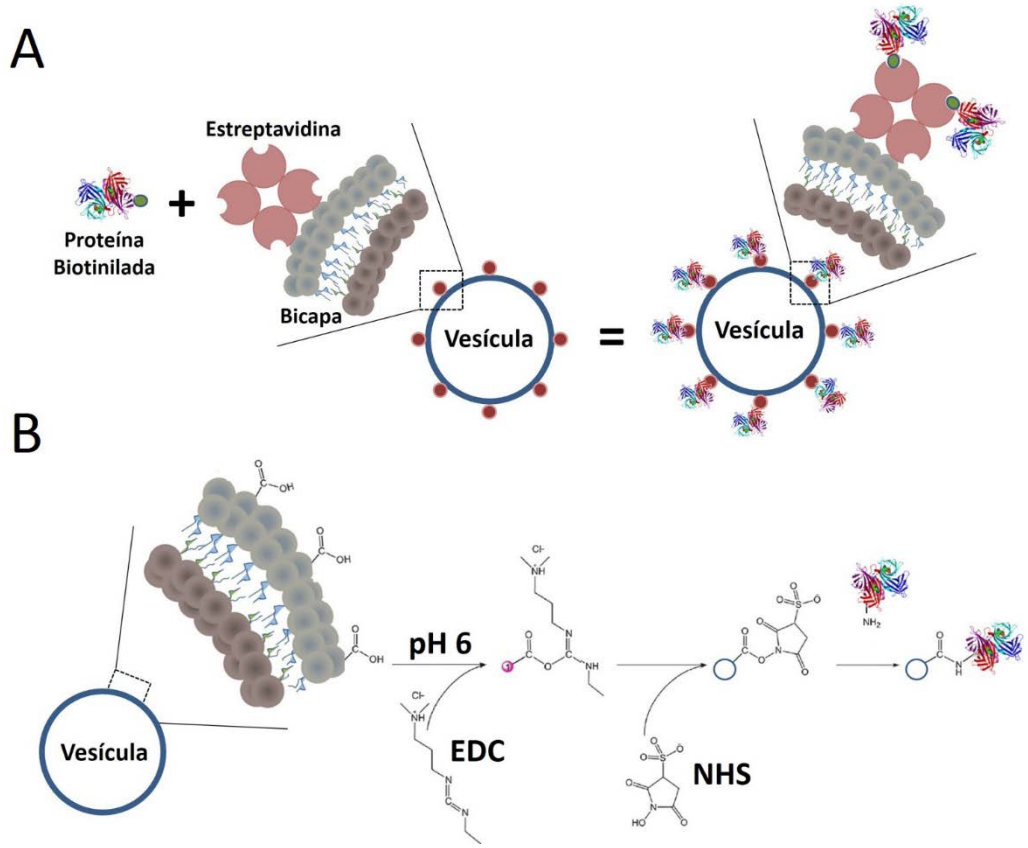

Figura 3.10. *(**A**) Estrategia de bioconjugación basada en la interacción Estreptavidina-Biotina, donde la Estreptavidina se conjuga previamente sobre la superficie de la bicapa mediante alguno de los métodos mostrados en la figura 10, y el otro elemento se encuentra biotinilado. (**B**) Conjugación de biomoléculas mediante el método de la carbodiimida empleando EDC/NHS como reactivos de conjugación. Este método puede ser empleado para la conjugación de Estreptavidina como se indica en el caso A.*

3.3.3. Purificación

<u>Diálisis</u>

Se trata de uno de los métodos más empleados en la literatura[127-129]. Este proceso está basado en los flujos osmóticos que se establecen a favor de gradiente de concentración. La suspensión de nanovesículas se contiene en un saco o dispositivo comercial separado del medio por una membrana, cuyo tamaño de poro deja pasar únicamente las moléculas de compuesto no encapsulado o conjugado (ver **Figura 3.11.A**). Como inconvenientes de esta técnica destacan: el tiempo requerido para completar la purificación y la necesidad de optimizarse para cada compuesto de forma

individual y la dilución de la muestra por entrada de medio de purificación hacia el interior del cartucho o bolsa. Como ventajas destacan la capacidad de purificar grandes lotes y la sencillez de la técnica.

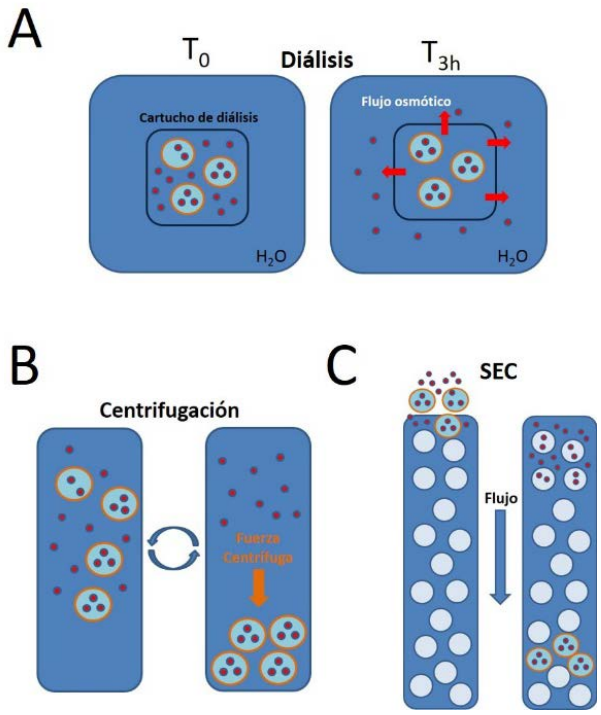

Figura 3.11. *Estrategias de purificación de vesículas para la eliminación del material no encapsulado o conjugado. (**A**) Diálisis, (**B**) (Ultra)centrifugación, y (**C**) Cromatografía de Exclusión de Tamaño (SEC) por filtración en gel.*

<u>Centrifugación/Ultracentrifugación</u>

Se trata de otro método muy frecuente,[130,131] y no solo para sistemas vesiculares. Este método emplea la mayor densidad de las vesículas, debido a su tamaño, respecto a los otros elementos en disolución, ya que al someter a una suspensión de vesículas a la fuerza centrífuga, éstas se irán al fondo del tubo pudiendo decantarse con facilidad el sobrenadante (ver **Figura 3.11.B**). Este método permite a su vez una concentración de la suspensión, ya que el pellet puede reconstituirse en un volumen menor. En función de la fuerza aplicada en el proceso, se habla de centrifugación o ultracentrifugación. A menudo este proceso se lleva a cabo a baja temperatura, para compensar el exceso de temperatura que genera el rotor a tales revoluciones.

Existe una modificación del método donde se lleva a cabo en un gradiente de densidad,[132] lo que permite separar los componentes en función de su densidad y así conocer este valor para elementos desconocidos.

Filtración por membranas

Se trata de una versión de la técnica anterior, en la que la centrifugación a cabo empleando dispositivos que poseen una membrana de tamaño selectivo por la que pasan los compuestos libres así como el medio de la suspensión, por lo que se puede emplear para una concentración simultánea a la purificación.[133] Presenta las mismas ventajas y desventajas que la técnica anterior.

Filtración en gel o Cromatografía de Exclusión por Tamaño (SEC)

Este método es una técnica cromatográfica, donde los compuestos se separan en función de una característica diferencial entre ellos, como es el tamaño o peso molecular en este caso.[134] El nombre de la técnica deriva del empleo de geles formado por polímeros entrecruzados que se emplean como fase estacionaria.

En este tamiz, los compuestos libres y las vesículas avanzan de forma diferente, ya que el bajo peso molecular respecto a las vesículas hace que éstos pueden seguir caminos más largos al ser capaces de penetrar por los poros de las partículas. Al contrario, las vesículas avanzan por el especio muerto que dejan las partículas entre sí, por lo que el orden de elución es: primero las vesículas y luego los compuestos libres en orden de mayor a menor peso molecular (ver **Figura 3.11.C**).

Los tipos de fase estacionaria más empleados para la purificación de vesículas son aquellos basados en partículas poliméricas de dextrano o agarosa entrecruzado que generan mallas de tamaño de poro diferentes. Sephadex® G25, G50 o G75;[135,136] o Sepharosa CL-2B o CL-4B[137,138] suelen ser los medios más empleados. En función del peso molecular del compuesto encapsulado/conjugado se emplea uno u otro, siendo CSephadex® empleado para moléculas de bajo/medio peso molecular y Sepharosa lo indicado más macromoléculas tipo proteínas o polímeros. En algunos casos, este método se emplea con fuerza centrífuga para una mayor rapidez y eficacia.[139]

Tabla 3.3. *Ventajas y desventajas de los métodos de purificación de vesículas.*

Método	Ventajas	Desventajas
Diálisis	Sencillez Equipamiento barato Escalable a nivel industrial	Optimización del tiempo necesaria para cada compuesto y medio Proceso largo
(Ultra)centrifugación	Elevada eficacia Rapidez del proceso	Posibilidad de aglomerar las vesículas al ser sometidas a fuerzas elevadas
Filtración por membranas	Escalable mediante multiplicación de los tubos	Posibilidad de que se rompan las vesículas Equipos costosos
Filtración en gel o SEC	Muy eficiente Versátil con amplio rango de fases estacionarias en función de los pesos moleculares de los cargos Dispositivos reutilizables Rápido	No escalable a nivel industrial Tiempos largos si se usa elución por gravedad

3.4. Exosomas: ejemplo de sistema vesicular natural con interés biotecnológico

Durante la última década, la comunidad científica ha presenciado una revolución en el conocimiento de los procesos fisiológicos, especialmente en cuestión de comunicación celular a nivel tisular y sistémico. Este hecho se debe en gran parte en los avances sobre cómo se producen y se desarrollan ciertas patologías gracias al mayor conocimiento sobre el papel fisio-patológico de las vesículas extracelulares, y en especial sobre los exosomas.[140]

Los exosomas son un tipo de vesículas extracelulares liberados al medio extracelular por todo tipo de células, y que pueden por ello encontrados en todo tipo de fluidos biológicos, además de en el medio de cultivo de células y tejidos cultivados *in vitro*.[141]

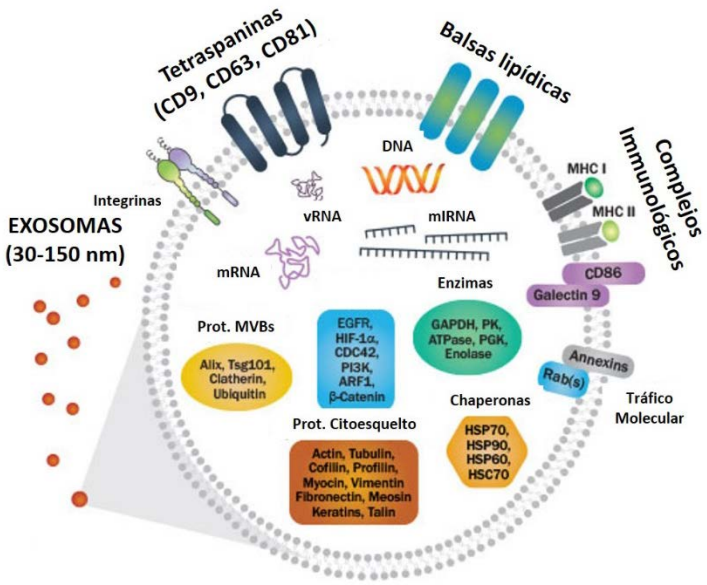

Figura 3.12. *Representación gráfica de la estructura y componentes de un exosomas natural. Figura adaptada de la referencia 142.*

Estas vesículas naturales que derivan de los *cuerpos multivesiculares* (orgánulos celulares encargados de la importación-exportación entre la célula y su entorno, poseen por ello una membrana similar a la plasmática, pero que difiere en términos de composición lipídica y proteica.[143] Este perfil bioquímico es definitorio pues de ellos, y sirve para su identificación y clasificación (entendiendo este proceso como la asignación de su origen y destino) (ver **Figura 3.12)**.[144]

El aumento de la información sobre la composición, biogénesis y los roles de los exosomas en procesos fisióligcos y patológicos ha introducido nuevas posibilidades en el campo del diagnóstico y de la terapia.[145] Los exosomas poseen características únicas que resultan de su origen celular y que los hace atractivos como nuevos biomarcadores de diagnóstico, estratificación de la enfermedad, o incluso como parámetro de medida de la respuesta y eficacia de un tratamiento.

Su composición molecular, tanto en términos de composición de membrana y de cargo, que incluye información lipidómica, proteómica y genómica, ofrece una fuente importante de conocimiento sobre su origen celular y el estado fisiológico del mismo. El hecho de poder analizar exosomas en fluidos biológicos fáciles de tomar (saliva, sangre, orina) que provengan de tejidos de difícil acceso (cerebral, medular) hace aún más atractivo su bioanálisis.

3.4.1. Exosomas como modelo de inspiración de vesículas mejoradas

Los exosomas combinan las ventajas de los vehículos de distribución de fármacos y de los agentes terapeúticos. De hecho, son considerados como los sistemas de distribución de compuestos más prometedores, especialmente en terapia génica para desórdenes genéticos o como agentes anti-tumorales.[146] Durante estos últimos años se han publicado números estudios sobre la modificación de elementos diana y sobre la encapsulación de elementos endógenos y exógenos en estas biopartículas, bien sea antes o después de su aislamiento de biofluidos o cultivos celulares.[147]

Estos trabajos han introducido el concepto de *exosomas semisintéticos*, un tipo de exosomas artificiales (modificados o creados en un laboratorio) que incluye a todos los exosomas que han sido modificados de alguna manera para su posterior uso en aplicaciones específicas.

3.4.2. Retos tecnológicos asociados a los exosomas y soluciones biomiméticas

Sin embargo, a pesar del desarrollo de estas metodologías, existen una serie de limitaciones relativas a su uso a nivel clínico, y que incluyen su aislamiento y purificación a escala de producción con un grado aceptable según estándares clínicos. Por otro lado, estas desventajas impiden a día de hoy la existencia de un material de referencia con el que poner a punto y comparar estrategias bioanalíticas que ayuden a profundizar en su estudio y permitan su plena instauración a nivel clínico.[148]

Estas desventajas han llevado a la comunidad científica a desarrollar estrategias para el diseño y producción de *exosomas totalmente artificiales*, creados en el laboratorio siguiendo metodologías propias de bionanotecnología. Estas metodologías se agrupan en dos grupos clásicos de la nanotecnología como son las metodologías *top-down* y *bottom-up*. La **Figura 3.13** muestra gráficamente el concepto de ambas, y resume brevemente sus ventajas y desventajas. En las secciones siguientes se explica brevemente en que consiste cada una. Información más detallada de cada una así como ejemplos encontrados en la literatura se expondrán ampliamente en el **capítulo 1**.

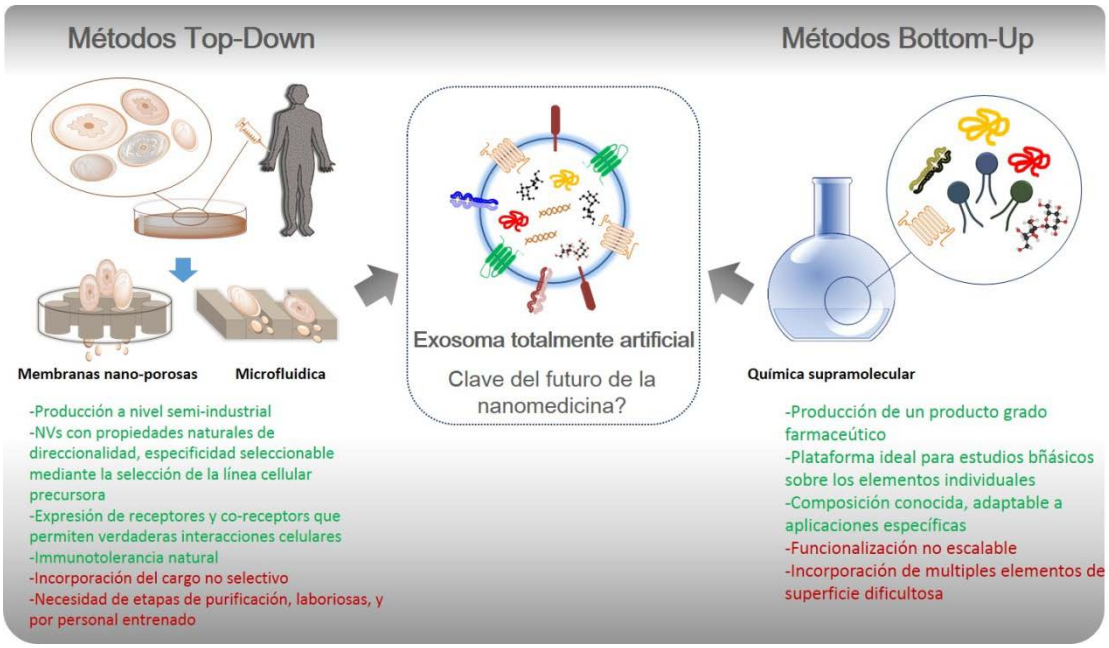

Figura 3.13. *Ventajas (**verde**) y desventajas (**rojo**) de los dos tipos de aproximaciones metodológicas basadas en bionanotecnología para la producción de exosomas puramente artificiales con fines teranósticos.*

Soluciones basadas en métodos Top-Down

Este conjunto de técnicas se basa en la producción de partículas en la nanoescala mediante la fragmentación de material de mayor tamaño y complejidad. La producción de exosomas artificiales en este caso comienza con el cultivo de células que serán empleadas como precursoras de fragmentos de membrana para la preparación de nanovesículas.

Esta "reducción" mediante fragmentación puede llevarse a cabo extrusión por membranas[149,150], o mediante dispositivos microfluídicos.[151,152] Ambos métodos han permitido encapsular material terapeútico (moléculas o nanoparticulado) o para producir partículas con propiedades regenerativas.

Ambas metodologías permiten la producción de cantidades suficientes para estudios clínicos, con una pureza aceptada, y lo que es más importante, con un perfil molecular y estructural muy similar al de los exosomas. Sin embargo, la encapsulación es un proceso poco selectivo, y las etapas de purificación siguen siendo largas, laboriosas y requieren de personal altamente cualificado.

Soluciones basadas en métodos Bottom-Up

Por contrario, esta aproximación crea elementos complejos y de tamaño nanométrico mediante el ensamblado molecular, empleado para ello principios físico-químicos como los mencionados en la sección 2.1 de la química supra-molecular. Es la aproximación en la que se basan los métodos de preparación de sistemas vesicular comentados en la sección 2.2. Por esto, la unidad básica en esta aproximación es la creación de una vesícula artificial que es funcionalizada con elementos típicos de exosomas mediante técnicas de encapsulación y bioconjugación.[153]

Estos métodos ofrecen la posibilidad de crear elementos muy puros, ya que la composición queda determinada por los precursores empleados, y por la pureza química de los compuestos empleados (tanto lípidos como proteínas son generalmente adquiridos en formas de elevada pureza, cercana al 100%). Por otra parte, muchos de estos procesos ya han sido adaptados y optimizados[154] a la encapsulación de ácidos nucleicos, moléculas caras y de difícil manejo.

Es por ello, un campo de trabajo muy interesante, donde la información que nos aporta el estudio de los exosomas naturales puede ayudar en la creación de nuevos liposomas mejorados, pero a su vez, éstos nos pueden permitir en el diseño y desarrollo de nuevos biomateriales complejos que puedan ser empleados en clínica y bionálisis.

3.5. Referencias bibliográficas

[1] Chen I.A., Walde P. (2010). From self-assembled vesicles to protocells. *Cold Spring Harbor Perspectives in Biology*, 2:a002170.

[2] Janney P.A., Kinnunen P.K.J. (2006). Biophysical properties of lipids and dynamic membranes. *Trends in Cell Biology*, 16(10):538-546.

[3] Wade L.G. Jr, editor. Organic Chemistry 5th edition. Pearson Prentice Hall, New Jersey, USA.

[4] Tandford C. (1973). The hydrophobic effect: formation of micelles and biological membranes. New York, *John Wiley and Sons, Inc*.

[5] Förster S., Zisenis M., Wenz E., Antonietti M. (1996). Micellization of strongly segregated block copolymers. *J. Chem. Phys*., 104:9956.

[6] Marianecci C., Di Marzio L., Rinaldi F., Celia C., Paolino D., Alhaique F., Esposito S., Carafa M. (2014). Niosomes from 80s to present: the state of the art. *Advances in Colloid and Interface Science*, 205:187-206.

[7] Antonietti M., Förster S. (2003). Vesicles and liposomes: a self-assembly principle beyond lipids. *Advanced Materials*, 15:1323-33.

[8] Lasic D.D. (1982b). A molecular model for vesicle formation. *Biochimica et Biophysica Acta*, 692:501-502.

[9] Lasic D.D. (1988). The mechanism of vesicle formation. *Biochemical Journal*, 256:1-11.

[10] Jahn A., Lucas F., Wepf R.A., Dittrich P.S. (2013). Freezing continuous-flow self-assembly in a microfluidic device: toward imaging of liposome formation. *Langmuir*, 29:1717-1723.

[11] Wang Z., He X. (2009). Dynamic of vesicle formation from lipid droplets: mechanism and controllability. *The journal of chemical physics*, 130(9):094905.

[12] Kasson P.M., Kelley N.W., Singhal N., Vrljic M., Brunger A.T., Pande V.S. (2006). Ensemble molecular dynamics yields submillisecond kinetics and intermediates of membrane fusion. *Proceedings of the National Academy of Sciences of the United States of America*, 103:11916.

[13] Weiss T.M., Narayanan T., Gradzielski M. (2008). Dynamics of spontaneous vesicle formation in fluorocarbon and hydrocarbon surfactant mixtures. *Langmuir*, 24:3759-3766.

[14] Sreekumaria A., Lipowsky R. (2018) Lipids with bulky head groups generate large membrane curvatures by small compositional asymmetries. *Journal of Chemical Physics*, 149:084901.

[15] Julicher F., Seifert U., Lipowsky R. (2013). Phase diagrams and shape transformations of toroidal vesicles. *Journal of Physics II*, 3:1681-1705.

[16] Manosroi A., Wongtrakul P., Manosroi J., Sakai H., Sugawara F., Yuasa M., Abe M. (2003). Characerization of vesicles prepared with various non-ionic surfactants mixed with colesterol. *Colloids and Surfaces B: Biointerfaces*, 30:129-138.

[17] Horiuchi T., Tajima K. (2000). Supramolecular Structure of Functionality Vesicles: Niosome Formation of Nonionic Amphiphiles and Physico-Chemical Properties in Aqueous Dispersion. *Journal of Japan Oil Chemists' Society* 49:1107.

[18] Peltonen L., Hirvonen J., Yliruusi J. (2001). The effect of temperature on sorbitan surfactant monolayers. Journal of Colloid and Interface Science, 239:134-138.

[19] Leng J., Egelhaaf S.U., Cates M.E. (2003). Kinetics of the Micelle-to-Vesicle Transition: Aqueous Lecithin-Bile Salt Mixtures. *Biophysical Journal*, 85:1624-1646.

[20] Zook J.M., Vreeland W.N. (2010). Effects of temperature, acyl chain length, and flow-rate ratio on liposome formation and size in a microfluidic hydrodynamic focusing device. Soft Matter, 6:1352-1360.

[21] Hu J., Weikl T., Lipowsky R. (2011). Vesicles with multiple membrane domains. *Soft Matter*, 7:6092-6102.

[22] Rai S., Pandey V., Rai G. (2017). Transfersomes as versatile and flexible nano-vesicular carriers in skin cancer therapy: the state of the art. *Nano Reviews & Experiments*, 8:1325708.

[23] Bangham A.D., Standish M.M., Watkins J.C. (1965). Diffusion of univalent ions across the lamellae of swollen phospholipids. *J. Mol. Biol.*, 13:238-252.

[24] Avanti Polar Lipids web, https://avantilipids.com/products, *última consulta 14/08/2019.*

[25] Pattni B.B., Chupin V.V., Torchilin V.P. (2015). New developments in liposomal drug delivery. *Chem Rev.*, 115:10938-10965.

[26] Hong Y.J., Kim J.C. (2011). Egg phosphatidylcholine liposomes incorporating hydrophobically modified chitosan: pH-sensitive release. *J. Nanosci. Nanotechnol.*, 11(1):204-9.

[27] Lu M., Zhao X., Xing H., Xun Z., Zhu S., Lang L., Yang T., Cai C., Wang D., Ding P.6. (2018). Comparison of exosome-mimicking liposomes with conventional liposomes for intracellular delivery of siRNA. *Int. J. Pharm.*, 550(1-2):100-113.

[28] Rinia H.A., de Kruijff B. (2001). Imaging domains in model membranes with atomic force microscopy. *FEBS Letters*, 504:194-199.

[29] Handjani-Vila R., Ribier A., Rondot B.A., Vanlerberghie G. (1979). Dispersions of lamellar phases of non-ionic lipids in cosmetic products, *Int. J. Cosmet. Sci.*, 1(5):303-314.

[30] Tavano L., Muzzalupo R., Mauro L., Pellegrino M., Andò S., Picc N. (2013). Transferrin-conjugated Pluronic niosomes as a new drug delivery system for anticancer therapy. *Langmuir*,29(41):12638-12646

[31] Manconi M., Vila A.O., Sinico C., Figueruelo J., Molina F., Fadda A.M. (2006). Theoretical and experimental evaluation of decypolyglucoside vesicles as potential drug delivery systems. *Journal of Drug Delivery Science and Technology*, 16:141-146.

[32] Planas M.E., Gonzalez P., Rodriguez L., Sanchez S., Cevc G. (1992). Noninvasive percutaneous induction of topical analgesia by a new type of drug carrier, and prolongation of local pain on sensitivity by anesthetic liposomes. *Anesth Analg*, 75:615-621.

[33] Caddeo C., Manca M.L., Peris J.E., Usach I., Diez-Sales O., Matos M., Fernàndez-Busquets X., Fadda A.M., Manconi M. (2018). Tocopherol-loaded transfersomes: In vitro antioxidant activity and efficacy in skin regeneration. *Int. J. Pharma.*, 551:34-41.

[34] Chaudhary H., Kohli K., Kumar V. (2013). Nano-transfersomes as novel carrier for transdermal delivery. *International Journal of Pharmaceutics*, 454:367-380.

[35] Saraf S., Paliwal S., Kaur C.D., Saraf S. (2011). Sphingosomes a novel approach to vesicular drug delivery. *Research Journal of Pharmacy and Technology*, 4(5):661-666.

[36] Zhigaltsev I.V., Maurer N., Akhong Q.-F., Leone R., Leng E., Wang J., Semple S.C., Cullis P.R. (2005). *Journal of Controlled Release*, 104:103–111.

[37] Boehlke L., Winter J.N. (2006).Sphingomyelin/cholesterol liposomal vincristine: a new formulation for an old drug. *Expert Opin. Biol. Th.*, 6(4):409-415.

[38] Salama A.H., Aburahma M.H. (2016). Ufasomes nano-vesicles-based lyophilized platforms for intranasal delivery of cinnarizine: preparation, optimization, ex-vivo histopathological safety assessment and mucosal confocal imaging. *Pharm Dev Technol.*, 21(6):706-15.

[39] Mittal R., Sharma A., Arora S. (2013). Ufasomes mediated cutaneous delivery of dexamethasone: formulation and evaluation of anti-inflammatory activity by carrageenin-induced rat paw edema model. *Journal of Pharmaceutics*, 2003: Article ID 680580.

[40] E. Touitou, N. Dayana, L. Bergelson, B. Godina, M. Eliaza. (2000). Ethosomes — novel vesicular carriers for enhanced delivery: characterization and skin penetration properties. *J. Control. Release*, 65(3):403-418.

[41] Dayana N., Touitou E. (2000). Carriers for skin delivery of trihexyphenidyl HCl: ethosomes vs. liposomes. *Biomaterials*, 21(18):1879-1885.

[42] Ferrer-Tasies L., Moreno-Calvo E., Cano-Sarabia M., Aguilella-Arzo M., Angelova A., Lesieur S., Ricart S., Faraudo J., Ventosa N., Veciana J. (2013). Quatsomes: vesicles formed by Self-Assembly of sterols and quaternary ammonium surfactants. *Langmuir*, 29:6519–6528.

[43] Tezel U., Pavlostathis S.G. (2015). Quaternary ammonium disinfectants: microbial adaptation, degradation and ecology. *Current Opinion in Biotechnology*, 33:296-304.

[44] Taubert A., Napoli A., Meier W. (2004). Self-assembly of reactive amphiphilic block copolymers as mimetics for biological membranes. *Current Opinion in Chemical Biology*, 8:598-603.

[45] Meng F., Zhong Z. (2011). Polymersomes spanning from nano- to microscales: advanced vehicles for controlled drug delivery and robust vesicles for virus and cell mimicking. *Journal of Physical Chemistry Letters*. 2:1533–1539.

[46] Schlaad H., Antonietti M. (2003) Block copolymers with amino acid sequences: molecular chimeras of polypeptides and synthetic polymers. *Eur Phys J E*, 10:17-23.

[47] Meier W., Nardin C., Winterhalter M. (2000). Reconstitution of channel proteins in (polymerized) ABA triblock copolymer membranes. *Angew Chem Int Ed Engl*, 39:4599-4602.

[48] Napper D.H. (1970). Colloid stability. Ind. Eng. Chem. Prod. Res. Develop., 9(4): 467-477.

[49] Huang Y., Chen J, Chen X, Gao J, Liang W. (2007). PEGylated synthetic surfactant vesicles (niosomes): novel carriers for oligomucleotides. *J. Mater. Sci. Mater. Med.*, 19:607-614.

[50] Awasthi V.D., Garcia D., Klipper R., Goins B.A., Phillips W.T. (2004). Neutral and anionic liposome-encapsulated hemoglobin: effect of postinserted poly(ethylene glycol)-distearoylphosphatidylethanolamine on distribution and circulation kinetics. *Journal of Pharmacology Experimental and Therapy*. 309:241–248.

[51] Bizmark N., Ioannidis M.A. (2015). Effects of Ionic Strength on the Colloidal Stability and Interfacial Assembly of Hydrophobic Ethyl Cellulose Nanoparticles. *Langmuir*, 31(34):9282-9289.

[52] Avanti Polar Lipids web, https://avantilipids.com/product-category/fluorescent-lipids. Ultimo acceso 14/08/2019.

[53] Pando D., Matos M., Gutiérrez G., Pazos C. (2015). Formulation of resveratrol entrapped niosomes for topical use. *Colloids Surf. B*, 128:398-404.

[54] Iwasakia Y., Tanaka S., Hara M., Ishihara K., Nakabayashia N. (1997). Stabilization of liposomes attached to polymer surfaces having phosphorylcholine groups. *J. Colloid. Interface Sci*., 192(2): 432-439.

[55] Jung. Y.K, Kim T.W., Park H.G., Soh H.T. (2010). Specific Colorimetric Detection of Proteins Using Bidentate Aptamer-Conjugated Polydiacetylene (PDA) Liposomes. *Adv. Funct. Mater*., 20(18):3092-3097.

[56] Shmeeda H., Liia Mak L., Tzemach D., Astrahan P., Tarshish M., Gabizon A. (2006). Intracellular uptake and intracavitary targeting of folate-conjugated liposomes in a mouse lymphoma model with up-regulated folate receptors. *Molecular Cancer Therapeutics*, 5(4):818-824.

[57] Li K., Chang S., Wang Z., Zhao X., Chen D. (2015). A novel micro-emulsion and micelle assembling method to prepare DEC205 monoclonal antibody coupled cationic nanoliposomes for simulating exosomas to target dendritic cells. *Int. J. Pharm*., 491:105-112.

[58] Lukyanov A.N., Elbayoumi T.A., Chakilam A.R., Torchilin V.P. (2004). Tumor-targeted liposomes: doxorubicin-loaded long-circulating liposomes modified with anti-cancer antibody. *J. Control Release*, 100(1):135-144.

[59] Patel D.M., Jani R.H., Patel C.N. (2011). Ufasomes: A Vesicular Drug Delivery. Systematic Reviews in Pharmacy, 2(2):72-78.

[60] Mukundan S. Jr., Ghaghada K.B., Badea C.T., Kao C.-Y., Hedlund L.W., Provenzale J.M., Allan Johnson G.A., Chen E., Bellamkonda R.V., Annapragada A. (2006). A liposomal nanoscale contrast agent for preclinical CT in Mice. *American Journal of Roentgenology*, 186: 300-307.

[61] Lee J., Lee H., Goh U., Kim J., Jeong M., Lee J., Park J.-H.. (2016). Cellular engineering with membrane fusogenic liposomes to produce functionalized extracellular vesicles. *ACS Applied Materials and Interfaces*, 8(11):6790-6795.

[62] Sato Y.T., Umezaki K., Sawada S., Mukai S., Sasaki Y., Harada N., Shiku H., Akiyoshi K. (2016). Engineering hybrid exosomes by membrane fusion with liposomes. *Sci. Rep*., 6:21933.

[63] Kakar R., Rao R., Goswami A., Nanda S., Saroha K. (2010). Proniosomes: An Emerging Vesicular System in Drug Delivery and Cosmetics. *Der Pharmacia Lettre*, 2(4): 227-239.

[64] N. Weiner, L. Lieb, S. Niemiec, C. Ramachandran, Z. Hu , K. Egbaria. (1994). Liposomes: A Novel Topical Delivery System for Pharmaceutical and Cosmetic Applications. *Journal of Drug Targeting*, 2(5):405-410.

[65] Rezvani M., Hesari J., Peighambardoust S.H., Manconi M., Hamishehka H., Escribano-Ferrer E. (2019). Potential application of nanovesicles (niosomes and liposomes) for fortification of functional beverages with Isoleucine-Proline-Proline: A comparative study with central composite design approach. *Food Chemistry*, 293:368-377.

[66] Gatt S., Bercovier H., Barenholz Y. Use of liposomes for combating oil spills and their potential application to bioreclamation. In: On-site bioreclamation: processes for xenobiotic and hydrocaron treatment, editado por Hinchee R.E. and Olfenbuttel R.F. 1991, Battelle Press, USA.

[67] Barani H. and Montazer M. (2008). A Review on Applications of Liposomes in Textile Processing. *Journal of Liposome Research*, 18(3):249-262.

[68] Liu Q., Boyd B.J. (2013) Liposomes in biosensors. *Analyst*, 138:391-409.

[69] Shweta Pawar S., Bhattacharya A., Nag A. (2019) Metal-Enhanced Fluorescence Study in Aqueous Medium by Coupling Gold Nanoparticles and Fluorophores Using a Bilayer Vesicle Platform. *ACS Omega*, 4(3):5983-5990.

[70] Edwards K.A., Korff R., Baeumner A.J. (2017). Liposome-Enhanced Lateral-Flow Assays for Clinical Analyses. *Methods in Molecular Biology*.1571:407-434

[71] Ho J.A., Wu L.-C. , Huang M.R., Lin Y.-J., Baeumner A.J., Durst R.A. (2007) Application of Ganglioside-Sensitized Liposomes in a Flow Injection Immunoanalytical System for the Determination of Cholera Toxin. *Analytical Chemistry*, 79:246-250.

[72] Chapman R., Lin Y., Burnapp M., Bentham A., Hillier D., Zabron A., Khan S., Tyreman M., Stevens M.M. (2015). Multivalent nanoparticles networks enable point-of-care detection of human phospholipase-A2 in serum. *ACS Nano*, 9:256-73.

[73] Bilek G., Kremser L., Blaas D., Kenndler E. (2006). Analysis of liposomes by capillary electrophoresis and their use as carrier in electrokinetic chromatography. *Journal of Chromatography B*, 841(1-2):38-51.

[74] Cipolla D., Wu H., Salentinig S., Boyd B., Rades T., Vanhecke D., Petri-Fink A., Rothin-Rutishauser B., Eastman S., Redelmeier T., Gondab I., Chana H.K.. (2016). Formation of drug nanocrystals under nanoconfinement afforded by liposomes. *RSC Advances*, 8:6223-6233.

[75] Miller J.P., Leo G. Herbette L.G., White R.E. (1996). X-ray Diffraction Analysis of Cytochrome P450 2B4 Reconstituted into Liposomes. *Biochemistry*, 35(5):1466-74.

[76] Biswas A., Sarkar S., Bhadra K., De S. (2015). Novel synthesis of biologically active CdS nanoclusters in cell-mimicking vesicles. *Journal of Experimental Nanoscience*, 11(9):681-694.

[77] De S., Kundu R., Biswas A. (2012). Synthesis of gold nanoparticles in niosomes. *Journal of Colloids and Interface Science*, 386:9-15.

[78] Olsona F., Hunt C.A., Szoka F.C., Vail W.J., Papahadjopoulos D. (1979). Preparation of liposomes of defined size distribution by extrusion through polycarbonate membranes. *Biochim. Biophys. Acta - Biomembranes*, 557:9-23.

[79] Yamaguchi T., Nomura M., Matsuoka T., Koda S. (2009). Effects of frequency and power of ultrasound on the size reduction of liposome. *Chemistry and Physics of lipids*, 160:58-62.

[80] Grimaldi N., Andrade F., Segovia N., Ferrer-Tasies L., Sala S., Veciana J., Ventosa N. (2016). Lipid-based nanovesicles for nanomedicine. *Chem. Soc. Rev.*, 45(23):6520-6545.

[81] Capretto L., Carugo D., Mazzitelli S., Nastruzzi C., and Zhang X. (2013) Microfluidic and lab-on-a-chip preparation routes for organic nanoparticles and vesicular systems for nanomedicine applications. *Advanced Drug Delivery Reviews*, 65:1496-1532

[82] Maestrelli F., González-Rodríguez M.L., Rabasco A.M. Mura P. (2006). Effect of preparation technique on the properties of liposomes encapsulating ketoprofen-cyclodextrin complexes aimed for transdermal delivery. *Int. J. Pharm.*, 312(1-2):53-60.

[83] Kremer J.M.H., Esker M.W.J., Pathmamanoharan C., Wiersema P.H. (1977). Vesicles of variable diameter prepared by a modified injection method. *Biochem.*, 16:3932-3935.

[84] Schieren H., Rudolph S., Finkelstein M., Coleman P., Weissmann G. (1978). *Biochim. Biophys. Acta,* 542:137–53.

[85] Abdelkader H., Ismail S., Kamal A., Alany R.G. (2011). Design and evaluation of controlled-release niosomes and discosomes for naltrexone hydrochloride ocular delivery. *J. Pharm Sci.*, 100(5):1833-1846.

[86] Szoka F., Papahadjopoulos D. (1978). Procedure for preparation of liposomes with large internal aqueous space and high capture by reverse-phase evaporation. *Proc. Natl. Acad. Sci. USA*, 75:4194–8.

[87] Alpes H., Allmann K., Plattner H., Reichert J., Rick R., Schulz S. (1986). Formation of large unilamellar vesicles using alkyl maltoside detergents. *Biochim. Biophys. Acta - Biomembr.*, 862:294–302.

[88] Alam M., Zubair S., Farazuddin M., Malik A., Mohammad O. (2013). Development, characterization and efficacy of niosomal diallyl disulfide in treatment of disseminated murine candidiasis. *Nanomedicine*, 9:247-256.

[89] Wallach D.F.H. (1993). In: Liposome Technology. Edited by Gregoriadis G, vol. 2. CRC Press.

[90] Mozafari S.M., Reed C.J., Rostrom C., Kocum C., Piskin E. (2005). Construction of stable anionic liposome-plasmid particles using the heating method. A preliminary investigation. *Cell. Mol. Bio. Lett.*, 7:923-927.

[91] Verma S., Singh S.K., Syan N., Mathur P., Valecha V. (2010). Nanoparticle vesicular systems: a versatile tool for drug delivery. *J. Chem. Pharm. Res.*, 2(2):496-509.

[92] Duncan R., Florence A.T., Uchegbu I.F., Cociacinch F. (1997). Drug polymer conjugates encapsulated within niosomes. *Patente internacional de aplicación*, ref. GB97:00072.

[93] Mokhtar M., Sammour O.A., Hammad M.A., Megrab N.A. (2008). Effect of some formulation parameters on flurbiprofen encapsulation and release rates of niosomes prepared from proniosomes. *Int. J. Pharm.*, 361:101-111.

[94] Espirito Santo I., Campardelli R., Cabral Albuquerque E., Vieira de Melo S., Della Porta G., Reverchon E. (2014). Liposomes preparation using a supercritical fluid assisted continuous process. *Chemical Engineering Journal*, 249:153-159.

[95] Kunastitchai S., Pichert L., Sarisuta N., Müller B.W. (2006). Application of aerosol solvent extraction system (ASES) process for preparation of liposomes in a dry and reconstitutable form. *Int. J. Pharm.*, 316(1-2):93-101.

[96] Manosroi A., Chutoprapat R., Abe M., Manosroi J. (2008). Characteristics of niosomes prepared by supercritical carbon dioxide ($scCO_2$) fluid. *Int. J. Pharm.*, 352(1–2):248-255

[97] Trucillo P., Campardelli R., Reverchon E. (2017). Supercritical CO_2 assisted liposomes formation: Optimization of the lipidic layer for an efficient hydrophilic drug loading. *Journal of CO_2 Utilization*, 18:181-188.

[98] Lorenzo Capretto L., Carugo D., Mazzitelli S., Nastruzzi C., Zhang X. (20139. Microfluidic and lab-on-a-chip preparation routes for organic nanoparticles and vesicular systems for nanomedicine applications. *Adv. Drug Deliv. Rev.*, 65:1496–1532.

[99] Carugo D., Bottaro E., Owen J., Stride E., and Nastruzzi C. (2016). Liposome production by microfluidics: potential and limiting factors. *Scientific Reports*, 19(6):25876.

[100] van Swaay D. and deMello A. (2013). Microfluidic methods for forming liposomes, *Lab Chip*, 13:752-767.

[101] Angelova M.I., Dimitrov D.S. (1986). Liposome electroformation. *Faraday Discuss. Chem. Soc.*, 81:303–311.

[102] Kuribayashi K., Tresset G., Coquet P., Fujita H., Takeuchi S. (2006). Electroformation of giant liposomes in microfluidic channels. *Meas. Sci. Technol.*, 17:3121.

[103] Le Berre M., Yamada A., Reck L., Chen Y., Baigl D. (2008). Electroformation of giant phospholipid vesicles on a silicon substrate: advantages of controllable surface properties. *Langmuir*, 24:2643–2649

[104] Y.C. Lin,M. Li, Y.T. Wang, T.H. Lai, J.T. Chiang, K.S. Huang, A new method for the preparation of self-assembled phospholipid microtubes using microfluidic technology, in: TRANSDUCERS'05 (Ed.), The 13th International Conference on Solid-State Sensors, Actuators and Microsystems, IEEE, 2005, pp. 1592-1595.

[105] Dittrich P.S., Renaud P., Manz A. (2006). On-chip extrusion of lipid vesicles and tubes through microsized apertures, *Lab Chip*, 6:488–493.

[106] Jahn A., Reiner J.E., Vreeland W.N., DeVoe D.L., Locascio L.E., Gaitan M. (2008). Preparation of nanoparticles by continuous-flow microfluidics, *J. Nanoparticle Res.*, 10:925–934.

[107] Phapal S., Sunthar P. (2013). Influence of micro-mixing on the size of liposomes self-assembled from miscible liquid phases. *Chem. Phys. Lipids*, 172–173:20–30.

[108] Kastner E., Verma V., Lowry D., and Perrie Y. (2015). Microfluidic-controlled manufacture of liposomes for the solubilisation of a poorly water soluble drug. *Int. J. Pharm.*, 485:122-130.

[109] Seo M., Paquet C., Nie Z., Xu S., Kumacheva E. (2007). Microfluidic consecutive flow-focusing droplet generators. *Soft Matter*, 3:986–992.

[110] Funakoshi K., Suzuki H., Takeuchi S. (2007). Formation of giant lipid vesicle like compartments from a planar lipid membrane by a pulsed jet flow, *J. Am. Chem. Soc.*, 129:12608–12609.

[111] Utada A., Lorenceau E., Link D., Kaplan P., Stone H., Weitz D. (2005). Monodisperse double emulsions generated from a microcapillary device. *Science*, 308:537–541

[112] Matos M., Gutiérrez G., Iglesias O., Coca J., Pazos C. (2015). Enhancing encapsulation efficiency of food-grade double emulsions containing resveratrol or vitamin B_{12} by membrane emulsification. *J. Food Eng.*, 166:212-220.

[113] Akbarzadeh A., Rogaie Rezaei-Sadabady R., Davaran S., Woo Joo S., Zarghami N., Hanifehpour Y., Samiei M., Kouhi M., Nejati-Koshki K. (2013). Liposome: classification, preparation, and applications. *Nanoscale Research Letters*, 8:102.

[114] Moghassemi S., Hadjizadeh A. (2014). Nano-niosomes as nanoscale drug delivery systems: an illustrated review. *J. Control. Release*, 185:22-36.

[115] Damera D.P., Krishna Venuganti V.V., Nag A. (2018). Deciphering the role of bilayer of a noisome towards controlling the entrapment and release of dyes. *ChemistrySelect*, 3:3930-3938.

[116] Ballie A.J., Coombs G.H. (1988). Vesicular systems (Niosome & Liposome) for delivery of Sodium Stibogluconate in experimental murine visceral leishmaniasis. *J. Pharma. Pharmacol.*, 40:161-165.

[117] Jeet K., Raines R.T. (2010). Advances in Bioconjugation. *Current Organic Chemistry*, 14(2):138-147.

[118] Marqués-Gallego P., de Kroon A.I.P.M. (2014). Ligation Strategies for Targeting Liposomal Nanocarriers. *BioMed Research International*, 2014: Article ID 129458.

[119] Zhang Yun D.W., Xiang Y., Zhang J.Z.H. (2003). New advance in chemistry: full quantum mechanical ab initio computation of Streptavidin−Biotin interaction energy. *J. Phys. Chem. B*, 107(44):12039-12041.

[120] Hermanson G.T (2013). (Strept)avidin-biotin interaction, Capitulo 11. En *Bioconjugate techniques*, Academic press, Londres, 1-125, 127-228.

[121] Papadia K., Markoutsa E., Antimisiaris S.G. (2014). A simplified method to attach antibodies on liposomes by biotin-streptavidin affinity for rapid and economical screening of targeted liposomes. *J. Biomed. Nanotechnol.*, 10(5):871-6.

[122] Lozano-Andrés, E., Libregts, S. F., Toribio, V., Royo, F., Morales, S., López-Martín, S., Valés-Gómez, M., Reyburn, H.T., Falcón-Pérez, J.M., Wauben, M.H., Soto, M., Yáñez-Mó, M. (2019). Tetraspanin-decorated extracellular vesicle-mimetics as a novel adaptable reference material. *Journal of Extracellular Vesicles*, 8(1), 1573052.

[123] Bioconjugate reagents, Chapter 3. En: *Bioconjugate techniques*, Hermanson G.T. (editor). *Academic Press*, Londres, 1-125, 127-228.

[124] Endoh H., Suzuki Y., Hashimoto Y. (1981). Antibody coating of liposomes with 1-ethyl-3-(3-dimethyl-aminopropyl)carbodiimide and the effect on target specificity. *J. Immunol. Methods*, 44:79-85.

[125] Li K., Chang S., Wang Z., Zhao X., Chen D. (2015). A novel micro-emulsion and micelle assembling method to prepare DEC205 monoclonal antibody coupled cationic nanoliposomes for simulating exosomas to target dendritic cells. *Int. J. Pharm.*, 491:105-112.

[126] NHS and SULFO-NHS Application note, Thermo Scientific. Disponible en la web.

[127] Gutiérrez G., Matos M., Barrero P., Pando D., Iglesias O., Pazos C. (2016). Iron-entrapped niosomes and their potential application for yogurt fortification. *Food Science and Technology*, 74:550-556.

[128] Pando D., Gutiérrez G., Coca J., Pazos C. (2013). Preparation and characterization of niosomes containing resveratrol. *Journal of Food Engineering*, 117(2):227-234.

[129] Pando D., Caddeo C., Manconi M., Fadda A.M., Pazos C. (2013). Nanodesign of olein vesicles for the topical delivery of the antioxidant resveratrol. *J. Pharm. Pharmacol.*, 65(8):1158-1167.

[130] Jain S., Chaudhari B.H., Swarnakar N.K. (2011). Preparation and characterization of niosomal gel for iontophoresis mediated transdermal delivery of isosorbide dinitrate. *Drug Deliv. Transl. Res.*, 1:309-321.

[131] Zubairu Y., Mohan L., Ngi Zeenat Iqbal N., Talegaonkar S. (2015). Design and development of novel bioadhesive niosomal formulation for the transcorneal delivery of anti-infective agent: In-vitro and ex-vivo investigations. *Asian Journal of Pharmaceutical Sciences*, 10(4):322-330

[132] Sánchez-López V., Fernández-Romero J.M., Gómez-Hens A. (2009). Evaluation of liposome populations using a sucrose density gradient centrifugation approach coupled to a continuous flow system. *Anal. Chim. Acta*, 645(1-2):79-85.

[133] Hirai M., Minematsu H., Hiramatsu Y., Kitagawa H., Otani T., Iwashita S., Kudoh T., Chen L., Li Y., Okada M., Salomon D.S., Igarashi K., Chikuma M., Seno M. (2010). Novel and simple loading procedure of cisplatin into liposomes and targeting tumor endothelial cells. *Int. J. Pharm.*, 391(1-2):274-283.

[134] Grabielle-Madelmont C., Lesieur S., Ollivon M. (2003). Characterization of loaded liposomes by size exclusion chromatography. *J. Biochem. Biophys. Methods.,* 56(1-3):189-217.

[135] Ruysschaert T., Audrey Marque A., Duteyrat J.-L., Lesieur S., Winterhalter M., Fournier D. (2005). Liposome retention in size exclusion chromatography. *BMC Biotechnol.*, 5:11.

[136] Ehnholm C., Zilversmit D.B. (1973). Exchange of various phospholipids and of cholesterol between liposomes in the presence of highly purified phospholipid exchange protein. *J. Biol. Chem.*, 248:1719-1724.

[137] Chen C.S., Yao J., Durst R.A. (2006). Liposome encapsulation of fluorescent nanoparticles: Quantum dots and silica nanoparticles. *Journal of Nanoparticle Research*, 8(6):1033-1038.

[138] Yang X., Zhao X., Phelps M.A., Piao L., Rozewski D.M., Liu Q., Lee L.J., Marcucci G., Grever M.R., Byrd J.C., Dalton J.T., Lee R.J. (2009). A novel liposomal formulation of flavopiridol. *Int. J. Pharm.*, 365(1-2):170-174.

[139] Gupta P.N., Mishra V., Rawat A., Dubey P., Mahor S., Jain S., S., Chatterji D.P., Vyas S.P. (2005b). Non-invasive vaccine delivery in tranfersomes, niosomes and liposomes: a comparative study. *Int. J. Pharm.*, 293:73-82.

[140] Raposo G. Stoorvogel W. (2013). Extracellular vesicles: Exosomes, microvesicles, and friends. *J. Cell Biol.*, 200(4):373.

[141] Yáñez-Mó M., Siljander P.R., Andreu Z., Zavec A.B., Borràs F.E., Buzas E.I., Buzas K., Casal E., Cappello F, Carvalho J, Colás E, Cordeiro-da Silva A., Fais S., Falcon-Perez J.M., Ghobrial I.M., Giebel B., Gimona M., Graner M., Gursel I., Gursel M., Heegaard N.H., Hendrix A., Kierulf P., Kokubun K., Kosanovic M, Kralj-Iglic V, Krämer-Albers E.M., Laitinen S., Lässer C., Lener T., Ligeti E., Linē A., Lipps G., Llorente A., Lötvall J., Manček-Keber M., Marcilla A., Mittelbrunn M., Nazarenko I., Nolte-'t Hoen E.N., Nyman T.A., O'Driscoll L., Olivan M., Oliveira C. Pállinger É., Del Portillo H.A., Reventós J, Rigau M., Rohde E, Sammar M., Sánchez-

Madrid F., Santarém N. Schallmoser K., Ostenfeld M.S., Stoorvogel W., Stukelj R., Van der Grein S.G., Vasconcelos M.H., Wauben M.H., De Wever O. (2015). Biological properties of extracellular vesicles and their physiological functions. *Journal of Extracellular Vesicles*, 14(4):27066.

[142] https://www.novusbio.com/research-areas/cell-biology. Último acceso 15/08/2019.

[143] Colombo M., Moita C. van Niel G., Kowal J., Vigneron J., Benaroch P., Manel N., Moita L.F., Théry C., Raposo G. (2013). Analysis of ESCRT functions in exosome biogenesis, composition and secretion highlights the heterogeneity of extracellular vesicles. *J. Cell. Sci.*, 126(24):5553-65.

[144] Kowal J., Arras G., Colombo M., Jouve M., Morath J.P., Primdal-Bengtson B., Dingli F., Loew D., Tkach M., Théry C. (2016). Proteomic comparison defines novel markers to characterize heterogeneous populations of extracellular vesicle subtypes. *Proc. Natl. Acad. Sci. U S A.*, 113(8):E968-77.

[145] Fuhrmann G., Herrmann I.K., Stevens M.M. (2015). Cell-derived vesicles for drug therapy and diagnosis: opportunities and challenges. *Nano Today*, 10:397-409.

[146] van der Meel R., Fens M.H.A.M., Vader P., van Solinge W.W., Eniola-Adefeso O., Schiffelers R.M. (2014). Extracellular vesicles as drug delivery systems: lessons from the liposome field. *J. Control. Release.*, 195:72-85.

[147] Johnsen K.B., Gudbergsson J.M., Skov M.N., Pilgaard L., Moos T., Duroux M. (2014). A comprehensive overview of exosomas as drug delivery vehicles – endogenous nanocarriers for targeted cancer therapy. *Bichim. Biophys. Acta*, 1846:75-87.

[148] Valkonen S., van der Pol E., Böing A., Yuana Y., Yliperttula M., R. Nieuwland, Laitinen S., Siljander P.R.M. (2017). Biological reference materials for extracellular vesicle studies. *Eur. J. Pharm. Sci.*, 98:4-16.

[149] Jang S.C., Kim O.Y., Yoon C.M., Choi D.S., Roh T.Y., Park J., Nilsson J., Lötvall J., Kim Y.K., Gho Y.S. (2013). Bioinspired exosome-mimetic nanovesicles for targeted delivery of chemotherapeutics to malignant tumors. *ACS nano*, 7:7698-7710.

[150] Hwang D.W., Hongyoon Choi H., Jang S.C., Yoo M.Y., Park J.Y., Choi N.E., Oh H.J., Ha S., Yun-Sang Lee, Y.-S., Jeong J.M., Gho Y.S., Lee D.S. (2015). Noninvasive imaging of radio-labelled exosome-mimetic nanovesicles using ^{99m}Tc-HMPAO. *Sci Rep.*, 5:15636.

[151] Jo W., Jeong D., Kim J., Cho S., Jang S.C., Han C., Kang J.Y., Gho Y.S., Park J. (2014). Microfluidic fabrication of cell-derived nanovesicles as endogenous RNA carriers. *Lab Chip*, 14:1261-1269.

[152] Yoon J., Jo W., Jeong D., Kim J., Jeong H., Park J. (2015). Generation of nanovesicles with sliced cellular membrane fragments for exogenous material delivery. *Biomaterials*, 59:12-20.

[153] Hermanson G.T. (2008). Preparation of liposome conjugates and derivatives. En Biconjugate Techniques, 2nd edition. Academic Press, London, UK.

[154] Shim G., Kim M.-G., Park J.Y., Oh Y.-K. (2013). Application of cationic liposomes for delivery of nucleic acids. *Asian Journal of Pharmaceutical Sciences*, 8(2):72-80.

4. Experimental

Capítulo 4. Experimental

Para una mejor comprensión de los resultados, tanto los materiales utilizados como los reactivos y los procedimientos empleados se van a detallar en cada uno de los capítulos experimentales de manera individual. De esta manera, el apartado experimental de la Tesis Doctoral recoge de manera general los principios de las técnicas y los detalles relacionados con la instrumentación empleada en la caracterización de las nanovesículas producidas a lo largo de la misma.

4.1. Dynamic Light Scattering (DLS): tamaño y potencial ζ

La dispersión dinámica de luz o *Dynamic Light Scattering* (DLS) es una técnica analítica no invasiva que se emplea para las medidas del tamaño de partícula (radio hidrodinámico) en suspensión, y de la distribución de tamaños. Esta técnica permite la medida de tamaños desde 0.3 nm hasta 10 μm aproximadamente.

Emplea un haz de luz láser que se dirige hacia la suspensión de partículas, siendo la luz reflejada por las mismas en múltiples direcciones. Este reflejo no posee ni una intensidad ni una direccionalidad fija, si no que debido al movimiento browniano de las partículas (por choques con moléculas del disolvente), éste fluctúa en el tiempo en proporción al tamaño de las partículas. Partículas pequeñas se mueven más rápido, mientras que partículas grandes se mueven despacio, por lo que se observan fluctuaciones que se producen de acuerdo a ese movimiento.

En un instrumento de DLS, la muestra se ilumina con un rayo láser y las fluctuaciones de la luz dispersada se detectan en un ángulo de dispersión conocido (θ) mediante un detector rápido de fotones. Las fluctuaciones de intensidad se detrminan mediante el cálculo de la función de correlación de intensidad g2(t). De esta correlación se obtiene coeficiente de difusión D de las partículas, que se relaciona con el radio hidrodinámico (R) de las partículas mediante la ecuación de Stokes-Einstein ($D=K(B)T/6\pi\eta R$), Donde k(B) es la constante de Boltzmann, T la temperatura y η la viscosidad.

El movimiento browniano de las macromoléculas depende de su tamaño, pero también de la temperatura y viscosidad del solvente, por lo que dichos datos son requeridos en un análisis por DLS.

Figura 4.1. *Equipo Zetasizer NANO-ZS, Malvern Instruments.*

En el caso de la presente Tesis Doctoral se ha utilizado un instrumento Zetasizer NANO-ZS (Malvern Instruments Ltd, Malvern, Reino Unido). Este intrumento (ver **Figura 4.**) es un analizador de tamaño de partícula con dos ángulos de detección (173° y 13°), utilizando la dispersión de luz dinámica con óptica NIBS (retrodispersión no invasiva o *Non-Invasive Backscatter*), lo que permite medir tanto suspensiones muy concentradas como diluidas. Opera con un láser de tipo He-Ne laser (633 nm, max. 4mW), a una temperatura por defecto de 25 °C (si bien es un parámetro que puede modificarse, hasta 120 °C). En esta Tesis, todas las medidas han sido realizadas a 25 °C.

Este equipo permite medir también potencial ζ a través de la luz dispersada. El potencial ζ se define como la carga que adquiere una partícula en un determinado medio, y que proviene de la carga superficial y de la concentración y tipo de iones en la solución. Estos iones son lo que se "ordenan" sobre la superficie de la partícula y generan la carga de la misma. Por tanto, El potencial zeta es una medida de la magnitud de la repulsión o atracción electrostática (o de carga) entre las partículas, y es uno de los parámetros fundamentales que afectan a su estabilidad coloidal. Su medida ofrece información de las causas de la dispersión, agregación o floculación, y se puede emplear en la mejora de las formulaciones.

Dicho parámetro se mide mediante una técnica denominada microelectroforesis de láser Doppler. En esta técnica, se aplica un campo eléctrico a una solución de moléculas o a una dispersión de partículas, que se mueven con una velocidad proporcional a su potencial ζ. Esta velocidad es medida mediante una técnica interferométrica de láser patentada denominada M3-PALS (Dispersión de luz para análisis de fase). Esta medida permite el cálculo de la movilidad electroforética, y a través dedicho valor se calcula el valor de potencial ζ.

4.2. Microscopía Electrónica de Trasmisión (TEM): morfología

El análisis morfológico de las vesículas se ha realizado mediante microscopía electrónica de transmisión por tinción negativa (NS-TEM), utilizando un microscopio electrónico de transmisión JEOL-2000 Ex II (Tokio, Japón). Es un instrumento que aprovecha los fenómenos espectroscópicos que se producen cuando un haz de electrones suficientemente acelerado colisiona con una muestra delgada convenientemente preparada, o una suspensión de partículas depositada sobre portamuestras adecuados.

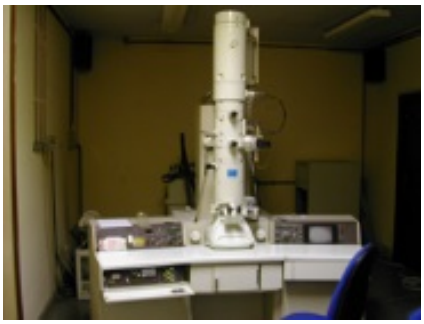

Figura 4.2. *Microscopio TEM JEOL-2000 ExII, Jeol.*

Cuando los electrones colisionan con la muestra, en función de su grosor y del tipo de átomos que la forman, parte de ellos son dispersados selectivamente, es decir, hay una gradación entre los electrones que la atraviesan directamente y los que son totalmente desviados. Todos ellos son conducidos y modulados por unas lentes para formar una imagen final sobre una cámara CCD que puede tener miles de aumentos con una definición inalcanzable para cualquier otro instrumento. La información que se obtiene es una imagen con distintas intensidades de gris que se corresponden al grado de dispersión de los electrones incidentes.

El caso concreto de la tinción negativa, es una técnica de microscopía que permite contrastar las muestras mediante una sustancia opaca a los fotones (microscopía óptica) o a los electrones (microscopía electrónica). En caso de microscopía electrónica de transmisión, se emplean metales pesados (de alto número atómico) que, por tanto, resultan opacas a los electrones transmitidos. Típicamente, estas sustancias son acetato de uranilo, citrato de plomo, ácido fosfotungstico, molibdato de amonio o tetraóxido de osmio.

En el caso particular de la presente Tesis Doctoral, el microscopio utilizado (ver **Figura 4.2**) está especialmente indicado para la nano-caracterización estructural y analítica de materiales. Posee 200 kV de aceleración lo que permite alcanzar una resolución de 3,4 Å entre líneas. El equipo dispone además de una cámara CCD de alta resolución (2048x2048 pixels). Se ha empleado ácido fosfotungstico (2% w/v, en agua ultrapura).

4.3. Turbiscan (Formulaction): estabilidad coloidal

La estabilidad coloidal de lad nanovesículas se ha determinado midiendo los perfiles de retrodispersión en un aparato Turbiscan Lab Expert (Formulaction, L'Union, Francia) provisto de una estación de envejecimiento (Formulaction, L'Union, Francia). Dicha estación de envejecimiento (ver **Figura 4.3**) permite el análisis, a largo plazo, de la estabilidad de todo tipo de dispersiones líquidas, de forma automatizada.

Figura 4.3. *Equipo Turbiscan LAB Expert con estación de envejecimiento, Formulaction.*

Este equipo emplea la técnica denominada dispersión estática de luz múltiple o *Static Multiple Light Scattering* (S-MLS). En esta técnica, la suspensión de partículas es iluminada con una fuente de fotones (880 nm, NIR), que son reflejados por las mismas en múltiples direcciones y en numerosas ocasiones (al ir siendo dispersada múltiples veces al ir encontrando varias partículas en su trayectoria de rebote). Finalmente, esta luz es detectada por dos detectores sincronizados, uno a 135° para luz dispersada y otro a 0° para luz trasmitida. La relación entre ellas y la intensidad individual será proporcional al tamaño de partícula y a su concentración. Esta medida se realiza a lo largo de la altura de la celda de medida, lo que crea un patrón de señal que permite monitorizar fenómenos de agregación, floculación, sedimentación o cremado, ya que

éstos se verán reflejos en un cambio de la señal detectada por ambos detectores y por consiguiente un cambio en ese patrón a lo largo del tiempo de medida.

4.4. HPLC fase reversa: eficacia de encapsulación

La cromatografía líquida de alta eficacia o high performance liquid chromatography (HPLC) de fase reversa es un tipo de cromatografía que emplea la polaridad de los analitos como característica en base a la cual se produce la separación. La separación cromatográfica se produce como consecuencia del avance diferencial de los componentes de la mezcla a través de una fase estacionaria de carácter hidrofóbico, de tal forma que los compuestos polares no interaccionan con la misma, y eluyen con el volumen muerto. Sin embargo, los compuestos apolares interaccionan con la fase estacionaria, y esta interacción es más fuerte cuanto mayor es la apolaridad del compuesto, avanzando más lento por la columna y eluyendo a tiempos de retención superiores.

La fase estacionaria está compuesta de partículas de sílica químicamente modificadas con hidrocarburos saturados, insaturados o aromáticos de diferentes tipos. Los compuestos apolares se eluyen de forma selectiva a medida que se incrementa la apolaridad de la fase móvil que los impulsa por la columna, de tal forma que a determinado porcentaje de disolvente orgánico (metanol, acetonitrilo o isopropanol), el compuesto pasa a la fase móvil y éste eluye de la columna.

Por lo tanto, para este tipo de cromatografías se emplean mezclas dinámicas de solventes polares, tales como agua, y acetonitrilo, acetato de etilo, acetona y alcoles alifáticos cuya proporción cambia con el tiempo, generando lo que se denomina gradiente cromatográfico. Alternativamente, se puede usar el modo isocrático, en el que la composición de la fase móvil permanece sin alterarse.

En el caso concreto de la presente Tesis Doctoral se ha utilizado un cromatógrafo HP serie 1100, (Hewlett-Packard, Palo Alto, CA), con un módulo de detección UV/Vis HP G1315A UV/ 281 (Agilent Technologies, Palo Alto, CA, USA), tal y como se puede observar en la **Figura 4.4**.

Se ha utilizado la siguiente columna cromatográfica: Zorbax Eclipse Plus C18 (Agilent Technologies, 284 Palo Alto, CA), con un tamaño de partícula de 5 µm y unas dimensiones de 4,6 mm × 150 mm. En todos los casos, se han empleado gradientes

analíticos cuyas espefificaciones se encuentran detalladas en las secciones experimentales de cada capítulo donde se ha empleado esta técnica.

Figura 4.4. *Equipo de HPLC HP serie 1100 con módulo de detección UV/Vis HP G1315A UV/281, Hewlett-Packard.*

4.5. Lector de placas

Un lector de placas (ver **Figura 4.5**) es un instrumento que permite detectar eventos biológicos, químicos o físicos en muestras contenidas en placas de microtitración. Los métodos comunes de detección para los ensayos de microplacas son: absorbancia, intensidad de fluorescencia, luminiscencia, fluorescencia resuelta en el tiempo y polarización de fluorescencia.

En el caso particular de esta Tesis, se ha empleado medidas de absorbancia del producto enzimático de la catálisis de dihidrocloruro de o-fenilendiamina (OPD) por parte de la enzima HRP, con una longitud de onda de detección λ = 492 nm, en un equipo Tecan Genios (Tecan Trading AG, Suiza)

Figura 4.5. *Lector de placas y absorbancia TECAN Genios, Tecan Trading AG.*

4.6. Analizador para la medida de Western Blot

Para la realización de las medidas por quimiluminiscencia en dot-blot se ha utilizado el analizador LAS4000 mini Image System analyser de GE Healthcare (ver **Figura 4.6**). Es un analizador específico para geles y blots, realizando la detección o bien por quimiluminiscencia o por fluorescencia. Posee una cámata CCD de FujifilmTM, con una resolución de imagen de 6.3 Mpixels.

En el caso particular de esta Tesis, se ha empleado quimiluminiscencia mejorada, proveniente de la reacción enzimática de un producto luminiscente que se forma por catálisis de la enzima HRP que se encuentra conjugada a los anticuerpos empleados para detección molecular específica.

Figura 4.6. *Analizador de imágenes de luminiscencia para geles y membranas LAS4000 mini Image System analyser de, GE Healthcare.*

4.7. Equipo de Differential Scanning Calorimetry

La calorimetría diferencial de barrido es una técnica analítica empleada en la caracterización de fenómenos que involucran cambios térmicos como consecuencia de procesos físico-químicos. Estos fenómenos producen cambios en la entalpía de las muestras, que son registrados a lo largo del tiempo y de un gradiente de temperatura. Dicho gradiente puede realizarse en modo de aumento de temperatura o en modo de descenso. Frecuentemente se suelen emplear ambos, para conocer la reversibilidad del proceso y así identificar su naturaleza.

Estas fluctuaciones térmicas se registran tanto para la muestra como para un material de referencia, y los cambios de flujos de calor son registrados como señal analítica. De esta forma se detectan procesos endo- y exotérmicos en forma de picos, cuya morfología y posición informan a cerca del fenómeno que los produce. En el caso

particular de los sistemas vesiculares, el cambio de estado gel a líquido cristalino de las bicapas se manifiesta como un pico endotérmico, ya que dicho cambio se produce gracias a energía en forma de calor. Su posición y forma de pico ofrece información acerca de la estabilidad y grado de empaquetamiento de los compuestos que forman la bicapa, y resulta en una técnica muy útil para la caracterización de formulaciones.

Figura 4.7. Equipo de DSC 822e, Mettler-Toledo.

En la presente Tesis Doctoral se ha empleado un equipo de DSC (ver **Figura 4.7**) modelo 822e (Mettler-Toledo, España). Las muestras han sido cargadas en crisoles sellados de aluminio, con flujo de nitrógeno para evitar procesos de degradación por oxidación.

5. Therapeutic biomaterials based on extracellular vesicles: classification of bio-engineering and mimetic preparation routes

Capítulo/Chapter 5

Therapeutic biomaterials based on extracellular vesicles: classification of bio-engineering and mimetic preparation routes

5.1. Extracellular vesicles in nanomedicine: possibilities and limitations

Extracellular vesicles (EVs) represent an important portion of the secretome. An overview of their functions in physiological conditions of EVs was compiled by a recent position paper of the International Society of Extracellular Vesicles (ISEV).[1] Some of the described properties can be used for therapeutic uses, and their testing has been transformed sometimes into several registered clinical trials.[2] Exosomes are being applied in antitumour immunotherapy,[3] as therapeutic agents against infectious diseases,[4] unmodified exosomes for immune-modulatory[5] and regenerative therapies,[6] and modified ones for targeted drug delivery,[7] especially in gene therapy.[8] Although some of the mechanisms behind their properties remains undescribed, some general characteristic of EVs make them advantageous over other therapeutic strategies.

Both the structure of the membrane and the formation route are the origin of the following advantageous aspects: (1) high selective targetability and minimum off-target effect, thanks to a set of molecules involved in targeting, signalling and receptor-mediated uptake, complete with all the co-receptors needed for the internalisation process; (2) capacity of extravasation due to a gel-state core derived from the presence of hydrated macromolecules (proteins and nucleic acids) combined with a minimum cytoskeleton that allows deformability while keeping the whole integrity of the vesicle; (3) Size distribution; (4) great stability in the blood due to the evasion of the innate immune system; (5) adaptative responses that cause clearance from the blood, with the corresponding decrease in bioavailability.

EVs can be used as therapeutic agent by themselves or as delivery systems. The great potential of EVs as drug delivery vehicles has been acknowledged in the literature.[7-12] In most cases, the encapsulated drug acts in collaboration with elements naturally present in the EVs, creating a synergetic effect. In other cases, EVs serve only

as vehicles to reach specific target population, sometimes highly protected from conventional administration routes.

Nevertheless, limitations of EVs as therapeutic agents have also been reported, including the absence of a good definition from a pharmaceutical point of view,[13] an incomplete understanding of their role in the development and spread of pathology, the absence of methods for the isolation of homogeneous populations and subpopulations of EVs, and cost-ineffective technology for the availability of sufficient quantities for clinical trials with constant characteristics. Moreover, it has been acknowledged that there is little understanding on how biological barriers are crossed by EVs, and a need for loading methods with scalable properties in clinical translation has been identified.[14]

5.2. Bio-engineered and mimetic EVs for nanomedicine: classification of artificial EVs

EVs have been modified in the search for broader therapeutic capability. Sometimes, this included the incorporation of new elements for targeted puporses, *in vitro* or *in vivo* traceability, or the material to be delivered. In other cases, modification was aimed at the enhancemt of colloidal stability, or change in surface charge to increase their uptake rate. These new approaches have generate new terms such as bioengineered exosomes, artificial exosomes,[15] exosome-mimetic nanovesicles,[16] exosome-like nanovesicles,[17,18] and exosome-based semi-synthetic vesicles.[19] These expressions have been used with different meanings in the literature, but to date, there has not been yet a clear criterion for their classification. One example is the term "exosome-like nanovesicles". In some works, this concept is used to name artificial vesicles made from cells through different techniques to mimic exosomes.[17-18] However, cell-derived vesicles with morphological and biochemical characteristics similar to exosomes were also named exosome-like nanovesicles by other authors.[19-20] Other authors working with non-animal research models used this term to refer to vesicles with size and flotation density values similar to exosomes. For example, Regente et al.[21] described the presence of exosome-like vesicles in sunflower plant fluids, and Prado et al.[22] showed evidence of vesicles quite similar to exosomes during pollen germination.

In order to provide a systematic classification to move around in this new emerging field, we suggest the nomenclature given in Figure 5.1. This Artificial EVs landscape is based on the concept behind the term. This way, "artificial EVs" will be used as general concept to designate all vesicles, modified or manufactured (from natural or synthetic sources) with the aim to mimic EVs (mainly exosomes) for therapeutic uses. Behind this term, two categories of artificial EVs could be discerned: "*semi-synthetic EVs*" and "*fully synthetic*" or "*EVs mimetic vesicles*", corresponding to modified natural EVs (pre- or post-isolation) and artificial structures, lab-made or generated from cultured cells.

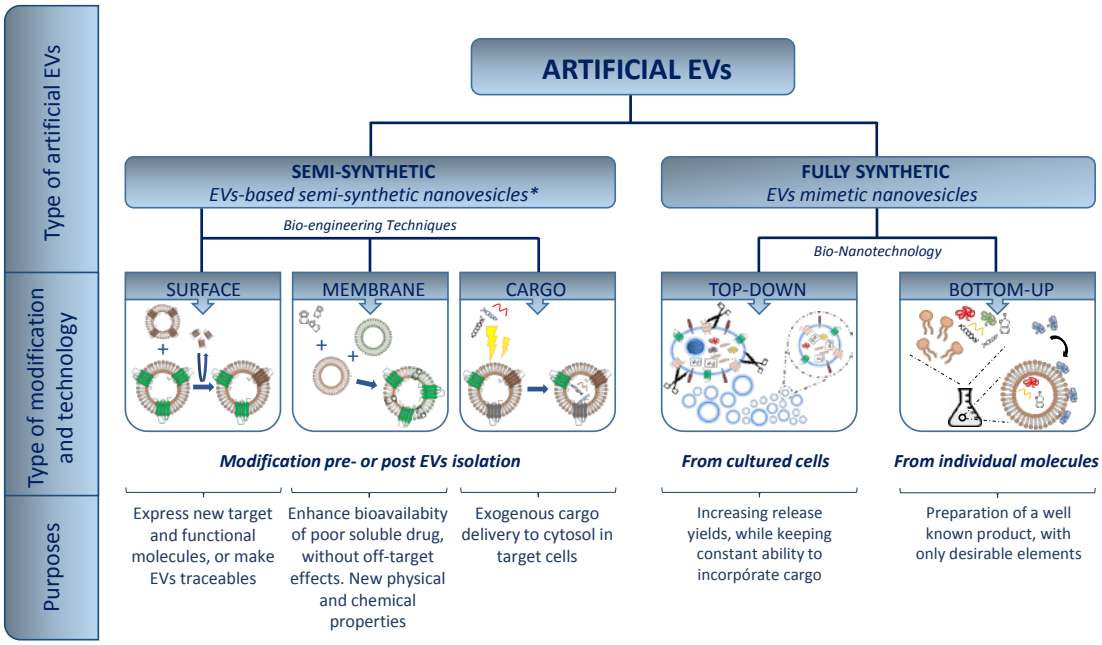

Figure 5.1. *Artificial EVs landscape: explored routes up-to-date for the preparation of artificial EVs for specific purposes.*EBSSNs (ref. 19)*

The former generate semi-synthetic products, as they start from a natural substrate, which can be subsequently modified before or after their isolation. The modification affects the structures of the outer surface of the vesicles, the membrane or the cargo that travels within, and could also include hydrophobic molecules at the membrane.

The term *fully synthetic,* on the other hand, stresses the artificiality of the product. We have recently briefly commented their potential in therapeutics.[23] These techniques can be classified on the basis of their manufacturing route: those starting from larger substrates (cells) that are reduced to units for the creation of small size vesicles (top-down nanotechnology) or those taking individual molecules (lipids, proteins, etc.) that self-assemble in higher order structures with tunable composition (bottom-up

nanotechnology). Top-down products differ from natural EVs in terms of micro-structure and biochemical composition, since they are formed from cell fragments: the characteristical membrane microdomains[24] (lipid rafts) and associated pools of surface markers (especially tetraspanins) are absent, and the minimal cytoskeleton is not present.

5.3. Impact of the artificial EVs classification at the design of new therapeutic agents based on EVs

The preparation route chosen is important for the final purpose of the artificial EVs, but it could be critical for the clinical trials and subsequent commercialization. The extense manipulation of EVs during the bio-engineering methods is the reason for their classification as advanced therapy medicinal products (ATMPs),[2] with a particular regulatory framewok. Following the same criteria, fully artificial EVs produced from cultured cells (top-down) should be also incorporated into this category.

On the other hand, botton up artificial mimetic EVs are more difficult to assign to one or another category. To date, a set of proteins has been fixed on lipidic vesicles with undefined purpose. While there is some evidence that the EVs membrane is important for the uptake process,[1] the role of the artificial membranes is not clear yet. Comparative studies of the effects over target cell lines with conventional liposomes and exosome-mimetic nanovesicles would be very useful to clarify this. The work in this field is reviewed in the section "Bottom-up methodologies: artificial membranes decorated with functional proteins to mimic EVs functions."

A critical evaluation of the *fully synthetic EVs* concept would imply providing an answer to questions such as: *What we are trying to mimic from EVs?; Is the biochemical composition, the morphology or the whole entity?; Is it worth mimicking a specific function?*. This is still a challenge in the field, since some of these questions are being answered at the same time for natural EVs. The best approach would involve an extensive biochemical characterization of natural EVs and a detailed description of their functions. Regarding functionality, other populations and not only the target cell lines should be assayed. This could give information about possible side effects. In the same way, multiple parameters should be registered as output factors, not just the process targetted by the EVs-based treatment. Proteins, nucleic acids, and lipid composition from specific types of exosomes are registered in specialized databases such as

ExoCarta,[25] EVpedia[26] and Vesiclepedia.[27] But this is not enough: a database with assays performed with EVs reporting treated cell lines, EVs type as therapeutical agents, tipe of assay (*in vitro* or *in vivo*) and experimental conditions could be of great interest to the scientific community. The combination of both sources of information would be the perfect scenario for the design of future artificial EVs-based therapies.

In any case, both types of artificial EVs should meet product specifications related to "purity, identity, quantity, potency and sterility" in concordance with the pharmaceutical market regulations.[28] Once more, there are some important differences in the definition of these parameters depending on the semi- or fully synthetic character of EVs. These key points will be considered and discussed in the following sections.

5.4. Semi-synthetic exosomes: biotechnological modification of naturally released exosomes

The simplest idea to manufacture EVs would be to use the natural mechanisms for the formation of vesicles, that is, the cellular machinery itself. It is known that the composition of the EVs at all levels responds to a high degree of control at very selective cellular mechanisms.[29] Therefore, the composition of the EVs could be controlled by intentional alteration of the cellular environment.

This method would lead to the creation of EVs with a composition profile adapted to a specific purpose. The technological methods used for bioengineering EVs are explained in the following sections. Two key aspects are the selection of producer cells (and their *in vitro* harvesting conditions) and the EVs isolation/enrichment procedures. Both choices will condition subsequent uses.

5.4.1 Selection of the EVs cellular origin

Cell lines could potentially release EVs vesicles, but there are great differences in release rate and biochemical composition and their susceptibility to modifications.[30] It is also accepted that before translation to clinical use of EVs, limitations regarding biocompatibility, economic viability, harvesting methods, and immunotolerance must be overcome. A summary of cell lines used for the production of EVs for clinical purposes, especially drug delivery, can be found in the literature.[31] Dendritic cells and cancer cell lines, such as melanoma, are the most used lines for EVs production.

Mesenchymal stem cells (MSCs) are one of the most promising sources of EVs, especially exosomes.[32] Yeo et al.[33] defended their use for mass production of exosomes with future therapeutic purposes based on some important facts related to their advantages over other cell lines. Mainly, MSCs are easy to obtain from all human tissues (even those considered as medical waste), and they have great *ex vivo* expansion capacity compatible with immortalization without compromising their therapeutic efficacy. These two facts are essential to establish a scalable and long-term source of well-characterised EVs, particularly exosomes.[14,28] In addition, their immunomodulatory effect gives them and their derived EVs important features in autologous and allogenic therapeutic applications.

Dendritic Cells (DCs) have important roles in immunity (both innate and adaptative). Some authors have paid attention to this cell line in order to enhance the production of clinical grade DC-derived exosomes for immunotherapy.[33] Properties of DCs have even been enhanced with different nanoparticles.[34] Exosomes from DCs modified to express indoleamine 2,3-dioxygenase (IDO), a tryptophan-degrading enzyme that is important for immune regulation and tolerance maintenance, have been used in the treatment of rheumatoid arthritis.[35] In another study, DC-derived exosomes modified to express FasL on the surface, (ligand involved in apoptosis induction), were tested as inflammatory and autoimmune therapy.[36] Other recent works are related to the role of tumour-released exosomes to load antigens into DCs for the therapy of malignant mesothelioma.[37]

To overcome the problem of low release rate, some authors lowered the micro-environmental pH, mimicking the natural cancer mechanism.[38] By culturing HEK293 cell lines at different pH, these authors found that low values of pH were the best to isolate high amounts of exosomes. In spite of the impact of these results, it would be necessary to test similar effects in non-cencerous cell lines and to determine how the change in the harvesting conditions affects EV composition (membrane components and cargo).

Not only human cell have been explored as EVs source: exosomes isolated from bovine milk and loaded with different drugs were a promising strategy for mass production of therapeutic EVs.[39] They can be easily isolated by differential centrifugation. The biocompatibility of milk-derived exosomes was checked by clinical

biochemical analysis in an animal model by oral gavage during 6 h (short-term toxicity) and 15 days (medium-term toxicity).

In recent years, some attention has been drawn to non-animal (especially plants) EVs and their potential use in therapy.[40] In particular, fruit-derived exosomes (lemon[41] and grapes[42]) have been isolated, characterized and tested as beneficial products. Perhaps this new source of EVs could be used in the near future for the development of EBSSNs following modifications to express the desired targeting molecules against specific cell lines. Evidences about immunotolerance should also be provided in order to avoid any interference in the results.

In any case, studies involving the encapsulation of the same drug into different cell lines-derived EVs would be desirable in order to clarify whether the beneficial effect is due to the drug or the combination of drug/type of carrier.

5.4.2 Obtaining a good substrate for modification: isolation procedures.

Since the final destination of artificial EVs would be the administration for therapeutic purposes, the highest level of standards would be required in order to preserve patient safety.[27,43] A key point in artificial EVs development is the enrichment from different biological samples, from cell-culture supernatants to several body fluids. There are different reviews[43-45] and technique-comparative papers[46-49] about isolation procedures. They involve ultracentrifugation, filtration, immunoaffinity isolation, polymeric precipitation and microfluidics techniques, with different degrees of purity for the final product.[50] In this chapter, we have focussed on scalability, reproducibility and synthetic EVs potential damage or physical modification.

Since the efficient function of EVs depends on their *size distribution,* aggregation and size changes after isolation are important. Lane et al.[47] studied these parameters in four isolation methods: two aggregation kits, a density-based method and ultracentrifugation. These authors found that some methods kept a constant vesicle size, but large differences were observed regarding yield of isolation (the two sedimentation methods gave recovery values two order of magnitude higher than the other methods). Another reported obstacle is the co-purification of material with similar physical characteristics to EVs.[42,51,52]

Scalability is also important, since the batch size is correlated- with the homogeneity of the final product; sometimes low-size batches are more prone to being susceptible to *bias* during the process, but on other occasions, higher batches yield more heterogeneous populations due to microenvironments during procedures.

The scale up step with ultracentrifugation (UC) is limited by the number of rotor positions and the maximum sample volume. On the other hand, methods such as Size Exclusion Chromatography (SEC) are easy to scale up by using large columns, but with the associated longer separation time. Pressure application to reduce processing time can disturb EVs.[43] Other methods, such as immunoaffinity isolations, are only used for small amounts of original sample because of the high price of the reagents required. Finally, microfluidic methods[45,53] are promising, with possibility to be coupled to online analysis.[54]

Reproducibility is crucial when the product is going to be used in the clinical field. Comparative results of UC are difficult to obtain due to the high number of models available in the market, and this could affect the quality of the isolated product.[43] The use of a fixed instrument would keep low variability between batches.[47]

Welton et al.[55] reported that ready-to-use SEC columns could overcome some problems related to homemade poured columns,[52] thereby avoiding variations from column to column, and facilitating robust protocols to be used routinely. The main problem associated with this method is dilution of EVs in the final sample and the subsequent need for concentration using precipitating agents or UC. This increases retention time and the possibilities of co-precipitation of other molecules with the same size and physical properties.

Considerable effort has been made in the field of EV isolation methods, which are still limiting the expansion of this field. There is not yet a perfect and universal method, and it is also accepted that selection of the isolation method could impact downstream steps.[56]

5.4.3 Strategies for biochemical modification

5.4.3.1 Pre-isolation modification using own cellular machinery

The advantages and disadvantages of the methods applied to incorporate proteins of nucleic acids are shown in **Table 5.2** and **Table 5.3**. Based on the study of exosome biogenesis-related mechanisms, several methods have been developed [50, 57-62].[50,57-62] The following criteria have been identified for their classification (see **Table 5.1**):

(I) location of exosomal functional entities, such as transmembrane proteins, and the use of their natural tropism to co-localized the exogenous element;

(II) strategies using molecular mechanisms for the introduction of exogenous molecules into EVs for cytosolic delivery;

(III) increasing the amount of molecules into the cellular plasma to be encapsulated by passive mechanism during MVB formation.

Table 5.1. *Classification of techniques for the production of artificial EVs, mainly exosomes, according to type of final product (semi- or fully synthetic) and the principle of the obtention mechanism*

Semi-synthetic exosome production: modification of vesicles naturally produced by cells	
Pre-isolation modification	
Class I	Co-localization of cargo and exosomal carrier moiety thanks to the natural tropism of the second
Class II	Use of sequences (i.e. nucleic acid-based sequences) for the exosomal biogenesis pathway signaling
Class III	Take the advantage of passive loading via increment of their presence, by genetic over-expression or active loading of producer cells
Post-isolation modification	
Class IV or *passive methods*	Methods that use passive adsorption of molecules into external surface of EVs, thanks to their hydrophobicity nature
Class V or *active methods*	*V.a (Physical methods)*, based on the creation of transitional alteration in the integrity of EVs that allows cargo to enter into the vesicles by concentration gradient or by passive incorporation during subsequent restoring of initial status post-stimuli V.b *(Chemical methods),* based on induced chemical reactions between EVs and cargo with or without previous introduction of functionalization agents into vesicles.
Creation of artificial mimetic structures of the natural exosomes	
Type I or *Top-down bionanotechnology*	Starting from larger substrates (cells) that are reduced to units for the creation of vesicles with reduced size
Type II or *Bottom-up bionanotechnology*	Starting with individual molecules (Lipids, proteins, etc.) that are assembled in a controlled way for generating complex structures of higher order

Class I methods (**Table 5.2**) involve the design of chimeric constructions of proteins by genetic engineering. In this case, the fusion between the gene of a protein to be incorporated and the gene of an exosomal-localized protein can be used for the

expression of the former on the outer surface of exosomes. This has been referred to in the literature as *Exosome Display* technology,[63] and it enables the manipulation of the protein content of exosomes and the subsequent tailoring of activities. The potential of the method was successfully demonstrated by the production of specific antibodies against human leukocyte antigen (HLA), a low immunogenic antigen.[64]

Lactadherin C1C2 domain was also used for similar purposes by Zeelemberg et al.[65] and Hartman et al.[66] to induce expression of chicken egg ovalbumin (OVA) peptide and the human epidermal growth factor receptor 2 antigen (HER2), respectively. Álvarez-Erviti et al.[67] described a method of inducing surface expression of the central nervous system–specific rabies viral glycoprotein (RVG) peptide on exosomes isolated from immature dendritic cells derived from mice. Complementarily, these brain-targeted exosomes were loaded with siRNA for the first time by electroporation. The delivery of GAPDH-siRNA specifically to neurons, microglia, and oligodendrocytes in the brain, resulted in a specific gene knockdown. This was considered the first example of EV-based genetic therapy. One of the most important facts of this work was the successful treatment of a highly protected tissue, the brain, in spite of the existence of brain-blood-barrier selectivity.

Tian et al.[68] used lysosome-associated membrane glycoprotein 2b to target electroporated doxorubicin loaded exosomes (20% of loading efficacy) produced in dendritic cells. Ohno et al.[69] used platelet-derived growth factor receptor transmembrane domain to anchor GE11 peptide, a ligand of the epidermal growth factor receptor (EGFR). This construction was transfected to Human Embryonic Kidney cell line 293 (HEK293) using pDisplay vector and FuGENE HD transfection reagent. As a model cargo, siRNA let-7 was selected for its ability to alter cell cycle progression and reduce cell division in cancer cells. This siRNA was introduced into EV producer cells by lipofection method. Modified exosomes (15-21 % of total released exosomes) were isolated by centrifugation and intravenously injected into an animal model with induced breast cancer. GE11 peptide as targeting moiety was selected by the elevated expression of his receptor (EGFR) in tumors of epithelial origin.

Table 5.2. *Pre-isolation methods for cargo incorporation into EVs*

Cargo incorporation previous to the release of exosomes					
Method	**EVs Modified component**	**Category of modification (according with table 1)**	**Advantages**	**Disadvantages**	**Molecules incorporated**
Genetic fusion of cargo gene with an exosomal protein gene	Surface	Class I	-Efficient exposure of targeting moiety on the surface of EVs -By selecting the EVs protein to be fusioned with, different expression rate can be achieved.	-Only successfully explored with exosomal membrane proteins	Peptides, small proteins such as GE11 peptide [69], HLA [63], OVA [65], HER2 [66], and RVG [67]
Exosome Surface Display Technology	Surface	Class I	-Suitable to induce expression of protein in both, extravesicular and intravesicular sides at the same time	-Not tested with high molecular weight proteins	-Fluorescent proteins [62] such as GFP and RFP
RNA zipcodes	Cargo	Class II	-Alternative to electroporation of miRNA	-Applicable only to mRNA and miRNA -Influence of mRNA size not tested	mRNA [70] and miRNA [71] modified with zipcodes
EXPLORE platform	Cargo	Class II	-Excellent platform to load proteins to be delivered to the cytosol of the target cell. -Expected better results than commercial solutions available.	-Limited loading capacity due to the presence of fluorescence reporter proteins in future work, this protein can be omitted	-mCherry, Bax, SrIκB and Cre recombinase proteins [61]
TAMEL platform	Cargo	Class II	-By selection of one component of the platform, the EV-enriched protein loading efficiency can be controlled	-High-cost effective method -Required highly experimented personal -EE values depending on RNA molecule size	RNA [59] with variable length
Over-expression of RNA cargo into producing cells	Cargo	Class III	-Used in all types of exosomes -Applicable to all types of RNA	-Nonspecific loading mechanism -Low efficiency, especially for mRNA	RNA and Proteins by expression of RNA into cell producer cytosol
Fusion with liposomes	Surface and/or cargo	Class III	-High efficiency -Both, hydrophilic and hydrophobic compounds can be loaded	-Cellular uptake rate can be decreased -Better efficiencies for hydrophobic molecules	-Hydrophobic and hydrophilic compounds, such as DiI and calcein respectively [72] -Photosensitizer drugs, such as ZnPc [72]

More recently, Stickney et al.[62] developed another genetic engineering method for surface expression of proteins in human cells, called *surface display technology*. In this case, tetraspanin CD63 was used as a scaffold for the presentation at both extravesicular and intravesicular orientations.

Class II methods englobe a heterogeneous group of strategies that have in common the use of specific molecular interaction between two elements and can be used to transport the complex into the exosomes.

One example of this strategy is the interaction between specific sequences in RNA molecules and proteins that are present in the route of exosomes formation.[16] Highly observed sequence motifs into RNA types studied into EVs, called EXOmotifs, was found in mRNA[70] and miRNA.[71] Exosomes for Protein Loading via Optically Reversible protein–protein interactions (EXPLORs) and Targeted and Molecular EV Loading (TAMEL) are technologies based on the molecular interaction between certain types of proteins or between RNA special structures and specific proteins. Proteins of interest can also be loaded into the inner compartment of exosomes for their direct delivery to the cytosol of the target cell as an alternative for therapeutic target locations. EXPLORs[61] has recently presented for that purpose. The system integrates two elements: one is composed by the genetic fusion of the photoreceptor cryptochrome 2 (CRY2) to the protein to be loaded, and the other is made by the fusion of a truncated version of the CRY-interacting basic-helix-loop-helix 1 (CIBN) to tetraspanin CD9. Both elements can be transitory attached by exposure to blue light, which induces the interaction between CRY and CIBN, and the interaction can be stopped once the blue light is not present.

TAMEL is another genetic engineering tool that has recently been published[59] for the active cargo of RNA. This platform is a fusion between an engineered EV-loading protein and the RNA to be loaded. Engineered EV-loading protein is also a fused product between an EV-enriched protein and an RNA-binding domain. This construction is transfected into EV producer cells to make his function. Different loading degrees can be obtained by selecting the EV-enriched protein. This is related to the natural expression of different proteins into EVs.

Class III methods includes the simplest method: passive loading into vesicles through their biogenesis. There can be two different approximations to this objective. First, the overexpression of RNA cargo in the producer cells. The major disadvantage of this method is the lack of selectivity in the loading process since it is gradient-driven (the higher the concentration in the cytoplasm, the higher its possibility of being trapped into exosomes during invagination of MVBs formation). On the other hand, the great advantage of the method is that by translation of mRNA into receptor cell cytoplasm, codified proteins can also be passively loaded into EVs.

The second approximation explores the active loading of the producer cells, i.e. by nanocarriers such as fusogenic liposomes. This strategy is based on physico-chemical properties that govern the type of mechanism (the fusiogenic properties of the two elements that take place in the method, cells and liposomes). Second, they modify the whole cell and not only the exosomes.

As an alternative method for the incorporation of exogenous molecules (specially designed for hydrophobic compound) into EVs, Lee et al.[72] presented the use of membrane fusogenic liposomes (MFLs). By the treatment of cells with MFLs loaded with a hydrophobic compound (DiI) and a hydrophilic molecule (calcein), these authors obtained EVs modified with both molecules. Only slight differences in the efficiency of incorporation into EVs were found, since a hydrophobic compound would remain in the plasma membrane after liposome fusion and in the subsequent formation of EVs membrane through their routes of biogenesis. In contrast, a hydrophilic molecule would be released into the cytosol. Intercellular transport of both molecules mediated by EVs was successfully observed *in vitro* in a multicellular tumor spheroid model.

A similar method was used to modify the composition of EVs, with special focus on the modification of the properties of the EV membrane.[57] Dyes, fluorescent lipids with different length and saturation grade of acyl chains, and chemotherapeutics were loaded into cells by means of EVs.

These authors carried out too a membrane surface modification, with the possibility of conjugation with molecules for targeting purposes. They first prepared MFLs containing azide-modified lipids which were fusioned with cells. By simple incubation with dibenzocyclooctyne (DBCO)-modified peptides, a covalent bond was created due

to the fast and selective reaction between DBCO and the azide group.[73] This strategy will allow new possibilities of surface ligand decoration on EVs for targeting purposes (such as peptides, aptens or antibodies) or for the introduction of molecules with therapeutic properties via interaction with selective receptors. By the combination of different head-group modified lipids, several different ligands could be incorporated into EVs outer membrane, including receptors and co-receptors.

5.4.3.2 Physical and chemical post-isolation modifications

These are the methods that require an external force (chemical or physical) to incorporate new molecules on previously isolated exosomes (**Table 5.3**).

Passive Methods. Incubation of EVs and cargo

The simplest way to incorporate any cargo into cell culture or body fluid isolated EVs is the co-incubation of both elements. This strategy was explored by Sun et al.[74] who found that curcumin exosome-loaded exhibited better stability and higher bioavailability in serum in an animal model. For these therapeutic-modified exosomes, an improvement at *in vivo* anti-inflammatory and septic-shock was observed.

In another study,[75] two anti-inflammatory compounds were loaded into exosomes and microparticles, and they were administrated intranasally, opening up new therapeutic possibilities. The effects of solvents and drug release kinetics from loaded exosomes by dialysis have been studied.[39,76]

Active Methods. Physical methods: electroporation and other temporary membrane disruptive methods

The most commonly used method for cargo incorporation into EVs after their release is electroporation.[77] This technique involves the temporary permeabilization of membranes through the creation of pores due to the application of high-voltage electricity. Some authors have pointed out that this method is not suitable for siRNA cargo into EVs due to technical problems, and an overestimated encapsulation into EVs could be observed. It has been reported that electroporation induces siRNA aggregation and co-pelletization with EVs during purification by ultracentrifugation, without dependence on electroporation buffer composition.[78] They also postulated that slight differences could be found between different EVs attending their cellular origin (e.g. primary cells).

Table 5.3. Post-isolation methods for cargo incorporation into EVs

Cargo incorporation after the release of exosomes					
Method	**EVs Modified component**	**Category of modification (according with table 1)**	**Advantages**	**Disadvantages**	**Molecules incorporated**
Co-incubation with exosomes	Cargo	Class IV	-The simplest method -Inexpensive -Compatible with the addition of a small amount of organic solvent for the enhancement of hydrophobic drug dissolution	-More suitable for hydrophobic molecules	Low and medium molecular weight hydrophobic molecules such as curcumin [74], placlitaxel [95], cucurbitacin I [75], celastrol [76] and different porphyrins [58] -Enzymes, such as Catalase [80]
Electroporation	Cargo	Class Va	-Used in all types of exosomes -Able to incorporate large compounds, such as 5 nm NPs	-Applicable only for hydrophilic compounds -RNA type-dependence effectivity -Slight differences in EE depending on the cellular origin (cell line) of the exosomes -Induce aggregation of siRNA, with valuable reduction in EE. -Exosome aggregation trend during electroporation process	-RNA, especially siRNA [67] -Different drugs such as placlitaxel [60], porphyrins [58] -SPIONs [79]
Extrusion	Cargo	Class Va	-Simple method	-Induces changes in EVs which reduce delivery efficiency	-Small molecules such as Porphyrins with different hydrophobicity [58], -Enzymes, such as Catalase [80]
Saponin-assisted loading	Cargo	Class Va	-Similar loading efficiency to electroporation, but without the associated problems -Saponin can enhance in some cases the efficiency of co-incubation	-Low efficiency for some big molecules, but better than simple incubation -Not tested with big molecules	
Hypotonic dialysis	Cargo	Class Va			
Sonication	Cargo	Class Va	-Enhance simple incubation through decreasing bilayer rigidity	-Not tested with hydrophilic molecules -Not tested with different EV populations	-Small molecules such as placlitaxel [95] or Doxorubicin -Enzymes, such as Catalase [80]
Click Chemistry	Surface	Class Vb	-Keep constant morphology or	-A two-step procedure with subsequent	-Fluorescent dyes such as azide-Flour 545 [81]

Another relevant problem concerning electroporation is exosome aggregation and subsequent decrease in functionality. To avoid these problems, Hood et al.[79] electroporated exosomes from mouse B16-F10 melanoma cells by incorporating 5 nm superparamagnetic iron oxide nanoparticles (SPIONs) as model exogenous cargo. Other authors compared the loading efficiency of different porphyrins with different hydrophobicities into EVs with various origins by passive loading (co-incubation), and by active loading, such as electroporation, extrusion, saponin-assisted drug loading and hypotonic dialysis.[58] The best results were obtained for hydrophobic compounds and for electroporation. Interestingly, zeta potential (ζ) related to the chemical composition of EV membranes seems to play a role in loading efficiency, since higher ζ values led to higher EE. The chemical properties of cargo are also relevant, since their charge will condition the final outcome. Electroporation did not induce drug precipitation.

In contrast, extrusion over polycarbonate membranes altered the morphology of vesicles and, subsequently, their delivery efficacy. Other authors used the sonication of EVs in the presence of drug solutions.[60] The loading efficacy was found to follow the order: incubation at RT < electroporation << mild sonication. A similar trend was observed for size changes after the loading procedure. On the other hand, surface charge and protein profile were similar after loading, evidencing no alteration in exosome stability. These authors explained the results concerning sonication as a decrease in bilayer rigidity after sonication, which allowed a better incorporation of the hydrophobic drug. Therefore, mild sonication should be considered as an enhancement of co-incubation. Additionally, loaded exosomes were stable over large periods of time at different temperatures.

A similar comparative study was carried reported, with the enzyme catalase.[80] For the preparation of exosomes modified with this oxidative stress-protecting agent used for the treatment of Parkinson's disease, these authors selected four methods: incubation at RT in the presence/absence of saponin, freeze/thaw, sonication, and extrusion. Sonication yielded the higher EE (26.1 %) and the more stable product. In contrast, this method also produced the higher increment in size, from 105 nm naïve exosomes to 183.7 nm in catalase-loaded exosomes. Associated with size increment, AFM observation also revealed a change in morphology, with a final non-spherical shape.

Despite these promising results regarding the encapsulation of different molecules into exosomes, standardization in systematic conditions followed by the study of several cell lines is still necessary to strongly support the use of these methods as routine practice in the clinical field.

Chemical methods: click-chemistry mediated functionalization and other targeted drug delivery strategies

The chemical copper-catalyzed reaction between an alkyne and an azide that forms a triazole linkage (*click-chemistry*) has been used for the surface functionalization of exosomes.[81] These were first chemically modified by the incorporation of alkyne groups into amine groups from proteins by carbodiimide chemistry.[82] These authors conjugated azide-Fluor 545 (a fluorescent compound) to activated EVs. Since no differences in morphological and functional properties were found, it was concluded that modification by *click chemistry* does not alter exosome characteristics, and allows the incorporation of exogenous molecules to the surface of EVs.

Finally, there is another type of cargo modification that has been applied into artificial vesicular systems (liposomes) with potential applicability to EVs. This method is based on the ability of some peptides to be incorporated into lipidic membranes causing disruption.[83,84] By fusion of the peptide D1-7 to an adhesion molecule expressed in cells, targeted lipidic carriers with therapeutic cargo were produced and successfully tested *in vitro* and *in vivo*. Another interesting application of this strategy is its ability to insert peptidic cargo into live cell membranes, giving possibilities of imaging live cells and modifying cell surface. This last property could be explored for the modification of plasma membrane in EV producer cells.

The modification of EVs membrane results in changes in surface charge, fusiogenic properties, immunogenicity decrease, and colloidal stability.[85] Engineered hybrid exosomes were prepared by membrane fusion with liposomes formulated with different types of lipids (i.e. zwitterionic, anionic, cationic and PEGlilated). Fusion properties with cell culture-derived exosomes were studied according to the chemical nature of liposomes lipids.[86] It was found that zwitterioninc and anionic lipids did not alter the uptake rate, while the introduction of cationic lipid greatly decreased the phenomena, and PEGilated lipid increased it by two-fold. Therefore, it can be

concluded that functional properties could be tuned by modifying the membrane composition.

5.5. Top-down and bottom-up methods for the development of full synthetic EVs

5.5.1. Production of artificial EVs by generation of plasma membrane fragments: a top-down inspired methodology

Approaches based on top-down nanotechnology have been developed for the production of EVs mimetic nanovesicles using cells as precursors of plasma membrane fragments. Those strategies rely on the principle of self-assembly of lipids and lipid membranes into spherical structures and the encapsulation of surrounding material into the aqueous cavity of generated nanovesicles. Current methods include extrusion over membrane filters,[16,17,87] hydrophilic microchannels[88] or cell slicing by Si_xN_y blades (see **Table 5.4**).[18]

5.5.1.1. Extrusion over polycarbonate membrane filters

Jang et al.[16] used a serial extrusion through polycarbonate membrane filters with a decreasing pore sizes (10 μm, 5 μm, and 1 μm) in a mini-extruder, similar to those commonly used for the preparation of liposomes. Human monocytes were chosen as precursors for membrane fragments. The yield production of NVs was 100 fold in comparison with the production of exosomes by using the same number of cells. Morphological studies of these NVs by crio-TEM and NTA showed many similarities with the exosomes, round shape and a peak diameter around 130 nm. Even the exosomal protein marker profile (CD63, Tsg101, moesin and beta-actin) checked by Western blot was identical for the NVs and exosomes. The chemotherapeutic drugs, doxorubicin, 5-FU, gemcitabine and carboplatin were added to the buffer where cells were resuspended. The encapsulation efficiency in the final purified NVs was found to be dependent on the initial amount of added drug.

Table 5.4. *Summary of the published work about the generation of mimetic EVs nanovesicles by Top-Down bionanotechnology. Cell source and type of cargo are encapsulated, and main characteristics are given.*

Generation technique	Precursor Cell Type	Type of material encapsulated	Nanovesicles characteristics	Reference
Manual extrusion over polycarbonate membrane filters	Monocytes and macrophages	Exogenous, chemotherapeutic drugs	-Mean size and distribution similar to exosomes -Exosomal protein profile similar to natural exosomes -EE of chemotherapeutics dependent on the original amount used during extrusion -High rate of drug release -100 times more nanovesicles than exosomes from the same number of cells -Results reproducible with different cell types	[16]
Pressurization and extrusion over hydrophilic parallel microchannels in a microfluidic device	Murine embryonic stem cells	Endogenous, proteins and RNA	- Average size in the exosome range - Similar intracellular and membrane protein and total RNA profile to the original cells and exosomes -Same ability to deliver RNA content as exosomes	[88]
Centrifugal force and extrusion over a filter with micro-size pores into a polycarbonate holder structure	Murine embryonic stem cells	Endogenous, proteins and RNA	-NVs size and morphology similar to exosomes -Cargo of RNA, intracellular proteins and plasma membrane proteins similar in types to exosomes -Small RNA profile differs in quantity, especially in miRNA respect to exosomes -Intravesicle contain twice concentrate in comparison to natural exosomes -250 fold times more vesicles than naturally secreted exosomes	[87]
Slicing living cell membrane with silicon nitride blades in a microfluidic device	Murine embryonic stem cells	Exogenous, polystyrene latex beads	- Generated NVs in the size range of exosomes - Nanovesicle production 100 fold time more productive than natural exosome -30% of EE for 22 nm nanoparticles as model of exogenous material encapsulation -NVs can deliver exogenous encapsulated material	[18]

Looking for a scaled-up process using extrusion as generation procedure of NVs, Jo et al.[87] developed a device that uses centrifugal force to extrude cells over polycarbonate filters (10 μm and 5 μm of pore sizes). The device has a central piece where filters are located and connected to two syringes where the sample is dispensed by the centrifugal force. Uniform-sized 100 nm NVs with a yield 250-fold higher than

that of exosome from the same number of cells was achieved. Analysis of the filters by TEM showed that many cells remained trapped in the structure.

The same device previously cited was employed by Jeon et al.[17] to produce exosome-mimetic NVs from murine embryonic stem cells for the treatment of mice isolated skin fibroblasts. These authors wanted to explore the potential of mimetic exosomes to induce proliferation and recovery after injury in an *in vitro* model. Genomic and proteical profiles similar to original cells were assessed by PCR and Western blotting of specific markers, and it was confirmed that successful delivery of genetic material by NVs was reached.

5.5.1.2 Pressurization, extrusion, and slicing over hydrophilic parallel microchannels in a microfluidic device

Jo et al.[87] produced exosome-mimetic nanovesicles by extruding cells over hydrophilic microchannels, with the aim of delivering endogenous RNA across plasma membrane with high efficiency and low toxicity. These authors developed a microfluidic device made of PDMS by soft lithography. This device had an array of 37 parallel microchannels, with a common inlet and outlet connection for the pumping with a syringe pump and the collection of NVs, respectively. The higher amount of nanovesicles generated by extrusion over hydrophilic channels with a similar size to exosomes was obtained with a length of 200 μm and a width of 5 μm. These results showed that an appropriate total shear force induced by the channel has to be reached in order to produce NVs with acceptable results. This force is responsible for NV generation due to elongation of the plasma membrane on the microchannel surface. When the elongated membrane reaches a certain value, it breaks into small portions that directly form nanovesicles, thanks to the self-assembly property of lipids in aqueous media.

With the appropriate channel morphology, these authors produced 100 nm nanovesicles similar in composition (proteinical and nucleic acid profile) to naturally produced exosomes. The analysis of these NVs[88] revealed that the formation of exosome-like NVs through hydrophilic channels produced a delivery system of endogenous material with identical results as exosomes.

More recently, Yoon et al.[18] reported the production of exosome-mimetic nanovesicles by the slicing of cells through Si_xN_y blades aligned to the flow direction

over hydrophilic microchannels. These authors combined the induced shear stress formation on NVs with the fragmentation of plasma membrane by the blades to obtain fragments for the generation of exosome-like nanovesicles and the co-encapsulation of exogenous material, (polystyrene latex beads as a model substance). It was found that NV diameter increased as the width channel increased. This is because channel morphology is proportional to Reynolds number (*Re*). In this particular case, *Re* is proportional to the hydraulic diameter and, therefore, to the inertial force, which directly increases with the channel width. In other words, NVs travelling through wide channels have higher inertial force when they reach the blades, generating larger sliced fragments that produce bigger NVs. These have a similar composition to that of parental cells and naturally released exosomes by those cell lines.

One of the most interesting works in the literature[18] describes the encapsulation of 22 nm fluorescent polystyrene latex beads as an exogenous simulated material, adding these nanoparticles to the media where cells were diluted before slicing. With a final corrected EE of 30 %, these NVs containing exogenous material were given to fibroblasts in an *in vitro* experiment. After a period of time, red dots corresponding to fluorescent beads were detected in the cytoplasm of fibroblast by confocal microscopy. The delivery efficiency of encapsulated beads into exosome-like NVs was higher than that of bead-aggregated NVs, revealing that exogenous material delivery with these NVs was possible, but the efficiency was still lower than that achieved with parental cell-components generated NVs.

5.5.2 Bottom-Up methodologies: artificial membranes decorated with functional proteins to mimic EVs functions

The third option for obtaining artificial EVs is their construction in a fully synthetic way by assembling individual molecules (lipids, proteins and cargo) into complex structures, such as a bilayer structure resembling EVs membranes functionalized with proteins for mimicking EVs function. This could be achieved by assuming that not all components in natural exosomes are essential for specific and efficient delivery,[13] including the transport of a message through direct contact with target cell receptors. Another assumption that encourages researchers to explore this route is that, from a structural and biochemical point of view, exosomes are liposomes with attached proteins. Therefore, this type of vesicular systems could be an ideal substrate to

develop exosome-mimetic structures. The main functional components of exosomes to be incorporated in mimetic materials have been reviewed.[13] The three main components of exosomes reported were lipids, membrane proteins and therapeutic cargo.

One of the main advantages of fully artificial EVs over previous strategies is the production of pure and well-defined biomaterial. In addition, production strategies of artificial EVs based on liposomes are more sustainble and easier to scaled up.[11,89] This fact is quite important for preclinical and clinical studies and in order to manufacture products ready to be sent to the market.[2]

Liposome preparation techniques have been extensively reviewed,[89-101] but not all the methods yield vesicles suitable to becoming an artificial exosome. It could be considered that only small unilamellar vesicles (SUVs) are ideal precursors due to their similarities to natural exosomes (size range and membrane disposition).

Methodologies for SUV preparation (**Table 5.5**) can be classified according to different criteria.[92] For example, number of steps to reach SUV. Another classification is based on the physical principle applied to prepare vesicles: mechanical processes, organic solvent replacement, detergent removal and other techniques as microfluidic-based methods. Reverse-phase evaporation, ethanol injection method, ether injection method (EtIM), thin-film hydration method (TFH), homogenization techniques, French press cell extrusion, microfluidization, extrusion over membranes, ultrasound and membrane contactors are some of the techniques developed for SUV preparation.

All these techniques rely on the self-assembly of amphiphilic molecules, such as lipids, in ordered structures due to their physicochemical behavior in aqueous media.[93,94] This principle is at the basis of bottom-up nanotechnology. Vesicles with a size-range close to that of natural EVs could be obtained[95] when operational variables were oprtimized by design of experiments. In addition, a wide spectrum of molecules with biological activity, independently of their physicochemical nature (hydrophilic or hydrophobic, low molecular weight or macromolecules) can be incorporated into liposomes, during or after their formation.[96]

Table 5.5. *Advantages and disadvantage of most frequently used methods for Small Unilamellar Vesicles (SUVs) preparation*

Method	One-step method for SUVs preparation	Physical method applied for preparation	Advantages	Disadvantages
Ether Injection Method (EIM)	Yes	Organic solvent replacement	-Scale-up adapted -High hydrophobic compound encapsulation -No mechanical degradation of compounds	-Not suitable for thermosensitive compounds -Solvent not suitable for some biocompounds
Ethanol Injection Method (EIM)	Yes	Organic solvent replacement	-Scale-up adapted -Non-dangerous substances are handled -High hydrophobic compound encapsulation -No mechanical degradation of compounds	-Ultrasounds are needed when concentrated samples are produced -Low encapsulation efficacies of low molecular weight hydrophilic compounds -Not suitable for thermosensitive compounds
Reverse-Phase Evaporation (RPE)	No	Emulsification/organic solvent replacement	- Widely used. -Suitable for mass production	-Frequently used solvents are not suitable for some biocompounds
Thin Film Hydration Method (TFH)	No	Mechanical processes	-Applied for any type of amphiphilic molecules -High encapsulation of Hydrophilic compounds compared to other methods	-Difficult to scale up production -Timely and costly ineffective due to necessary downsizing techniques
Downsizing Techniques **-French press cell extrusion** **-Microfluidization** **-Extrusion over membranes**	/	Mechanical processes	-Good reproducibility -Adapted to scale-up requirements	-Product loss associated with clogging of membrane by concentrated samples
Ultrasounds	Yes	Mechanical processes	-Simple methodology -Possibility to be scaled-up	-Degradation of biological compounds -Scale-up un-adapted

Functionalization of liposomes with biomolecules is possible, owing to the different headgroup-modified lipids that are available.[97] Headgroup modification usually includes a molecule of polyethylene glycol as a spacer between the functional group and the polar region of the lipid. This avoids the sterical hindrance caused by the proximity of biomolecules and liposome surface. The chemical modification includes the introduction of different types of functional groups, such as biotin, amine, maleimide, carboxylic acid, folate, cyanur, DBCO, azide, and succinyl. These groups

determine the crosslinking strategy[98-101] which should not compromise the biological function. Bioconjugation should ideally show ideally be carried out under mild conditions, aqueous media, chemoselectivity, and with a high yield.

Successful conjugation of peptides/proteins with liposomes can be checked using conventional molecular biology techniques such as dot-blot,[15] SDS-PAGE, or even flow cytometry.[102] A preliminary purification step is required in order to remove unconjugated biomolecules. For this purpose, authors have used classical separation methods, such as ultracentrifugation[102] or gel filtration[15,103] (SEC) with high exclusion limit resins (Sepharose CL-2B, 4B mainly). Dyalisis, however, is not used due to the high molecular weight of biomolecules selected for mimicking exosomes.

Undecorated liposomes have also been used in the EVs research field, as EV model for comparing isolation efficacy and physical integrity,[47] detection by flow cytometry,[104] and EV refractive index study.[105] However, their use as scaffold for artificial EV development could offer new possibilities in basic research about EVs and theranostic applications. To date, there are been few examples of this approximation for the development of mimetic exosomes, and no comparative results are available owing to the great differences between the methods used. A summary of the main experimental work on mimicking exosome by bottom-up nanotechnology is given at **Table 5.6** and briefly commented below.

The most frequent preparation technique for SUVs as templates for EVs mimicking is the TFH method combined with extrusion over polycarbonate membranes and with[102] or without[15] previous freeze-thaw cycles. Martínez-Lostao et al.[102] had a formulation that included lipids and stoichiometry inspired in natural exosomes. The introduction of only 5% (w/w) of an iminodiacetic acid derivative or DOGS-NTA allowed the binding of APO2L/TRAIL-His_{10} to liposomes in a single step. Its bioactivity was a higher activity than that of the soluble ligand. Moreover, a treatment based on these synthetic exosomes achieved 60% of disease improvement in a rheumatoid arthritis-induced animal model. In another study, liposome-bound Apo2L/TRAIL overcame the resistance to the soluble ligand exhibited by chemorresistive tumor cell mutants.[106] The mechanism of action of LUV-TRAIL in hematologic cells[107] was also studied by using mimetic structures of exosomes.

Table 5.6. *Summary of published work about the development of mimetic EVs nanovesicles by bottom-up bionanotechnology. Formulation of the vesicles, molecules for the surface functionalization and main physical characteristic (size) are given.*

Formulation	Preparation Method	Conjugation strategy	Size	Protein for functionalization	Reference
PC:SM:Cho:DOGS-NTA (55:30:10:5) weight ratio For fluorescent labelling, 0.25% mole/mole **DSPE-RhodB**	Thin film Hydration Method (KCl 100 mM, HEPES 10 mM pH 7.0, EDTA 0.1 mM; KHE buffer) Filtered and degassed + Extrusion over 200 nm membranes	Ni^{2+}NTA headgroup functionalized lipid + histidine-tagged recombinant peptides 37° C, 30 min	150-200 nm	APO2L/TRAIL-His_{10}	[102]
PC:Cho:DSPE-PEG:DSPE-PEG-MAL (1:0.5:0.04:0.01) Molar ratio For fluorescent labelling, 1% of PC amount of **DSPE-RhodB**	Thin film Hydration Method (Hepes 25mM, NaCl 140mM; pH 7.4) Filtered and degassed + Extrusion over 100 nm membranes	Maleimide headgroup functionalized lipid + Traut's reagent protein activation 1h RT 20/1 ratio	100 nm	MHC class I peptide complexes and FAB regions against T cell receptors (adhesion, early and late activation, and survival)	[15]
Microemulsion phase **PC:CpEL** (7:3, w/w) Micelle phase In 10:1 v/v DE:A **DOPE:DC-Cho** (4:1, w/w) In 1:2 v/v EtOH:DW	Micro-emulsion and micelle combining method + Sonication Step for 3min	Carboxilic group from ChoS and amine group from protein EDC/NHS 4°C for 12 h	82 nm	Monoclonal antibody against DEC205 antigen expressed on Dendritic Cells	[103]

Another approximation to artificial EVs (exosomes) for therapeutic purposes was carried out by De la Peña et al.[15] using a reported formulations.[108,109] The main components were phosphatidylcholine and cholesterol, and headgroup-modified lipids such as DSPE-PEG-MAL. In order to make traceable NVs, both *in vivo* and *in vitro*, a fluorescent lipid was included into the formulation, and magnetic nanoparticles (SPIONs) were encapsulated during thin-film hydration step. After optimization of chemical-activated ligands binding, mimetic SNVs simulating DCs derived exosomes were successfully tested as new tools in basic and clinical immunology. A T-Cell expansion rate higher than that with previously reported experiences using conventional methods was achieved.

An innovative methodology for the production of protein encapsulated nanoliposomes was also reported.[103] They produced 82 ± 4 nm antibody-coated liposomes with aprox. 93 % EE of BSA. The preparation route that combined a micro-emulsion containing the protein to be encapsulated, with micelles, in order to create a lipid bilayer formed through layer-by-layer assembling. In this work, authors selected a Box-Behnken experimental design to optimize (maximize) the EE by adjusting some formulation parameters. The final optimized formulation is summarised in Table 4.9. In this particular case, researchers selected mimetic exosomes for the potential transmission of antigen to DCs by a controlled target delivery using a conjugated monoclonal antibody anti-DEC205, a highly expressed receptor on the surface of DCs. The introduction of cholesterol succinate in the outer layer of the liposomes allowed the bioconjugation of the Ab by EDC/NHS chemistry.

Despite the promising results and the advantages of these methods for the development of liposome-based artificial EVs, there are some limiting aspects that hinder the transfer to the clinical field. While technological progress has allowed the design, development and production of nanomedicines with high pharmaceutical grade, their clinical impact has been smaller than expected due to a lack of sufficient information about *in vivo* interactions and fates inside the human body.[11] Specific challenges[13] are related to the functionalization of vesicle surface with a combination of functional proteins at the same time because actual methodologies are time-consuming and because of the incorporation of nucleic acids with acceptable efficiencies. The dependence of vesicle formulation on parameters such as fusion properties and stability could be another limit of special relevance to immunotolerance. Finally, the knowledge about key components in exosomes is not yet complete, since they may vary from one cell line to another. They could even be health-state-dependent and sensitive to harvesting conditions.

Despite attempts to mimic the exosome natural lipid composition, there is a need for actually checking whether the formulation is active and involved in the expected functions or is just a passive element involved only in the scaffolding of true functional elements. Comparison of the efficiency of the intended integrated component in differently formulated vesicles could be an interesting experiment to elucidate the role of membrane components. Parameters of uptake route and incorporation efficiency could also be measured with different cell lines, in order to assess the role of the target

cell. Other compounds as an alternative to lipids, with a high grade of biocompatibility, could also be used for the formulation of artificial exosome bilayers. One option is to use non-ionic surfactants[110] for the preparation of niosome-based artificial exosomes. These compounds offer some advantages[111] over lipids, such as price, versatility and sustainability. On the other hand, their chemical structure offers enhanced stability from both a chemical and physical points of view. Niosomes with size range close to EVs can also be produced.[95]

In recent years, microfluidics has been playing an important role in the development of enhanced vesicular systems, enabling robust and highly controlled preparation routes of vesicles[112] and allowing rapid characterization of products.[113] Another important aspect in the development of exosome-based therapy, regarding any preparation route, is the creation of reduced systems for the study of traffic and delivery into *in vivo* microenvironments.[19] Again, microfluidic-based systems are opening new possibilities by the development of organ-on-a-chip platforms that enable the study of these processes in an innovative and highly efficient way.[114]

It is expected that microfluidic synthesis of nanovesicles will open the path for new artificial EVs routes, with the required control of size and EE, and minimal consumption of reagents.

Other recently explored drug-delivery systems have developed platelet-mimetic nanoparticles by also using bottom-up technology. These authors have produced unilamellar polymeric nanoparticles functionalized with immunomodulatory and adhesion antigens, and they have tested them as another approach to diseasetargeted delivery.[115]

5.6. Conclusions and future perspectives

Knowledge about all the biological aspects related with EVs, especially exosomes, has opened up new frontiers in the clinical field. After an explosion of publications in recent years about the role of EVs in physiological and pathological conditions, novel opportunities for the development of enhanced therapeutic biomaterials have arisen. These observations could help in the production of new materials inspired by natural vesicles, without the classical inconveniences associated with up-to-date synthetic alternatives (liposomes, polymersomes, inorganic nanoparticles, etc.). EV-based therapies include tissue regeneration or immunomodulation, but drug delivery is one

of the most promising applications. Production, isolation, modification, and purification at large-scale clinical grade are the main limitations of EVs becoming a true clinically settled therapeutic agent.

These limitations have promoted the development of mimetic material inspired by EVs, the so-called artificial EVs. In this chapter we have introduced a systematic classification of the types of artificial EVs according to their preparation routes. Two well-defined strategies have been developed: semi-synthetic or fully synthetic products. The first strategy uses natural exosomes as precursors that are modified at the moment of their biogenesis (pre-isolation modifications), whereas the second strategy modifies the vesicles after their release by cells and their isolation from cultured media or biological fluids. Genetic engineering-based modifications, active loading platforms, specific signaling sequences for selective sorting or precursor cell modifications with nanomaterials are some of the methods developed for exosome-based semi-synthetic nanovesicle production.

Fully synthetic vesicles with EVs mimetic properties can be produced by bio-nanotechnology. Top-down techniques that produce vesicles made of membrane fragments obtained from the extrusion or slicing of cells, or bottom-up techniques that take advantage of supra-molecular chemistry (mainly self-assembly) to produce vesicles from individual molecules, represent the technology developed for that purpose.

Despite the great potential of artificial EVs, some limitations to their development as therapeutic tools have been identified. There is not a perfect technique, and, depending on the final purpose of artificial EVs, combinations of procedures could offer new insights in the field. Systematic studies with different cellular origins and target cell lines would expand and consolidate the applications of artificial exosomes. Comparative work including the encapsulation into different artificial vesicles would be interesting in order to identify effects due to the carrier.

Multidisciplinary teams with complementary actions in the fields of applied biology, pharmacology, chemical engineering, material sciences and medicine, would allow the definitive consolidation of these therapeutic biomaterials in clinical routines.

5.7. Referencias bibliográficas

[1] Yáñez-Mó, M., Siljander, P.R.M., Andreu, Z., Bedina Zavec, A., Borràs, F.E., Buzas, E.I., ... & Colás, E. (2015). Biological properties of extracellular vesicles and their physiological functions. Journal of extracellular vesicles, 4(1):27066.

[2] Lener T., Gimona M., Aigner L., et al. Applying extracellular vesicles based therapeutics in clinical trials – an ISEV position paper. J. Extracell. Vesicles 2015;4:30087.

[3] Tran TH, Mattheolabakis G, Aldawsari H, et al. Exosomes as nanocarriers for immunotherapy of cancer and inflammatory diseases. Clin Immunol. 2015;160:46-58.

[4] Aline F, Bout D, Amigorena S, et al. (2004). Toxoplasma gondii antigen-pulsed-dendritic cell-derived exosomes induce a protective immune response against T. gondii infection. Infect Immun. 2004;74:4127-37

[5] Dalal J, Gandy K, Domen J. Role of mesenchymal stem cell therapy in Crohn's disease. Pediatr Res. 2012;71:445-51.

[6] Lamichhane TN, Sokic S, Schardt JS, et al. Emerging roles for extracellular vesicles in tissue engineering and regenerative medicine. Tissue Eng. Part B Rev. 2015;21:45-54.

[7] Batrakova EV, Kim MS. Using exosomes, naturally-equipped nanocarriers, for drug delivery. J. Control. Release. 2015;219:396-405.

[8] Tan A, Rajadas J, Seifalian AM. Exosomes as nano-theranostic delivery platforms for gene therapy. Adv. Drug Deliv. Rev. 2013;65:357-367.

[9] van Dommelen SM, Vader P, Lakhal S, et al. Microvesicles and exosomes: Opportunities for cell-derived membrane vesicles in drug delivery. J. Control. Release. 2012;161:635-644.

[10] Ha D, Yang N, Nadithe V. Exosomes as therapeutic drug carriers and delivery vehicles across biological membranes: Current perspectives and future challenges. Acta Pharm. Sin. B. 2016;6:287-296.

[11] van der Meel R, Fens MHAM, Vader P, et al. Extracellular vesicles as drug delivery systems: Lessons from the liposome field. J. Control. Release. 2014;195:72-85.

[12] El Andaloussi S, Lakhal S, Mäger I, et al. Exosomes for targeted siRNA delivery across biological barriers. Adv. Drug Deliv. Rev. 2013;65:391-397.

[13] Kooijmans SAA, Vader P, van Dommelen SM, et al. Exosome mimetics: A novel class of drug delivery systems. Int. J. Nanomedicine. 2012;7:1525-1541.

[14 Lakhal S, Wood MJA. Exosome nanotechnology: An emerging paradigm shift in drug delivery. Bioessays. 2011;33:737-741.

[15] De La Peña H, Madrigal JA, Rusakiewicz S, et al. Artificial exosomes as tools for basic and clinical immunology. J. Immunol. Methods. 2009;344:121-132.

[16] Jang SC, Kim OY, Yoon CM, et al. Bioinspired exosome-mimetic nanovesicles for targeted delivery of chemotherapeutics to malignant tumors. ACS Nano. 20013;7:7698-7710.

[17] Jeong D, Jo W, Yoon J, et al. Nanovesicles engineered from ES cells for enhanced cell proliferation. Biomaterials. 2014;35:9302-9310.

[18] Yoon J, Jo W, Jeong D, et al. Generation of nanovesicles with sliced cellular membrane fragments for exogenous material delivery. Biomaterials. 2015;59:12-20.

[19] Forterre A, Jalabert A, Berger E, et al. Proteomic analysis of C2C12 myoblast and myotube exosome-like vesicles: A new paradigm for myoblast-myotube cross talk?. PLoS One. 2014;9:e84153.

[20] Bryniarski K, Ptak W, Jayakumar A, et al. Antigen-specific, antibody-coated, exosome-like nanovesicles deliver suppressor T-cell microRNA-150 to effector T cells to inhibit contact sensitivity. J. Allergy Clin. Immunol. 2013;132:170-181.

[21] Regente M, Corti-Monzón G, Maldonado AM, et al. Vesicular fractions of sunflower apoplastic fluids are associated with potential exosome marker proteins. FEBS Letters. 2009;583:3363-3366.

[22] Prado N, de Dios Alché J, Casado-Vela J, et al. Nanovesicles are secreted during pollen germination and pollen tube growth: A possible role in fertilization. Mol. Plant. 2014;7:573-577.

[23] García-Manrique P, Gutiérrez G, Blanco-López MC, Fully Artificial Exosomes: Towards New Theranostic Biomaterials, Trends in Biotechnology, in press.

[24] Laulagnier K, Motta C, Hamdi S, et al. Mast cell- and dendritic cell-derived exosomes display a specific lipid composition and an unusual membrane organization. Biochem. J. 2004;380:161-171.

[25] Simpson RJ, Kalra H, Mathivanan S. ExoCarta as a resource for exosomal research. J. Extracell. Vesicles 2012;1: 18374.

[26] Kim DK, Lee J, Simpson RJ, et al. EVpedia: A community web resource for prokaryotic and eukaryotic extracellular vesicles research. Semin. Cell Dev. Biol. 2015;40:4-7.

[27] Kalra H, Simpson RJ, Ji H, et al. Vesiclepedia: A compendium for extracellular vesicles with continuous community annotation. PLoS Biol. 2012;10:e1001450.

[28] Gimona M, Pachler K, Laner-Plamberger S, et al. Manufacturing of human extracellular vesicle-based therapeutics for clinical use. Int. J. Mol. Sci. 2017;18:1190.

[29] Villarroya-Beltri C, Baixauli F, Gutiérrez-Vázquez C, et al. Sorting it out: Regulation of exosome loading. Sem. Cancer Biol. 2014;28:3-13.

[30] Yeo RWY, Lai RC, Zhang B, et al. Mesenchymal stem cell: An efficient mass producer of exosomes for drug delivery. Adv. Drug Deliv. Rev. 2013;65:336-341.

[31] B. Johnsen, J.M. Gudbergsson, M.N. Skov, L. Pilgaard, T. Moos, M. Duroux, A comprehensive overview of exosomes as drug delivery vehicles—Endogenous nanocarriers for targeted cancer therapy. Biochim. Biophys. Acta - Reviews on Cancer. 1846 (2014) 75-87.

[32] Lai RC, Yeo RWY, Tan KH, et al. Exosomes for drug delivery—a novel application for the mesenchymal stem cell. Biotechnol. Adv. 2013;31:543-551.

[33] Lamparski HG, Metha-Damani A, Yao JY, et al. Production and characterization of clinical grade exosomes derived from dendritic cells. J. Immunol. Methods. 2002;270:211-226.

[34] Klippstein R, Pozo D. Nanotechnology-based manipulation of dendritic cells for enhanced immunotherapy strategies. Nanomedicine: Nanotechnology, Biol. Med. 2010;6:523-529.

[35] Bianco NR, Kim SH, Ruffner MA, et al. Therapeutic effect of exosomes from indoleamine 2,3-dioxygenase–positive dendritic cells in collagen-induced arthritis and delayed-type hypersensitivity disease models. Arthritis Rheumatol. 2009;60:380-389.

[36] Hee Kim S, Bianco N, Menon R, et al. Exosomes derived from genetically modified DC expressing FasL are anti-inflammatory and immunosuppressive. Mol. Ther. 2006;13:289-300.

[37] Mahaweni N, Lambers M, Dekkers J, et al. Tumour-derived exosomes as antigen delivery carriers in dendritic cell-based immunotherapy for malignant mesothelioma. J. Extracell. Vesicles. 2013;2: 22492.

[38] Ban JJ, Lee M, Im W, et al. Low pH increases the yield of exosome isolation. Biochem Biophys Res Commun. 2015;461:76–79.

[39] Munagala R, Aqil F, Jeyabalan J, et al. Bovine milk derived exosomes for drug delivery. Cancer Lett. 2016;371:48–61.

[40] Zhang M, Viennois E, Xu C, et al. Plant derived edible nanoparticles as a new therapeutic approach against diseases. Tissue Barriers. 2016;4(2):e1134415.

[41] Raimondo S, Naselli F, Fontana S, et al. Citrus limon derived nanovesicles inhibit cancer cell proliferation and suppress CML xenograft growth by inducing TRAILmediated cell death. Oncotarget. 2015;6:19514–19527.

[42] Pérez-Bermúdez P, Blesa J, Soriano JM, et al. Extracellular vesicles in food: experimental evidence of their secretion in grape fruits. Eur J Pharm Sci. 2017;98:40–50.

[43] Witwer KW, Buzás EI, Bemis LT, et al. Standardization of sample collection, isolation and analysis methods in extracellular vesicle research. J Extracell Vesicles.

2013;2:20360.

[44] Sunkara V, Woo HK, Cho YK. Emerging techniques in the isolation and characterization of extracellular vesicles and their roles in cancer diagnostics and prognostics.

Analyst. 2016;141:371–381

[45] Liga A, Vliegenthart ADB, Oosthuyzen W, et al. Exosome isolation: A microfluidic road-map. Lab Chip. 2015;15:2388–2394.

[46] Andreu Z, Rivas E, Sanguino-Pascual A, et al. Comparative analysis of EV isolation procedures for miRNAs detection in serum samples. J Extracell Vesicles. 2016;5:31655.

[47] Lane RE, Korbie D, Anderson W, et al. Analysis of exosome purification methods using a model liposome system and tunable-resistive pulse sensing. Sci Rep. 2015;5:1–7.

[48] Tauro BJ, Greening DW, Mathias RA, et al. Comparison of ultracentrifugation, density gradient separation, and immunoaffinity capture methods for isolating human colon cancer cell line LIM1863-derived exosomes. Methods. 2012;56:293–304.

[49] Greening DW, Xu R, Ji H, et al. A protocol for exosome isolation and characterization: evaluation of ultracentrifugation, density-gradient separation, and immunoaffinity capture methods. In: Posch A, editor. Proteomic profiling: methods and protocols. New York: Springer; 2015. p. 179–209.

[50 Marcus ME, Leonard JN. FedExosomes: engineering therapeutic biological nanoparticles that truly deliver. Pharmaceuticals. 2013;6:659–680.

[51 Yamada T, Inoshima Y, Matsuda T, et al. Comparison of methods for isolating exosomes from bovine milk. J Vet Med Sci. 2012;74:1523–1525

[52] Böing AN, van der Pol E, Grootemaat AE, et al. Singlestep isolation of extracellular vesicles by size-exclusion chromatography. J Extracell Vesicles. 2014;3:23430.

[53] Davies RT, Kim J, Jang SC, et al. Microfluidic filtration system to isolate extracellular vesicles from blood. Lab Chip. 2012;12:5202–5210.

[54] He M, Crow J, Roth M, et al. Integrated immunoisolation and protein analysis of circulating exosomes using microfluidic technology. Lab Chip. 2014;14:3773–3780.

[55] Welton JL, Webber JP, Botos LA, et al. Ready-made chromatography columns for extracellular vesicle isolation from plasma. J Extracell Vesicles. 2015;4:27269.

[56] Taylor DD, Shah S. Methods of isolating extracellular vesicles impact down-stream analyses of their cargoes. Methods. 2015;87:3–10.

[57] Lee J, Lee H, Goh U, et al. Cellular engineering with membrane fusogenic liposomes to produce functionalized extracellular vesicles. ACS Appl Mat Interfaces. 2016;8:6790–6795.

[58] Fuhrmann G, Serio A, Mazo M, et al. Active loading into extracellular vesicles significantly improves the cellular uptake and photodynamic effect of porphyrins. J Control Release. 2015;205:35–44.

[59] Hung ME, Leonard JN. A platform for actively loading cargo RNA to elucidate limiting steps in EV-mediated delivery. J Extracell Vesicles. 2016;5:31027.

[60] Kim MS, Haney MJ, Zhao Y, et al. Development of exosome-encapsulated paclitaxel to overcome MDR in cancer cells. Nanomed Nanotechnol Biol Med. 2016;12 (3):655–664.

[61] Yim N, Ryu SW, Choi K, et al. Exosome engineering for efficient intracellular delivery of soluble proteins using optically reversible protein–protein interaction module. Nat Commun. 2016;7:1–9.

[62] Stickney Z, Losacco J, McDevitt S, et al. Development of exosome surface display technology in living human cells. Biochem Biophys Res Commun. 2016;472(1):53–59.

[63] Delcayre A, Estelles A, Sperinde J, et al. Exosome display technology: applications to the development of new diagnostics and therapeutics. Blood Cells, Mol Dis. 2005;35:158–168

[64] Delcayre A inventor, Le PJB inventor; Methods and compounds for the targeting of protein to exosomes. European patent WO2003016522 A2. 2003.

[65] Zeelenberg IS, Ostrowski M, Krumeich S, et al. Targeting tumor antigens to secreted membrane vesicles in vivo induces efficient antitumor immune responses. Cancer Res. 2008;68:1228–1235.

[66] Hartman ZC, Wei J, Glass OK, et al. Increasing vaccine potency through exosome antigen targeting. Vaccine. 2011;29:9361–9367.

[67] Alvarez-Erviti L, Seow Y, Yin H, et al. Delivery of siRNA to the mouse brain by systemic injection of targeted exosomes. Nat Biotechnol. 2011;29:341–345.

[68] Tian Y, Li S, Song J, et al. A doxorubicin delivery platform using engineered natural membrane vesicle exosomes for targeted tumor therapy. Biomaterials. 2014;35:2383–2390.

[69] Ohno SI, Takanashi M, Sudo K, et al. Systemically injected exosomes targeted to EGFR deliver antitumor microRNA to breast cancer cells. Mol Ther. 2013;21:185–191.

[70] Bolukbasi MF, Mizrak A, Ozdener GB, et al. miR-1289 and "Zipcode"-like sequence enrich mRNAs in microvesicles. Mol Ther Nucleic Acids. 2012;1:1–10.

[71] Villarroya-Beltri C, Gutiérrez-Vázquez C, Sánchez- Cabo F, et al. Sumoylated hnRNPA2B1 controls the sorting of miRNAs into exosomes through binding to specific motifs. Nat Commun. 2013;4:1–10.

[72] Lee J, Kim J, Jeong M, et al. Liposome-based engineering of cells to package hydrophobic compounds in membrane vesicles for tumor penetration. Nano Lett. 2015;15:2938–2944.

[73] Chang PV, Prescher JA, Sletten EM, et al. Copper-free click chemistry in living animals. Proc Natl Acad Sci USA. 2010;107:1821–1826.

[74] Sun D, Zhuang X, Xiang X, et al. A novel nanoparticle drug delivery system: the anti-inflammatory activity of curcumin is enhanced when encapsulated in exosomes. Mol Ther. 2010;18:1606–1614.

[75] Zhuang X, Xiang X, Grizzle W, et al. Treatment of brain inflammatory diseases by delivering exosome encapsulated anti-inflammatory drugs from the nasal region to the brain. Mol Ther. 2011;19:1769–1779.

[76] Aqil F, Kausar H, Agrawal AK, et al. Exosomal formulation enhances therapeutic response of celastrol against lung cancer. Exp Mol Pathol. 2016;101:12–21.

[77] Weaver JC. Electroporation: A general phenomenon for manipulating cells and tissues. J Cell Biochem. 1993;51:426–435.

[78] Kooijmans SAA, Stremersch S, Braeckmans K, et al. Electroporation-induced siRNA precipitation obscures the efficiency of siRNA loading into extracellular vesicles. J Control Release. 2013;172:229–238.

[79] Hood JL, Scott MJ, Wickline SA. Maximizing exosome colloidal stability following electroporation. Anal Biochem. 2014;448:41–49.

[80] Haney MJ, Klyachko NL, Zhao Y, et al. Exosomes as drug delivery vehicles for Parkinson's disease therapy. J Control Release. 2015;207:18–30.

[81] Smyth T, Petrova K, Payton NM, et al. Surface functionalization of exosomes using click chemistry. Bioconjug Chem. 2014;25:1777–1784.

[82] Hermanson GT. Zero-length crosslinkers. In: Hermanson GT, editor. Bioconjugate Techniques. 3rd ed. Boston: Academic Press; 2013. p. 259–273.

[83] Sessa G, Freer JH, Colacicco G, et al. Interaction of a lytic polypeptide, melittin, with lipid membrane systems. J Biol Chem. 1969;244:3575–3582.

[84] Pan H, Myerson JW, Ivashyna O, et al. Lipid membrane editing with peptide cargo linkers in cells and synthetic nanostructures. Faseb J. 2010;24:2928–2937.

[85] Sato YT, Umezaki K, Sawada S, et al. Engineering hybrid exosomes by membrane fusion with liposomes. Sci Rep. 2016;6:1–11.

[86] Morris GJ, McGrath JJ. The response of multilamellar liposomes to freezing and thawing. Cryobiology. 1981;18:390–398.

[87] Jo W, Kim J, Yoon J, et al. Large-scale generation of cell derived nanovesicles. Nanoscale. 2014;6:12056–12064.

[88] Jo W, Jeong D, Kim J, et al. Microfluidic fabrication of cell-derived nanovesicles as endogenous RNA carriers. Lab Chip. 2014;14:1261–1269.

[89] Wagner A, Vorauer-Uhl K. Liposome technology for industrial purposes. J Drug Deliv. 2011;2011:1–9.

[90] Mozafari MR. Liposomes: an overview of manufacturing techniques. Cell Mol Biol Lett. 2015;10:711–719.

[91] Szoka JF, Papahadjopoulos D. Comparative properties and methods of preparation of lipid vesicles (liposomes). Annu Rev Biophys Bioeng. 1980;9(1):467–508.

[92] Abdus S, Sultana Y, Aqil M. Liposomal drug delivery systems: an update review. Curr Drug Deliv. 2007;4:297–305.

[93] Antonietti M, Förster S. Vesicles and liposomes: A selfassembly principle beyond lipids. Adv Mat. 2003;15:1323–1333.

[94] Lasic D.D. (1988). The mechanism of vesicle formation. Biochem J., 256:1–11.

[95] García-Manrique P, Matos M, Gutiérrez G, et al. (2016). Using factorial experimental design to prepare size-tuned nanovesicles. Ind Eng Chem Res., 55:9164–9175.

[96] Gregoriadis G, editor. Entrapment of drugs and other materials into liposomes.Volume II, Liposome Technology. Boca Ratonn: CRC Press; 2007.

[97] Avanti Polar Lipids products. Available from: http:// www.avantilipids.com

[98] Sullivan SM, Connor J, Huang L. (1986). Immunoliposomes: preparation, properties, and applications. Med Res Rev., 6:171–195.

[99] Hermanson GT. The reactions of bioconjugation. In: Hermanson GT, editor. Bioconjugate techniques. 3rd ed. Boston: Academic Press; 2013. p. 229–258.

[100] Nobs L, Buchegger F, Gurny R, et al. (2004). Current methods for attaching targeting ligands to liposomes and nanoparticles. J Pharm Sci., 93:1980–1992.

[101] Schuber F. Chemistry of ligand-coupling to liposomes. In: Schuber F, Philippot JR, editors. (). Liposomes as tools in basic research and industry. Boca Raton: CRC Press; 1995. p. 21–39.

[102] Martinez-Lostao L, García-Alvarez FC, Basáñez G, et al. (2010). Liposome-bound APO2L/TRAIL is an effective treatment in a rabbit model of rheumatoid arthritis. Arthritis Rheum., 62:2272–2282.

[103] Li K, Chang S, Wang Z, et al. A novel micro-emulsion and micelle assembling method to prepare DEC205 monoclonal antibody coupled cationic nanoliposomes for simulating exosomes to target dendritic cells. Int J Pharm. 2015;491:105–112.

[104] Chandler W.L, Yeung W., Tait J.F. (2011). A new microparticle size calibration standard for use in measuring smaller microparticles using a new flow cytometer. J Throm Haemost., 9:1216–1224.

[105] Gardiner C, Shaw M, Hole P, et al. (2014). Measurement of refractive index by nanoparticle tracking analysis reveals heterogeneity in extracellular vesicles. J Extracell Vesicles, 3:25361.

[106] De Miguel D, Basáñez G, Sánchez D, et al. (2013). Liposomes decorated with Apo2L/TRAIL overcome chemoresistance of human hematologic tumor cells. Mol Pharm., 10:893–904.

[107] de Miguel D, Gallego-Lleyda A, Galan-Malo P, et al. (2015). Immunotherapy with liposome-bound TRAIL overcomes partial protection to soluble TRAIL-induced apoptosis offered by down-regulation of Bim in leukemic cells. Clin Trans Oncol., 17:657–667.

[108] Pagnan G, Stuart DD, Pastorino F, et al. (2000). Delivery of c-myb antisense oligodeoxynucleotides to human neuroblastoma cells via disialoganglioside GD2-Targeted immunoliposomes: antitumor effects. J Natl Cancer Inst., 92:253–261.

[109] Pastorino F, Brignole C, Marimpietri D, et al. (2003). Doxorubicin-loaded Fab′ fragments of anti-disialoganglioside immunoliposomes selectively inhibit the growth and dissemination of human neuroblastoma in nude mice. Cancer Res.,63:86–92.

[110] Marianecci C, Di Marzio L, Rinaldi F, et al. (2014). Niosomes from 80s to present: the state of the art. Adv Colloid Interface Sci., 205:187–206.

[111] Moghassemi S, Hadjizadeh A. (2014). Nano-niosomes as nanoscale drug delivery systems: an illustrated review. J.Control Release., 185:22–36.

[112] Capretto L, Carugo D, Mazzitelli S, et al. (2013). Microfluidic and lab-on-a-chip preparation routes for organic nanoparticles and vesicular systems for nanomedicine applications. Adv Drug Deliv Rev., 65:1496–1532.

[113] Birnbaumer G, Kupcu S, Jungreuthmayer C, et al. (2011). Rapid liposome quality assessment using a lab-on-achip. Lab Chip., 11:2753–2762.

[114] Bhise NS, Ribas J, Manoharan V, et al. (2014). Organ-on-achip platforms for studying drug delivery systems. J Control Release., 190:82–93.

[115] Hu CMJ, Fang RH, Wang KC, et al. (2015). Nanoparticle biointerfacing by platelet membrane cloaking. Nature., 526:118–121.

6. Using factorial experimental design to prepare size-tuned nanovesicles

Capítulo/Chapter 6

Using factorial experimental design to prepare size-tuned nanovesicles

6.1. Introduction

Controlled preparation of nanoparticles has attracted great interest in recent years.[1] Nanovesicles are an important family of organic nanoparticles, produced by bottom-up nanotechnology, with relevant applications in biomedicine,[2] food science,[3] analytical chemistry,[4,5] or biosensors.[6] They are considered *soft nanoparticles* because interactions among their molecular components are similar to those arising from biological systems.[7] Most of the work describing their preparation for specific uses focuses on the optimization of their composition with the aim of maximizing encapsulation efficiency or delivery or delivery control.

However, size is one of the most critical properties (together with shape and surface chemistry) for understanding cell-uptake process and, therefore, bioavailability and targetability.[7] Several studies have focused on the optimization of the drug encapsulation efficiency, while considering size as just a property for controlling administration parameters, such as penetration kinetics in topical formulations. For example, Padamwar et al.[8] studied the encapsulation of Vitamin E in liposomes and found that the amount of lipids yielded a positive correlation with size, which was, in turn, negatively correlated with penetration efficiency into the skin. Sometimes, size has been found to increase with higher amounts of membrane components, such as cholesterol, whereas it decreased with higher amounts of surfactants (e.g., Tween® 80). Simultaneously, cholesterol or surfactants could affect encapsulation efficiency (EE). Optimal situations can be reached as a compromise at intermediate levels of both factors. In that case, Taha[9] also reported an interaction between membrane components concentration and size reduction by ultrasounds, making factor optimization an essential task. In other cases, an opposite effect was observed, and higher concentrations of membrane components (such as Span® 60 and cholesterol) produced larger sizes and increased EEs. It is useful to deliver efficient amounts of a selected drug into superficial

skin layers without systemic absorption.[10] On this basis, the goal of our work was to set up a bulk-method for producing nanovesicles of controlled size that could be subsequently modified for specific applications.

Vesicles are colloidal particles in which a concentric bilayer made up of amphiphilic molecules surrounds an aqueous compartment. These vesicles are commonly used to encapsulate both hydrophilic and lipophilic compounds, for food, cosmetic, pharmaceutical or medical applications, such as diagnosis or therapy.[11] Hydrophilic compounds are entrapped into the aqueous compartments between bilayers, whereas lipophilic compounds are preferentially located inside these bilayers.[12,13] The most common types of vesicles are liposomes and niosomes.

Liposomes were first described by Bangham et al. in 1965,[14] and they are basically spherical bilayer vesicles formed by the self-assembly of phospholipids. This self-assembly process is based on the interactions occurring between phospholipids and water molecules, where the polar head groups of phospholipids are exposed to the aqueous phases (inner and outer), and the hydrophobic hydrocarbon tails are forced to face each other in a bilayer.[15] Because of the presence of both lipid and aqueous phases in liposomes structure, they can be used for encapsulation, delivery, and controlled release of hydrophilic, lipophilic, and amphiphilic compounds.[15,16]

On the other hand, niosomes are vesicles formed by the self-assembly of nonionic surfactants in aqueous media resulting in closed bilayer structures.[13,17,18] As liposomes, their formation process is a consequence of unfavorable interactions between surfactants and water molecules, and they can also entrap hydrophilic, lipophilic, and amphiphilic compounds.[19,20]

Niosomes exhibit a number of advantages over liposomes, such as higher stability, easy access to raw materials, lower toxicity, high compatibility with biological systems, non-immunogenicity, and versatility for surface modification.[20]

Cholesterol is commonly used as a membrane additive for nanovesicle preparation in order to improve vesicles stability, entrapment efficiency, and release under storage.[20] It increases vesicle size and rigidity, improving encapsulation efficiency, but at high concentrations, it could adversely affect the encapsulation rate.[21,22] Cholesterol also plays a fundamental role in niosomes formation when hydrophilic surfactants are used (hydrophile/lipophile balance around 10).[20]

More than 20 different methods have been identified for nanovesicle preparation, and these methods were recently reviewed.[23,24] In this work, a modified ethanol injection method (EIM) is used, because it offers some advantages over other methods, such as simplicity, absence of potentially harmful chemicals, and suitability for scaleup.[25]

The conventional EIM was first described in 1973.[26] In this technique, lipids/surfactants and additives are first dissolved in an organic solvent, such as diethyl ether or ethanol, and then injected slowly through a syringe into an aqueous phase containing the compound of interest. Then, the organic solvent is removed using a vacuum rotary evaporator. When ethanol is used as organic solvent, the spontaneous formation of vesicles occurs as soon as the organic solution is in contact with the aqueous phase,[27] but vigorous agitation is needed to obtain narrower size distributions. For this purpose, a final sonication stage was applied in this study after organic phase removal by vacuum evaporation.

However, there is large number of variables involved in this modified EIM, and selection of the most important of them (screening) is a crucial step in rationally preparing vesicles by this versatile method. In this work, Z-average size and polydispersity index (PDI) were selected as the dependent variables. They are considered to be of great importance in nanovesicles design because most of the final applications of these vesicular systems are directly related to these two parameters. Factorial experimental design and analysis of variance (ANOVA) methodology are appropriate and efficient statistical tools that permit the effects of several factors that influence responses to be studied by varying the factors simultaneously in a limited number of experiments.

In the recent past years, Design of Experiments (DoE) has been extensively used for the study and optimization of vesicles and other similar organic materials. Different designs can be applied to reduce the number of factors involved in the preparation techniques[28] and, therefore, to minimizing the number of experiments without losing valuable information. Plackett-Burman desing is a type of fractional design involving relatively few runs,[29] commonly used for the screening of variables.

Another important role of DoE is the optimization of nanovesicles composition for the enhancement of intended purposes. For instance, it has been applied to the formulation of liposomes (phospholipid and cholesterol ratio) for topical delivery of

vitamin E,[8] hybrid liposomes (with both low- and high-transition-temperature phospholipids) to improve the encapsulation and delivery of silymarin,[30] and niosomes for topical delivery applications.[10,31] DoE has also been used to enhance transdermal flux of raloxifene hydrochloride[32] or diclofenac diethylamine[33] loaded transfersomes, and of other polymeric nanoparticles encapsulating an anticancer drug.[34] Moreover, the interaction between vesicles and proteins, such as pectin, to improve drug-delivery properties has been studied by DoE.[35] Nanostructured lipid carriers (NLCs) loaded with flurbiprofen were also produced under optimal conditions using full factorial design.[36]

In this work, an initial fractional factorial design with two levels (Plackett-Burman) was used to screen the most important factors in vesicles preparation by the EIM. Then, a 2^3 two-level full factorial design using center-point replicates was applied to study the influence of the main factors and their interactions on Z-average size and PDI. Once the appropriate operating conditions were determined, vesicles stability was studied by using multiple light scattering technology and by measuring the encapsulation efficiencies (EE) of different compounds.

6.2. Materials and methods

6.2.1 Materials

Phosphatidylcholine (PC) (predominant species: $C_{42}H_{80}NO_8P$, MW= 775.04 g/mol) from soybean (Phospholipon 90G) was a kind gift from Lipoid (Ludwigshafen, Germany). Sorbitan monostearate (Span® 60, S60) ($C_{24}H_{46}O_6$, MW=430.62 g/mol) and Cholesterol (Cho) ($C_{27}H_{46}O$, MW=386.65 g/mol) were purchased from Sigma Aldrich (St. Louis, MO, USA). All membrane components were dissolved in absolute ethanol (Sigma-Aldrich).

Methanol, acetonitrile, 2-propanol, and acetic acid of high-performance liquid chromatography (HPLC) grade were supplied by Sigma-Aldrich.

A phosphate buffer (PB) solution (10 mM, pH 7.4) was used in all experiments as the aqueous phase. The buffer solution was prepared in Milli-Q water by dissolving proper amounts of sodium dihydrogen phosphate and sodium hydrogen phosphate, supplied by Panreac (Barcelona, Spain). Sodium chloride from Panreac was added to increase the ionic strength when it was required according to experiments listed in Table 1. For the encapsulation experiments, Fat Red Bluish or Sudan Red 7B dye ($C_{24}H_{21}N_5$, MW= 379.46

g/mol) and cholecalciferol or Vitamin D_3 ($C_{27}H_{44}O$, MW=384.64 g/mol) were purchased from Sigma-Aldrich.

6.2.2 Factorial design of experiments

Factors that could potentially affect the size of vesicles produced by the EIM were classified in four groups, according to the different steps involved in this preparation method: *formulation* (organic/aqueous phase volume ratio, phospholipid concentration, and ionic strength), *injection* (injection flow, temperature, and stirring speed), *evaporation* (temperature and rotation speed), and *sonication* (amplitude and time of sonication).

To identify the relative effect of variables on the response, a two-level fractional factorial design was used. A Plackett-Burman (P-B) resolution III design with n=16 runs was proposed of the initial factors screening. Two levels were selected for each variable.

Table 6.1 list the factors and levels involved in the P-B fractional factorial design used, where O/A is the organic/aqueous phase volume ratio, C is the concentration of phospholipid, I is the ionic strength, Q_V is the injection flow, T_I is the injection temperature, N_S is the stirring speed during injection, T_E is the evaporation temperature, N_E is the evaporator rotation speed, A is the sonication amplitude, and t is the sonication time.

In a second step, a 2^3 full factorial design with center-point repetitions (n=5) was carried out to study the main effects and interactions between factors previously selected by the screening design (**Table 6.2**). All the other factors were fixed at a certain value.

***Table 6.1**. Plackett-Burman Fractional Factorial Design: Responses, Levels, and Factors*

RESPONSES Y_1 Z-average size PC-liposomes Y_2 PDI PC-liposomes		FACTORS									
		FORMULATION			INJECTION			EVAPORATION		SONICATION	
	LEVELS	O:A (X_1)	C (X_2) (g/L)	I (X_3) (mM)	Q_V (X_4) (mL/h)	T_I (X_5) (°C)	N_S (X_6) (rpm)	T_E (X_7) (°C)	N_R (X_8) (rpm)	A (X_9) (%)	t (X_{10}) (min)
	-1	5:50	2.5	10	50	30	350	35	30	25	15
	1	20:50	6.0	150	215	60	900	60	120	42	30

BATCH	X_1	X_2	X_3	X_4	X_5	X_6	X_7	X_8	X_9	X_{10}	Y_1	Y_2
PB1	1	1	-1	-1	-1	-1	1	-1	1	1	90	0.254
PB2	1	-1	-1	1	-1	1	1	1	1	-1	93	0.129
PB3	-1	-1	-1	-1	-1	-1	1	1	-1	-1	97	0.152
PB4	1	-1	1	-1	1	0	1	-1	1	-1	72	0.205
PB5	-1	1	-1	1	-1	-1	1	-1	-1	1	258	0.413
PB6	1	1	1	1	-1	-1	-1	1	-1	-1	102	0.176
PB7	-1	-1	1	1	-1	-1	-1	-1	1	1	84	0.218
PB8	1	-1	-1	1	1	1	-1	1	-1	1	106	0.240
PB9	-1	-1	-1	-1	1	1	-1	1	1	1	71	0.229
PB10	1	-1	1	-1	-1	-1	-1	-1	-1	1	81	0.141
PB11	-1	1	1	-1	1	-1	1	1	-1	1	152	0.316
PB12	1	1	1	1	1	1	1	1	1	1	65	0.260
PB13	-1	-1	1	1	1	1	1	-1	-1	-1	87	0.189
PB14	-1	1	1	-1	-1	1	-1	1	1	-1	115	0.273
PB15	1	1	-1	-1	1	1	-1	-1	-1	-1	113	0.199
PB16	-1	1	-1	1	1	-1	-1	-1	1	-1	74	0.271

***Table 6.2.** Full factorial design (2^3) with center point repetitions (n=5): factors, levels and responses*

RESPONSES		LEVELS	FACTORS O:A (X_1)	C (X_2) (g/L)	A (X_3) (%)
Y_1	Z-average size PC-liposomes	-1 (Low)	5:50	2	30
Y_2	PDI PC-liposomes	0 (Medium)	12.5:50	5	42.5
Y_3	Z-average size S60:Cho niosomes	1 (High)	20:50	8	55
Y_4	PDI S60:Cho niosomes				

BATCH	X_1	X_2	X_3	Y_1	Y_2	Y_3	Y_4
FF1	1	-1	1	65	0.299	305	0.075
FF2	1	1	-1	97	0.249	362	0.136
FF3	-1	1	-1	149	0.296	294	0.206
FF4	-1	1	1	88	0.307	262	0.291
FF5	-1	-1	1	64	0.342	242	0.120
FF6	1	1	-1	100	0.257	360	0.143
FF7	1	1	1	64	0.272	241	0.182
FF8	-1	-1	-1	90	0.196	235	0.078
FF9	0	0	0	82	0.219	301	0.195
FF10	1	-1	-1	84	0.205	253	0.032
FF11	-1	1	1	107	0.297	276	0.235
FF12	-1	1	-1	156	0.308	275	0.145
FF13	1	-1	1	65	0.378	248	0.066
FF14	1	-1	-1	97	0.246	268	0.045
FF15	-1	-1	-1	84	0.173	239	0.094
FF16	0	0	0	75	0.224	305	0.253
FF17	0	0	0	84	0.250	317	0.118
FF18	1	1	1	55	0.307	224	0.203
FF19	0	0	-1	77	0.242	308	0.241
FF20	0	0	0	84	0.251	337	0.171
FF21	-1	-1	1	69	0.343	233	0.124

In both designs, mean diameter (Z-average size) and PDI were selected as response variable. MINITAB statistical software (version 17) was used for all data analysis. Analysis of variance (ANOVA) was used for this purpose.

Once the models were obtained taking into account significant factors and interactions, a set of selected size-tuned vesicles were prepared and characterized.

6.2.3 Vesicles preparation

For liposomes preparation, appropriate weighed amounts of PC were dissolved in different volumes of absolute ethanol (5-20 mL range). The same procedure was applied to niosomes preparation by weighing and dissolving S60 and Cho in 1:0.5 weight ratio. Then, the organic solution was injected, with a syringe pump (KD Scientific, Holliston, MA, USA) at a flow rate of 120 mL/h, into Milli-Q water that was kept at 60ºC and stirred at 500 rpm. Once vesicles were formed, ethanol was removed at 40°C under reduced pressure (90 kPa) in a rotary evaporator. The resulting vesicular systems were further sonicated for 15 min (CY-500 sonicator, Optic Ivymen System, Biotech SL, Barcelona, Spain), using 30-55% amplitude, 500 W power, and 20 kHz frequency. The sonication probe was placed in a 100 mL glass beaker at a constant depth, 1.5 cm over the container bottom.

6.2.4. Vesicles characterization

6.2.4.1. Vesicles size

Z-average size and PDI of vesicles were determined via Dynamic Light Scattering (DLS) using a Zetasizer Nano ZS (Malvern Instruments Ltd, Malvern, UK). Three independent samples were taken from each formulation, and measurements were performed three times at room temperature without dilution.

6.2.4.2. Vesicles morphology

Morphological analysis of vesicles was carried out by negative staining transmission electron microscopy (NS-TEM), using a JEOL-2000 Ex II TEM (Tokyo, Japan). A sample drop was placed on a carbon-coated copper grid and sample excess was removed with filter paper. Then, a drop of 2% (w/v) phosphotungstic acid solution (PTA) was applied to the carbon grid and allowed to stand for 1 minute. Once the excess of staining agent

has been removed with filter paper, the sample was air-dried, and the thin film of stained and fixed vesicles was observed with the transmission electron microscope.

6.2.4.3. Vesicles stability

Vesicles stability was determined by measuring backscattering (BS) profiles in a Turbiscan Lab Expert apparatus (Formulaction, L'Union, France) provided with an Ageing Station (Formulaction).

Samples were placed in cylindrical glass test cells, and backscattered light was monitored at 30 °C as a function of time and cell height every 2 h for 7 days.

The optical reading head scans the sample in the cell, providing BS data every 40 µm in percentages relative to standards as a function of the sample height (in millimeters). These profiles build up a macroscopic fingerprint of the sample at a given time, providing useful information about changes in size distribution or appearance of a creaming layer or a clarification front with time.[3,37,38]

6.2.4.4. Encapsulation Efficiency (EE)

EE also provides useful information related to the stability of the vesicle membrane. Hydrophilic compounds are entrapped in aqueous compartments between bilayers, whereas lipophilic compounds are preferentially located within surfactant or lipid bilayer.[39] Substances as drugs, bioactive compounds, dyes, and nanomaterials incorporated into vesicles can also affect the morphology and stability of the final dispersion.

For the purpose of determining EEs, Sudan Red 7B and vitamin D_3 (hydrophobic compounds) were encapsulated in the two different formulations.

Each compound was analyzed by Reverse-Phase High Performance Liquid Chromatography (RP-HPLC) (HP series 1100 chromatograph, Hewlett Packard, Palo Alto, CA, USA). Before RP-HPLC analysis could be performed, the non-encapsulated compound had to be removed by passing the sample through a Sephadex G-25 column (GE Healthcare Life Sciences, Wauwatosa, WI, USA). Then, both filtered and non-filtered samples were diluted 1:10 (v/v) with methanol to facilitate vesicle rupture and to extract the encapsulated compound. EE was calculated according to **Equation 2**.

$$EE = \frac{\text{peak area of filtered sample}}{\text{peak area of non-filtered sample}} \times 100$$

Equation 2

The RP-HPLC system was equipped with a HP G1315A UV/VIS absorbance detector (Agilent Technologies, Palo Alto, CA, USA). The column was a Zorbax Eclipse Plus C18 with a particle size of 5 µm, 4.6 mm × 150 mm (Agilent Technologies). The mobile phase consisted of a mixture of (A) 100% Milli-Q-water and (B) 100% methanol with gradient elution at 0.8 mL/min. The step gradient started with a mobile phase of 80% A, running 100% mobile phase B in minute 5 for 10 minutes. The mobile phase B was fed for 2 minutes after each injection to prepare the column for the next sample. The separation was carried out at 30°C. Different wavelengths were used for UV/VIS detector, namely, 533 nm for Sudan Red 7B and 270 nm for Vitamin D_3.

6.3. Results and discussion

6.3.1. Effects of variables on morphological characteristics

The responses (Z-average size and PDI) of each batch from P-B design were measured by DLS. The relative importance of the main effects on Z-average size and PDI of PC liposomes are shown in the Pareto chart given in **Figure 6.1**.

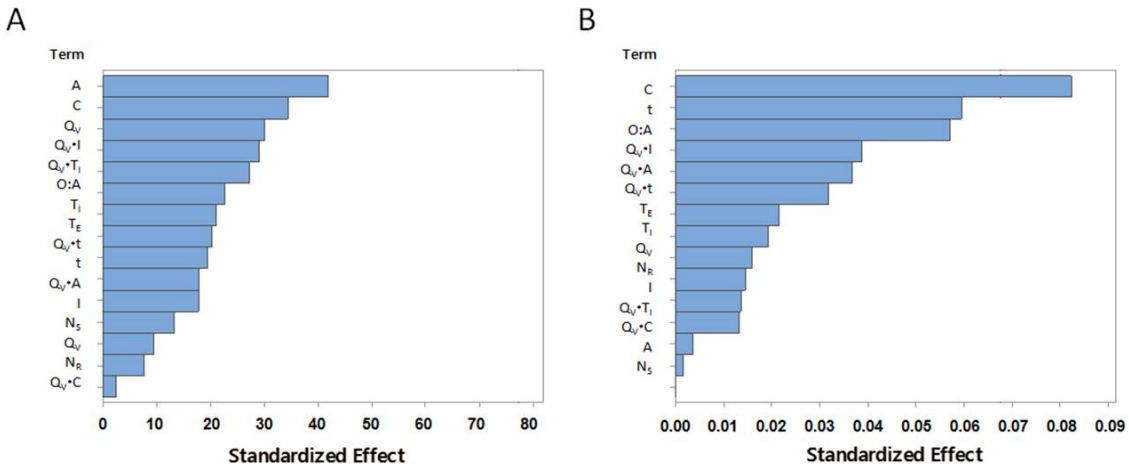

Figure 6.1. *Pareto chart of the standardized effects of independent variables (factors) on (**A**) Z-average size and (**B**) PDI of PC liposomes for the Plackett-Burman fractional factorial design*

Researchers must be aware of the confusion of main effects with two-factor interactions in this type of design (resolution III), where the alias structure is too

complex. However, we decided to use the initial Plackett−Burman design only for screening purposes and selection of the main factors from the Pareto chart, as is usually accepted. Effects were selected by applying the hierarchical ordering principle, known sometimes as the sparsity-of-effects principle, where higher-order effects (three- or four-way interactions) are sacrificed to study lower-order effects (main effects first and two-way interactions next). This principle suggests that priority should be given to the estimation of lower-order effects, especially when resources (time and money) are scarce. This postulate is an empirical principle whose validity has been confirmed by the analysis of many real experiments.

According to these data, the most important variables on both responses are organic/aqueous phase volume ratio, the (final aqueous phase) phospholipid concentration, and the sonication amplitude. These results are in good agreement with previous studies carried out by Kremer et al.,[40] who evaluated the effect of some preparation variables on the size and polydispersity of liposomes made from two different natural phosphatidylcholines. Their experimental results showed that the most important factor in the final size of liposomes was the lipid concentration in the alcohol injected into the buffer solution. This factor corresponds to the interaction of lipid amount and flow rate of organic solvent injected, two factors present in the Pareto chart in **Figure 6.**. The same explanation was postulated by other authors,[8,41,42] confirming that the lipid concentration clearly affects the liposome size. This factor was found to be the most relevant one for controlling morphological characteristics of phosphatidylcholine liposomes. Szoka et al.[43] found that stirring, ionic strength, and temperature of aqueous phase could also contribute to final size, but the effects of these factors were smaller than those observed for lipid concentration, organic/aqueous phase ratio, and chemical nature of the organic solvent (a parameter not included in our study). Therefore, experimental results in **Figure 6.1** confirm the previously reported observations.[43]

The ethanol injection method is usually chosen because it avoids the sonication step, which is needed in several other methods of liposome preparation, such as the thin-film hydration method. Preliminary experiments (data not shown) indicated that sonication is a crucial step for reducing the size of both liposomes and niosomes. Alternatively, small vesicles can be produced without sonication by using low concentration of lipids/surfactants, but with low yield. This is why we decided to include this step as a factor at the present study.

6.3.2. PC liposomes

The first three main effects from the Pareto chart obtained for the P-B design were selected for the 2^3 full factorial design. The ANOVA results for Z-average size and PDI values are listed in **Table 6.3** and **Table 6.4**, respectively, whereas the corresponding Pareto chart is shown in **Figure 6.2**. Mean sizes in the range of 55-156 nm with PDI values between 0.173 and 0.378 were obtained for PC liposomes (with standard deviations ranging from 0.304 to 4.40 nm for size and from 0.003 to 0.053 for PDI). Similar size ranges were also obtained using the EIM in other previously reported studies.[22,27,41,43,44]

Table 6.3. *ANOVA results (coded units) for Z-average size of PC-liposomes for the 23 full factorial design; results for S60:Cho niosomes are also given (cursive numbers)*

Source	DF	Seq SS	Adj SS	Adj MS	F	P
Main effects	3	9349.7	9349.7	3116.6	86.7	0.000
		11209.8	*11209.8*	*3736.6*	*14.9*	*0.000*
2-Way Interactions	3	2805.3	2805.3	935.1	26.0	0.000
		8828.3	*8828.3*	*2942.8*	*11.7*	*0.001*
3-Way Interactions	1	113.2	113.2	113.2	3.2	0.101
		4116.8	*4116.8*	*4116.8*	*16.4*	*0.002*
Curvature	1	326.9	326.9	326.9	9.1	0.011
		7370.0	*7370.0*	*7370.0*	*29.3*	*0.000*
Residual Error	12	431.2	431.2	35.9		
		3015.0	*3015.0*	*251.3*		
Pure Error	12	431.2	431.2	35.9		
		3015.0	*3015.0*	*251.3*		

ANOVA indicates analysis of variance; DF, degrees of freedom; SS, sum of squares; MS, mean of squares; F, Fischer's ratio; P, p-value.

Table 6.4. *ANOVA results (coded units) for PDI of PC-liposomes for the 23 full factorial design; results for S60:Cho niosomes are also given (cursive numbers)*

Source	DF	Seq SS	Adj SS	Adj MS	F	P
Main effects	3	0.0256	0.0256	0.0082	16.72	0.0000
		0.0728	*0.0728*	*0.0243*	*18.30*	*0.0000*
2-Way Interactions	3	0.0162	0.0162	0.0054	11.02	0.0010
		0.0017	*0.0017*	*0.0006*	*0.43*	*0.7370*
3-Way Interactions	1	0.0017	0.0017	0.0017	3.39	0.0900
		0.0002	*0.0002*	*0.0002*	*0.18*	*0.6830*
Curvature	1	0.0069	0.0069	0.0069	14.05	0.0030
		0.0136	*0.0136*	*0.0136*	*10.22*	*0.0080*
Residual Error	12	0.0059	0.0059	0.0005		
		0.0159	*0.0159*	*0.0013*		
Pure Error	12	0.0059	0.0059	0.0005		
		0.0159	*0.0159*	*0.0013*		

ANOVA indicates analysis of variance; DF, degrees of freedom; SS, sum of squares; MS, mean of squares; F, Fischer's ratio; P, p-value.

The normality, variance homogeneity, and randomness assumptions were tested with the normal probability plot, frequency histogram, and residuals *versus* fits plot and residuals *versus* order plots, respectively.

No clear aberrant tendencies were observed, because the residuals tended to form a line, no typical cornet pattern was observed, and no time-based pattern was detected. Only some outliers values were detected (Cook's distance and DFITS values are given in **Table 6.5**).

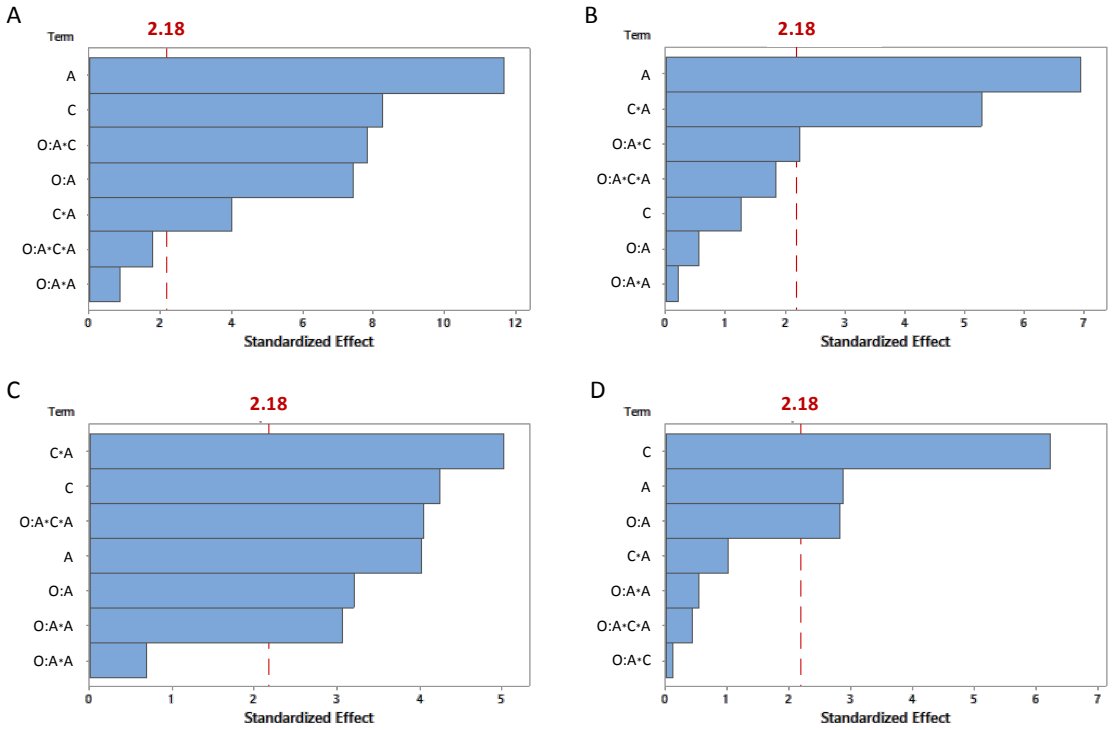

Figure 6.2. *Pareto chart of the standardized effects of independent variables (factors) on the (A, C) Z-average size and (**B,D**) PDI of (**A,B**) PC liposomes and (**C,D**) S60:Cho niosomes (1:0.5, w/w) for the 23 full factorial design.*

Table 6.5. *COOK's distance and DFITS values obtained for each response in the full factorial designs*

BATCH	COOK Y_1	DFIT Y_1	COOK Y_2	DFIT Y_2	COOK Y_3	DFIT Y_3	COOK Y_4	DFIT Y_4
FF1	0.000	-0.019	0.708	-3.530	0.706	3.518	0.003	0.168
FF2	0.015	-0.358	0.007	-0.245	0.001	0.073	0.002	-0.130
FF3	0.089	-0.889	0.016	-0.369	0.077	0.823	0.156	1.207
FF4	0.530	-2.693	0.011	0.307	0.046	-0.626	0.131	1.096
FF5	0.028	-0.486	0.000	-0.031	0.020	0.413	0.001	-0.074
FF6	0.015	0.358	0.007	0.245	0.001	-0.073	0.002	0.130
FF7	0.116	1.024	0.139	-1.131	0.063	0.740	0.018	-0.393
FF8	0.058	0.705	0.060	0.720	0.004	-0.173	0.011	-0.299
FF9	0.001	0.103	0.023	-0.457	0.022	-0.440	0.000	-0.009
FF10	0.255	-1.614	0.191	-1.355	0.046	-0.626	0.007	-0.242
FF11	0.530	2.693	0.011	-0.307	0.046	0.626	0.131	-1.096
FF12	0.089	0.889	0.016	0.369	0.077	-0.823	0.156	-1.207
FF13	0.000	0.019	0.708	3.530	0.706	-3.518	0.003	-0.168
FF14	0.255	1.614	0.191	1.355	0.046	0.626	0.007	0.242
FF15	0.058	-0.705	0.060	-0.720	0.004	0.173	0.011	0.299
FF16	0.033	-0.554	0.012	-0.325	0.010	-0.291	0.086	0.980

The ANOVA results allowed for an analysis of the contributions of the effects of the independent variables on the response function (mean size of PC liposomes). In this case, significant two-way interactions were identified: (O/A)×C and C×A (see **Figure 6.3**). Larger sizes are reached when the organic solution has higher lipid concentration (more than 20 g/L). On the other hand, C×A interaction reveals that the degree of size reduction upon application of a higher amplitude depends on the total lipid concentration present in the medium (referred to final volume of dispersion).

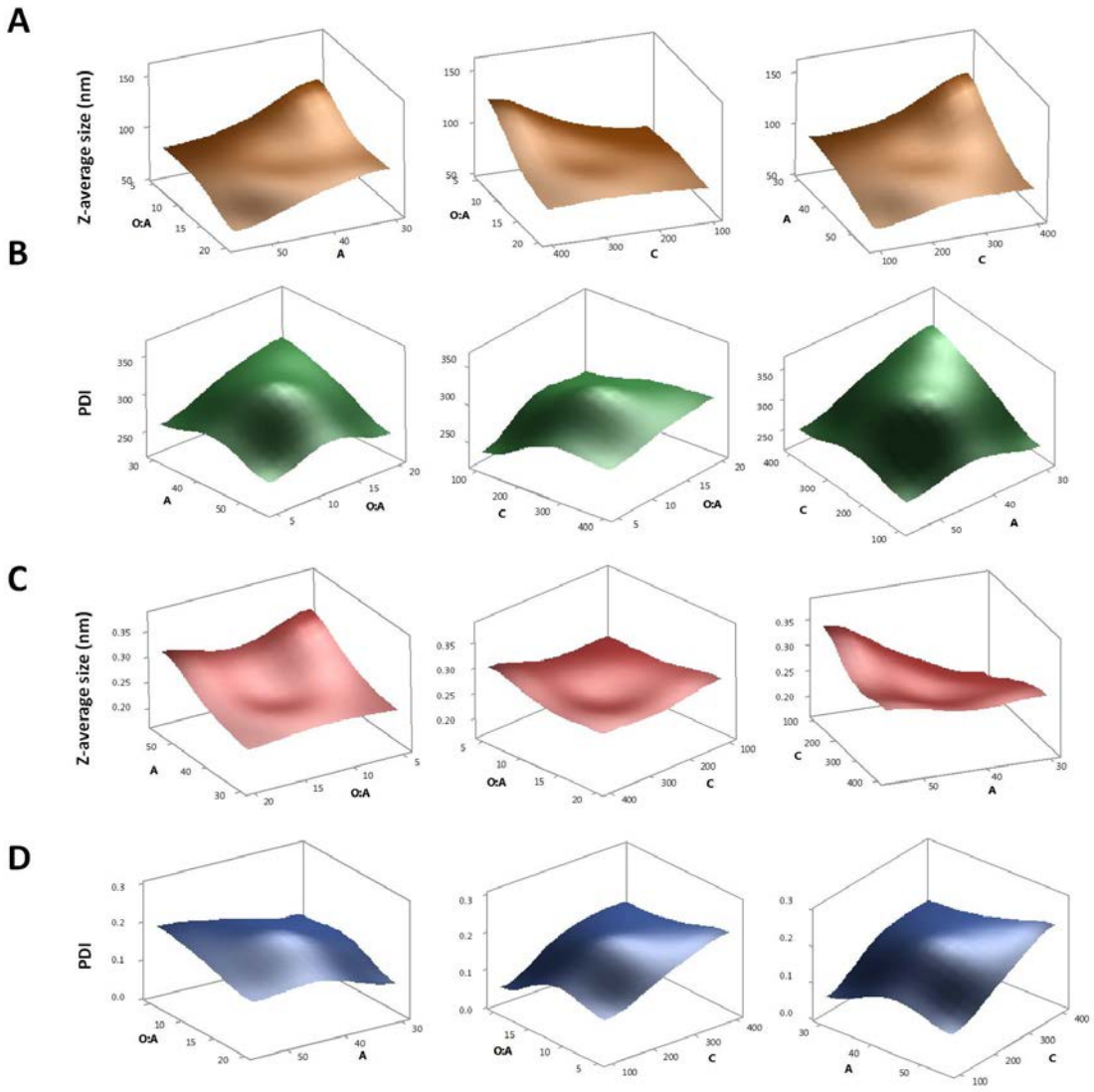

Figure 6.3. *Three-dimensional (3D) response surface plots for the factors O/A (organic/aqueous phase volume ratio), C (lipid or surfactant/stabilizer concentration, g/L), and A (sonication amplitude, %) for the (A,C) Z-average size and (B,D) PDI of (A,B) PC liposomes and (C,D) S60:Cho niosomes (1:0.5, w/w).*

All of the main effects are significant (p-value < 0.05), with a positive effect on mean size (a higher response value with an increase in the factor level) for the lipid total

concentration and a negative effect (a lower response value with a decrease in factor level) for organic/aqueous phase volume ratio and the sonication amplitude.

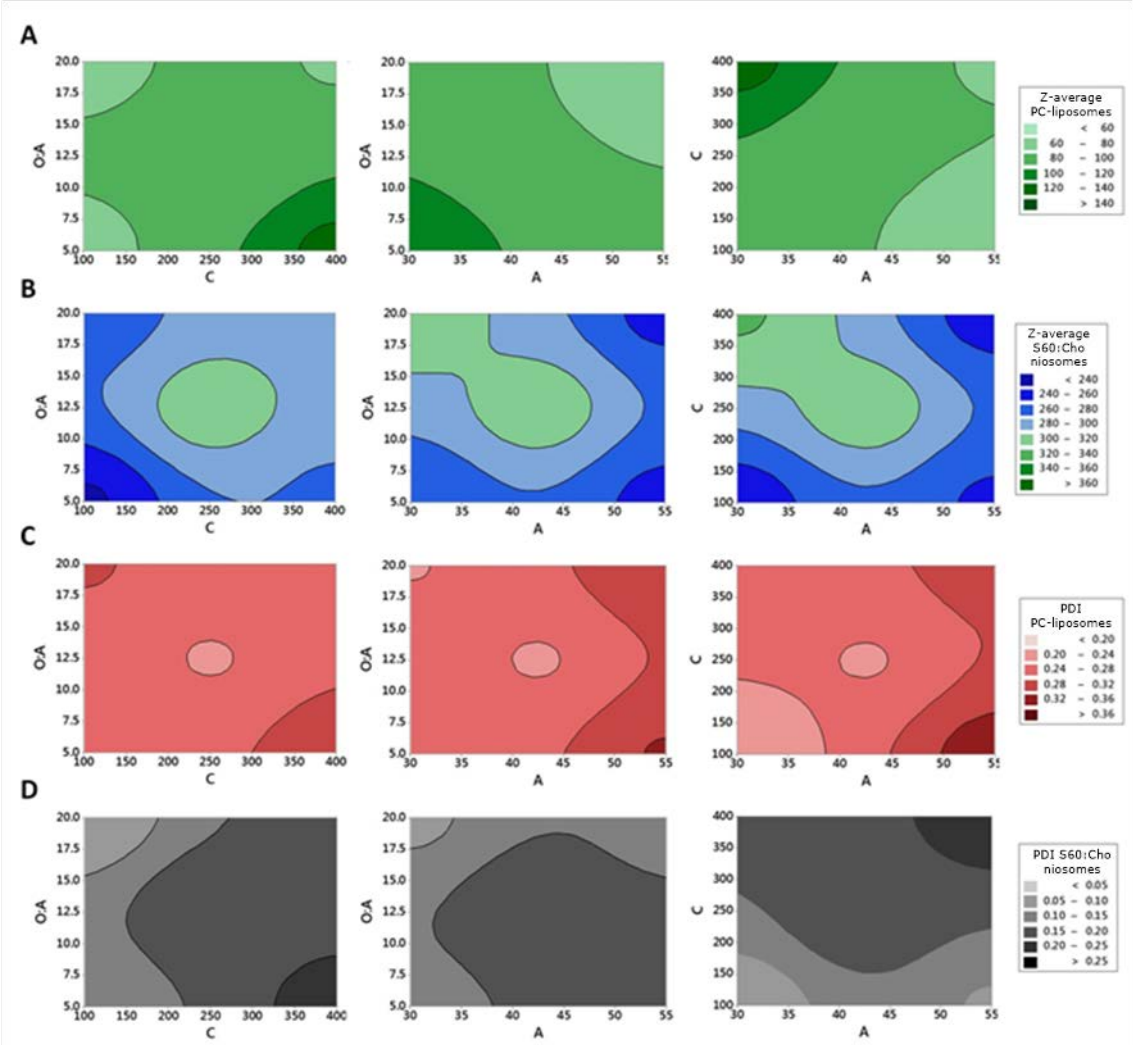

Figure 6.4. *Contour Plot for the factors O:A (organic:aqueous phase volume ratio), C (lipid or surfactant/stabilizer concentration, g/L) and A (sonication amplitude, %) on Z-average size, nm (A) and PDI (C) of PC-liposomes, and Z-average size, nm (B) and PDI (D) of S60:Cho niosomes (1:0.5, w/w).*

These effects can be explained according to a previously reported vesicle formation model.[45-47] This model relies on the formation of vesicles through intermediate structures, such as phospholipid bilayer fragments and sheet-like micelles. These intermediates are the result of amphiphilic self-assembly because of their characteristic physical-chemical properties.[48]

During the injection of ethanol droplets into the aqueous phase, lipids reorganization inside these dispersed droplets to form bilayers is favored by the fact that lipids energetically prefer a parallel molecular arrangement.[45] These planar structures give rise

to closed vesicles when their size induces enough surface tension to close the structure and to minimize the bending energy.

The size of these intermediates depend directly on the number of lipid molecules (concentration) and the dispersion degree (solubilization) in the organic phase. It is obvious from the previous assessment that higher concentration of lipids in the droplets will form higher membrane fragments, as our experimental results and previous observations confirm.[8,40-42]

It is also important to know how easily lipid droplets are dispersed, as well as their size and homogeneity. Lipids of higher solubility will then form smaller lipid droplets and, consequently, short membrane fragments (and ultimately tiny vesicles).[40] This explains, in a simplified way, why higher organic/aqueous phase ratio yields smaller liposomes.

The negative effect of sonication amplitude is explained by vesicles rupture, which takes place when an excess of energy is applied to vesicles during the sonication process as a result of the effect of induced cavitation.[49,50] The final effect of ultrasounds can be controlled by varying the input power, ultrasound frequency, sonication time, and probe depth into the container. As frequency increases, liposomes of smaller size are produced as a result of stronger acoustic cavitation events. This assumption was confirmed by our results, in accordance with previous studies.[49,50] It is important to point out that, to minimize the effects of variations in the probe depth, this factor was kept constant at 1.5 cm above the container bottom.

Another aspect to be taken into consideration is the effect of sonication time. It has been reported by Silva et al.[49] that sonication time plays an important role in decreasing vesicles size, although they observed that this effect reached a plateau at about 21 min. Our P-B design revealed a positive effect of sonication time on Z-average size (from 15 to 30 min), although it was weaker than the effects of the other variables selected for the 2^3 full factorial design (especially sonication amplitude). A similar influence is observed for PDI response, but with a stronger effect. We preferred to select sonication amplitude instead of sonication time because one of the goals of controlling factors is to obtain a narrow size distribution.

As the design included a center point with several repetitions (n=5), the presence of curvature in the response variables could be tested (**Tabla 9.**). Because curvature seemed

to be significant (p-value < 0.05), a term involving center point (Ct Pt) was included in the equations for its estimation.

With all this information about the effects and their estimated coefficients, an equation (R^2 = 96.69 %) for Z-average size value of PC liposomes (Y_1) was generated in Equation 3.

$$Y_1 = 62.8 + 2.55\ (O/A) + 0.449\ C - 0.185\ A - 0.0185\ (O/A)\times C - 0.00555\ C\times A - 9.26\ (Ct\ Pt) \quad (2)$$

Equation 3

Different behavior was observed regarding PDI, which was strongly affected by the sonication amplitude as the only significant main effect and its interaction with total lipid amount. There is also another interaction (O/A)×C, but with a lower effect on the PDI response.

To understand the C×A interaction, it is important to take into account the effect of the sonication amplitude as the main effect. An increase in this factor level leads to less monodisperse size distribution, that is, higher PDI values. However, according to the interaction, this response depends highly on the total amount of lipids present in the sample. At a low level of lipids amount, the reduction in size is more effective (as previously mentioned), but the size distribution is large. However, at a high level of the lipids amount, this enlargement of the size distribution is significantly lower.

Curvature in the response was also tested, again revealing a significant presence (p-value < 0.05). For PDI response (Y_2), the following equation with a R^2 value of 89.35 % was obtained in Equation 4.

$$Y_2 = -0.160 + 0.00939\ A - 0.0000420\ (O/A)\times C - 0.0000250\ C\times A - 0.0425\ (Ct\ Pt) \quad (3)$$

Equation 4

These equations are formulated with uncoded coefficients, making it easier to use them to predict selected target size and PDI values.

6.3.3. S60:Cho niosomes

To investigate whether the selected factors in the P−B design for PC liposomes (a reference model for vesicular systems) produced similar effects with other different formulations, the same 2^3 full factorial design using center-point replicates was performed for a typical noisome formulation, in this particular case, S60:Cho niosomes (1:0.5, w/w). The main variables were the organic/aqueous phase volume ratio (O/A), the total concentration of surfactant and stabilizer (C), and the sonication amplitude (A).

The ANOVA results for Z-average size and PDI values are listed in **Table 6.3**, and the corresponding Pareto chart and three-dimensional surface plot are shown in **Figure 6.2** and **Figure 6.3**, respectively. Mean sizes in the range 224-362 nm with PDI values between 0.032 and 0.291 were obtained for S60:Cho niosomes (with standard deviation ranging from 1.05 to 7.28 nm for size and from 0.009 to 0.052 for PDI). Similar size and PDI ranges were reported for niosomes prepared by EIM using Span 60 as membrane component.[17]

Two-way interactions ((O/A)×A, C×A) and a three-way interaction (O/A)×C×A) were detected, with sonication amplitude (A) as the common factor in these interactions (see **Figure 6.2.C**). Therefore, it can be postulated that sonication amplitude is the key factor in the niosomes size response. The response depends on both the O/A and C factor levels, with a higher interaction between sonication amplitude and total amount of membrane components. Differences in the magnitude of the coefficient of this factor between liposomes and niosomes can be attributed to the initial size before sonication (smaller for liposomes) and vesicles stability.[50]

The three main effects are significant, but in contrast to the case for liposomes, the organic/aqueous phase volume ratio (O/A) shows a positive effect on niosomes size. This behavior could be due to different molecular features of the surfactant and stabilizer that result in different interactions with the organic phase and, therefore, poor or not enough solubility.

The other two variables (C, A) have effects similar to those described above for liposomes. Therefore, the same explanation regarding surfactant concentration and sonication amplitude can be applied here to justify their effects on niosomes size. In this

case, the stronger effect of C is explained by the influence of cholesterol on the final size of vesicles, as reported by Padamwar et al.[8]

Once again, curvature was detected for Z-average size response. The following equation (Equation 5) was obtained to model this case, with an adjusted correlation coefficient (R^2) of 91.27 %.

$$Y_3 = 236.9 - 4.31\,(O/A) - 0.012\,C - 0.56\,A + 0.0461\,(O/A)\times C + 0.00363\,C\times A - 0.00114\,(O/A)\times C\times A + 44.00\,(Ct\ Pt) \quad (4)$$

Equation 5

On the other hand, a completely different behavior was observed regarding the PDI response. Only the three main effects (O/A, C, A) were found to be significant, and no interactions were found. Two positive effects on the niosome PDI were detected: surfactant/stabilizer concentration and sonication amplitude. In this case, the total concentration of membrane components seemed to have an important role in the vesicle size distribution, as can be seen in the correspondent Pareto chart (**Figure 6.2**). This observation once again can be attributed to the solubilization of membrane components in the organic phase. Higher concentration of these components requiere better solubilization in dispersed droplets to reach small membrane fragments.

It is important to note that some combinations of factors yield narrow size distributions, namely, PDI ≤ 0.100, a value frequently obtained by other preparation methods, such as microfluidic hydrodynamic focusing[51] also using also S60/Cho as the formulation.

A negative effect was detected for organic/aqueous phase volume ratio (O/A). As the final concentration of ethanol increased during the injection process, a smaller size distribution was obtained. As previously mentioned, no interaction between this factor and the total concentration of membrane components was observed.

The Equation 6 with a R^2 value of 84.73 % was obtained for the niosome PDI model response (Y_4):

$$Y_4 = 0.053 - 0.00392\,(O/A) + 0.000039\,C + 0.00067\,A + 0.0597\,(Ct\ Pt) \quad (5)$$

Equation 6

The estimated coded coefficients for the considered effects on the Z-average sizes and PDIs of PC liposomes and S60:Cho-niosomes are listed in **Table 6.6**, as a summary of the factors´influence. Coded coefficients were used to maintain the orthogonality of the designs and to allow for a direct comparison between coefficients.

Table 6.6. *Estimated coded coefficients for the considered effects on Z-average size and PDI of PC liposomes and S60:Cho niosomes (1:0.5, w/w)*

Responses	Coefficients							
	Constant	**X_1**	**X_2**	**X_3**	**X_1X_2**	**X_1X_3**	**X_2X_3**	**$X_1X_2X_3$**
				Z-average size				
Liposome (Y_1)	89.68	-11.14	12.40	-17.50	-11.75	-	-5.97	-
Niosome (Y_3)	269.82	12.72	16.87	-15.94	-	-12.15	-19.92	-16.04
				PDI				
Liposome (Y_2)	0.280	-	-	0.038	-0.012	-	-0.029	0.010
Niosome (Y_4)	0.136	-0.026	0.057	0.026	-	-	-	-

6.3.4. Vesicles characterization

Size-tuned vesicles were prepared under selected operating conditions by applying the models obtained from the experimental design (Equation 3-6) and the assistance of response optimizer and response prediction at Minitab statistical software (version 17). This tools can be applied to the simultaneous optimization of several responses only when the same set of factors are studied separately, because a common experimental region is needed.

The operating conditions were selected to prepare PC liposomes with a mean size of 70 nm and the minimum PDI value (predicted value of Y_1= 67 ± 4, and Y_2= 0.317 ± 0.013), and S60-Cho niosomes with a mean size of 240 nm and the minimum PDI value (predicted value of Y_3= 239 ± 11, and Y_4= 0.120 ± 0.025). These sizes and PDI values were selected only as an example. The factor output values were O/A= 5:50 , C= 2 g/L and

A= 55 % for the liposomes and O/A= 5.9:50, C= 2 g/L and A= 55 % for the niosomes. **Figure 6.5** and **Figure 6.6** show optimization plots and values of individual and composite desirability for size-tuned liposomes and size-tuned niosomes, respectively.

The experimental results showed that the models obtained with the experimental design were accurate, since mean sizes of 69 ± 0.5 nm (PDI= 0.245 ± 0.005) and 233 ± 3 nm (PDI= 0.112 ± 0.004) were obtained for PC liposomes and S60:Cho niosomes, respectively. The relative error was low for the experimental results regarding mean size (3% for Y_1 and Y_3), but higher for the size distributions (22% for Y_2 and 7% for Y_4).

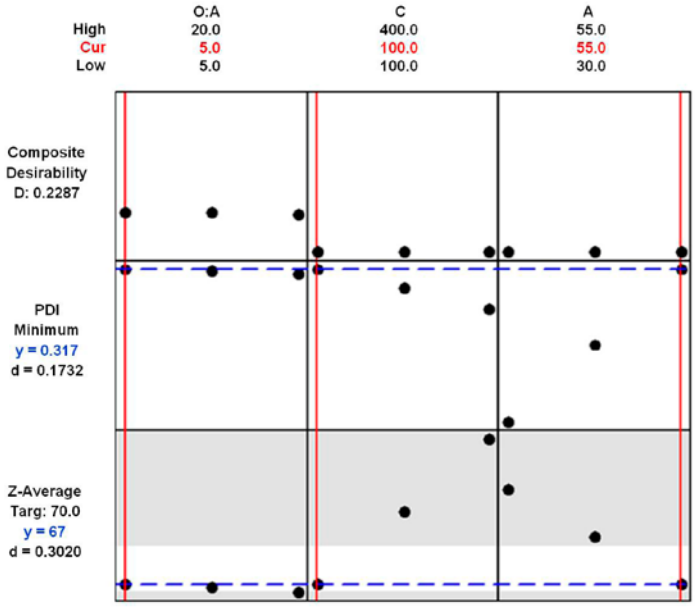

Parameters

Response	Goal	Lower	Target	Upper	Weight	Importance
Z-Average PC-Liposomes	Target	65	70.000	75.000	1	1
PDI PC-Liposomes	Minimum		0.173	0.378	1	1

Solution

Solution	O:A	C	A	Z-Average PC-Liposomes Fit	PDI PC-Liposomes Fit	Composite Desirability
1	5	100	55	67	0.317	0.2287

Response	Fit	SE Fit	95% CI	95% PI
Z-Average PC-Liposomes	67	4	(57, 76)	(51, 83)
PDI PC-Liposomes	0.317	0.013	(0.308, 0.377)	(0.284, 0.402)

Figure 6.5. *Optimization plot and values of individual (d) and composite (D) desirability provided by the response optimizer (Minitab, version 17) for an example of size-tuned PC liposome (desired size = 70 nm, with a minimum PDI value).*

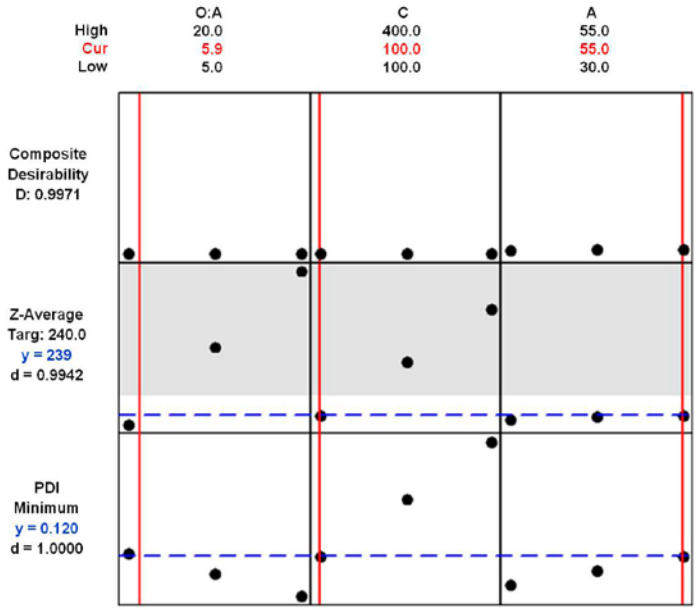

Parameters

Response	Goal	Lower	Target	Upper	Weight	Importance
Z-Average S60:Cho Niosomes	Target	235	240.000	245.000	1	1
PDI S60:Cho Niosomes	Minimum		0.120	0.291	1	1

Solutions

Solution	O:A	C	A	PDI S60:Cho Niosomes Fit	Z-Average S60:Cho Niosomes Fit	Composite Desirability
1	5.9	100	55	0.120	239	0.9971

Response	Fit	SE Fit	95% CI	95% PI
Z-Average S60:Cho Niosomes	239	11	(217, 263)	(198, 281)
PDI S60:Cho Niosomes	0.120	0.025	(0.066, 0.172)	(0.024, 0.214)

Figure 6.6. *Optimization plot and values of individual (d) and composite (D) desirability provided by the response optimizer (Minitab, version 17) for an example of size-tuned S60:Cho niosome (1:0.5 w/w) (desired size = 240 nm, with a minimum PDI).*

The sizes and morphologies of the vesicles were investigated by TEM, using a negative contrast. **Figure 6.7** shows black-stained vesicles, as a result of the interactions of the electron beam with PTA, which produces a selective deposit of metal ions that enhances morphological details. Themicrographs show spherical structures of approximately 80 nmfor the liposomes (**Figure 6.7.C**) and about 250 nm for the niosomes (**Figure 6.7.D**). These values agree with the DLS measurements.

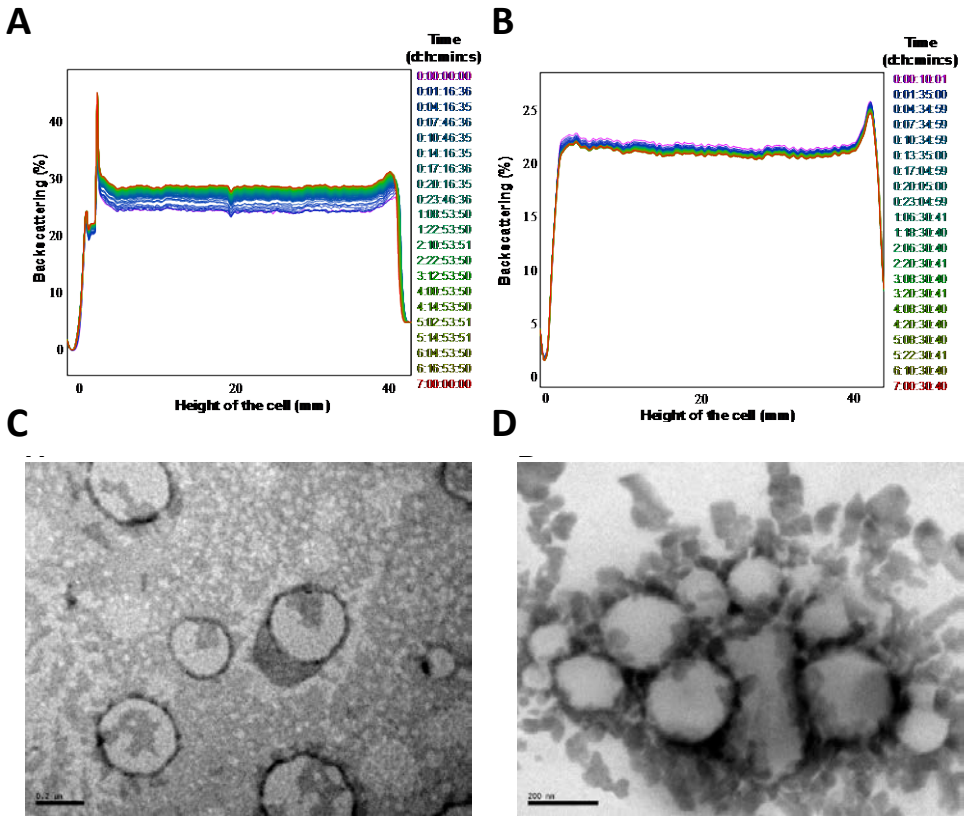

*Figure 6.7. (**A,B**) BS profiles and (**C,D**) TEM micrographs of empty vesicles designed with a controlled size and PDI values by applying the models obtained from experimental design: (**A,C**) PC liposomes and (**B,D**) S60:Cho niosomes (1:0.5, w/w).*

Figure 6.7.D shows clusters of niosomes that are all similar in size. Aggregation arose during the drying step prior to TEM measurements, because no flocculation phenomena were monitored with Turbiscan apparatus.

Slight differences were noticed in zeta potential measurements, exhibiting low values for both types of vesicles. Niosomes had values of about -16.8 ± 0.7 mV, whereas the liposomes had values of -6.9 ± 0.3 mV. This small value for liposomes could be due to neutralization of the negative charge from phosphate groups by sodium cations present in the medium (from sodium chloride in the PBS buffer).

The formulated vesicles exhibited a high stability after 1 week of monitoring time. BS profiles obtained for PC liposomes are given in **Figure 6.5**, where a variation of 4.5% in the middle part of the cell (from 10 to 30 mm) is noticed. A simultaneous slight clarification process was observed in the middle and top parts of the cell in the corresponding transmission profile (results not shown). This was promoted by some movement of PC liposomes towards the bottom of the cell, resulting in a slight increase

in BS (sedimentation). However, this was a reversible process, caused by differences in concentration, with the sample remaining stable and maintaining its initial properties (size and PDI). The vesicles were again characterized after gentle agitation of the cell at the end of the monitoring time with analogous results.

For S60:Cho niosomes (**Figure 6.7.B**), the BS profile remained nearly constant (variations of approximately 0.5%) with time, showing high stability. Some variation was also observed in transmission profile profile all along the cell height, since the sample was not translucent.

6.3.4.1. Encapsulation efficiency (EE)

Vesicles containing Sudan Red 7B and Vitamin D_3 as model compounds (both lipophilic) were also prepared and characterized. No differences were observed regarding mean size and PDI values or TEM, zeta potential or Turbiscan measurements, meaning that entrapped compounds did not affect vesicle´s behavior.

High EE values were obtained for both Sudan Red 7B and Vitamin D_3, as expected taking into account their hydrophobic character. EE values up to 90.1% and 88.0% corresponded to Sudan Red 7B encapsulated in PC liposomes and S60:Cho niosomes, respectively. Experiments carried out with Vitamin D_3 led to EE values of 99.2% for PC liposomes and 73.9% for S60:Cho niosomes. These results are in good agreement with those previous studies, where compounds with similar chemical properties were encapsulated.[12,13,27]

6.4. Conclusions

In this work, an adequate approximation using DoE was applied to study the influence of experimental factors of the EIM on the mean size and size distribution of PC liposomes and S60:Cho niosomes (1:0.5, w/w).

An initial screening design enabled a reduction of the number of variables. This was a necessary step before carrying out a full factorial design. Finally, response models were applied to prepare selected size-tuned nanovesicles, which were characterized from a stability point of view.

This was achieved with a low number of experiments (58 runs). This methodology enabled two different formulations (liposomes and niosomes, the most common types of

nanovesicles) to be studied in a comparative way. Stable liposomes and niosomes of the targeted sizes were successfully prepared with the model equations obtained, with encapsulation efficiencies higher than 73.9 % in all cases for selected hydrophobic compounds.

The most important variables identified by ANOVA were the organic/aqueous phase volume ratio, the (final aqueous phase) phospholipid concentration and the sonication amplitude.

These results offer new insights into the mechanism and effects of the factors involved in nanovesicles preparation by the EIM, one of the most easily scaled-up methods for preparing vesicles for several fields of interest.

6.5. Bibliographic references

[1] Capretto L., Carugo D., Mazzitelli S., Nastruzzi C., Zhang X. (2013). Microfluidic and lab-on-a-chip preparation routes for organic nanoparticles and vesicular systems for nanomedicine applications. *Adv. Drug Deliv. Rev.*, 65:1496-1532.

[2] Rongen H.A.H., Bult A., van Bennekom W.P. (1997). Liposomes and immunoassays. *J. Immunol. Methods*, 204:105-133.

[3] Pando D., Gutiérrez G., Coca J., Pazos C. (2013). Preparation and characterization of niosomes containing resveratrol. *J. Food Eng.,* 117:227-234.

[4] Gómez-Hens A., Fernández-Romero J.M. (2005). The role of liposomes in analytical processes. *Trac-Trends Anal. Chem.*, 24:9-19.

[5] Edwards K.A., Bolduc O.R., Baeumner A.J. (2012). Miniaturized bioanalytical systems: enhanced performance through liposomes. *Curr. Opin. Chem. Biol.*, 16:444-452.

[6] Liu Q., Boyd B.J. (2013) Liposomes in biosensors. *Analyst*, 138:391-409.

[7] Canton I., Battaglia G. (2012). Endocytosis at the nanoscale. *Chem. Soc. Rev.*, 41:2718-39.

[8] Padamwar M.N., Pokharkar V.B. (2006). Development of vitamin loaded topical liposomal formulation using factorial design approach: Drug deposition and stability. *Int. J. Pharm.*, 320:37-44.

[9] Taha E.I. (2014). Lipid vesicular systems: formulation optimization and ex vivo comparative study. *J. Mol. Liq.*, 196:211-216.

[10] Abdelbary A.A., AbouGhaly M.H.H. (2015). Design and optimization of topical methotrexate loaded niosomes for enhanced management of psoriasis: Application of Box–Behnken design, in-vitro evaluation and in-vivo skin deposition study. *Int. J. Pharm.*, 485:235-243.

[11] Jadhav S.M., Morey P., Karpe M., Kadam V. (2012). Novel vesicular system: An overview. *J. Appl. Pharm. Sci.*, 02:193-202.

[12] Rajera R., Nagpal K., Singh S.K., Mishra D.N. (2011). Niosomes: a controlled and novel drug delivery system. *Biol. Pharm. Bull.*, 34:945-53.

[13] Uchegbu I. F., Vyas S.P. (1998). Non-ionic surfactant based vesicles (niosomes) in drug delivery. *Int. J. Pharm.,* 172:33-70.

[14] Bangham A.D., Standish M.M., Watkins J.C. (1965). Diffusion of univalent ions across the lamellae of swollen phospholipids. *J. Mol. Biol.*, 13:238-252.

[15] da Silva Malheiros P., Daroit D.J., Brandelli A. (2010). Food applications of liposome-encapsulated antimicrobial peptides. *Trends Food Sci. Tech.*, 21:284-292.

[16] du Plessis J., Weiner N., Müller D.G. (1994). The influence of in vivo treatment of skin with liposomes on the topical absorption of a hydrophilic and a hydrophobic drug in vitro. *Int. J. Pharm.*, 103:R1-R5.

[17] Manconi M., Sinico C., Valenti D., Loy G., Fadda A.M. (2002). Niosomes as carriers for tretinoin I: Preparation and properties. *Int. J. Pharm.*, 234:237-248.

[18] Manca M.L., Manconi M., Nacher A., Carbone C., Valenti D., Maccioni A.M., Sinico C., Fadda A.M. (2014). Development of novel diolein–niosomes for cutaneous delivery of tretinoin: Influence of formulation and in vitro assessment. *Int. J. Pharm.*, 477:176-186.

[19] Mahale N.B., Thakkar P.D., Mali R.G., Walunj D.R., Chaudhari S.R. (2012). Niosomes: Novel sustained release nonionic stable vesicular systems — An overview. *Adv. Colloid Interface Sci.*, 183–184:46-54.

[20] Moghassemi S., Hadjizadeh A. (2014). Nano-niosomes as nanoscale drug delivery systems: An illustrated review. *J. Control. Release*, 185:22-36.

[21] Mali N., Darandale S., Vavia P. (2013). Niosomes as a vesicular carrier for topical administration of minoxidil: formulation and in vitro assessment. *Drug Deliv. Transl. Res.*, 3:587-592.

[22] Fan M., Xu S., Xia S., Zhang X. (2008). Preparation of salidroside nano-liposomes by ethanol injection method and in vitro release study. *Eur. Food Res. Technol.*, 227:167-174.

[23] Marianecci C., Di Marzio L., Rinaldi F., Celia C., Paolino D., Alhaique F., Esposito S., Carafa M. (2014). Niosomes from 80s to present: The state of the art. *Adv. Colloid Interface Sci.*, 205:187-206.

[24] Akbarzadeh A., Rezaei-Sadabady R., Davaran S., Joo S.W., Zarghami N., Hanifehpour Y., Samiei M., Kouhi M., Nejati-Koshki K. (2013). Liposome: classification, preparation, and applications. *Nanoscale Res. Lett.*, 8:102.

[25] Justo O.R., Moraes Â.M. (2011). Analysis of process parameters on the characteristics of liposomes prepared by ethanol injection with a view to process scale-up: Effect of temperature and batch volume. *Chem. Eng. Res. Des.*, 89:785-792.

[26] Batzri S., Korn E.D. (1973). Single bilayer liposomes prepared without sonication. *Biochim. Biophys. Acta-Biomembr.*, 298:1015-1019.

[27] Pham T.T., Jaafar-Maalej C., Charcosset C., Fessi H. (2012). Liposome and niosome preparation using a membrane contactor for scale-up. *Colloid Surf. B-Biointerfaces*, 94:15-21.

[28] Loukas Y.L. (1998). Experimental studies for screening the factors that influence the effectiveness of new multicomponent and protective liposomes. *Anal. Chim. Acta*, 361:241-251.

[29] Shah S.R., Parikh R.H., Chavda J.R., Sheth N.R. (2013). Application of Plackett–Burman screening design for preparing glibenclamide nanoparticles for dissolution enhancement. *Powder Technol.*, 235:405-411.

[30] El-Samaligy M.S., Afifi N.N., Mahmoud E.A. (2006). Increasing bioavailability of silymarin using a buccal liposomal delivery system: Preparation and experimental design investigation. *Int. J. Pharm.*, 308:140-148.

[31] Shaikh K.S., Chellampillai B., Pawar A.P. (2010). Studies on nonionic surfactant bilayer vesicles of ciclopirox olamine. *Drug. Dev. Ind. Pharm.*, 36:946-53.

[32] Mahmood S., Taher M., Mandal U.K. (2014). Experimental design and optimization of raloxifene hydrochloride loaded nanotransfersomes for transdermal application. *Int. J. Nanomed.*, 9:4331-4346.

[33] Chaudhary H., Kohli K., Kumar V. (2013). Nano-transfersomes as a novel carrier for transdermal delivery. *Int. J. Pharm.*, 454:367-380.

[34] Derakhshandeh K., Erfan M., Dadashzadeh S. (2007). Encapsulation of 9-nitrocamptothecin, a novel anticancer drug, in biodegradable nanoparticles: Factorial design, characterization and release kinetics. *Eur. J. Pharm. Biopharm.*, 66:34-41.

[35] Alund S.J., Smistad G., Hiorth M.A. (2013). A multivariate analysis investigating different factors important for the interaction between liposomes and pectin. *Colloid Surf. A.*, 420:1-9.

[36] Gonzalez-Mira E., Egea M.A., Garcia M.L., Souto E.B. (2010). Design and ocular tolerance of flurbiprofen loaded ultrasound-engineered NLC. *Colloid Surf. B*, 81:412-421.

[37] Pando D., Caddeo C., Manconi M., Fadda A.M., Pazos C. (2013). Nanodesign of olein vesicles for the topical delivery of the antioxidant resveratrol. *J. Pharm. Pharmacol.*, 65:1158-1167.

[38] Pando D., Matos M., Gutiérrez G., Pazos C. (2015). Formulation of resveratrol entrapped niosomes for topical use. *Colloid Surf. B*, 128:398-404.

[39] Devaraj G.N., Parakh S.R., Devraj R., Apte S.S., Rao B.R., Rambhau D. (2002). Release Studies on Niosomes Containing Fatty Alcohols as Bilayer Stabilizers Instead of Cholesterol. *J. Colloid Interface Sci.*, 251:360-365.

[40] Kremer J.M.H., Van der Esker M.W., Pathmamanoharan C., Wiersema P.H. (1977). Vesicles of variable diameter prepared by a modified injection method. *Biochemistry*, 16:3932-3935.

[41] Pons M., Foradada M., Estelrich J. (1993). Liposomes obtained by the ethanol injection method. *Int. J. Pharm.*, 95:51-56.

[42] Justo O.R., Moraes A.M. (2005). Kanamycin incorporation in lipid vesicles prepared by ethanol injection designed for tuberculosis treatment. *J. Pharm. Pharmacol.*, 57:23-30.

[43] Szoka F.C., Jr. (1996). Preparation of liposome and lipid complex compositions. U.S. Patent 5, 549, 910.

[44] Ghanbarzadeh S., Arami S. (2013). Enhanced Transdermal Delivery of Diclofenac sodium via conventional liposomes, ethosomes, and transfersomes. *Biomed Res. Int.*, 1-7.

[45] Antonietti M., Förster S. (2003). Vesicles and liposomes: a self-assembly principle beyond lipids. *Adv. Mater.*, 15:1323-1333.

[46] Wang Z., He X. (2009). Dynamics of vesicle formation from lipid droplets: Mechanism and controllability. *J. Chem. Phys.*, 130:094905.

[47] Lasic, D.D. (1988). The mechanism of vesicle formation. *Biochem. J.*, 256:1-11.

[48] Janmey P.A., Kinnunen P.K.J. (2006). Biophysical properties of lipids and dynamic membranes. *Trends Cell Biol.*, 16:538-546.

[49] Silva R., Ferreira H., Little C., Cavaco-Paulo A. (2010). Effect of ultrasound parameters for unilamellar liposome preparation. Ultrason. *Sonochem.*, 17:628-632.

[50] Yamaguchi T., Nomura M., Matsuok T., Koda S. (2009). Effects of frequency and power of ultrasound on the size reduction of liposome. *Chem. Phys. Lipids*, 160:58-62.

[51] Lo C.T., Jahn A., Locascio L.E., Vreeland W.N. (2010). Controlled self-assembly of monodisperse niosomes by microfluidic hydrodynamic focusing. *Langmui*r, 26:8559-8566.

7. Continuous flow production of size-controllable niosomes using a thermostatic microreactor

Capítulo/Chapter 7

Continuous flow production of size-controllable niosomes using a thermostatic microreactor size-tuned nanovesicles

7.1. Introduction

A precise control over local environment during production of colloids is essential to minimise perturbations in chemical characteristics that could lead to heterogeneous populations, and then, differences in particle properties. To achieve such homogeneity and uniform properties, a strict control of particle size is necessary.[1,2]

Nanovesicles (organic colloids) are particles formed by self-assembled amphiphilic molecules into closed bilayered structures with an inner aqueous core. Depending on the chemical nature of bilayer constituents, these particles are categorised into liposomes (lipids), niosomes (non-ionic surfactants) or polymersomes (block copolymers), as most frequently found in the literature.[3-5]

Niosomes exhibit unique advantages over the other types of vesicular systems due to their inherent characteristics of non-ionic surfactants.[6,7] These advantages include; (i) better chemical and physical stability of suspensions due to the absence of oxidation-related degradation, (ii) easy derivatization to introduce different functional groups for stability enhancement or bioconjugation, (iii) wide range of surfactant types available (with single or double acyl chain, with different length or saturation), (iv) high immunological tolerance, and (v) cost effectiveness. Firstly introduced in the cosmetic industry by L'Oreal for dermal bioactive compounds delivery,[8] over the last 15 years their applications have expanded to many fields. Food fortification,[9] diagnostic agents,[10] analytical chemistry,[11] nanomaterial synthesis,[12] and drug delivery[13] are just some of examples. For all of these applications, a product with specific characteristics, homogeneity and reproducibility is desired, and in particular, controlled size and monodispersity are essential.

Effort has been made to the production of niosomes by traditional methods with tight control over size and size distribution[14] for some specific applications.[15] For example, in

our previous work,[16] we have used experimental design to study the influence of variables in the ethanol injection process, in order to improve particle size tunability.

One of the most popular chemical families for niosome production involves sorbitan esters (commercially available as Span®). Span family members differ in terms of acyl chain length and saturation, with a big range of hydrophilic-lipophilic balance values (HLB), where HLB is an important parameter with implications in drug encapsulation efficiency and morphological characteristics of particles. This parameter is also related to the physical state at room temperature (RT), and influences the minimum temperature (together with *gel-to-liquid* transition temperature, or T_c) that is required at the very stage of the particle formation. On the other hand, some of the compounds used in formulations with great loading capacity, low release rate and stability in solution are solid at RT. For these reasons, a higher and controlled temperature level is mandatory for this process.

Microfluidics technology is very promising for precise control over input variables when mixing chemical species.[17] Other advantages include low consumption of chemicals (relevant in formulation optimization), scale-up possibilities for industrial production, on-line coupling to other processes (such as purification steps), and efficient control over temperature if required.[18] Jahn et al.[19] reported for the first time the hydrodynamic flow focussing (HFF) technique (**Figure 7.1**) for liposomes production. Following that, other researchers have used this method to examine various liposomes formulations and for encapsulating either hydrophobic or hydrophilic molecules.[20,21] Under laminar flow conditions within the HFF configuration, a stream of lipids in organic phase is focussed between two aqueous streams in microchannels, allowing the mixing of chemical species by molecular diffusion. At the two organic/aqueous interfaces, bilayers can be formed and self-assembled into liposomes once a critical concentration is reached. By controlling the flow, the extension of mixing and hence the size of liposomes, could also be controlled. However, the production of niosomes through microfluidic routes remains less explored, and limited attention has been paid to using HFF technique.[22-24]

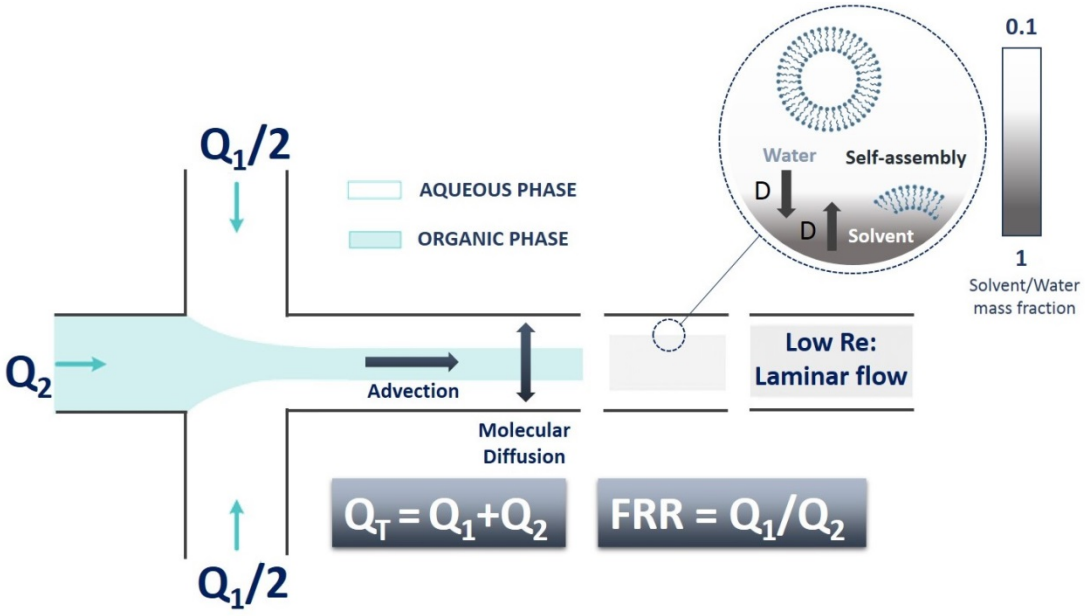

Figure 7.1. *Schematic diagram of a continuous flow microreactor based on hydrodynamic flow focusing for vesicular systems production. The reduction of focused stream width under laminar flow conditions makes possible the mixing of chemical species by molecular diffusion, since time for mixing decreases with the square root of distance. By changing flow rates, the kinetics and extension of mixing can be modified, and then, the size of particles. Amphiphilic molecules are self-assembled into bilayers once critical concentration of solvent is reached, and molecules acquired an ordered state to minimize the interaction with water molecules. At a certain size bending modulus induce planar bilayer to be closed into vesicles.*

At present, the high temperature required for the preparation of niosomes has not been well taken into account in microfluidics routes. For example, the previous work that firstly explored microfluidics assembly of niosomes faced such temperature related challenge, thus only included Span® 20 and Span® 80 (T_m = 25 °C and -30 °C, respectively) in the study.[22]

Along with the wide application of continuous flow microreactors for organic colloids preparation[18] is the development of microreactor itself, including design and manufacturing of such microdevices, with simpler and more affordable production methods.[25] As a result, some traditional fabrications methods which stem from the photo-electronics field, such as photolithography,[26] are being substituted by new processes that require less expensive equipment and can be performed in common labs with no need for clean rooms facilities.[27] Among the techniques explored, additive manufacturing, especially 3D-printing, has emerged as a promising method for microfluidic device manufacturing.[28] The rapid development of 3D-printing technology and the commercialization of desk printers have enabled researchers to explore its utility

in microfluidic prototyping and manufacturing,[29-31] that generally use low cost raw materials and can print objects with desired resolution.

The aim of the present work was to develop a thermostatic microreactor platform for the continuous flow production of niosomes in a size-controllable manner. The microfluidic reactor was designed with a hydrodynamic flow focusing configuration, and fabricated in order to allow visualization of the dynamic process including molecular diffusion, with the aid of an inverted microscope and a digital image acquisition system. 3D-printing technology was used for fabricating the microfluidic device (positive mould) and thermostatic system. The effect of operational parameters was investigated on the final morphological characteristic of niosomes. Niosomes were formulated with non-ionic surfactants with different transition temperatures (T_m) with controlled temperature as a tailoring parameter to tune the size and homogeneity of particles.

7.2. Materials and methods

7.2.1. Materials

Sorbitan monostearate or Span® 60 (Sigma-Aldrich), sorbitan monolaureate or Span® 20 (Sigma-Aldrich), cholesterol from lamb wool (Akros Organics), Phosphate Buffer Saline (10 mM, pH 7.4) prepared from tablets according to manufacture instructions (Sigma-Aldrich), Bromoxylenol blue (Sigma-Aldrich), and technical grade solvents such as ethanol absolute, 2-propanol (or isopropyl alcohol, IPA), and acetone (all from J.T. Baker, Avantor, USA) were used in this work. Ultrapure water was used for all experiments. Poly(dimethylsiloxane) monomer Sylgard® 184 or PDMS was purchased from Dow Corning Corporation (Auburn, AL, USA). Other materials used for devices fabrication are specified in the following respective sections.

7.2.2. Thermostatic system fabrication

Thermostatic chamber was design in Autodesk® Inventor® and 3D-printed with PLA filaments using a special printer for fused deposition modelling (Ultimaker 2+ 3D printer, Ultimaker B.V., The Netherlands). Main chamber and cap of the device were produced separately. A microscope glass slide of 50 x 70 mm (Corning® microscope slides, Sigma-Aldrich, Gillingham, UK) was sealed to the chamber with a 2-phase

adhesive glue special for plastic materials, bought in a local store. A transparent piece of plastic was glued to the cap aperture with the same adhesive used with the other piece. Teflon tape was used to enhance the closure of both elements in a removable way. Holes for the inlets and outlet pipes of the microfluidic device were manually prepared with a sharp tool.

The previously described chamber was connected to a temperature-controllable recirculation system (F12-MC, Julabo GmbH, Germany) through the inlet, and a peristaltic pump (MasterFlex®, Cole-Parmer Instruments Company, USA) through the outlet. The plastic pipes were those from the recirculator, and connections to the chamber were made with common plastic adapters (see supplementary material).

External supply of the recirculator was set approximately at a flow rate of 55 % of the total volume, while peristaltic pump revolution rate was adjusted to remove water from the chamber at a rate that allowed a continuous and constant flow through it. Temperature inside the chamber was monitored with a digital temperature probe (Testo 110, Testo SE & Co., Germany). The sensor probe was introduced into the chamber through a hole placed in one side of plastic window of the cap (see **Figure 7.2**).

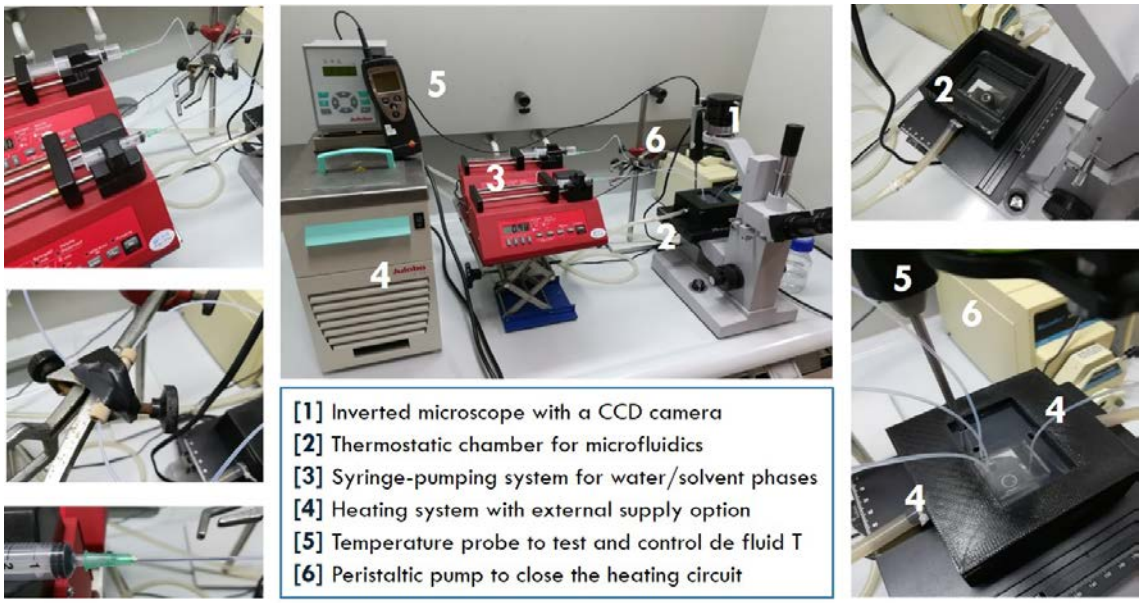

Figure 7.2. *Pictures composition showing the whole setup (central) and detailed components (sides) used in this work for niosomes production by Hydrodynamic Flow Focusing with controlled temperature.*

7.2.3. Microfluidic devices manufacturing and channel characterization

Master mould of devices was designed in Solidworks® CAD 2016 software and 3D-printed onto VeroClear™ resin with the HR-3D printer Objet350 Connex™ (Stratasys Ltd., USA). A post-printing process was also needed. First, mould was flushed with (I) IPA, (II) deionized water, (III) acetone, and finally compressed air. Then, it was cured overnight at 60 °C, and on the following day a treatment of the inner surface was carried out with Aquapeel® (to avoid interference of the resin with PDMS curing process). Three individual moulds were printed.

Once the positive mould was ready, a mixture of degassed PDMS curing agent (1:10 w/w) was poured into it, and left overnight in an oven at 40 °C. For degassing the PDMS mixture, a bench centrifuge was used at 3000 rpm for 10 min. It should be noted that pouring into master mould must be done slowly to minimise bubble formation. On the following day, the replica of the mould was carefully peeled off from the mould, and inlets and outlet holes were prepared with a 1.5 mm biopsy punch with plunger (Miltex®, Fischer Scientific, UK).

Oxygen plasma (PVA-TePla 300 plasma cleaner, Wettenberg, Germany) treatment was applied to bond a microscope glass slide (50 x 70 mm; Corning® microscope slides, Sigma-Aldrich, Gillingham, UK) to the PDMS replica to complete the microfluidic channel. Four pieces of thermic resistant plastic (Ø 8 mm and 3 mm height) were glued in each corner at the bottom of the glass slide, to elevate the device allowing a flow of hot water under the channels.

Polytetrafluoroethylene (PFTE, 0.5 mm I.D.) pipes (Cole-Parmer, UK) were inserted into the holes, and the other end was attached to a syringe needle to create a connection for introduction of the fluids from syringe pumps (NE-300, NEW ERA Pump Systems Inc., USA). Luer lock syringes (Becton, Dickinson and Company, UK) of 1, 10 or 20 mL were used depending on the selected Flow Rate Ratio (FRR), i.e. volumetric flow rate of total aqueous phase/ volumetric flow rate of organic phase.

The mixing channel (23 mm long) on the 3D-printed positive mould was characterized in terms of morphology, accuracy and reproducibility by mechanical profilometry (Talysurf-120L, Taylor-Hobson, United Kingdom). Three equidistance

measurements were taken (2 mm across the channel, perpendicular to it), and data were processed with OriginPro 18 (OriginLab Corporation, USA) software.

The whole setup (microfluidic device inside the thermostatic chamber with respective inlets and outlets) was placed over the stage of an inverted microscope (IN200TAB series, AmScope, USA) with a digital imaging system to capture images (5M.P USB CCD camera, AmScope, USA) supported with the software supplied by the camera manufacturer. The entire experimental setup is illustrated in **Figure 7.2**.

7.2.4. Niosomes production and morphological characterization

Working solutions of 5 and 20 mM of Span® 60:cholesterol and Span® 20:cholesterol (1:0.5 molar ratio) were prepared by dilution from a 50 mM stock solution. Ethanol absolute was used as organic solvent, since it is miscible in aqueous buffer (PBS, 10 mM pH 7.4). Aqueous and organic phases were pumped into microfluidic device once appropriate temperature was reached. Three different total flow rates (Q_T) were studied (50, 100 and 200 µL/min), and aqueous:organic flow rates were adjusted to five different flow rates ratios (FRR) (5, 15, 25, 35 and 50). Span® 20:cholesterol formulation was injected at 30, 40, 50 and 60 °C; while Span®60: cholesterol was only injected at 50 °C. All the combination of membrane components concentration, Q_T, FRR, and temperature was conducted by duplicate.

A total volume of 2.5 mL was collected from the outlet of the device for each experimental condition in a glass vial. Size (z-average or peak value, depending on the number of peaks in the size distribution) and homogeneity (PDI) of particles were measured by Dynamic Light Scattering (DLS) in a Zetasizer NANO-ZS equipment (Malvern Instruments Ltd, Malvern, UK). Samples were measured undiluted by triplicate, with the 173° backscatter detector in disposable low volume cuvettes (Malvern Instruments Ltd, Malvern, UK).

7.2.5. Mixing efficiency visualization

Solvent and no-solvent diffusion by hydrodynamic flow focusing was monitored by an adaption of a previous published methodology.[32] Briefly, a change in colour of a pH indicator dye (bromoxylenol blue) was used, since this dye exhibits a strong yellowish colour at pH below 6.0 and blue at pH above 7.6. A saturated solution of dye in absolute ethanol acidified with acetic acid was focused by PBS adjusted to pH 10.0 with 2M

NaOH solution. Once focused, a change in colour of the stream from yellow blue indicated a molar fraction of aqueous phase close to one, and then, completes mixing by diffusion.

7.3. Results and discussion

With the microreactor platform developed, systematic characterisation and operation were conducted in terms of 3D printing outcomes and nanoproduction, as detailed below. (The performance and optimization of the thermostatic system are shown in **Figure 7.3**).

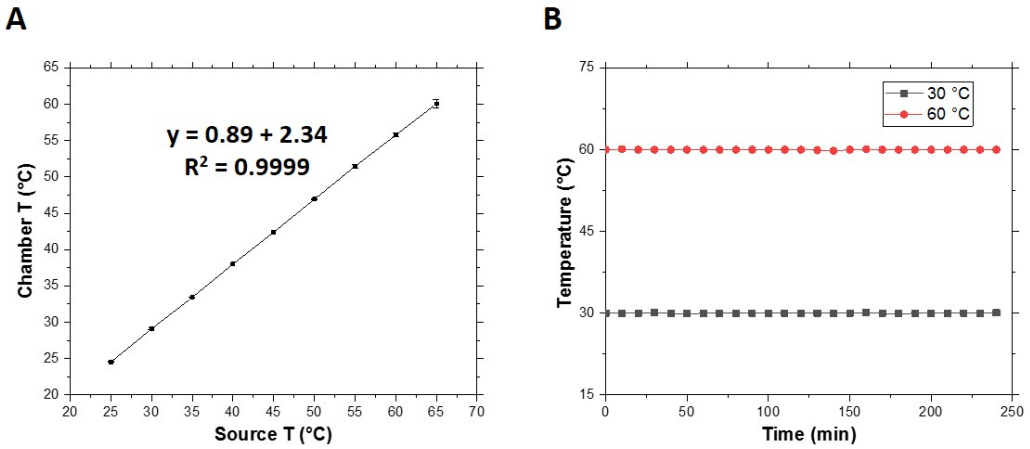

Figure 7.3. *Calibration plot (A) and temperature stability (B) of the in-house designed thermostatic chamber for microfluidics chips, fabricated by 3D-printing technology with PLA filaments. Values represented are the average of three independents measurements.*

7.3.1. High resolution 3D-printing of master moulds for microfluidic devices fabrication

As a key element of the device, mixing channel morphology was characterized by mechanical profilometry onto 3D-printed positive moulds. A considerable difference in nominal dimensions between Computer Aided Design (CAD) and printed object was observed (**Table 7.**). With an original squared cross sectional geometry of 100 µm width and 100 µm height, printed features onto VeroClear® resin showed a curved morphology five times wider and approximately half of the height. At the same time, variations in width and height of the mixing channel were found between the three 3D-printed positive moulds (see **Table 7.1**) even following the same fabrication procedure.

However, these dimensions were reasonably constant along the mixing channel length, especially for channel height.

***Table 7.1**. Morphological characteristics of mixing channel for original Solidworks® CAD 2016 design and 3D-Printed positive moulds (3D-PM) onto VeroClearTM resin with the 3D printer Objet350 ConnexTM (Stratsys). Average and standard deviation values are given for the parameters.*

Mould	Width (μm)	Height (μm)	Cross sectional area (μm)
CAD	100	100	10000
3D-PM1	535 ± 40	47 ± 2	13090 ± 485
3D-PM2	423 ± 14	51 ± 1	11605 ± 262
3D-PM3	507 ± 28	68 ± 3	18007 ± 1092

A possible explanation for these variations in channel dimensions could be related to printer operational parameters. Objet350 Connex3 printer used Polyjet™ inkjet-head patented technology for a layer-by-layer process based on Stereolithography.[33] The jetting head dispensed a proper amount of a photopolymer resin onto a build tray and instantly cured them with UV light. The process took place in XY-axes to create a 2D sheet (down to 16 microns thickness), and by lowering the build tray, another layer was created over the previous one. The cycle was repeated until the whole design was completed. With a resolution of 600 x 600 x 1600 dpi (X-Y-Z-axes respectively) and an accuracy of 20-85 microns for features below 50 mm (up to 200 microns for full model size), the final features depended on geometry (proximity between elements), build parameters (exposure time, printing speed) and model orientation.[29] Comina et al.[29] reported the successful printing of positive moulds for microfluidics devices with elements from 50 μm to 2 mm, however, some artefacts were described between close elements with 50 μm in dimension differences, though working with optimized parameters. Unfortunately, no details about cross section geometry were given for these channels. Some other authors[34] have reported differences between CAD and printed designs with efforts in resin formulation optimization.

In our recent work,[31] we found that 3D printed channels with the Objet350 Connex3 printer were smoother than channels printed with a conventional desk 3D printer (Ultimaker 2+). However, for the same dimensions and aspect ratio, accuracy in cross sectional shape was lower for the HR-3D printer even at large dimensions (1 mm

squared channels). It suggested that further studies are needed to understand this effect with the scale and for different materials in order to inform printing parameters optimization in terms of element dimensions, geometry, and printing materials. Apart from the difference between CAD and 3D-PMs, the cross sectional area of Mould 3 was similar to that previously used by Lo et al.,[22] on which the selected operational parameters of the present work were based.

7.3.2. Production of nanoparticles with temperature control for formulations with high T_m non-ionic surfactants

The use of non-ionic surfactants for the formulation of organic colloids, especially for NVs preparation, exhibits numerous advantages.[4,6] However, a strict control of the temperature is necessary if Span®60 (T_m = 45 °C), one of the most commonly used surfactant in niosome formulation) is involved. **Figure 7.4** shows its precipitation at RT in microchannels once reaching the focusing region, highlighting the significance of temperature effect.

In **Figure 7.4** surfactant precipitation was observed at the focussing region and persists along the channel length when Span® 60 is used at 25 °C. However, at 50 °C a complete mix of both phases were produced without the presence of any surfactant precipitation. Moreover, the production of niosomes at this temperature conditions were observed using Transmission Electron Microspcopy (TEM) and negative staining protocol.

This technique has been less explored than traditional bulk preparation routes,[18] and with important advantages such as better control over particle preparation and the subsequent final characteristics (size and monodispersity, i.e.). This is important for biomedical,[1] food[35] and analytical chemistry[2] applications. In this regard, the influence of operational conditions over particles physical properties was tested by analysing the results of 3 total flow rates (Q_T), two different concentrations of bilayer components, for 5 different FRR. Particle size (nm) and size distribution (PDI) were measured by DLS as output variables. All the combinations were conducted at 50 °C, a temperature over surfactant T_m.

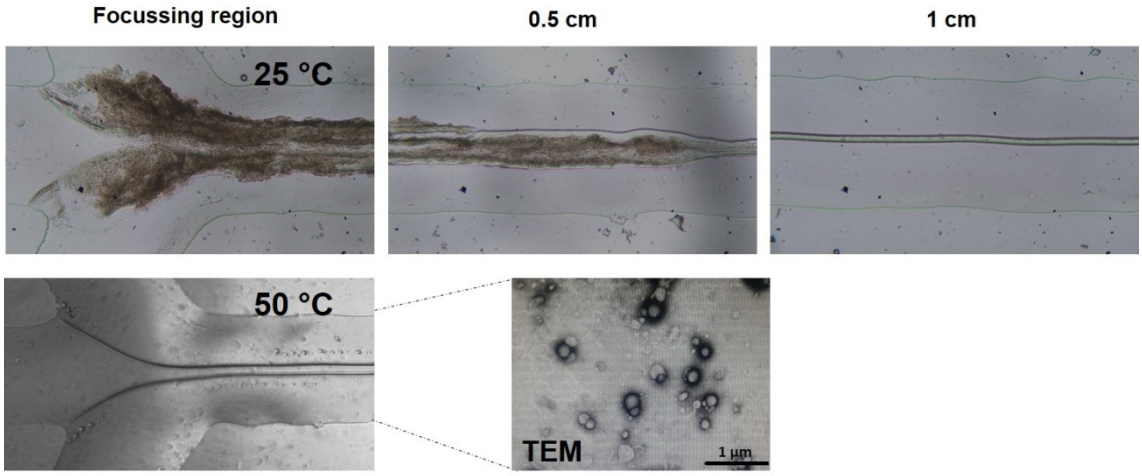

Figure 7.4. *Figure 2. Precipitation of Span® 60 (Tm=45 °C) at room temperature (upper arrow) at the focusing region (left), 0.5 and 1.0 cm downstream (centre and right). At a temperature above surfactant Tm, focusing is complete and vesicles formation could be checked by negative staining (Phosphotungstic acid 2%) and Transmission Electron Microscopy (TEM).*

In general terms, smaller particles were produced as the FRR increased (**Figure 7.5.A** and **Figure 7.5.B**) for both concentrations (5 and 20 mM), and for all the Q_T levels. At a concentration of 5 mM (**Figure 7.5.A**), the particle size decreased from 278, 298 and 358 nm (when FRR = 5) to 155, 129 and 143 nm (when FRR = 50), where Q_T = 50, 100 and 200 µL/min, respectively. At a concentration of 20 mM (**Figure 7.5.B**), similarly, the particle size reduced from 342, 361 and 386 nm (when FRR = 5) to 164, 147 and 151 nm (when FRR = 50) at the three Q_T levels of 50, 100 and 200 µL/min, respectively. Size reduction was rapidly reached with an increment in FRR from 5 to 15, and this reduction became less pronounced from FRR 15 to 50. It is important to take into account that when FRR increased the total amount of bilayer components decreased, not only producing vesicle with smaller size, since particle concentration was also reduced.

No significant effect of different Q_T was observed, while only some differences were noticed in some particular combinations of parameters at low surfactant concentration (5 mM), as seen in **Figure 7.5.A**. These observations were in accordance with previous studies[22] carried out with identical chip configuration for the production of niosomes formulated with other sorbitan esters (Span®20 and 80), and also for the production of liposomes.[19,20,36,37] At lower Q_T, also the linear velocity was lower (hence larger residence time) what can counteract the effect of the bilayer components concentration.

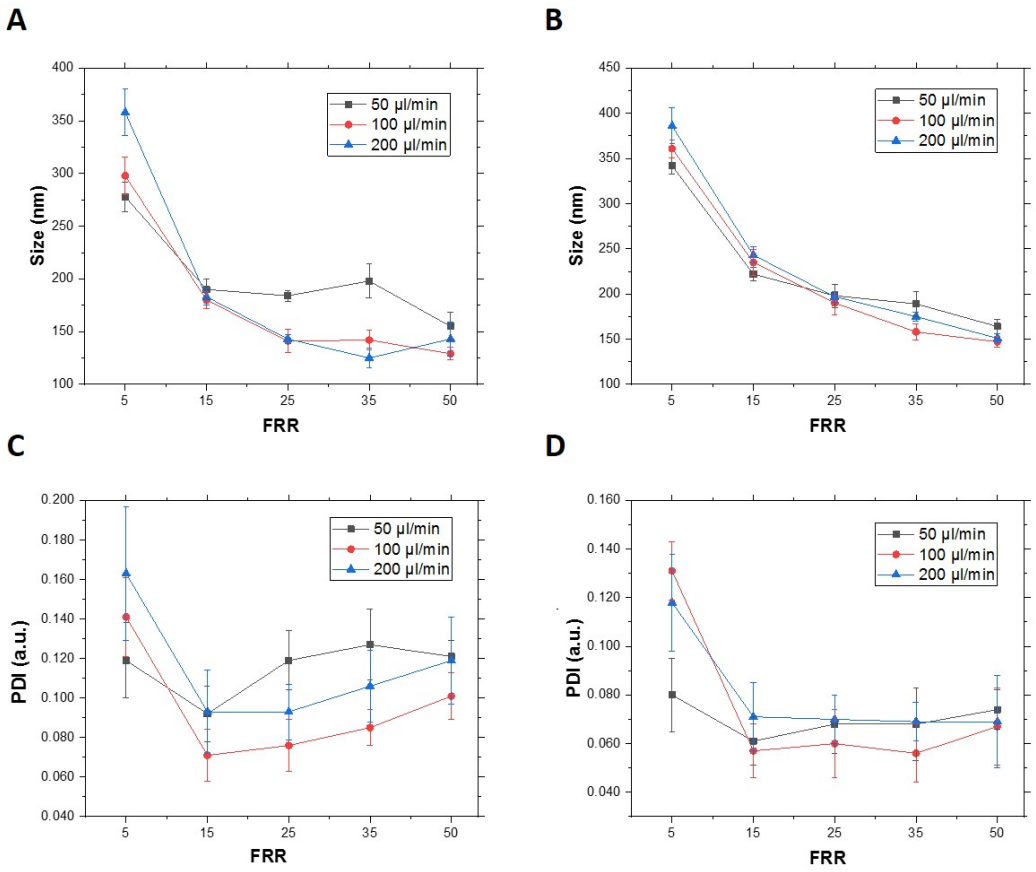

Figure 7.5. *Size (nm) and size distribution (PDI, a.u.) measured by DLS in undiluted samples from niosomes formulated with Span® 60:Cholesterol (1:0.5 molar ratio) at 5mM (A,C) and 20mM (B,D) in a continuous flow microreactor based on hydrodynamic flow focusing at controlled temperature (50 °C). Each condition was tested twice, and each batch was measured by triplicate.*

The increase in FRR, and the subsequent decrease in initial focused width (W_f), reduced the time needed for a complete mixing between solvent and no-solvent (t_{mix}), thus the critical concentration to induce molecules self-assembly was reached faster. This led to smaller vesicles since the total amount of bilayer components was reduced.[38] On the other hand, the reduction of solvent introduced in the mixing channel also decreased the possibility of particle fusion into bigger unities by Ostwald-ripening phenomena.[20,39] A reduced t_{mix} also led to complete mixing in limited length channels. In other cases, no diffused solvent containing amphiphilic molecules self-assembled out of the channel under entirely different conditions (outlet pipes, with no laminar flow characteristics).

Regarding size distribution of particles (**Figure 7.5.C** and **Figure 7.5.D**), PDI value reduced as FRR increased from 5 to 15, (for 5 mM: from 0.119, 0.141 and 0.163 nm at FRR = 5 to 0.092, 0.071 and 0.093 nm at FRR = 50; for 20 mM: from 0.080, 0.131 and 0.118 nm at FRR = 5 to 0.061, 0.057 and 0.071 nm FRR = 50; for both concentration values are

indicated for Q_T = 50, 100 and 200 µL/min respectively), and remained without significant changes at higher FRR for both concentrations. Some authors[19,20,32] reported a significantly increase in PDI with the increment of FRR for an identical chip configuration, but for liposomes production instead. However, our observation was in line with that of Bottaro et al. [32] in a "Y"-shaped device, while Joshi et al.[21] described also a reduction in PDI as FRR increase during liposome formation. No significant differences on PDI were observed for all Q_T levels applied.

The use of microreactors with different channel configurations, and the use of static mixing enhancers,[40] could be the reason of different results among published works. Some of them have highlighted the influence of channel dimensions and configurations over mixing efficiency and particle properties.[19,22,36] The preparation of solvent mixture containing bilayer precursors can also influence the extension and homogeneity of solubilisation, and in consequence, nanoprecipitation process. In the present work, ethanol was used as solvent for microfluidic-based preparation of niosomes for the first time, and this limited the possibility for comparison with other studies.

We have noticed that at high FRRs some transitory perturbations of the focused fluid were recorded, especially at 50 µL/min. The focused stream exhibited a "beating pulse" like effect that was likely produced by the syringe pump due to its own pumping mechanism. These pulses created really short increments in the width of the focused fluid that introduced alteration in solvent exchange kinetics and the subsequent changes in the local concentration of bilayer precursors and solvent concentration.

Surprisingly, lower PDI values were obtained at 20 mM for all FRRs at the three different Q_T. Indeed, these differences were higher at 50 µL/min. At low concentration, those mentioned instabilities can induce more pronounced local changes in bilayer precursor's abundances, with the corresponding effect in particle monodispersity. To gain insights into these observations further studies are needed.

On the other hand, larger particles were obtained when a higher concentrated ethanolic solution of bilayer components was used (20 mM *vs.* 5 mM). This was observed at all Q_T and FRR levels (see in **Figure 7.6**). The same observation was also reported by other authors when producing liposome using microchannels,[37] and in agreement with the mechanism of vesicle formation under microfluidic flow dynamic mixing.

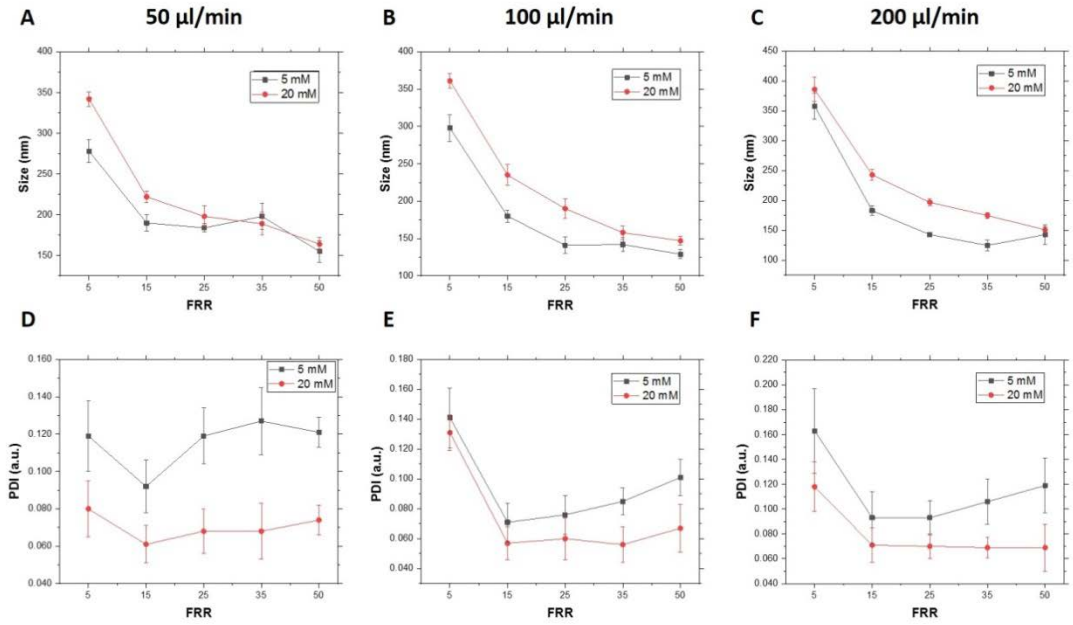

Figure 7.6. *Effect of bilayer components concentration for niosomes formulated with Span® 60:Cholesterol (1:0.5 molar ratio) and produced under the same flow conditions (QT and FRR) for size (upper row) and size distribution (lower row).*

The efficiency of mixing under the assayed working conditions was studied following a published methodology.[32] With this method, mixing efficiency was measured through the change in colour of a pH indicator dye (bromoxylenol blue), that changed from yellow (acidic ethanolic solution containing bilayer precursors) to blue (basic aqueous phase, PBS pH= 10). A shift in focused fluid colour from yellow to blue indicated that molar fraction of water into the stream was close to 1 and the subsequent molar fraction of EtOH became close to 0, evidencing a complete mixing by solvent and aqueous effluents. This change in colour was easily detected in the inverted microscope, and recorded with the digital camera. As an example, results for Q_T = 100 µl/min at several FRRs are shown in **Figure 7.7**.

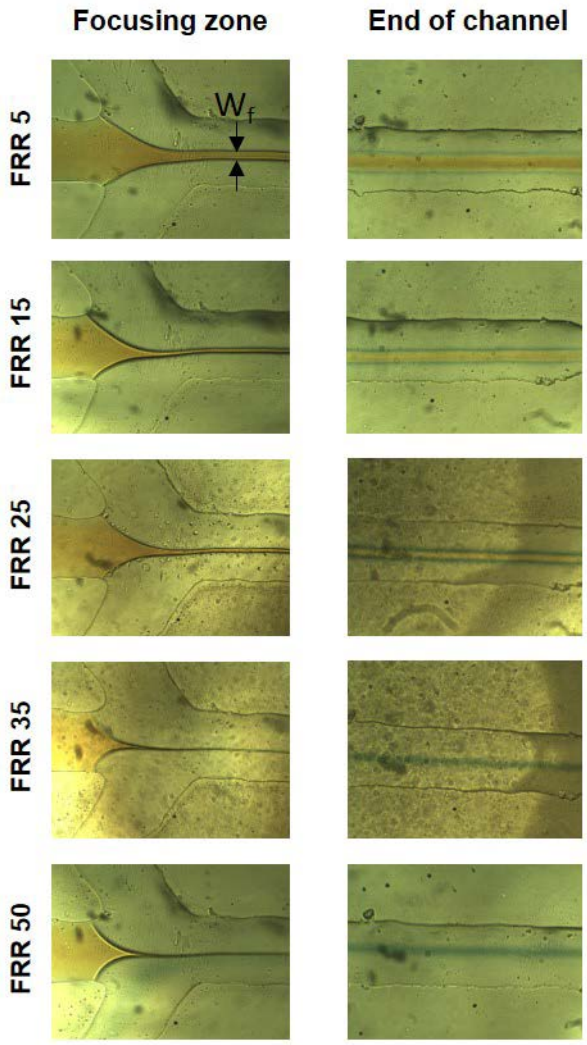

Figure 7.7. *Images (4X) of focusing region and end of the mixing channel evidencing hydrodynamic flow focussing of a central ethanol stream at different FRR values for QT=100 µL/min and 50 °C. Yellow colour indicates acid pH (pure EtOH, no mixing), while blue colour indicates basic pH (complete mixing by codiffusion of solvent and no solvent). Bromoxylenol blue dye was dissolved in EtOH (acidified with acetic acid), and PBS was adjusted with NaOH to pH 10.*

Complete mixing was only reached at high values of FRR (35 and 50) for Q_T = 50 µl/min and Q_T = 100 µl/min, and only at the high FRR (50) for Q_T = 200 µl/min. As Q_T increased, residence time of the fluid inside mixing channel reduced (from 0.5 s at 50 µl/min to 0.13 s at 200 µl/min), preventing to stay the necessary time to reach complete mixing. Only at high FRR value, t_{mix} was short enough to be compatible with low values of residence time for our channel dimension (t_{mix} = 17 ms and 8 ms for FRR = 35 and 50, respectively, predicted according to a theoretical model (**Equation 7**,[41]). In this model W_f represents the width of focused stream, where w is the channel width and D is solvent diffusion coefficient.

$$t_{mix} \sim \frac{W_f^2}{4D} \approx \frac{w^2}{9D} \frac{1}{(1+FRR)}$$ *Equation 7*

As seen in **Figure 7.5**, W_f decreased as FRR increased, and a dependence of W_f with Q_T was observed at lower FRR values (**Figure 7.8.A**). It was also observed that a lower Q_T generated wider focused streams probably due to the lower pressure exercised by the lateral aqueous flows to the middle solvent flow, but these differences became less pronounced at higher FRRs. A similar trend was observed by Bottaro et al.[32] in an identic channels configuration, but contrary to Jahn et al.[19] who reported a non-variation in W_f with modifications in Q_T.

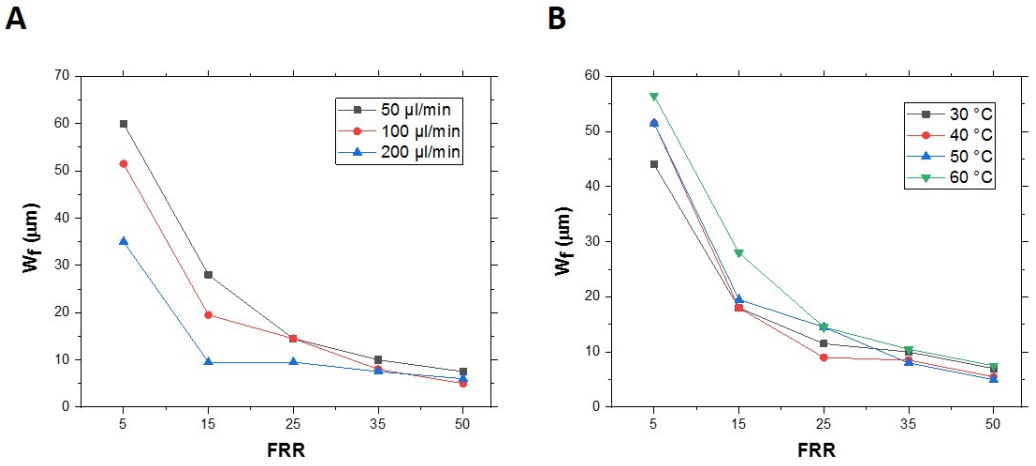

Figure 7.8. *Values of ethanol focused stream (Wf, µm) as flow rate ratio (FRR) increased for different values of volumetric rates (QT) at constant temperature (50 °C), and different temperatures at constant QT (100 µL/min). Values represent the average of two independent measurements, taken at approx. at 100 µm from the end of focussed region.*

Moreover, an intense inverse correlation (potential) between FRR and W_f was observed at all the Q_T levels (**Table 7.2**). However, a strong negative correlation (linear) between particle size and W_f was observed at the two different concentrations studied. These correlations reflect that particle size is governed by focusing parameters. It is clear that niosomes size can be tuned with the selection of the appropriate FRR and Q_T values, which are key parameters for W_f and residence time.

Table 7.2. *Correlation factor between flow focusing parameters (FRR and Wf) and particle size at different concentration of bilayer components and variable QT (A), and at fixed concentration and QT for different working temperatures (B).*

(A)

R^2 *(T = 50 °C)*	50 µl/min	100 µl/min	200 µl/min
(*) FRR *vs* W_f	0.99	0.97	0.92
(**) W_f *vs* Particle size	0.86 *(5 mM)*	0.98 *(5 mM)*	0.97 *(5 mM)*
	0.98 *(20 mM)*	0.99 *(20 mM)*	0.93 *(20 mM)*

FRR, Flow Rate Ratio; Q_T, Total volumetric rate; W_f, initial width of focused stream; (*) potential correlation; (**) linear correlation

(B)

R^2 *(Q_T = 100 µl/min)*	30 °C	40 °C	50 °C	60 °C
(*) FRR *vs* W_f	1.00	0.99	0.97	0.98
(**) FRR *vs* Particle size	0.24	0.56	0.91	0.65

FRR, Flow Rate Ratio; Q_T, Total volumetric rate; W_f, initial width of focused stream; (*) potential correlation; (**) linear correlation

7.3.3. Production of niosomes at different temperatures to study potential tailoring effect over particle morphology

In this part of work Q_T of 100 µL/min and 5 mM of components concentration were selected, since these have been the best operating conditions in terms of smaller particles with narrower size distributions.

The effect of temperature was examined in a rage of 30 °C and 60 °C as another operating parameter on size-tuned niosomes formation through flow-focused based microfluidics. For this purpose, a non-ionic surfactant with low T_m was needed that allowed to test a wide range of working temperatures. Sorbitan monolaureate or Span® 20 (T_m = 25 °C and HLB 8.6) was selected, another common surfactant used for niosomal formulations,[42] and surfactant:cholesterol molar ratio was kept in 1:0.5 as for Span® 60 in order to allow formulations comparisons.

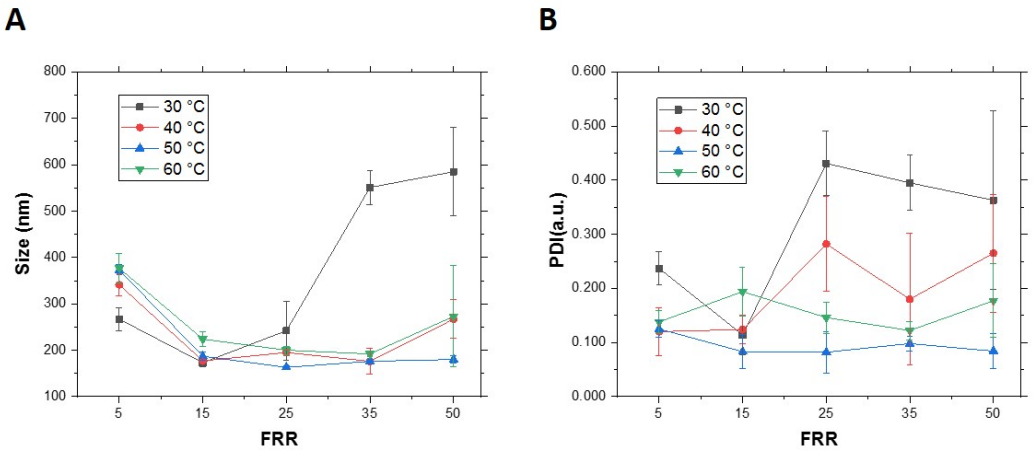

Figure 7.9*.Size (nm) (**left**) and size distribution (PDI, a.u.) (**right**) measured by DLS in undiluted samples from niosomes formulated with Span® 20:Cholesterol (1:0.5 molar ratio) at 5mM in a continuous flow microreactor based on hydrodynamic flow focusing at different controlled temperatures (30, 40, 50, and 60 °C). Each condition was tested twice, and each batch was measured by triplicate.*

Figure 7.9 depicts the results of particle size at the same FRRs previously used for Span® 60 niosomes at different working temperatures: 30, 40, 50 and 60 °C. At 30 °C, a reduction in particle size from FRR=5 to FRR=15 was observed. As FRR increased size became also larger (even higher that those particles produced at FRR = 5). This phenomenon could be related to the observation of cholesterol precipitates inside the mixing channel that were formed immediately after focusing region. The low solubility of cholesterol in water at nearly room temperature induced its precipitation as crystals. Those precipitates modified the flow properties and introduced turbulences that induced micro domains in the fluid with different concentrations of bilayer components, and particles with different morphologies. Also the depletion of cholesterol could generate different particles than those produced in their presence. These perturbations were magnified at higher FRR, since as seen in **Figure 7.9.B** the width of focused fluid became smaller with the increment of FRR, and this stream was relatively smaller than the formed crystals (around 100 μm structures).

For the rest of temperatures, a similar behaviour as for Span® 60 niosomes was observed. Particles size became smaller with an inverse correlation with FRR. At higher temperatures, focused ethanol stream was wider, and these differences were reduced with the increment in FRR. Only slight differences in particle size could be detected (**Figure 7.9.A**).

Regarding temperature effect some authors reported an increase in particle size as temperature increased[24] which were attributed to the bilayer expansion at higher temperature.[43] In our case, such increase in particle size was not observed. It is know that collapse pressure and surface compressional moduli decrease with temperature for all surfactants, and this implies that Span monolayers are more expanded with increments in temperature. However, as temperature increases planar bilayer precursors are less rigid, which could be easily bended to closed structures, and this effect could lead then to smaller particles.[38]

Regarding size distribution and temperature, it was observed that the increment of temperature yielded more monodisperse particles, especially at 50 °C. Complete mixing can be reached at FRR = 35 and FRR = 50 at any temperature. Only at 50 and 60 °C PDI values remained nearly constant (after a first reduction from FRR=5 to 15) with the increment in FRR.

7.3.4. Effect of surfactant acyl chain length over particles size and monodispersity

Another interesting finding resulted from the comparison between niosomes formulated with different non-ionic surfactants under identical preparation conditions. In this work niosomes with sorbitan esters with different saturated acyl chain lengths (C12 and C18 for Span® 20 and 60 respectively) were prepared. As seen in **Figure 7.10,** shorter chains generally yielded larger niosomes. That was contrary to what would be expected; it is generally understood that shorter chains increase the curvature radius of the bilayer, according to the critical packing parameter (cpp) of the molecules,[6] allowing smaller particles. However, if was taken into account the higher hydrophilic character of Span® 20 compared to Span® 60 (higher HLB value) the higher hydrophilicity could enhance water soak into the inner core of the vesicle, resulting in larger vesicles size. Similar results were reported by Gutierrez et al.[44] when niosomes were prepared by mechanical agitation. Regarding niosome size distributions, no differences between both types of surfactants were observed.

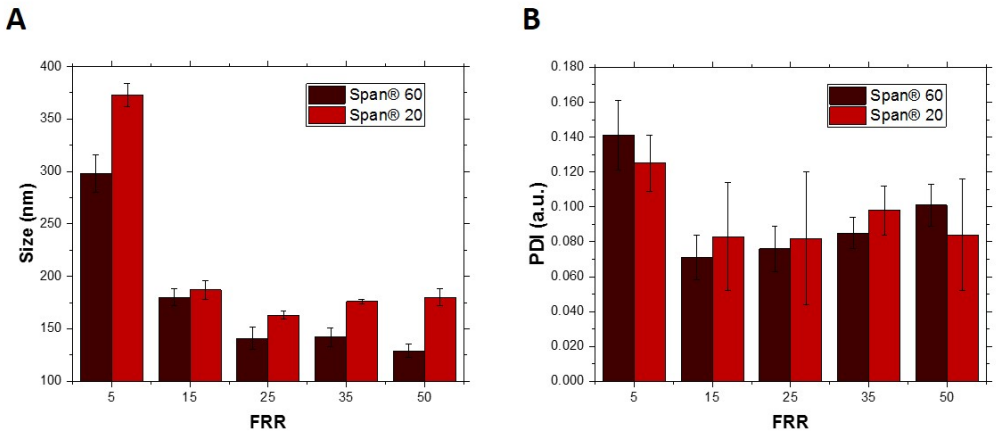

Figure 7.10. *Influence of acyl chain length (C12 and C18 for Span® 20 and Span® 60 respectively) of two different sorbitan sters used in niosomes formulation (surfactant: cholesterol 1:0.5 molar ratio, 5 mM), and produced under different conditions by hydrodynamic flow focusing at controlled temperature (50 °C) and a flow rate QT=100 µl/min.*

7.4. Conclusions

Novel prototyping and additive manufacturing techniques with such as (HR)3D-printing have been applied for the fabrication of a microfluidic continuous flow reactor for hydrodynamic flow focusing at controlled temperature compatible with commercial inverted microscopes. Despite some alteration in cross sectional dimensions and morphology accuracy with respect to the original CAD design, high resolution 3D-printed positive moulds allow us to create functional microreactors for organic colloid production under different working conditions, and to study their effect on aqueous/solvent mixing efficiency through molecular diffusion, and its relationship with particles morphology.

This work shows that temperature is an essential parameter that must be taken into consideration when formulating niosomes with surfactants with T_m over RT. Also it can be used to modify the properties of particles (size and dispersity) produced with non-ionic surfactants with T_m above RT.

We have found that flow focussing at controlled temperature follows the same patterns as for RT, with the ratio between aqueous and solvent streams being the main parameter to control focused stream width and hence, mixing efficiency and kinetics. However, total flow rate only has insignificant effect when FRRs are set to low values, whilst it can influence residence time, and subsequently, mixing efficiency. In general

terms, an increase in FRR yields a focused stream being narrower, and then, smaller particles due to the reduction in residual solvent and the introduction of less amount of bilayer components. This reduction allows complete mixing, even at high total flow rate, resulting in the size distribution of generated particles being more homogeneous. The counterpart is that production yield is reduced, since particles are generated in a less concentrated suspension. Another variable found to be relevant is the component concentration in ethanol feeding solution, with a direct effect on particle size and monodispersity. A more concentrated solution induces an increment in particle size at any total flow rate, but surprisingly, better size distribution. Complementary, we have checked the influence of acyl chain length over particles morphology, and the versatility that introduces this parameter into the properties and functionalities of this type of biomaterial.

The effect of ethanol stratification due to differences in density was not taken into account, which need further investigation in for future work, in particular in its relationship with focusing temperature.

The findings in this works provide valuable information about microfluidics-based production of niosomes at different operational conditions, and are expected to support the expansion of this technique for the preparation of a wider range of organic colloids with important characteristics for related industries with growing interest in different application fields.

7.5. Bibliographic references

[1] Albanese A., Tang P.S., Chan W.C. (2012). The effect of nanoparticle size, shape, and surface chemistry on biological systems. *Annu. Rev. Biomed. Eng.*, 14:1-16.

[2] Kelly K.L., Coronado E., Zhao L.L., Schatz G. (2003). The optical properties of metal nanoparticles: the influence of size, shape, and dielectric environment. *J. Phys. Chem. B*, 107:668-677.

[3] Tarun G., Amit K.G. (2014). Liposomes: targeted and controlled delivery system. *Drug Deliv. Lett.*, 4:62-71.

[4] Abdelkader H., Alani A.W.G., Alany R.G. (2013). Recent advances in non-ionic surfactant vesicles (niosomes): self-assembly, fabrication, characterization, drug delivery applications and limitations. *Drug Deliv.*, 21:87-100.

[5] Lee J.S., Feijen J. (2012). Polymersomes for drug delivery: design, formation and characterization. *J. Control. Release*, 161:473-483.

[6] Marianecci C., Di Marzio L., Rinaldi F., Celia C., Paolino D., Alhaique F., Esposito S., Carafa M. (2014). Niosomes from 80s to present: The state of the art. *Adv. Colloid Interface Sci.*, 205:187−206.

[7] De S. and Prasad M.R., Self-assembled cell-mimicking vesicles composed of amphiphilic molecules: structure and applications, Volume 1, Encyclopedia of biocolloids and Biointerface Science, First Edition, Hiroyuki Ohshima (Ed.), 2016, John Wiley & Sons.

[8] Handjani-Vila R., Ribier A., Rondot B.A., Vanlerberghie G. (1979). Dispersions of lamellar phases of non-ionic lipids in cosmetic products. *Int. J. Cosmet. Sci.*, 1979, 1:303-314.

[9] Gutiérrez G., Matos M., Barrero P., Pando D., Iglesias O., Pazos C. (2016). Iron-entrapped niosomes and their potential application for yogurt fortification. *Food Sci. Technol.,* 74:550-556.

[10] Demir B., Baris B.F., Pinar G.Z., Unak P., Timur S., (2018) Theranostic niosomes as a promising tool for combined therapy and diagnosis: "all-in-one" approach. *Appl. Nano Mater.*, 1:2827-2835.

[11] García-Manrique P., Lozano-Andrés E., Estupiñán-Sánchez O.R., Gutiérrez G., Matos M., Pazos C., Yañez-Mo M., Blanco-López C. (2016). Biomimetic small extracelular vesicles, 3rd GEIVEX Simposium, San Sebastian, Spain, 29-30 September, Poster communication.

[12] De S., Kundu R., Biswas A. (2012). Synthesis of gold nanoparticles in niosomes. *J. Colloid. Interface Sci.*, 386:9-15.

[13] Bartelds R., Hadi N.M., Pols T., Stuart M.C.A., Pardakhty A., Asadikaram G., Poolman B. (2018). Niosomes, an alternative for liposomal delivery. *PLoS ONE*, 13:e0194179.

[14] Justo O.R., Moraes A.M. (2011). Analysis of process parameters on the characteristics of liposomes prepared by ethanol injection with a view to process scale-up: Effect of temperature and batch volume. *Chem. Eng. Res. Des.*, 89:785−792.

[15] Danaei M., Dehghankhold M., Ataei S., Davarani Hasanzadeh F., Javanmard R., Dokhani A., Khorasani S., Mozafari M.R. (2018). Impact of particle size and polydispersity index on the clinical applications of lipidic nanocarrier systems. *Pharmaceutics*, 57:1-17.

[16] García-Manrique P., Matos M., Gutierrez G., Estupiñán O.R., Blanco-López M.C., Pazos C. (2016). Using factorial experimental design to prepare size-tuned nanovesicles. *Ind. Eng. Chem. Res.*, 55:9164-9175.

[17] van Swaay D., deMello A. (2013). Microfluidic methods for forming liposomes. *Lab Chip*, 13:752-767.

[18 Capretto L., Carugo D., Mazzitelli S., Nastruzzi C., Zhang X. (2013). Microfluidic and lab-on-a-chip preparation routes for organic nanoparticles and vesicular systems for nanomedicine applications. *Adv. Drug Deliv. Rev.*, 65:1496-1532.

[19] Jahn A., Vreeland W.N., DeVoe D.L., Locascio L.E., Michael G. (2007). Microfluidic directed formation of liposomes of controlled size. *Langmuir*, 23:6289-6293.

[20] Kastner E., Verma V., Lowry D., Perrie Y. (2015). Microfluidic-controlled manufacture of liposomes for the solubilisation of a poorly water soluble drug. *Int. J. Pharm*., 485:122-130.

[21] Joshi S., Hussain M.T., Carla B.R., Anderluzzi G., Kastner E., Salmaso S., Kirby D.J., Perrie Y. (2016). Microfluidics based manufacture of liposomes simultaneously entrapping hydrophilic and lipophilic drugs. *Int. J. Pharm.*, 514:160-168.

[22] Lo C.T., Jahn A., Locascio L.E., Vreeland W.N. (2010). Controlled self-assembly of monodisperse niosomes by microfluidic hydrodynamic focusing. *Langmuir*, 26:8559-8566.

[23] Obeid M.A., Khadra I., Mullen A.B., Tate R.J., Ferro V.A. (2017). The effects of hydration media on the characteristic of non-ionic surfactant vesicles (NISV) prepared by microfluidics. *Int. J. Pharm*, 56:52-60

[24] García-Salinas S., Himawan E., Gracia M., Arruebo M., Sebastian V. (2018). Rapid on-Chip assembly of niosomes: batch versus continuous flow reactors. *Appl. Mater. Interfaces*, 10:19197-19207.

[25] Gross B.C., Erkal J.L., Lockwood S.Y., Chen C., Spence D.M. (2014). Evaluation of 3D printing and its potential impact on biotechnology and the chemical sciences. *Anal. Chem.*, 86:3240-3253.

[26] Dong J., Liu J., Kang G., Xie J., Wang Y. (2014). Pushing the resolution of photolithography down to 15 nm by surface plasmon interference. *Sci Rep*, 4:5618.

[27] Carugo D., Lee J.Y., Pora A., Browning R.J., Capretto Lorenzo, Nastruzzi C., Stride E., (2016). Facile and cost effective production of microscale PDMS architecture using a combined micromilling-replica moulding (μMI-REM) technique. *Biomed. Microdevice*s, 18:1-10.

[28] Au A.K., Huynh W., Horowitz L.F., Folch A. (2016). 3D-Prinded microfluidics. *Angew. Chem. Int. Ed*., 55:3862-3881.

[29] Comina G., Suska A. Filippini D. (2014). PDMS lab-on-a-chip fabrication using 3D printed templates. *Lab Chip*, 14:424-430.

[30] Hwang Y., Paydar O.H., Candler R.N. (2015). 3D Printed molds for non-planar PDMS microfluidic channels. *Sens. Actuator A-Phys.,* 226:137-142.

[31] Cristaldi D.A., Yanar F., Mosayyebi A., García-Manrique P., Stulz E., Carugo D., Zhang X. (2018). Easy-to-perform and cost-effective fabrication of continuous-flow reactors for their application for nanomaterials synthesis. *N Biotechnol*., 47:1-7.

[32] Bottaro E., Mosayyebi A., Carugo D., Nastruzzi C. (2017). Analysis of the diffusion process by pH indicator in microfluidic chips for liposomes production. *Micromachines*, 8:209.

[33] 3D Printing and additive manufacturing-Fifth Edition, Principles and Applications, 2017, Chee Kai Chua andKah Fai Leong (editors), World Scientific Publishing Co. Pte. Ltd. Singapore.

[34] Gaal G., Mendesa M., de Almeideb T.P., Piazzettad M.H.O., Gobbi Â.L., Riul Jr A., Rodrigues V. (2017). Simplified fabrication of integrated microfluidic devices using fused deposition modeling 3D printing. *Sens. Actuators B Chem*., 242:35-40.

[35] Ezhilarasi P.N., Karthik P., Chhanwal N., Anandharamakrishnan C. (2013). Nanoencapsulation techniques for food bioactive components: a review. *Food Bioprocess Technol.*, 6:628–647.

[36] Carugo D., Bottaro E., Owen J., Stride E., Nastruzzi C. (2016). Liposome production by microfluidics: potential and limiting factors. *Sci Reports*, 19:25876.

[37] Hood R.R., DeVoe D.L. (2015). High-throughput continuous flow production of nanoscale liposomes by microfluidic vertical flow focusing. *Small*, 11:5790-5799.

[38] Antonietti M., Förster S. (2003). Vesicles and Liposomes: a self-assembly principle beyond lipids. *Adv. Mater.*, 15:1323-1333.

[39] Zhigaltsev I.V., Belliveau N., Hafez I., Leung A.K.K., Huft J., Hansen C., Cullis P.R. (2012). Bottom-Up design and synthesis of limit size lipid nanoparticle systems with aqueous and triglyceride cores using millisecond microfluidic mixing. *Langmuir*, 28:3633-3640.

[40] Kastner E., Kaur R., Lowry D., Moghaddam B., Wilkinson A., Perrie Y. (2015). High-throughput manufacturing of size-tuned liposomes by a new microfluidics method using enhanced statistical tools for characterization. *Int. J. Pharm.*, 477:361-368.

[41] Karnik R., Gu F., Basto P., Cannizzaro C., Dean L., Kyei-Manu, Langer R., Farokhzad O.C. (2018). Microfluidic platform for controlled synthesis of polymeric nanoparticles. *Nano Lett.*, 8:2906-2912.

[42] Manosroi A., Wongtrakul P., Mnosroim J., Sakai H., Sugawara F., Yuasa M., Abe M., (2003). Characterization of vesicles prepared with various non-ionic surfactants mixed with colesterol. *Colloid Surface B,* 30:129-138.

[43] Peltonen L., Hirvonen J., Yliruusi J. (2001). The effect of temperature on sorbitan surfactant monolayers. *J. Colloid Interf. Sci.,* 239:134-138.

[44] Gutiérrez G. Benito J.M., Pazos C., Coca J. (2014). Evaporation of aqueous dispersed systems and concentrated emulsions formulated with non-ionic surfactants. *Int. J. Heat Mass Transf.*, 69:117-128.

8. Particle size and encapsulation efficiency dependence with cargo molecular weight and film hydration solution for niosomes formulated with mixture of surfactants

Capítulo/Chapter 8

Particle size and encapsulation efficiency dependence with cargo molecular weight and film hydration solution for niosomes formulated with mixture of surfactants

8.1. Introduction

Vesicles are commonly used as drug delivery systems for different active compounds. Vesicles show special promise as drug carries due to their unique properties such as nanometric size, high surface-volumen ratio, and ease of drug-release modulation.[1] Niosomes are a specific type of vesicles formed by the self-assembly of non-ionic surfactants in aqueous media that leads to closed bilayers.[2] This structure enables them to encapsulate aqueous solutions leading either the encapsulation of hydrophilic and hydrophobic compounds.[3]

Niosomes offer some advantages over other encapsulation technologies such as their low cost, chemical stability, biocompatibility, among others.[4] Furthermore, non-ionic surfactants self-assemblies are easily derivatized, which provides functional versatility to their structure.[5]

In recent years, niosomes have been used for encapsulating drugs,[6] nutraceuticals,[7] antioxidants,[8,9] micronutrients,[10] etc. There are still many challenges in the development of delivery systems that could encapsulate hydrophilic compounds effectively. There are colors, nutraceuticals and vitamins of industrial interest that need to be protected of chemical degradation, to inhibit adverse interaction with other components, to mask off-flavors, or to obtain a particular release profile. For example, some water soluble colors are susceptible to chemical degradation under certain conditions, e.g., pH, light or temperatura.[11] Water soluble vitamins are not stored in the body, and could be washed out during food processing making necessary to replenish them daily.[12]

In this work, three different bioactive hydrophilic compounds with different molecular weight and industrial interest were encapsulated (**Figure 8.1**): ascorbic acid (Vitamin C), rhodamine B (Fluorescent organic dye) and cobalamin (Vitamin B_{12}). Ascorbic acid, found in citrus fruits, berries and vegetables, acts mainly as antioxidant, but also promotes the production of noradrenaline, collagen, bile acids, and increases the intestinal absorption of non-heme iron.[12,13] Rhodamine B is a synthetic and highly soluble molecule used as pigment in drug and cosmetic formulations due to its absorption and emission properties.[14,15] Finally, cobalamin belongs to the B-complex vitamins and can be found in cheese, fish, milk or eggs. It functions as coenzyme and as an important intermediate in the metabolism of folic acid, a compound really important to prevent congenital disorder during the first stage of pregnancy.[12]

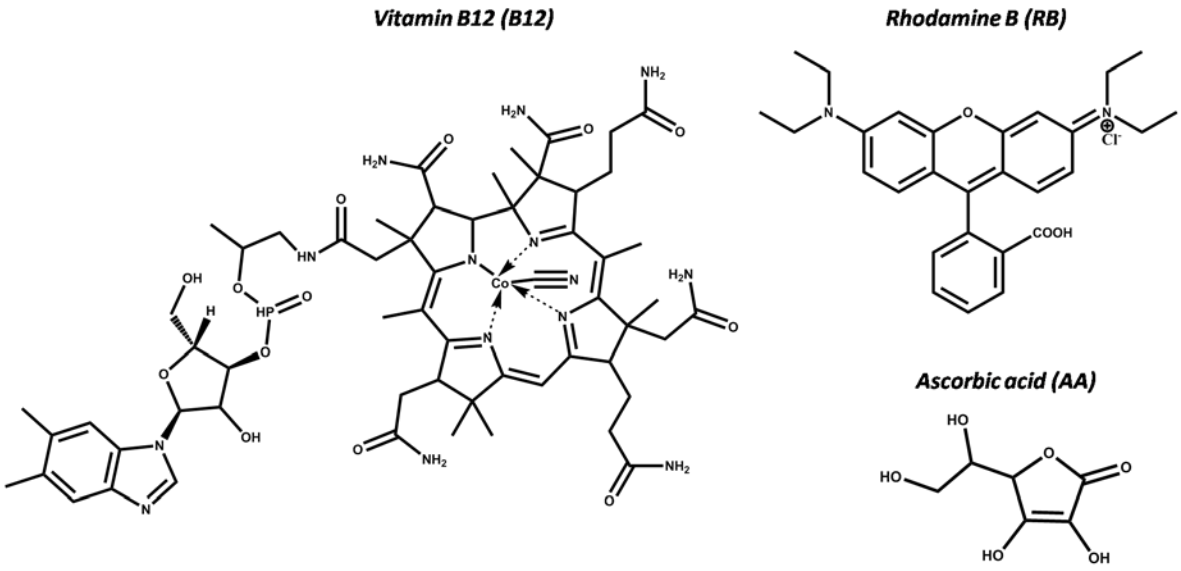

Figure 8.1. *Chemical structures of the encapsulated compounds*

On the other hand, it is important to consider the effect of the composition of aqueous solution used to hydrate the film, over particles morphology (size and PDI) and functional characteristics such as encapsulation efficiency (EE), with special focus on hydrophilic compounds encapsulation. The use of different co-solvents in the self-assembly process of the niosomes, expands their application through the possibilities of tune particle size and EE values, depending on selected applications. For example, glycerol has been used to enhance the solubility of bioactive compounds,[16] but also as cryoprotector agent for

liophilization,[17] or to enhance the drug carriers penetration for transdermal administration.[16,18] In addition, polyethylene glycol (PEG), a water soluble polymer with several molecular weight versions, has been used to prepare highly stable niosomes,[19] and as sterical stabilizer of liposomes,[20] allowing longer circulation times in blood.[21]

In this work, we prepared niosomes with a formulation based on an equimolar mixture of surfactants Tween® 80 and Span® 80. Moreover, in some formulations dodecanol was used as membrane additive, and using aqueous solutions of water, glycerol and polyethylene glycol solutions as hydration media. We found that these prepared niosomes are able to encapsulate hydrophilic compounds of different molecular weights. We were able to compare two different purification methods, dialysis and gel filtration (SEC Chromatography) used to separate encapsulated from the free compounds in solution.

8.2. Materials and methods

8.2.1. Materials

Niosomes were formulated by the use of non-ionic surfactants Tween® 80 (Tw80, MW 1310 g/mol, HLB 15.0) and Span® 80 (Sp80, MW 428.60 g/mol, HLB 4.3), from Sigma Aldrich (San Luis, MO, USA) and Fluka Analytical (Bucharest, Romania) respectively. 1-Dodecanol 98 % (Dc, Mw 186.34 g/mol) from Sigma Aldrich was used as optional membrane additive. L-(+)-ascorbic acid (AA, MW 176.12 g/mol) was obtained from J.T. Baker (), while Rhodamine B purity ≥ 95 % (RB, MW 479.02 g/mol), and Vitamin B_{12} purity ≥ 98.5 % (B12, MW 1355.38 g/mol) were also purchased from Sigma Aldrich.

For the film hydration solution, polyethylene glycol 400 (PEG-400, MW 380-420 g/mol, density 1.128 g/cm3, VWR International LLC, BDH PROLABO), glycerol bidistilled 99.5 % (Gly, MW 92.09 g/mol, density 1.261 g/cm3, VWR International LLC, BDH PROLABO) and, ultrapure water were used.

Absolute ethanol from J.T. Baker was used for bilayer components stock solutions. Methanol HPLC grade from VWR International LLC, BDH PROLABO), and acetic acid solution (49-51 %, HPLC grade) from Sigma Aldrich were used for liquid chromatography (HPLC) performance.

8.2.2 Niosomes preparation

Niosomes were prepared by a modified Thin Film Hydration method (TFH). The corresponding amount of surfactants and membrane additives were placed into a 100 mL round bottom flask in an equimolar ratio (from ethanolic stock solutions). The organic solvent was removed using a rotary evaporator (Buchi Labortechnik AG, Flawil, Switzerland), until get a homogeneous dried film. This film was then hydrated using different aqueous-based solutions at 60 ºC, and agitated at 100 rpm during 30 minutes. Suspension on vesicles were let acquire room temperature prior to purification and/or characterization.

Niosomes containing the active principle inside, were prepared by the hydration of the thin films formed after the evaporation with the corresponding aqueous solutions: ultrapure water (or MQ), water:glycerol (60:40, v/v) or GLY, and water:PEG-400 (55.3:44.7, v/v) or PEG. Both solutions have the same density.

Two different formulations of niosomes were studied. The first one contained an equimolar ratio of Tw80 and Sp80, while the second was a mixture of Tw80, Sp80, and Dc as bilayer stabilizer in a 1:1:1 molar ratio. The total concentration of membrane components was kept constant at 10 mM (final concentration in vesicles suspension). The molar ratio between both surfactants were selected to yield an HLB value of 10**.**

8.2.3. Niosomes purification

The purification of niosomes suspension was carried out by using two different methods: dialysis and gel permeation chromatography.

8.2.3.1. Dialysis

Loaded niosomes suspensions were placed in a dialysis bag (dialysis tubing, 10 K MWCO, Thermo Scientific, Waltham, MA, USA), and let floating in the corresponding hydration media in a 1:100 v/v ratio. Dialysis time was adjusted depending on the encapsulated compound (3h, 4h and 8h for AA, RB and B12, respectively).

Dialysis times were optimized by using a control solution containing the encapsulated compound at the same concentration used for encapsulation experiments. Samples were

collected for the external phase, once the concentration on the external media was more than the 99.8% of the original concentration, it was considered that the dialysis time was enough for the purification.

HPLC was used to determine the concentration of free compound in the collected samples.

8.2.3.2. Gel permeation chromatography

AA and RB loaded niosomes (with the exception of RB-niosomes in PEG) were purified using a Sephadex G-25 Superfine column (HiTrap™ desalting columns, GE Healthcare Life Sciences, UK); while B12 and RB loaded niosomes in PEG were purified using a gravity elution PD Column (V_0 = 2.5 mL) packed with Sepharose CL-4B (both from, GE Healthcare Life Sciences). Sepharose CL-4B was used since in optimization steps, we realized that RB and B12 PEG solution was not properly retain in Sephadex G25. **Table 8.1** summarize the purification conditions based on gel filtration. Control solutions of the corresponding compounds in the selected media were utilized to assess the efficiency of the used method.

HPLC was used to determine the absence of free compound in the first collected fractions from the column, were niosomes eluted, to assess the suitability of the SEC column.

8.2.4. Niosomes size and distribution analysis

Mean diameter (z-average, nm) and Polydispersity Index (PDI, a.u.) for the prepared niosomes were measured by Dynamic Light Scattering (DLS) on a Zetasizer NanoZS Series (Malvern Instruments Ltd., Malvern, UK). Measurements were performed by triplicate with undiluted samples, and at 25 °C. Low volume plastic disposable cuvettes were used during size characterization (Malvern Instruments Ltd., Malvern, UK).

Table 8.1. *Chromatography mediums used for gel filtration based purification of loaded niosomes*

Component Encapsulated	Hydration media	Gel filtration medium used
Ascorbic acid	MilliQ	Sephadex G25
Ascorbic acid	MilliQ/Glycol	Sephadex G25
Ascorbic acid	MilliQ/PEG	Sephadex G25
Rodamine	MilliQ	Sephadex G25
Rodamine	MilliQ/Glycol	Sephadex G25
Rodamine	MilliQ/PEG	Sepharose CL-4B 25
Vitamin B12	MilliQ	Sephadex G25
Vitamin B12	MilliQ/Glycol	Sephadex G25
Vitamin B12	MilliQ/PEG	Sepharose CL-4B 25

8.2.5. Niosomes encapsulation efficiency (EE)

Encapsulation efficiency was calculated as the ratio between the quantity of encapsulated compound (after proper purification), and the total amount in the unpurified suspension according to **Equation 8**.

$$\% EE = \frac{[compound]_{encapsulated}}{[compound]_{initial}} \times 100 \qquad \textit{Equation 8}$$

Purified niosomes were diluted 1:10 (v/v) using methanol in order to break the niosomal bilayers and release the encapsulated compounds. The quantification of the cargo molecules was carried out by reverse phase liquid chromatography, or RP-HPLC (HP series 1100 chromatograph, Hewlett Packard, Agilent Technologies), with a Zorbax Eclipse Plus C18 column (4.6 mm x 150 mm, 5 µm, Agilent Technologies, Santa Clara, California, USA). UV/vis (HP G1315A detector, Agilent Technologies) and fluorescence (1260 Infinity A detector, from Agilent Technologies), were used as detection coupled to the chromatographic separation. The following HPLC programs were used:

Ascorbic Acid

A linear gradient was performed with 0.1 % (v/v) acetic acid in MQ (mobile phase A) and methanol (mobile phase B). The gradient started with 95 % of A, reaching 20 % of A at min. 15, and kept constant for 5 min. The flow rate was 0.9 mL/min. Retention time for AA was 2.28 min at λ = 278 nm.

Rhodamine B

A linear gradient was used with MQ (mobile phase A) and methanol (mobile phase B). The gradient started with 2 % of B, running 100 % of B at min. 21, and kept constant for 5 min. The flow rate 1 mL/min. Retention time for RB was 19 min at λ = 554 nm.

Vitamin B_{12} (B12)

A linear gradient was used with MQ (mobile phase A) and methanol (mobile phase B). The gradient started with 20 % of B, obtaining 100 % of B at 5 min and kept constant for 10 min. The flow rate was 0.8 mL/min. Retention time for B12 was 4.35 min at λ = 361 nm.

8.2.6. Differential Scanning Calorimetry (DSC)

Differential Scanning Calorimetry measurements were conducted in aluminum sealed pans (10mg sample), heating mode (5 °C/min), from – 40 °C to 25 °C, under N_2 atmosphere, in a DSC Mettler Toledo model 821e (Mettler Toledo International Inc., Barcelona, Spain).

8.3. Results and discussion

In the present work, the effect of hydration solution composition in the thin film hydration method for niosomes preparation has been studied. More precisely, glycol compounds such as glycerol and polyethylene glycol 400 have been tested to prepare niosomes for the encapsulation of hydrophilic compounds. A mixture of surfactant has been used in the formulation, with and without a bilayer stabilizer, such as dodecanol.

8.3.1. Niosomes size *vs* hydration solution composition and cargo molecular weight

Hydration solution composition seems to have an important role in particle size. In particular, bigger particles were obtained with PEG solution than with GLY solution, and the last compared to hydration with MQ (see **Figure 8.2**). This observation was reported for Tw80-Sp80 and Tw80-Sp81-Dc formulations, with an influence with compound molecular weight, since for the same hydration solution, different size values are observed depending on the compound, but without any clear tendency. However, these differences in size are less marked for RB and B12 with Tw80-Sp80-Dc formulation.

The influence of dodecanol over particle size has a discrete effect. For example, it highly influenced niosomes size when encapsulated AA and PEG was used as hydration solution. On the other hand, Dc seems to reduce particle size for RB and B12 loaded niosomes when Gly and PEG are used for hydration.

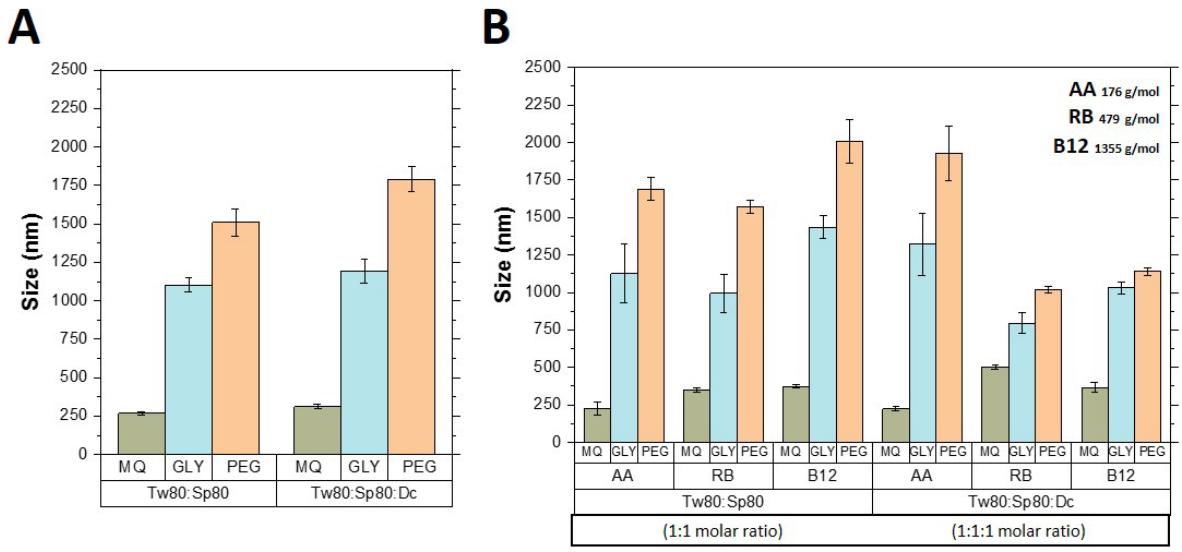

Figure 8.2. *(**A**) Size values of empty vesicles. Tw80: tween® 80; Sp80: span® 80; Dc: dodecanol. (**B**) Effect of hydration solution and cargo molecular weight over particle size, for niosomal formulations Tw80:Sp80 (1:1 molar ratio) and Tw80:Sp80:Dc (1:1:1 molar ratio) prepared by Thin Film Hydration method (TFH).*

Empty vesicles allows to study the effect of the hydration solution used and the presence of Dc on the final particle size. The presence of Dc increases the drop size independently of the hydration medium used, this is due to their location at the membrane layer and their reduction on the surfactant curvature on the presence of alcohol. In order hand the use of Gly and PEG solutions as hydration media increases significantly the particle size of the vesicles formed. It is important to point that these compounds can be attached to the membrane compounds producing higher stability to the system but also could increase the particle size.[16,28]

Molecular weight of encapsulated compounds into the vesicles has not a clear effect over particle size. For vesicles formulated with Tw80 and Sp80 the particle size seems to increase when larger molecular weight compounds are encapsulated, these effect is especially noticeable for the B12, probably due to their significantly major molecular weight value.

The addition of polyethylene glycol with different MW in aqueous solution for vesicles (especially niosomes preparation has been also studied.[19,22-24] PEG-400 and PEG-6000 are the most popular options, frequently used for surfactant mixture based formulations,

where Tween® and Span® (60 and 80) are widely used. The concentration of PEG-400 in aqueous solutions was reported to influence the niosomal formation in a formulation¡Error! Marcador no definido. based on Tween® 80. Similar, PEG-6000 concentration influenced the particle size of niosomes formulated with Tw80:Sp80 1:0.3 mass ratio.¡Error! Marcador no definido. Similar size values to the ones reported in this work have been found by other authors when Span® 60 is combined with PEG-400.¡Error! Marcador no definido.

These glycol compounds alter the packing of the bilayer and increase their curvature, which is manifested as an increment in particle radius. For example, glycerol has the property to change the dielectric constant of the bilayer interior, and bilayer components can re-arrange with different interactions.[18] PEG molecules can interact by H bonds with Tween® 80 molecules, so al low concentration can be part of the bilayer, which is less rigid. However, al high concentration it can decrease the stability of the membrane until the disruption. In that case, the instability of niosomes could led to fusion of particles and large vesicles can be obtained. This may be the mechanism that explains our size results when PEG is used as hydration solution.

Some works[16] have checked the influence of chemical composition of the film hydration solution for niosomal formulation, with special focus on the presence of poly-ol compounds (alcohols). These authors reported the influence alcohol type and concentration over particle size, and they found differences. Particularly, they reported that glycerol concentration in hydration solution has positive effect: as glycerol concentration increases (up to 40%, like our study) bigger particles were obtained without any impact over monodispersity.

Some other works[18] using aqueous-glycerol solutions for vesicles preparation by direct hydration with sonication, have reported that empty and loaded vesicles did not differ in terms of size, however other hydration solutions such as propylene glycol (1:1, v/v), more similar to PEG, yields bigger particles compared to MQ or GLY solutions. These authors have attributed this phenomena to the interaction of this compound with bilayer components.¡Error! Marcador no definido.

Surprising the size of encapsulating RB and B12 vesicle is reduced around 30% when Dc is used as a membrane component and PEG solution as a hydration method. This phenomena indicates that even encapsulated dompounds are hydrophilic and hence are encapsulated at the iner part of the vesicle they have some interacions with the membrane compounds.

Regarding the monodispersity of the suspensions, in all the cases, both empty and loaded vesicles showed a PDI value from 0.3 ± 0.1 for empty Gly niosomes (with Dc) to 0.7 ± 0.1 for AA loaded MQ niosomes (with Dc). Encapsulation seems to not influence the value, since in some cases loaded vesicles exhibit better monodispersity than loaded niosomes.

8.3.2. Encapsulation Efficiency *vs* hydration solution composition and cargo molecular weight

Regarding the EE of the different compounds we observed differences related with the molecular weight of the cargo, and for both formulations. The best EE values were obtained for AA when MQ is used as hydration solution, with independence of the purification method (**Figure 8.3**). For this compound it seems that hydration solution composition is not a key factor for encapsulation, since in almost all the cases the EE values were similar. Only some particular differences are observed in the formulation where Dc is used as membrane stabilizer (Gly yields the lowest EE value, 68%, using dialysis as purification method, and MQ the higher EE value, 100%, using gel filtration as purification technique).

However, RB and B12 seems to have an important dependence with hydration solution composition, since a great difference in EE values can be observed depending on medium chemistry. In the case of RB, EE ranges between 8.4% (Gly) and 60% (PEG) when dialysis is used as purification method, and from 9% (MQ) to 22% (PEG) in the case of Dc containing formulation with same purification method.

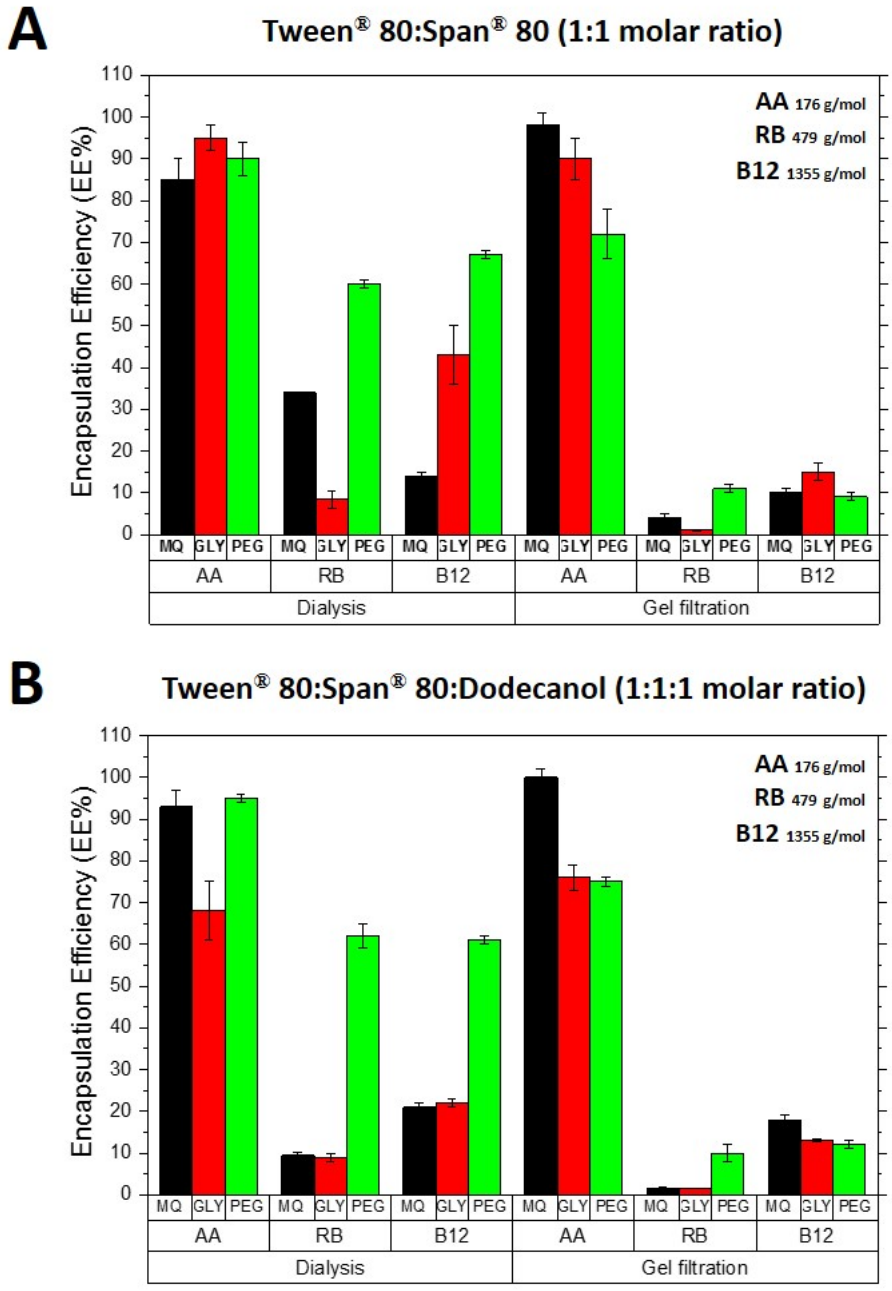

Figure 8.3. *Effect of hydration solution and cargo molecular weight over encapsulation efficiecy, for niosomal formulations (**A**)Tw80:Sp80 (1:1 molar ratio) and (**B**) Tw80:Sp80:Dc (1:1:1 molar ratio) prepared by Thin Film Hydration method (TFH). Tw80: tween® 80; Sp80: span® 80; Dc: dodecanol. Dialysis (10 MWCO membranes) and gel filtration (Sepahdex G25 or Seharose CL-4B, depending on the compound) were used as purification methods.*

It seems that PEG greatly improve RB encapsulation. Besides these good results, when gel filtration is used EE remains with similar values and in general, offering lower values

than dialysis purified vesicles for both types of formulation. A possible explanation is given into the next section.

A similar pattern of results is described for B12 encapsulation. Again, the use of PEG as hydration solution yields the higher EE values (67%) for dialysis purified vesicles for both formulation, but a not clear effect of medium composition can be observed for gel-filtrated niosomes. Dc addition into the formulation is not an important parameter for his encapsulation.

Muzzalupo et al.[16] reported that 40% of glycerol yields the higher EE% compared to other alcohols for sulfadiazine, and hydrophilic drug. They attributed this effect to the presence of multiple –OH groups in the alcohol that could help the drug to be totally solubilized thanks to H bonds between both molecules. A similar effect could be related to B12 EE% without Dc, but may be not useful for RB encapsulation. However, PEG increase EE of both, RB and B12, for both formulations. PEG has been tested to enhance the solubility of amphiphilic compounds such as ellagic acid,**¡Error! Marcador no definido.** quercetin,[25] paclitaxel,[26] however no data about hydrophilic compounds have been found.

Interestingly, our formulation offers better AA EE% than liposomes found in the literature, where only 10% was reached.[27] Regarding vitamin B12, PEG niosomes with/without Dc offer better encapsulation than liposomes,[28] however there is a great difference in size (2 μm for niosomes *vs* less than 100 nm for liposomes). On the other hand, EE% values for RB are unusual, since the papers only report the encapsulation, without interest in maximize this parameter.

These results evidence that exists and interaction between cargo molecular weight and hydration solution composition without any clear influence of niosomes formulation, at least for the introduction of Dc as bilayer stabilizer. Only in the case of MQ and dialysis, a clear influence of cargo MW is observed, with a reduction in EE as MW increase. The composition of film hydration solution could be a key parameter for some compounds EE optimization, with a possible relationship with their molecular weight (medium or high molecular weight compounds), and particular dependence of chemical nature of the compounds, since a not general pattern was observed. In our opinion, the enhancement of

EE% values using Gly, and especially PEG, is an interaction of solubility enhancement and the effect of increase particle size, which for hydrophilic compounds is translated into a bigger capacity of niosomes to carry more cargo molecules due to physical (volume) capacity.

Regarding the purification strategies, dialysis is the most popular option chosen to purified vesicles encapsulating hydrophilic and amphiphilic compounds[18,19,¡Error! Marcador no definido.,¡Error! Marcador no definido.]. However, if the permeating through the bilayer is not clear understood for a specific formulation, realease and purification can be overlapped, and EE% could be underestimated. To assess this for our formulation we selected SEC chromatography as alternative method,[29] to be able to compare the performace of both techniques.

As described previously, important differences in EE values are obtained when the two purification methods are compared, and those discrepancies seems to be magnified with hydration medium composition. The general trend is to observe a lower EE value for niosomes suspensions purified by gel filtration.

The greatest differences are in all the cases observed for the use of PEG in both formulations, and in the majority of them, MQ offers no differences between methods. Also, a positive interaction with molecular weight is described for GLY and PEG.

To assess if this result relies on physical forces involved in the purification methods, empty niosomes prepared in the three different aqueous solutions were subjected to gel filtration. Particle size, size distribution and concentration were measured by Nanoparticle Tracking Analysis (NTA) before and after the process **(Figure 8.4**).

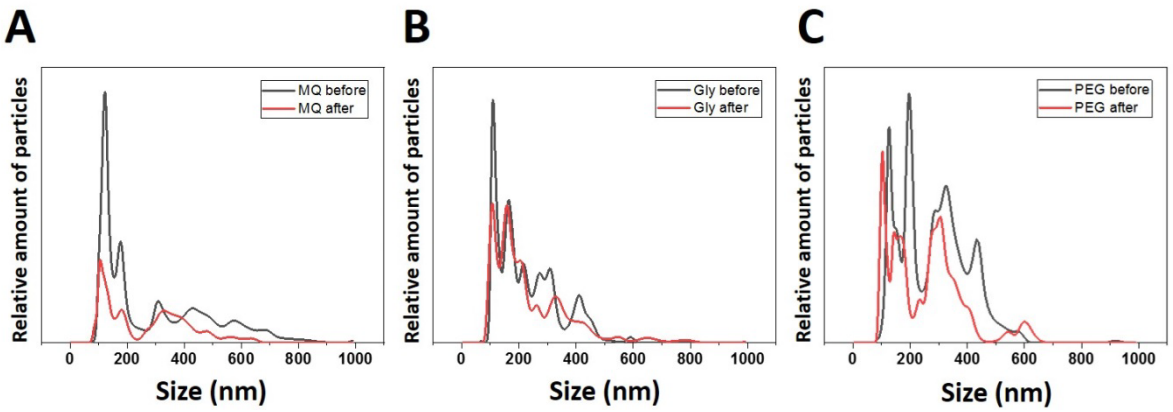

Figure 8.4. *Naparticle Tracking Analysis (NTA) of the three different hydration solution based niosomes after and before SEC purification. MQ and Gly vesicles were purified using Sephadex G25 and PEG vesicles by Sepharose CL-4B.*

The results showed a reduction in mean size, and particle concentration for PEG based niosomes suspension. It seems that a retention of vesicles of a mechanical disruption of particles may occur during their flow through the column. During the process, the bed of the column experiments a visible compaction due to the high viscosity of the fluid even at low flow rate recommended by the manufacturer for viscous solutions. This phenomena could yield to mechanical stress of the vesicles due to shear forces as they pass through the compacted gel. Subsequently, loaded vesicles could collapse and their content could be release to the medium where is trapped by the effect of the gel even when is compacted. A reduction in EE value could be then observed for this case as reported.

Interestingly, particles in GLY solutions seems to keep their integrity, since no changes in measured parameters have been reported. And also curiously, MQ suspended niosomes experiment a slight reduction in size and concentration, what could be related to entrapment phenomena of the smallest and highest niosomes by capture and clogging with the stationary phase respectively.

Besides being a popular choice for vesicles purification, SEC has some drawbacks that must be taken into consideration. For example, it has been reported that vesicles can be retained by stationary phase[30], and this retention is dependent of particles pores and not by particles size itself. Sepharose CL-40 contains particles with 20 nm pore size, which is enough to allow the flow of small vesicles through them. However, large flexible particles

like PEG-hydrated may clog the pores and disturb the process, leading to underestimation of EE% by vesicles loss and vesicles disruption into the columns. This fact could be potentiated by viscous solution, such as 45% PEG in water.

8.3.3. Thermal behavior of formulation in the hydration solutions

Differential Scanning Calorimetry (DSC) is a useful technique carried out to study the phase behavior of lipids and surfactant based bilayers, and gives information about molecular interactions of the structure, which allows getting information about stability and fluidity of the vesicle bilayer.[31] Also, this technique has been applied to measure the EE% of hydrophobic compounds,[32] since they are loaded into the structure and then, alter the cohesion of the bilayer.

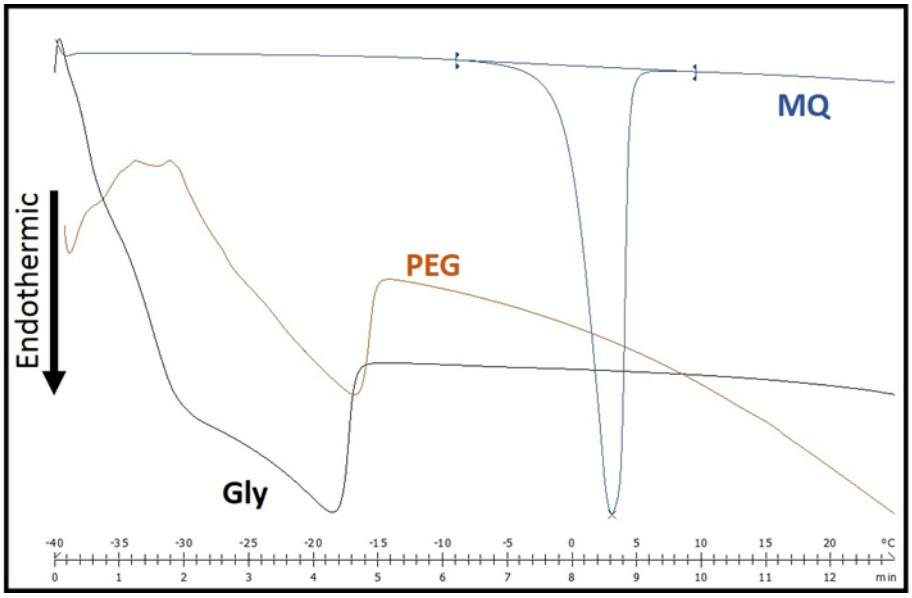

Figure 8.5. *DSC curves acquired in heating mode for the formulation without dodecanol in the three different hydration solutions: ultrapure water (MQ), water:glycerol 60:40 v/v (Gly), and water:PEG-400 55:45 v/v (PEG).*

Figure 8.5 represents the DSC curves obtained for empty vesicles prepared into the three different hydration solutions. It is clear, that the incorporation of PEG and Gly changes the stability of the bilayer, since T_c is decreased and the morphology of the peaks shows a less ordered structure, evidenced for broad peak transition and loss of symmetry. Gly and PEG transitions from gel-to-liquid seems to be in two steps, showing

heterogeneity of the bilayer. As consequence, bilayer becomes more fluid, and bigger particles could be formed.

8.4. Conclusions

The preparation of niosomes encapsulating different hydrophilic compounds with differences in molecular weight and by thin film hydration method performed with different aqueous based solutions, allowed us to check the existence of the influence of these parameters over particle size and encapsulation efficiency, two important and related characteristics for niosomes aimed to bioactive compound protection and/or delivery bio-applications.

Hydration solution composition has been correlated with particle size for a niosomal formulation based on surfactant mixture with/without dodecanol as membrane stabilizer. In addition, a possible interaction with cargo molecular weight could exist, since in particular cases, particles become slightly bigger as molecular weight increase. This increment in size is correlated with an increase in EE for these compounds. Since bigger particles can encapsulated more compound molecules than smaller ones, especially for hydrophilic compounds where they are loaded into the aqueous inner cavity of vesicles, the relationship between EE and hydration solution composition seems to be purely due to vesicles physical aspects (loading volume capacity). DSC curves showed a change in bilayer structure with the use of glycerol and polyethylene glycol 400, that may interact with surfactants and create a less organized structure.

Encapsulation efficiency obtained using dialysis method were higher than obtained for gel filtration for the same samples. In addition, when dialysis was used, encapsulation efficiency strongly depended of the hydration media while no differences were observed when gel permeation was used as purification method. It seems that gel filtration is not an appropriate purification method for suspensions of large vesicles, especially for viscous solutions. Mechanical stress of particles during separation could lead to unsatisfactory results in terms of particle integrity and subsequent EE values.

8.5. Bibliographic references

[1] Marianecci C., Petralito S., Rinaldi F., Hanieh P.N., Carafa M. (2016). Some recent advances on liposomal and niosomal vesicular carriers. *J. Drug Deliv. Sci. Technol.*, 32:256–269.

[2] Uchegbu I.F., Florence A.T. (1995). Non-ionic surfactant vesicles (niosomes): Physical and pharmaceutical chemistry. *Adv. Colloid Interface Sci.*, 58:1–55.

[3] Uchegbu I.F., Vyas S.P. (1998). Non-ionic surfactant based vesicles (niosomes) in drug delivery. *Int. J. Pharm.*, 172:33–70.

[4] Salim R., Minanikawa M., Sugimura H., Hashim A. (2014). Amphiphilic designer nano-carriers for controlled release, from drug delivery to diagnostics. *Med. Chem. Commun.*, 5:1602–1618.

[5] Marianecci C., Di Marzio L., Rinaldi F., Celia C., Paolino D., Alhaique F., Esposito S., Carafa M. (2014). Niosomes from 80s to present: The state of the art. *Adv. Colloid Interface Sci.*, 205:187–206.

[6] Alomrani A.H., Al-Agamy M.H., Badran M.M. (2015). In vitro skin penetration and antimycotic activity of itraconazole loaded niosomes: Various non-ionic surfactants. *J. Drug Deliv. Sci. Technol.*, 28:37–45.

[7] Pando D., Beltrán M., Gerone I., Matos M., Pazos C. (2015). Resveratrol entrapped niosomes as yoghurt additive. *Food Chem.*, 170:281–287.

[8] Tavano L., Muzzalupo R., Picci N., De Cindio B. (2014). Co-encapsulation of antioxidants into niosomal carriers: Gastrointestinal release studies for nutraceutical applications. *Colloids Surf. B.*, 114:82–88.

[9] Tavano L., Muzzalupo R., Picci N., De Cindio B., (2014). Co-encapsulation of lipophilic antioxidants into niosomal carriers : Percutaneous permeation studies for cosmeceutical applications. *Colloids Surf. B.*, 114:144–149.

[10] Gutierrez G., Matos M., Barrero P., Pando D., Iglesias O., Pazos C. (2016). Iron-entrapped niosomes and their potential application for yogurt fortification. *LWT - Food Sci. Technol.*, 74:550–556.

[11] McClements D.J. (2015). Encapsulation, protection, and release of hydrophilic active components: Potential and limitations of colloidal delivery systems. *Adv. Colloid Interface Sci.*, 219:27–53.

[12] Fathima S.J., Nallamuthu I., Khanum F. (2017). Vitamins and minerals fortification using nanotechnology: bioavailability and Recommended Daily Allowances. *Nutr. Deliv.*, 457–496.

[13] Du J., Cullen J.J., Buettner G.R. (2012). Ascorbic acid: Chemistry, biology and the treatment of cancer. *Biochim. Biophys. Acta.*, 1826:443–457.

[14] Kim H.N., Lee M.H., Kim H.J., Kim J.S., Yoon J., (2008). A new trend in rhodamine-based chemosensors: application of spirolactam ring-opening to sensing ions. *Chem. Soc. Rev.*, 37:1465–72.

[15] Ulusoy H.İ., (2017). A versatile hydrogel including bentonite and gallocyanine for trace Rhodamine B analysis. *Colloids Surf. A*, 513:110–116.

[16] Muzzalupo R., Tavano L., Lai F., Picci N. (2014). Niosomes containing hydroxyl additives as percutaneous penetration enhancers: Effect on the transdermal delivery of sulfadiazine sodium salt. *Colloids Surf. B.*, 123:207–212.

[17] Stark B., Pabst G., Prassl R. (2010). Long-term stability of sterically stabilized liposomes by freezing and freeze-drying: Effects of cryoprotectants on structure, *Eur. J. Pharm. Sci.*, 41:546–555.

[18] Vitonyte J., Manca M.L., Caddeo C. Valenti D., Peris J.E., Usach I. Nacher A., Matos M., Gutiérrez G., Orrù G., Fernàndez-Busquets X., Fadda A.M., Manconi M. (2017). Bifunctional viscous nanovesicles co-loaded with resveratrol and gallic acid for skin protection against microbial and oxidative injuries. *Eur. J. Pharm. Biopharm.*, 114:278-287.

[19] Hua W., Liu T. (2007). Preparation and properties of highly stable innocuous niosome in Span 80/PEG 400/H2O system. *Colloids Surf. A*, 302:377-382.

[20] Yongzhuo Huang Y., Chen J., Chen X., Gao J., Liang W. ().PEGylated synthetic surfactant vesicles (Niosomes): novel carriers for oligonucleotides. *J. Mater. Sci.: Mater. Med.*, 19(2):607-614.

[21] Gianasi E., Cociancich F., Uchegbu I.F., Florence A.T., Duncan R. (1997). Pharmaceutical and biological characterisation of a doxorubicin-polymer conjugate (PK1) entrapped in sorbitan monostearate Span 60 niosomes. *Int. J. Pharm.*, 148:139–148.

[22] Liu T., Guo R. (2005). Preparation of a highly stable niosome and its hydrotrope-solubilization action to drugs. *Langmuir*, 21:11034-11039.

[23] Junyaprasert V.B., Singhsa P., Suksiriworapong J., Chantasart D. (2012). Physicochemical properties and skin permeation of Span 60/Tween 60 niosomes of ellagic acid. *Int. J. Pharm.*, 423:303– 311.

[24] Liu T., Guo R. (2005). Preparation of a highly stable niosome and its hydrotrope-solubilization action to drugs. *Langmuir*, 21:11034-11039.

[25] Priprem A., Watanatorn J., Sutthiparinyanont S., Phachonpai W., Muchimapura S. (2018). Anxiety and cognitive effects of quercetin liposomes in rats. *Nanomed. Nanotechnol.*, 4:70-78.

[26] Yang T., Cui F.-D., Choi M.-K., Lin H., Chung S.-J., Shim C.-K., Kim D.-D. (2007). Liposome formulation of paclitaxel with enhanced solubility and stability. *Drug Delivery,* 14:301–308.

[27] Chen W., Compton R.G. (2014). Investigation of Single-Drug-Encapsulating Liposomes using the Nano-Impact Method. *Angwandte,* 53(50):13928-13930.

[28] Bochicchio S., Barba A.A., Grassi G., Lamberti G. (2016). Vitamin delivery: Carriers based on nanoliposomes produced via ultrasonic irradiation. *LWT - Food Science and Technology*, 69:9-16.

[29] Gabrielle-Madelmont C., Lesieur S., Ollivon M. (2003). Characterization of loaded liposomes by size exclusion chromatography. *J. Biochem. Bioph. Meth.*, 56:189-217.

[30] Ruysschaert T., Marque A., Duteyrat J.-L., Lesieur S., Winterhalter M., D. Fournier. (2005). Liposome retention in size exclusion chromatography. *BMC Biotechnology*, 5(11).

[31] Demetzos C. (2008). Differential Scanning Calorimetry (DSC): A tool to study the thermal behavior of lipid bilayers and liposomal stability. *J. Liposome Res.*, 18:159–173.

[32] Montenegro L., Panico A.M., Bonina F. (1996). Quantitative determination of hydrophobic compound entrapment in dipalmitoylphosphatidylcholine liposomes by differencial scanning calorimetry. *Int. J. Pharm.*, 138:191-197.

9. Selected tetraspanins functionalized niosomes as potential standards for exosomes detection based on immunoassays

Capítulo/Chapter 9

Selected tetraspanins functionalized niosomes as potential standards for exosomes detection based on immunoassays

9.1. Introduction

Extracellular vesicles have emerged as a novel mechanism of intercellular communication over the last years, playing an important role in both biological and pathological processes.[1] Exosomes are a subtype of extracellular vesicles (EVs), released by membrane fusion of multivesicular bodies (MVB) with the plasma membrane.[2] Exosomes are vesicular subcellular particles (30-150 nm) with an average size around 100-150 nm, characterized by a particular protein profile which offer information about the original cell line from which are released, the target cell population, and valuable information about health status and possible (patho)physiological roles.[3,4]

Their possibilities as biomarkers for diagnosis[5] and treatment-response monitoring[6] promote their determination in biological fluids and cell culture media as a routine practice in cell biology labs, but also in the clinical research. However, as the information about EVs is constantly growing and evolving, routine practices with possibilities to be incorporated in hospital facilities must be addressed and validated,[7] which represent a technological challenge were reference material (RM) play an essential role. Up to date, several strategies for EV isolation, detection and quantification have been developed, as reviewed elsewhere.[8-10]

EVs can be quantified directly or based on the quantification of biomolecules present in the vesicles, in the majority of the cases a molecule present in the membrane.[8] The specific recognition of these molecules can be performed by the use of antibodies, aptamers or other type of molecules with selective interactions, such as proteins with binding capabilities over lipids. Several strategies have been developed based on this principle, and optical[11,12] or electrochemical[13,14] transduction are the most popular principles for

biosensing of EVs. Regarding the molecules, tetraspanins CD9, CD63 or CD81 are commonly used as membrane markers, since EVs are enriched in these transmembrane proteins.[15]

During the development and validation of a new analytical tool or method, the use of standards is essential for the development stage, but also to characterized their performance, possibilities and potential limitations. Traditionally, for EVs quantification, suspensions enriched in exosomes isolated from body fluids or cell cultures media have been used for these purpose. However, the absence of a well characterized and validated strategy for EVs isolation makes difficult the existence of a robust RM for the evaluation and performance of methods inter-comparison studies. The co-isolation of other biological entities (mainly protein aggregates), and the isolation of heterogeneneous EV fractions in terms of size (i.e., exosomes or microvesicles) or sub-types (i.e., exosome populations from different cell lines) are some of the most commonly limitations of isolation procedures for the establishment of EVs-based RM.[8]

Scientists have focused the attention on mimetic particles and their used in EVs-related research.[16,17] Synthetic vesicular systems, such as liposomes or niosomes (prepared from lipids and non-ionic surfactants, respectively) have been postulated as powerful tools due to their similarities in terms of morphology and chemical behavior to natural EVs. Some works have explored the applications of synthetic vesicles for the study of EVs biology.[18] On the other hand, some studies have applied these particles for exosomes modifications for new intended purposes, mainly for diagnostic and therapy.[19]

Also, these vesicles have been used in methods comparison studies. For example, Lane et al.[20] compared different exosome purification methods using a model liposome system, and they concluded that the studied purification methods (ultracentrifugation, two sedimentation reagents, a density gradient method, and the ExoSpin exosome purification system) possessed different efficiencies, but keep constant vesicles size and size distribution from real sample. Maas et al.[21] used liposomes to compare methods based on single-particle analysis (nanoparticle tracking analysis or NTA, tunable resistive pulse sensing or tRPS and high-resolution flow cytometry or hFC) for EVs quantification, and found absolute quantification differences between techniques and between synthetic

counterparts and natural EVs. Interestingly, also some differences were observed for liposomes with different size. However, the use of this synthetic vesicles for methodological comparisons is limited to their physical properties and not to functional characteristics such as the presence of specific molecular markers. This is important, since some physical properties such as size and monodispersity can influence the outcome of the analysis by limiting the sensitivity for smaller particle detection and a bias into the quantification. The introduction of molecular recognition coupled to a proper size, could create a robust RM that allows to expand the range of techniques to be tested, but also introduce new possibilities of information acquisition for deep inter-comparison studies.

During the last years, several technologies have raised in order to overcome the limitations for the use of natural exosomes in biomedical applications, and the so called artificial exosomes have emerged with a full range of possibilities and capabilities for diagnosis and therapy.[22,23] However, their use as true standards for analytical purposes have remained unexplored, and only some probes of concept have been developed.[24,25]

The aim of the present work was the design, development and functional characterization of a potential standard of EVs (RM), more precisely exosomes, for their application in immunoassay-based methods. **Figure 9.1** capture the molecular composition and structure of our proposal. Recombinant constructions (large extracellular loops, LEL) of tetraspanins CD63 and CD9 were bioconjugated to the external surface of niosomes prepared with a size distribution similar to natural exosomes. Mono- (CD9 or CD63) and double (CD9 and CD63) functionalized particles have been prepared and tested in an ELISA assay. Their potential as RM for EVs bioanalytics is evaluated, and a versatile strategy for their customized production is presented.

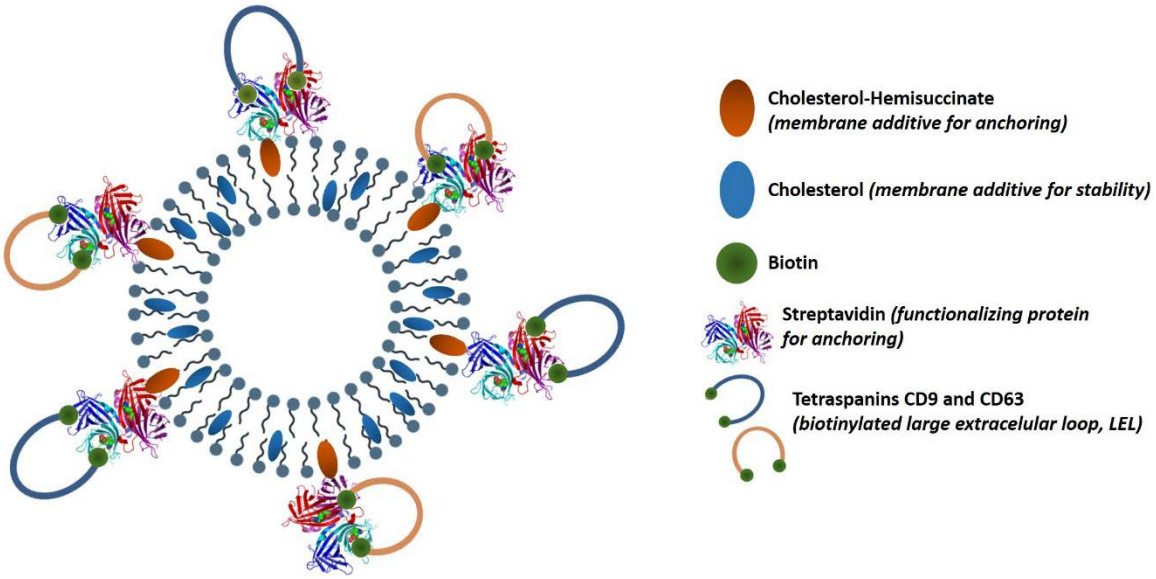

Figure 9.1. *Schematic fully artificial exosome produced by bottom-up bio-nanotechnological methods based on supramolecular chemistry. The different molecular components are detailed with their functions.*

9.2. Material and methods

Sorbitan monostearate or Span® 60 (Sp60), Cholesterol hemisuccinate (Cho-suc), and Phosphate Buffer Saline or PBS (10 mM, pH 7.4) prepared from tablets according with manufacture instructions, were acquired from Sigma Aldrich (San Luis, MO, USA). Cholesterol from lamb wool (Cho) was from Across Organics (Geel, Belgium), and streptavidin (Str) was from G Biosciences (Geno Technology Inc., USA). Ultrapure water was used for buffer preparation.

Other biochemical have been: Biotinylated-HRP (Life Technologies, Thermo Fisher, Waltham, MA, USA) TMB, and nitrocellulose membrane (GE Healthcare Life Sciences, USA).

HiTrap columns packed with Sephadex G-25 (5 mL bed volume) and Sepharose CL-2B/CL-4B gel filtration media were acquired from GE Healthcare Life Sciences (Pittsburgh, USA).

Biotinylated and purified monoclonal antibodies against CD9 (VJ1/20) and CD63 (Tea3/18) were acquired from Immunostep (Salamanca, Spain). Polyclonal antibody against CD9 was from Santa Cruz Biotechnology (Dalas, TX, USA) and for CD63 was acquired from Sigma Aldrich. Secondary antibodies HRP-conjugated, and streptavidin-HRP were acquired from Thermo Scientific.

9.2.1. Niosomes preparation and size measurement

Nanovesicles formulated with Sp60:Cho:Cho-suc (1:0.5:0.01 molar ratio) were prepared following a method previously described.[26] Briefly, 20 mL of a 6 mM ethanolic solution containing bilayer precursors at the mentioned molar ratio were injected (130 mL/h) into 50 mL of ultrapure water at 60 °C and constant stirring (500 rpm). Injection was performed with a syringe Pump (KDS Instruments, Beijing, China) on a beaker glass over a heating/stirring plate (IKA, Staufen, Germany). Residual ethanol was removed by evaporation under vacuum (50 °C, 90 Bar and 35 rpm) (Bütchi Labortechnik AG, Flawil, Switzerland), and aqueous volume was reduced to 25 mL by water evaporation by reducing the vacuum down to 50 Bar for approximately 45 min.

Produced vesicles were characterized in terms of size and size distribution by measuring 3 undiluted independent samples by Dynamic Light Scattering in a ZetaSizer NANO ZS instrument (Malvern Instruments, Malvern, UK) at 25 °C and 3 runs per measurement using forward scatter (173°) detector. Low disposable plastic cuvettes from equipment manufacturer were used for that purpose.

9.2.2. Streptavidin conjugation to niosomes surface

Protein (recombinant streptavidin) conjugation to niosomal surface was carried out following the carbodiimide method.[27] 1-Ethyl-3-(3-dim((ethylaminopropyl)carbodiimide (EDC) and sulfo N-hydroxysulfosuccinimide (sulfo-NHS) were added to the selected volume of niosomes suspension to reach 4.3 mM and 9.2 mM, respectively; carboxylic groups were activated for 30 min at RT with gently shaking. Excess of conjugation reagents were removed by gel filtration with HiTrap desalting columns packed with Sephadex G-25. Elution was performed with PBS 10 mM, pH 7.4, a suitable condition for conjugation to the primary amine-containing molecule. Then, streptavidin was added, and

a total sample volume of 2.5 mL was reached by addition of ultrapure water. The solution was kept at constant mechanical agitation in a vortex for 2 h. To quench possible activated NHS esters, 1 mg of glycine was added to the suspension.

Removal of unconjugated protein was carried out by gravity elution gel filtration in a PD-10 empty column packed with Sepharose CL-4B (8.6 mL, bed volume) conditioned with PBS. A total elution volume of 3.5 mL was recovered in a flow cytometer-grade tube with sealing cap (BD Plastipak, Vaud, Switzerland), and 0.1% sodium azide in PBS was used as eluent solution. This concentration was checked to keep vesicles without modification in colloidal state. A protein quantification kit (based on bicinchoninic acid assay or BCA, according to manufacturer instruction) was used to determine the elution profile of a solution of streptavidin to check the suitability of chromatography separation for purification.

The efficiency of streptavidin conjugation was checked by dot blot, using biotinilated-HRP enzyme (B-HRP) as protein detection probe and insoluble TMB (suitable for membranes) as substrate. Briefly, 1 µL of samples (fractions from SEC column) and protein standards were applied over nitrocellulose membranes (GE Healthcare Life Sciences, Pittsburgh, USA) and air dried at RT. Membranes were blocked in 5% BSA in PBS-0.05% Tween® 20 (PBS-T) and then incubated in a 4 µg/mL solution of B-HRP in 0.1% BSA in PBS-T for 45 min. Membranes were washed and incubated with TMB at variable times, monitoring the signal from the highest concentration standard to avoid signal saturation.

9.2.3. Tetraspanins (CD9/63) large extracellular loops (LELs) production

Production of tetraspanin LELs has been performed as previously described.[25]

9.2.4. Vesicles functionalization with tetraspanins LELs constructions

For mono-functionalization of niosomes with LEL_CD9 or LEL_CD63, 700 µL of selected LEL stock was added to 1.5 mL of vesicles suspension and incubated overnight at 4ºC with gently shaking. Excess of biotin was used to saturate possible free binding sites of

streptavidin in order to avoid possible unspecific signal from biotinylated antibodies used in ELISA assays.

In the case of double functionalized vesicles, 300 µL of LEL_CD63 was added, while the amount of LEL_CD9 was reduced to 150 µL according to a previous report showing that their production yield is approximately the double of CD63.[25] This was intended to keep the ratio of LEL types to 1:1 molar ratio.

In order to remove unbound LEL, sepharose CL-2B columns (10 mL bed volume) were prepared in plastic syringes (BD Plastipak) with a nylon filter to retain the gel into the column. A 3 way stopcock (BD Plastipak) was attached to column outlet to control the elution flow. After equilibration of the column with filtered PBS, the total amount of vesicles suspension plus LEL was added and a total of 20 fractions (0.5 mL) were collected into glass vials, and stored at 4 °C.

To check the effectiveness of LEL coupling to streptavidin-coated niosomes, all the fractions were checked by dot blot analysis with specific monoclonal antibodies against CD9 and CD63 as primary antibodies, and anti-mouse-HRP as secondary antibody. Blots were developed with the ECL detecton system (Supersignal® West Femto maximum sensitivity substrate, Thermo Scientific) in a LAS4000 mini Image System analyzer from Fujifilm and software ImageQuant-TL (GE Healthcare).

9.2.5. Immunoassays for artificial EVs detection

ELISA assays were performed in 96-well plates (Corning, Corning, NY, USA). Microplate wells were coated at 4 °C overnight with monoclonal antibodies (10 µg/mL, in borate buffer saline or BBS buffer, 10 mM and pH 8.2), and blocked with BSA 2% in PBS for 2h at 37 °C. Samples (100 µL/well) were incubated at 4 °C overnight. Detection was performed using biotinylated monoclonal antibodies (12.5 µg/mL in PBS) and polyclonal antibodies (1:250 and 1:500 for anti-CD9 and anti-CD63, respectively) incubated for 1h at 37 °C. Streptavidin-HRP (1:2000) and anti-rabbit IgG-HRP (1:3000) was used as secondary detection probes. The reaction was developed with o-phenylenediamine dihidrochloride (OPD, Sigma Aldrich) substrate for colorimetric detection, and signal intensity was measured at 492 nm in a microplate reader (Tecan Genios, Tecan Trading AG,

Switzerland) after addition of stop solution. Washing steps were performed with PBS-T between incubation steps, and PBS prior to the addition of OPD.

9.3. Results and discussion

The strategies for the development of artificial exosomas have been reviewed in a previous publication of our group.[23] Their biochemical composition should provide them with similar physical, optical and functional characteristics to natural EVs, providing a new range of RM for different isolation and detections strategies. In this work, we have followed a strategy based on bio-nanotechnology and supramolecular chemistry to create a synthetic bilayer made of non-ionic surfactants and additives (niosomes) that was then functionalized with proteins typical of exosomes, against specific receptors are directed in assays based of molecular recognition such as immunoassays.

9.3.1. Streptavidin-coated niosomes development as generic scaffold for artificial EVs production

In a previous work,[26] the influence of ethanol injection method (EIM) preparation variables over particle size and monodispersity of the niosomal formulation Span® 60:Cholesterol (1:0.5 molar ratio) was deeply studied. It was found that organic/aqueous phase volume ratio, the (final aqueous-phase) surfactant-cholesterol concentration, and the sonication amplitude were the parameters with stronger effects. In order to improve the results, we decided to use all the information provided by the models, with the aim of obtaining smaller niosomes with an acceptable size distribution which represented values in agreement with those observed for natural exosomes.

In a deep study (data not published) we observed that higher sonication amplitude needed for size reduction really decrease the life time of the probe, and TiNPs could be observed by TEM in the prepared suspensions. Also, the ageing of the probe introduce not controlled alterations in the process, and becomes not reproducible as sonication probe ages. So, it was decided to avoid the use of sonication, and his influence was compensated by reasonably changing the value of the other two factors. Concentration of membrane components in the organic phase was reduced to the half, while its volume was kept at 20

mL. In order to compensate the dilution of the prepared nanovesicles solution, we used evaporation under vacuum (50 °C, 45 bar) to reduce the final aqueous suspension down to 25 mL instead of 50 mL.

With these modifications of initial conditions, niosomes with 150 ± 3 nm (PDI 0.060) were obtained. For bioconjugation purposes, cholesterol-hemisuccinate was added. This additive not only introduces surface available carboxylic groups as anchor elements, but it also provides negative charges that enhance the stability of bared niosomes during storage. The addition of cholesterol-hemisuccinate did not modify the average size of the vesicles in comparison with formulations lacking cholesterol-hemisuccinate.

Once we got the optimal suspension of niosomes in terms of size, monodispersity and particle concentration, protein (streptavidin) could be conjugated with the niosomes at the external surface to create a generic platform for the development of different types of artificial EVs. The carbodiimide-based bioconjugation strategy is a two-step procedure to permanently link two biomolecules, or a molecule with a surface or a nanomaterial [28]. This method creates a covalent bond between an amine and an activated carboxylic group by the use of EDC and NHS. In this particular case, between amine groups from basic aminoacids in the streptavidin molecule and the carboxylic group from cholesterol hemisuccinate introduce into niosomal formulation as additive.

This strategy has been previously followed for the conjugation of biomolecules with nanovesicles, and some examples can be found in the literature.[29,30] Interestingly, carbodiimide method has been applied in the development of artificial exosome for therapy.[31] The process is carried out in two steps in order to avoid protein aggregation induced by cross-linked molecules, since proteins exhibit both functional groups, the amine and the carboxylic. The pH value of each step (acid for the first, neutral to basic for the second) was carefully adjusted in order to maximize the coupling process. Two different amounts of protein were tested in order to check variable dependence over bioconjugation yield. However, no differences were observed, and the lower amount was selected in order to keep the process cost-effective.

The elution profile from the SEC column of a solution of streptavidin is shown in **Figure 9.2.A**. The elution is enough delayed from the death volume, where nanovesicles

eluted, checked by passing through the column a suspension of NVs with a loaded red dye for visual purposes (**Figure 9.2.A, detail**).

As shown in **Figure 9.2.B**, five different batches (L1 – L5) of streptavidin-functionalized niosomes (Nio_Str) were analyzed by an adapted dot blot to check the presence of the protein and the effectiveness of the functionalization method. As shown, reproducibility is acceptable, with values around 63 µg/ml.

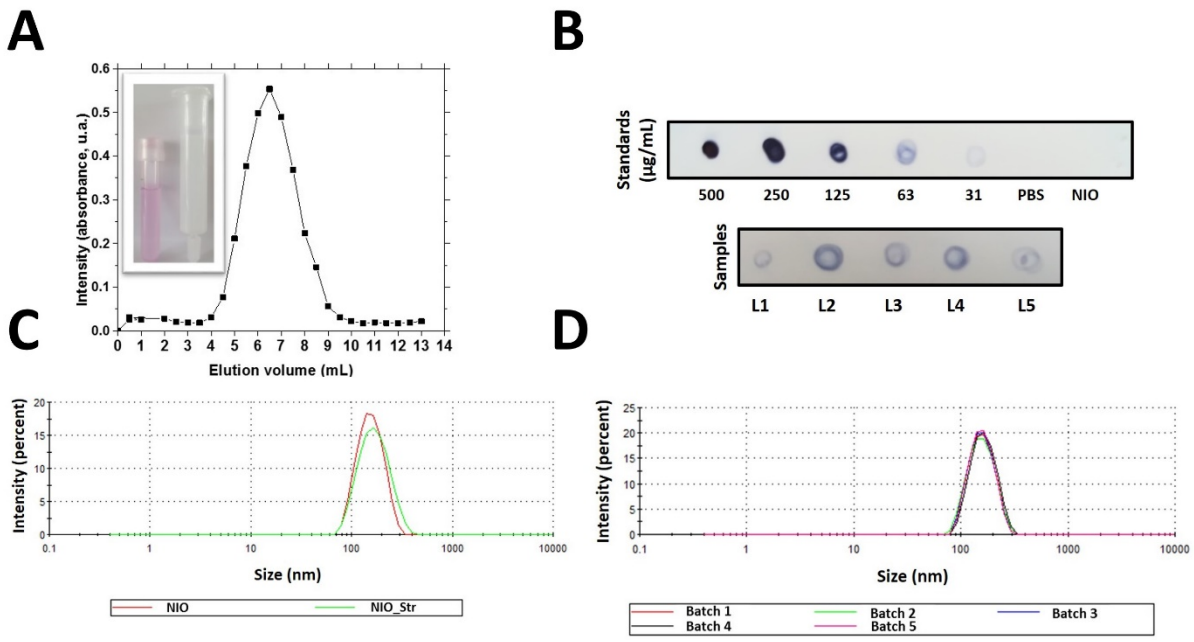

Figure 9.2. *Figure 2. (**A**) Elution profile of a solution of streptavidin from a Sepharose CL-4B SEC gravity elution column. Signal quantification of each 0.5Ml fraction was measured by BCA total protein assay according with manufacturer instruction. Graph insight shows (left) the first 3.5 mL collected of a suspension of red dye loaded niosomes to allow their visualization, after their elution from the SEC column; (right) the SEC column after the elution of the 3.5 mL of dyed niosomes. Both elements, niosomes and free protein, eluted from the column enough separate to allow their separation based on Sepharose CL-4B gravity elution coloumns. (**B**) Dot-Blot assay for checking the effectively of streptavidin bioconjugation to niosomes through carbodiimide method (EDC/NHS). Standards of different concentrations allows the semiquantification of the process by comparison of spot intensity. The result shows the 5 different batches. Biotinylated-HRP (4µg/mL) was used as detecting agent. (**C**) Size distribution by DLS of bared niosomes (or NIO) and streptavidin-conjugated niosomes or (NIO_Str). The average size increment (2nm) shown as peak displacement demonstrate the effective conjugation of the protein. (**D**) Size distribution by DLS of the 5 different batches of NIO_Str (152 ± 3 nm), to demonstrate the reproducibility of the process.*

As expected, an increase (2 nm) in hydrodynamic radius of the particles was observed after bioconjugation of streptavidin over niosomes surface (**Figure 9.2.C**), and this increment can be monitored by DLS as routine technique to check the process efficacy.[32]

All the batches were characterized in terms particle size and size distribution (**Figure 9.2.D**), showing a good reproducibility, with an average value of 152 ± 2 nm.

9.3.2. Artificial EVs production using Nio_Str functionalized with tetraspanin LEL

In order to develop a functional RM based on artificial exosomes, Nio_Str particles were incubated with tetraspanin CD9 and/or CD63 large extracellular loops (LEL), to create mono- or double functionalized niosomes named Nio_LEL (-LEL9, -LEL63, or LEL9/63). Biotinylated recombinant tetraspanin LELs production has been previously described.[25] Briefly, each construction is biotinylated at the N- and C- terminal by the introduction of 15 aminoacids of the AviTag peptide, which allows site-specific biotinylation by the biotin ligase A (BirA) from *Escherichia coli*. This double biotinylation will allow LELs to bind them to streptavidin molecules, and this binding process will help LELs to acquire the proper spatial conformation for antibodies specific recognition during molecular recognition assays performance, such as dot blot and ELISA assays.

LELs coupling to Nio_Str was performed by co-incubation at constant stirring overnight at 4 °C in a tube rotator. In the special case of Nio_LEL9/63, niosomes were incubated with both type of LEL at a molar ratio 1:1, in order to obtained particles with equal amount of surface tetraspanins.

After incubation, excess of LELs was removed by gel filtration (Sepharose CL-2B), and several fractions were collected into glass vials. The fractions were analyzed by dot blot for immunodetection of the LEL. **Figure 9.3.A** shows the detection of LEL_CD9 and LEL_CD63 constructions in both mono- and double-functionalized niosomes, and confirms the single and co-functionalization with LELs. The first five fractions correspond to the void volume of the column and no signal was detected. A progressive increment in the signal was observed in fractions 5/6 to 9/10, which correspond to those that showed the characteristics pale white color of the vesicles in suspension. Then, a reduction in signal is observed prior to another increment in the signal corresponding to the elution of free LEL that is used in excess.

Both characteristics (color ad signal) were taken into consideration, and the 5 fractions showing higher signals were pooled, so the final volume achieved of Nio_LEL was 2.5 mL for each type of modified niosomes. Signal differences between CD63 and CD9 for double functionalized vesicles are due to differences in exposure time. It was needed longer exposures for CD63 detection. Nio_LEL particles were produced in the range of 5.2×10^{11} – 1.0×10^{12} particles/mL, measured by NTA.

Nio_LEL were also characterized by NTA to check particle average size and size distribution, and a sample of natural exosomes was also measured for comparative purposes. Besides differences in terms of peaks intensities across the distributions (**Figure 9.3.B**), average size of Nio_LEL9, Nio_LEL63, Nio_LEL9/63 and natural exosomas are similar (185, 160, 159 and 162 nm respectively), and the size distribution limits are similar for all the particles. However, artificial vesicles are more homogeneous (as expected) since they are lab-made products, while natural exosomas are more heterogeneous regarding their natural origin. Mono- and double-functionalized particles remains similar between types of particles.

The next step was to test the recognition of the Nio_LEL by their specific anti-tetraspanin antibody and the possible unspecific signal from the other anti-tetraspanin. Negative controls were introduced (bared niosomes, and niosomes functionalized with Streptavidin with/without biotin saturation), and a sample of natural exosomes (mesenchymal triple-negative breast cancer cell line SUM159) was used as positive control. Both polyclonal and monoclonal antibodies (biotinylated or purified) were tested. Effective molecular recognition was carried out by dot blot assay as performed to check niosomes-LEL functionalization. This rapid and simple technique is suitable for screening of antibodies.[33]

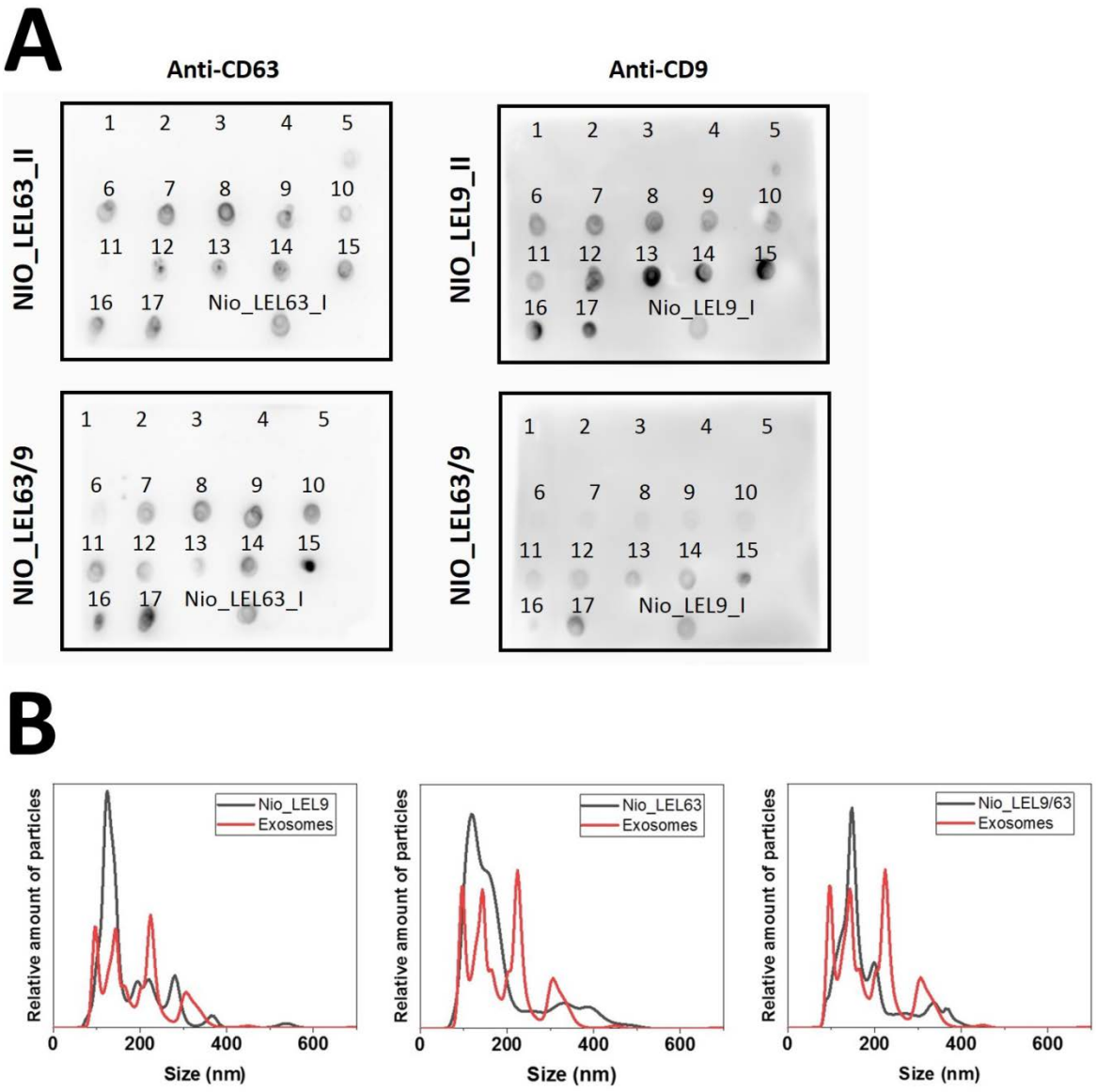

Figure 9.3. *(**A**) Dot-blot assays for revelation of LEL, CD9 or CD63, positive fractions collected from a Sepharose CL-2B gravity elution SEC column. Mon- and double-functionalized Nio_Str have been produced. (**B**) Size distribution measured by NTA (Nanosight, Malvern Instruments) of previous described fully artificial exosomas (NIO_LEL). A sample of natural exosomas isolated from mesenchymal triple-negative breast cancer cell line SUM159 was also measured for comparison purposes.*

The results of the different assays carried out showed that the best detection was obtained with the polyclonal antibodies (**Figure 9.4**), in terms of specificity (referred to Nio_LEL recognition and discrimination). Those antibodies exhibit some unspecific recognition for the other tetraspanin, but less intense than the observed for biotinylated monoclonal antibodies. In addition, the signal from negative controls was more intense for

both types of monoclonal antibodies. However, between them, purified ones offered better results. Based on these observations, capture by purified monoclonal antibodies and detection using polyclonal antibodies were selected as configuration for a sandwich-based ELISA experiments to detect artificial, according to a classical configuration for this type of immunoassays.[34]

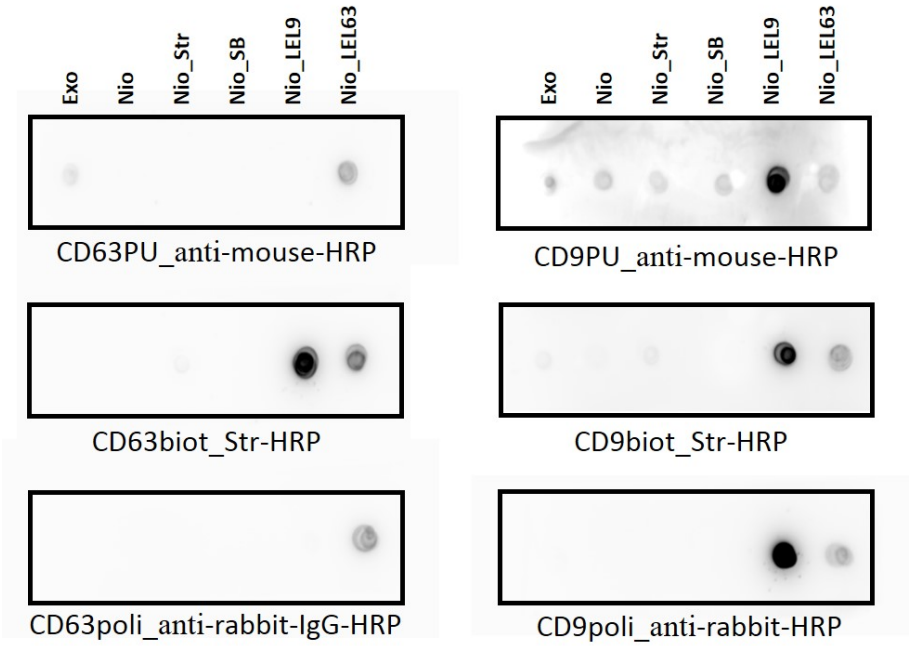

Figure 9.4. *Dot-blot assay for the screening and selection of a-tetraspanin antibodies for their future use in ELISAs for the detection of fully artificial exosomes (NIO_LEL). Secondary antibodies labelled with HRP were appropriate selected. Different negative controls were also introduced (bared niosomes, niosomes functionalized with streptavidin with and without biotin saturation), as the use of isolated exosomas from mesenchymal triple-negative breast cancer cell line SUM159 as positive control. Values are uniplicate assays. (PU) monoclonal purified antibody; (biot) Biotynilated monoclonal antibody; (poli) polyclonal antibody.*

9.3.3. Development of ELISA assays using artificial exosomas

9.3.3.1. Single tetraspanin functional particles

To test the potential use of monofunctionalized Nio_LEL as RM, ELISA assays were carried out using different combinations of capture/detection antibodies for both types of vesicles (Nio_LEL9 and Nio_LEL63). This proposed ELISA assay with colorimetric detection used monoclonal antibodies for capture and polyclonal antibodies for primary detection, with the use of adequate HRP-labeled secondary. The combination of the proper

detection and capture antibodies is crucial in the development of ELISA assays, especially in terms of *signal-to-noise* ratio and specificity. Multiple antibodies combinations were tested, and their unspecific signal were also studied.

From negative controls (**Figure 9.5.A**), unspecific recognition (capture or detection-based) can be measured. In this particular case, both types of mono-functionalized niosomes are recognized by the anti-tetraspanin against the non-carrying protein. Cross detection of these particles confirms something previously observed by dot-blot assay, that this unspecific recognition is higher for CD63 compared to CD9. The signal observed for capture/detection of NIO_LEL63 using anti-CD9 antibodies is higher than that observed when using anti-CD63. This result was obtained with both batches, and differences in signal intensity between both batches are probably related to particle concentration (6.9×10^{11} and 8.2×10^{11} particles/mL for batch 1 and 2 respectively in the case of NIO_LEL9 and 1.0×10^{12} and 7.4×10^{11} for NIO_LEL63).

Then, monofunctionalized niosomes were tested under the different antibodies combination, to test their selectivity (how efficiently Nio_LEL are discriminated) and sensibility (how intense is the specific signal). The same controls as for dot blot assay were used, and Nio_LEL particles were tested in the produced concentration without dilution.

As seen in **Figure 9.5.B**, a better signal was observed for all the cases were anti-CD9 was used for detection, even when the assayed particles were Nio_LEL63, or in the case of Nio_LEL9 captured by anti-CD63. These two conditions offer then the unspecific signal for detection, clearly lower than the specific signal, and in accordance with dot-blot results.

In the case of detection based on anti-CD63, when capture by anti-CD9, this detection can discern ($p<0.005$) between types of Nio_LEL with a really low sensibility, and coupled to capture also by anti-CD63 is the only combination that cannot differentiate Nio_LEL type.

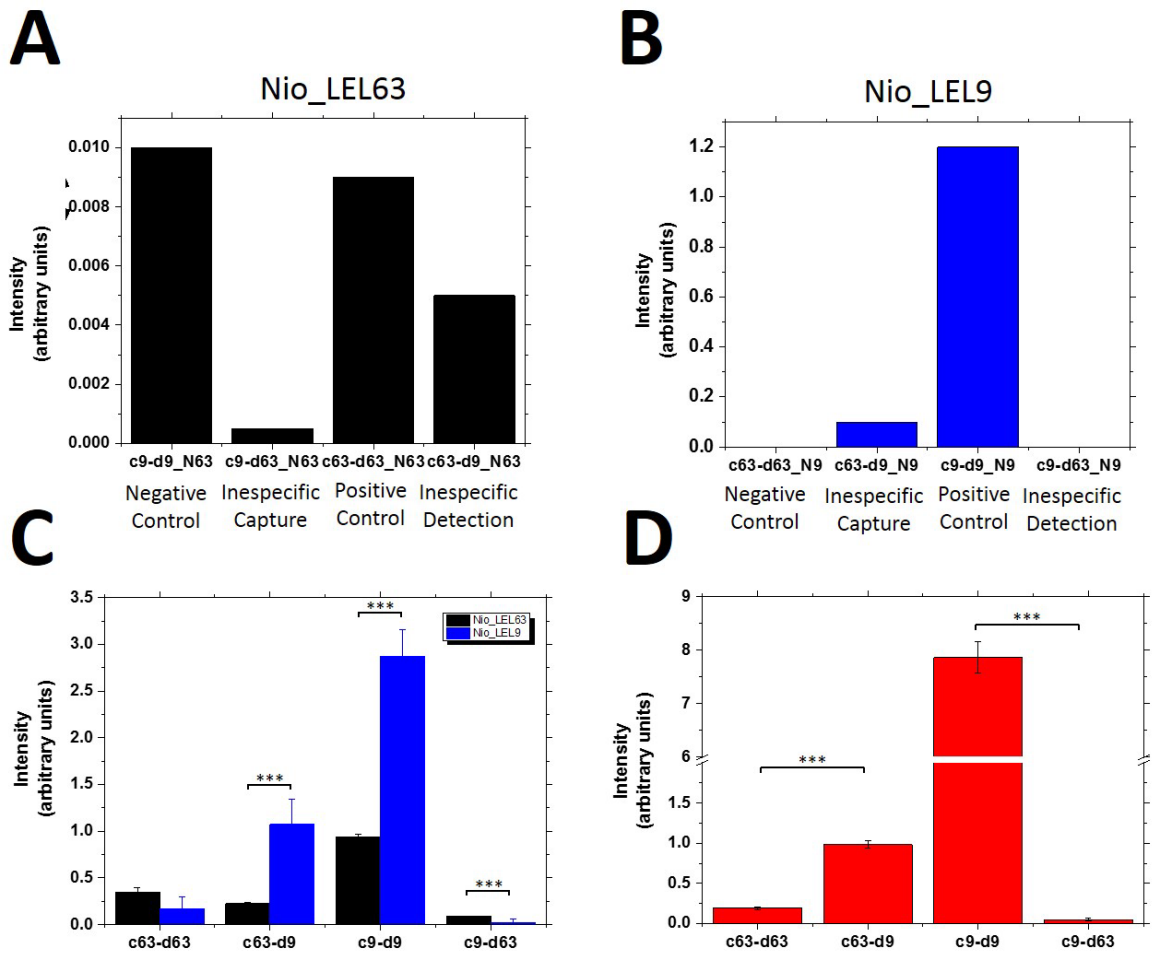

Figure 9.5. *(**A,B**) Cross-reactive responses for mono-functionalized LEL-tetraspanin niosomes (fully articial exosomas) for different configuration of capture (c) and detection (d) anti-tetraspanin antibodies. (**C**) ELISA assays for the detection of NIO_LEL9 (N9) and NIO_LEL63 (N63) fully artificial exosomes using different combination of capture (c) and detection (d) antibodies. Monoclonal a-CD9 or a-CD63 antibodies were used for capture, whereas polyclonal a-CD9 or a-CD63 antibodies were used for detection. (**D**) ELISA assays for the detection of NIO_LEL9/63 using different combinations of capture (c) and detection (d) antibodies. The graphs shows the mean ± SD of 3 independent experiments. *** p<0.005, Student's t-test.*

The large difference between specific capture-detection of Nio_LEL9 y –LEL63 could be explained by differences in antibodies affinity, since differences in particles concentration are no so evident (6.9×10^{11} *vs* 1.0×10^{12} for Nio_LEL9 and Nio_LEL63 respectively). Based on these results, capture and detection by anti-CD9 seems to offer the better sensibility with capabilities to discern the type of vesicles.

9.3.3.2. Double tetraspanin functional particles

However, single molecule detection is often used, but the simultaneous detection of two different tetraspanins (at least one of them must be CD63, being the others CD9 or CD81) is accepted as a molecular identification of the endosomal origin of the exosomes, and can be used as molecular markers in exosomes detection based on immunoassays.[35] For this purpose, double functionalized niosomes (Nio_LEL9/63) were produced and tested by the same antibodies combination in order to identify which one offers better sensibility.

Nio_LEL9/63 are recognized by all the combinations of capture/detection antibodies (**Figure 9.5.D**), however a clear higher detection is observed when using anti-CD9 as capture and detection ($p<0.005$). The next combination with acceptable sensibility is the one that uses capture by anti-CD63 and detection by anti-CD9. The other two possibilities (c9-d63 and c63-d63) offer a really low sensibility. These observations are in accordance with those described for mono-functionalized particles, and clearly confirm that antibodies for CD9 offer better possibilities probably due to a higher affinity constant.

In a previous work of our group,[36] an ELISA procedure was developed for the detection of exosomes based on the simultaneous recognition of two tetraspanin (one used for capture, and the other for detection). For this purpose, melanoma cell line (Ma-Mel-86c) derived exosomes isolated by ultracentrifugation were used, and different combination of antibodies recognizing CD9, CD63, and CD81 were tested. Results revealed that capture by CD81 and detection carried out by CD9 presented the best signal-to-noise ratio. However, the same exosomes were better detected in a Lateral Flow Immunoassay (LFIA) using CD9 for capture and CD63 for detection, besides this combination offered a higher background signal in ELISA compared to CD81/CD9 for capture/detection respectively.

In this type of analytical platforms, only Nio_LEL9/63 could be tested, since mono-fucntionalized particles are not suitable due to how it works a LFIA test. However, the best capture-detection pair described for this systems is in our case the less sensible one, so our proposal of RM based on artificial exomes is adequate for ELISA and could not be for LFIA.

Finally, only in the combinations where anti-CD9 is used as detection, the sensibility was enough to allow the visualization of dose-response signals (**Figure 9.6**). This result is the manifestation of those observed in figure 34.D, where it can be seen that detection based on CD63 is not a good option. In all the cases, a linear correlation is observed. When the signal intensity proportioned by a specific antibody configuration was enough to allow visualization of dose-response, this response was fitted to a linear equation, demonstrating that working condition where into the linear range of the typical sigmoidal response related to a sandwich assay, which confirms that our RM proposal is suitable.

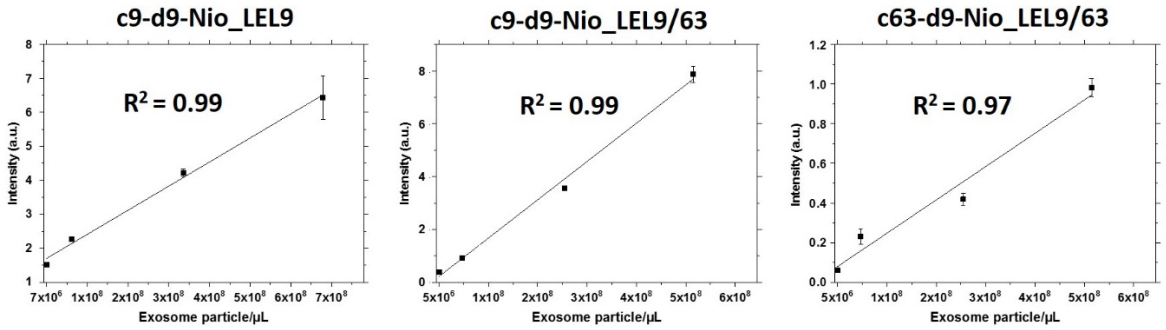

Figure 9.6. *Dose-response graphs for different types of fully artificial exosomas detected by ELISA assay using monoclonal and polyclonal antibodies a-tetraspanins CD9 y CD63 for capture and detection respectively. As secondary appropriate a-IgG-HRP was used. N9 and N9/63 are NIO_LEL9 and NIO_LEL9/63 respectively, which are mono- and double-functionalized LEL-tetraspanin niosomes.*

9.3.4. Commercial potential of our artificial exosome model

The work of Lane et al.[20] has highlighted the physical similarities between synthetic vesicles and EVs, and those particles have been used as reference materials for methodological comparisons (NTA, tRPS and hFC). However, all those methods are classified as unspecific concentration determination methods[37] since they rely on general physical characteristics and not in a specific molecular marker which allows also phenotyping possibilities. In this scientific challenge we propose fully artificial exosomes[22] as a new potential tool to help into the development and validation of new analytical methods and platforms, as demonstrated with our results. In our opinion, our proposed RM could be competitive to those in the market up to date.

Tabla 9.1. *Some commercial available kits based on ELISA for exosomes quantification in biological samples. Most of them are based on colorimetric signal quantification based on HRP substrates, with a typical format of 96 well microtiter plate.*

Product	Manufacturer	Biomarkers	Assay format	Standard used for calibration plots
ExoELISA	SBI System Biosciences	CD9/CD63/CD81 for detection	Exosomes are immobilized directly into the well	Lyophilized Exosomes
ExoTestTM	HansaBioMed	CD9 for detection	Sandwich assay using CD9 for detection. Capture not specified by the manufacturer	Exosome lyophilized
ExoQuant	Centaur Genprice	CD9 for detection	Sandwich assay using pan-Exosome biomarkers (data not specify by the manufacturer	Lyophilized Exosomes
ExoEL-CD81A1	BioVision	CD9 for detection	Sandwich assay using pan-Exosome biomarkers (data not specify by the manufacturer	Exosome lyophilized
PS CaptureTM Exosome ELISA KIT	Fujufilm Wako Pure Chemical Corporation	CD63 for detection	Exosomes are captured by a phosphatidylserine binding protein immobilized in the wells	Lyophilized Exosomes
CD9/CD63 Exosome ELISA Kit	Cosmo BIO CO. Ltd	CD63 for detection	Sandwich assay using CD9 for capture	CD9/63 Fusion protein
ExoAssayTM	CD Creative Diagnostics®	Not specified by the manufacturer	Sandwich assay using CD9 for capture	Lyophilized Exosomes

Details extracted from products data sheets or proportionated by the manufacturer

Commercially available kits based on ELISA assays are marketed with different configurations (**Tabla 9.1**). Some of them are based on direct capture of exosomes into plate wells (such as ExoELISA-(Ultra), SBI System Biosciences), while other relies on exosome-capture mediated by antibodies-coated weels (such as ExoTESTTM, HansaBioMed). Majority of them, use lyophilized exosomes as standards, and some

manufactures let clear that signal can be different depending on the amount of protein per vesicle between different types of exosomes, with potential bias of extrapolated concentration. This fact hinders the quantification of these types of analytes, since the same intensity could be related to a higher concentration of analytes with a reduced expression level of detection antigen, or a low concentration of analytes carrying a higher number of detection epitopes. This is a key point to take into account for analytes such as exosomas, where the expression levels of CD9 and CD63 differs between cell lines,[38] or even exosomas from cells with different heath status. This is something that clearly difficult the development of a universal standard for EVs quantification, especially for exosomes, as mentioned previously.

In this diverse market our proposal can be compatible, since both types of Nio_LEL (mono- and double-functionalize) could be potentially applied. On the other hand, our platform is really versatile, since antigen density can be tuned by changing the density of streptavidin over their surface, and any biotinylated peptide could be used to functionalize, giving lots of options to create specific types of artificial exosomas. Complementary studies about measurements of effective concentration of LEL in the NVs and their stoichiometry in the case of multiple protein functionalization) will re-enforce the results presented here. Also, the application of calibration curves obtained with this innovative RM to different real sample will help to consolidate our model.

9.5. Conclusions and future work

The results demonstrate the potential use of this new biomaterial as analytical standard for molecular recognition based assays, such as immunoassays or aptamer-based assays. The development of artificial exosomes based on tetraspanin (recombinant LEL) surfaced functionalized niosomes have been described. The production of mono- and double-functionalized vesicles with CD9 and/or CD63 is possible, and these particles can be detected and discerned by sandwich ELISAs, using a classical format based on capture through monoclonal antibodies and detection based on polyclonal antibodies with secondary enzyme-labeled antibodies. Dose-response of this particles has been checked, since a linear fitted response is essential for their use as standard for obtaining calibration plots used for quantification purposes.

The methodology proposed in this study allows the preparation with a tunable functionalization based on changes in density surface functionalization (by variation in cholesterol hemisuccinate molar ratio) or changes in the stoichiometry of proteins (by variation in molar ratio of proteins during coupling to streptavidin-coated niosomes). The exploration of this variables could be an interesting starting point for future works. Also, further validation studies must be performed, in order to test their usability for different cell-line derived exosome quantification. Additional proteins, different than classical tetraspanins, could be used for the development of pathology-specific standards.

Another interesting field to be explored is the exploration of other methods for niosomes production, such as microfluidics, that allows an exceptional control of size control while the chemical consumption is really low. This is essential when formulation use really expensive compounds, or scarce material such as highly purified proteins are needed. Furthermore, microfluidics may be a potential platform for the assembly or reconstitution of proteins into synthetic bilayers while those are being self-assembled.

9.5. Bibliographic references

[1] Yáñez-Mó M., Siljander PR., Andreu Z., Zavec AB, Borràs FE, Buzas EI, Buzas K, Casal E, Cappello F, Carvalho J, Colás E, Cordeiro-da Silva A, Fais S, Falcon-Perez JM, Ghobrial IM, Giebel B, Gimona M, Graner M, Gursel I, Gursel M, Heegaard NH, Hendrix A, Kierulf P, Kokubun K, Kosanovic M, Kralj-Iglic V, Krämer-Albers EM, Laitinen S, Lässer C, Lener T, Ligeti E, Linē A, Lipps G, Llorente A, Lötvall J, Manček-Keber M, Marcilla A, Mittelbrunn M, Nazarenko I, Nolte-'t Hoen EN, Nyman TA, O'Driscoll L, Olivan M, Oliveira C, Pállinger É, Del Portillo HA, Reventós J, Rigau M, Rohde E, Sammar M, Sánchez-Madrid F, Santarém N, Schallmoser K, Ostenfeld MS, Stoorvogel W, Stukelj R, Van der Grein SG, Vasconcelos MH, Wauben MH, De Wever O. Biological properties of extracellular vesicles and their physiological functions. J Extracell Vesicles. 2015 May 14;4:27066

[2] Kalra, H., Drummen, G., Mathivanan, S. (2016). Focus on extracellular vesicles: introducing the next small big thing. International journal of molecular sciences, 17(2), 170.

[3] Azmi, A. S., Bao, B., & Sarkar, F. H. (2013). Exosomes in cancer development, metastasis, and drug resistance: a comprehensive review. Cancer and Metastasis Reviews, 32(3-4), 623-642.

[4] Corrado, C., Raimondo, S., Chiesi, A., Ciccia, F., De Leo, G., & Alessandro, R. (2013). Exosomes as intercellular signaling organelles involved in health and disease: basic science and clinical applications. International journal of molecular sciences, 14(3), 5338-5366.

[5] Azmi A.S., Bao B., Sarkar F.H. (2013). Exosomes in cancer development, metastasis, and drug resistance: a comprehensive review. *Cancer Metastasis Rev.*, 32(3-4), 623-642.

[6] Cappello, F., Logozzi, M., Campanella, C., Bavisotto, C. C., Marcilla, A., Properzi, F., Fais, S. (2017). Exosome levels in human body fluids: a tumor marker by themselves?. European Journal of Pharmaceutical Sciences, 96, 93-98.

[7] van der Meel R., Krawczyk-Durka M., van Solinge W.W., Schiffelers R.M. (2014). Toward routine detection of extracellular vesicles in clinical samples. *Int J Lab Hematol*., 36:244-253.

[8] Boriachek, K., Islam, M. N., Möller, A., Salomon, C., Nguyen, N. T., Hossain, M. S. A., Yamauchi, Y., Shiddiky, M. J. (2018). Biological functions and current advances in isolation and detection strategies for exosome nanovesicles. Small, 14(6), 1702153.

[9] Peterson, M. F., Otoc, N., Sethi, J. K., Gupta, A., & Antes, T. J. (2015). Integrated systems for exosome investigation. Methods, 87, 31-45.

[10] Van Der Pol, E., Hoekstra, A. G., Sturk, A., Otto, C., Van Leeuwen, T. G., & Nieuwland, R. (2010). Optical and non-optical methods for detection and characterization of microparticles and exosomes. Journal of Thrombosis and Haemostasis, 8(12), 2596-2607.

[11] Rupert, D. L., Lässer, C., Eldh, M., Block, S., Zhdanov, V. P., Lotvall, J. O., Bally, M., Höök, F. (2014). Determination of exosome concentration in solution using surface plasmon resonance spectroscopy. Analytical chemistry, 86(12), 5929-5936.

[12] Boriachek, K., Islam, M. N., Gopalan, V., Lam, A. K., Nguyen, N. T., Shiddiky, M. J. (2017). Quantum dot-based sensitive detection of disease specific exosome in serum. Analyst, 142(12), 2211-2219.

[13] Doldán, X., Fagúndez, P., Cayota, A., Laíz, J., Tosar, J. P. (2016). Electrochemical sandwich immunosensor for determination of exosomes based on surface marker-mediated signal amplification. Analytical chemistry, 88(21), 10466-10473.

[14] Zhou, Q., Rahimian, A., Son, K., Shin, D. S., Patel, T., & Revzin, A. (2016). Development of an aptasensor for electrochemical detection of exosomes. Methods, 97, 88-93.

[15] López-Cobo, S., Campos-Silva, C., Moyano, A., Oliveira-Rodríguez, M., Paschen, A., Yáñez-Mó, M., Blanco-López, M.C., Valés-Gómez, M. (2018). Immunoassays for scarce tumour-antigens in exosomes: detection of the human NKG2D-Ligand, MICA, in tetraspanin-containing nanovesicles from melanoma. Journal of nanobiotechnology, 16(1), 47.

[16] Jang SC, Kim OY, Yoon CM, et al. Bioinspired exosome-mimetic nanovesicles for targeted delivery of chemotherapeutics to malignant tumors. ACS Nano. 2013;7:7698–7710.

[17] Jeong D, Jo W, Yoon J, et al. Nanovesicles engineered from ES cells for enhanced cell proliferation. Biomaterials. 2014;35:9302–9310.

[18] Hood J.L., Scott M.J., Wickline S.A. (2014). Maximizing exosome colloidal stability following electroporation. Analytical Bichemistry, 448:41-49.

[19] Lee J., Kim J., Jeong M., Lee H., Goh U., Kim H, Kim B., Park J-H. (2015) Liposome-based engineering of cells to package hydrophobic compounds in membrane vesicles for tumor penetration. Nano Letters, 15:2938-2944.

[20] Lane, R. E., Korbie, D., Anderson, W., Vaidyanathan, R., & Trau, M. (2015). Analysis of exosome purification methods using a model liposome system and tunable-resistive pulse sensing. Scientific reports, 5, 7639.

[21] Maas, S. L., De Vrij, J., Van Der Vlist, E. J., Geragousian, B., Van Bloois, L., Mastrobattista, E., Schiffelers, R.M., Wauben, M.H.M., Broekman; M.L.D., Nolte, E. N. (2015). Possibilities and limitations of current technologies for quantification of biological extracellular vesicles and synthetic mimics. Journal of Controlled Release, 200, 87-96.

[22] García-Manrique, P., Gutiérrez, G., & Blanco-López, M. C. (2018). Fully artificial exosomes: towards new theranostic biomaterials. Trends in biotechnology, 36(1), 10-14.

[23] García-Manrique, P., Matos, M., Gutiérrez, G., Pazos, C., & Blanco-López, M. C. (2018). Therapeutic biomaterials based on extracellular vesicles: classification of bio-engineering and mimetic preparation routes. Journal of extracellular vesicles, 7(1), 1422676.

[24] García-Manrique P., Lozano-Andrés E., Estupiñán-Sánchez O.R., Gutiérrez G., Matos M., Pazos C., Yañez-Mo M., and Blanco-López C., Biomimetic small extracelular vesicles, 3rd GEIVEX Simposium, San Sebastian, Spain, 29-30 September 2016. Poster communication.

[25] Lozano-Andrés, E., Libregts, S. F., Toribio, V., Royo, F., Morales, S., López-Martín, S., Valés-Gómez, M., Reyburn, H.T., Falcón-Pérez, J.M., Wauben, M.H., Soto, M., Yáñez-Mó, M. (2019). Tetraspanin-decorated extracellular vesicle-mimetics as a novel adaptable reference material. Journal of Extracellular Vesicles, 8(1), 1573052.

[26] García-Manrique, P., Matos, M., Gutiérrez, G., Estupiñán, O. R., Blanco-López, M. C., & Pazos, C. (2016). Using factorial experimental design to prepare size-tuned nanovesicles. Industrial & Engineering Chemistry Research, 55(34), 9164-9175.

[27] Introduction to Bioconjugation, Chapter 1, and The Chemistry of Reactive Groups, Chapter 2. In Bioconjugate techniques, Edited by Hermanson G.T. Academic press, Londres, 1-125, 127-228.

[28] Bioconjugate reagents, Chapter 3. In Bioconjugate techniques, Edited by Hermanson G.T. Academic press, Londres, 1-125, 127-228.

[29] Endoh H., Suzuki Y., Hashimoto Y. (1981). Antibody coating of liposomes with 1-ethyl-3-(3-dimethyl-aminopropyl)carbodiimide and the effect on target specificity. Journal of Immunological Methods, 44:79-85.

[30] Tan D.M-Y, Fu J-Y, Fu-Shun Wong F-S, Er H-M, Chen Y-S, Nesaretnam K. (2017). Tumor regression and modulation of gene expression via tumor-targeted tocotrienol niosomes. Nanomedicine, 12(20):2487-2502.

[31] Li K., Chang S., Wang Z., Zhao X., Chen D. (2015). A novel micro-emulsion and micelle assembling method to prepare DEC205 monoclonal antibody coupled cationic nanoliposomes for simulating exosomas to target dendritic cells. International journal of Pharmaceutics, 491:105-112.

[32] Jans, H., X. Liu, Austin L, Maes G, Huo Q. (2009). Dynamic Light Scattering as a Powerful Tool for Gold Nanoparticle Bioconjugation and Biomolecular Binding Studies." Analytical Chemistry 81(22): 9425-9432.

[33] Renart J., Behrens M.M., Fernández-Renart M., Martínez J.L., Immunoblotting Techniques, Chapter 23, in Immunoassay, edited by Christopoulos T.K. and Diamandis E.P, Academic Press Inc., San Diego, California, USA.

[34] Christopoulos T.K. and Diamandis E.P., Immunoassay configurations, Chapter 10, in Immunoassay, edited by Christopoulos T.K. and Diamandis E.P, Academic Press Inc., San Diego, California, USA.

[35] Kowal, J., Arras, G., Colombo, M., Jouve, M., Morath, J. P., Primdal-Bengtson, B., Florent Dingli, F., Loew, D., Tkach, M., Théry, C. (2016). Proteomic comparison defines novel markers to characterize heterogeneous populations of extracellular vesicle subtypes. Proceedings of the National Academy of Sciences, 113(8), E968-E977.

[36] Oliveira-Rodríguez, M., López-Cobo, S., Reyburn, H. T., Costa-García, A., López-Martín, S., Yáñez-Mó, M., Cernuda-Morollón, E., Paschen, A., Valés-Gómez, M., Blanco-López, M. C. (2016). Development of a rapid lateral flow immunoassay test for detection of exosomes previously enriched from cell culture medium and body fluids. Journal of extracellular vesicles, 5(1), 31803.

[37] Rupert, D. L., Claudio, V., Lässer, C., & Bally, M. (2017). Methods for the physical characterization and quantification of extracellular vesicles in biological samples. Biochimica et Biophysica Acta (BBA)-General Subjects, 1861(1), 3164-3179.

10. Conclusiones/Conclusions

Capítulo 10. Conclusiones

La conclusión general que se extrae de los resultados obtenidos a lo largo de la presente Tesis Doctoral es la probada posibilidad de realizar un correcto control sobre la producción de nanovesículas con tamaño controlado y monodispersas. Por otra parte, se mejora la encapsulación de compuestos hidrofílicos y estudia su relación con el tamaño de partículas. Además, se demuestra su potencial para el desarrollo de modelos bio-miméticos de exosomas, un tipo natural de vesículas extracelulares con elevado interés clínico y biológico, y su empleo a modo de estándar analítico. Esta conclusión es el resumen de los siguientes puntos:

- Se planteó el estudio del efecto de las variables de un método clásico, como es la inyección de etanol, sobre las propiedades finales de las partículas (liposomas y niosomas), concretamente el tamaño y la monodispersidad. El adecuado planteamiento de los diseños de experimentos ha permitido reducir de diez variables metodológicas iniciales con posible efecto sobre las respuestas a sólo tres (concentración final de compuestos de membrana en la fase acuosa, relación de volumen entre fase acuosa y orgánica, y amplitud de sonicación), que son las de mayor efecto. Se han establecido modelos matemáticos en forma de ecuaciones polinómicas que permiten predecir el tamaño y la dispersión del mismo (PDI) en función de los valores de los factores metodológicos.

  Adicionalmente, estudios de estabilidad coloidal llevados a cabo mediante medidas de potencial Zeta (ζ) y de perfiles de retro-dispersión de luz, así como de eficacia de encapsulación de compuestos bioactivos, han demostrado su potencial uso en aplicaciones biotecnológicas diversas, como la distribución y liberación controlada de compuestos bioactivos, sistemas de amplificación de señal analítica, y desarrollo de elementos biomiméticos.

- Se ha evaluado la impresión 3D tanto convencional como de alta resolución a la hora de la fabricación de un dispositivo de microfluídica y su módulo termostatizado. Esta técnica, ha permitido la fabricación de dispositivos funcionales y de bajo coste, aunque la morfología y dimensiones de los microcanales del chip difieren de aquellos planteados en el diseño por

ordenador. Estas diferencias podrían atribuirse a parámetros operacionales de las impresoras, y deben ser estudiados más a fondo en futuros trabajos.

Los resultados de este estudio han mostrado la idoneidad de este tipo de dispositivos a la hora de preparar nanovesículas. El desarrollo de un sistema de control de temperatura adaptado al dispositivo microfluídico, ha permitido el uso de tensioactivos no iónicos con elevada temperatura de transición (T_m), los cuales se ha demostrado que son los más adecuados en la formulación de niosomas.

Por un lado, el diseño del dispositivo y su acoplamiento a un microscopio invertido ha permitido obtener información de procesos clave en la formación de estas partículas como es la difusión molecular en flujo paralelo. También se ha observado el papel de la temperatura sobre dicha difusión y sobre el principio en el que se basa el dispositivo microfluídico: el enfoque hidrodinámico de fluidos. De forma análoga al estudio anterior, se ha podido establecer la importancia de los parámetros metodológicos, siendo la relación de flujos orgánico:acuoso el parámetro fundamental para controlar la eficiencia del mezclado y las propiedades morfológicas de las partículas.

Por otra parte, la concentración de los componentes de membrana en la fase orgánica se ha demostrado que condiciona los tamaños finales y los valores de PDI. Sin embargo, el flujo volumétrico total posee un escaso efecto, y sin embargo influye de forma importante sobre la eficacia del mezclado de fases, así como sobre el tiempo de producción. La temperatura puede llegar a mejorar las propiedades de las partículas, como reducir el tamaño promedio y los valores de PDI.

- La encapsulación de compuestos hidrófilos en sistemas vesiculares representa un reto, y no es adecuada de llevar a cabo mediante métodos de inyección de solventes. Por ello se llevó a cabo un estudio de la influencia de la composición del medio de hidratación durante el método *denominado hidratación de película delgada.* Se ha podido comprobar como la eficacia de encapsulación (EE) se puede mejorar con la composición del método de hidratación, y además se observó una clara influencia del mismo sobre el tamaño de partícula final.

Por otra parte, se han descrito efectos particulares del peso molecular de los compuestos a encapsular tanto sobre el tamaño de partícula como sobre la EE de dichos compuestos en las vesículas formuladas.

Mediante técnicas calorimétricas, se ha podido comprobar como la composición del medio de hidratación altera el orden y empaquetado de las bicapas, pudiendo ser el responsable de los cambios encontrados en la distribución de tamaño y la EE.

Además, se ha podido comprobarla idoneidad de la diálisis y la filtración en gel para la purificación de estos sistemas vesiculares formulados en medios viscosos. Se ha observado una discrepancia entre ellos para este tipo de suspensiones, y se ha concluido que medios muy viscosos impiden una correcta separación e introducen un sesgo de tamaño en la población de vesículas.

- Por último, la información que se ha obtenido de los modelos obtenidos para la inyección de etanol ha sido empleada para la mejora de las características de los niosomas formulados con Span® 60: Colesterol (relación molar 1:0,5). En concreto, la relación de fases orgánica:acuosa se ha mantenido elevada mientras que se ha reducido la concentración de los componentes de membrana. Esto ha permitido obtener niosomas de un tamaño similar al de exosomas naturales, con valores de PDI adecuados, y todo ello evitando procesos de sonicación, ya que se ha observado que el envejecimiento de la sonda introduce variabilidad en el proceso.

  Estas partículas han sido funcionalizadas en la superficie con moléculas de estreptavidina tras una optimización del proceso, y han permitido la posterior funcionalización con tetraspaninas recombinantes biotiniladas, en concreto CD9 y CD63. Se han podido obtener partículas mono- y bi-funcionalizas con tamaños similares a exosomas naturales, aunque con distribuciones de tamaño ligeramente diferentes, probablemente debido al proceso de purificación por cromatografía de exclusión de tamaños empleado en etapas finales para su preparación. Estos exosomas totalmente artificiales y producidos mediante técnicas bio-nanotecnológicas basadas en química supramolecular, han sido reconocidos y diferenciados en función de la tetraspanina en superficie

mediante immunoensayos sándwich de tipo ELISA. A su vez, la señal analítica responde a la concentración de dichas partículas, lo que en conjunto las hace candidatas idóneas a ser empleadas como estándares analíticos en este tipo de métodos de detección basados en reconocimiento molecular.

Sin embargo, el diseño de estas partículas condiciona la selección de anticuerpos que pueden usarse para su detección, debiendo evaluarse si dichas configuraciones son adecuadas para muestras biológicas. Además, estos exosomas deber ser caracterizados en mayor profundidad para conocer la densidad superficial de proteínas, así como la relación molar real entre ellas cuando son doblemente funcionalizados. Este parámetro es importante para explicar la diferencia en concentración de exosomas naturales en una muestra que se ha obtenido al emplear un calibrado obtenido con exosomas artificiales y el valor obtenido mediante NTA (*Nanoparticle Tracking Analysis*). Esta información ayudará a la mejora del diseño de este tipo de biomaterial con fines analíticos, y a su adecuación al tipo de exosomas naturales que se desee mimetizar, ya que es conocida la enorme diversidad fenotípica que existe.

Chapter 10. Conclusions

The general conclusion that can be drawn from the results obtained throughout the work carried out in this Ph.D. Thesis is the possibility to carry out a correct control over the production of nanovesicles with controlled size and monodisperse size distribution. On the other hand, the encapsulation of hydrophilic compounds and their relation to particle size is improved. In addition, it is demonstrated their potential for the development of biomimetic models of exosomes, a natural type of extracellular vesicles with high clinical and biological interest, and its use as an analytical standard. This conclusion is based on the following points:

- The study of the effect of the variables of a classical method, such as Ethanol Injection Method or EIM, on the final properties of the particles (liposomes and niosomes), specifically size and monodispersity was proposed. The adequate approach of the DoE has allowed reducing from ten initial methodological variables with potential effect on the responses to only three (organic/aqueous phase volume ratio, membrane precursors final concentration in the aqueous phase, and sonication amplitude), which are those with a higher effect. Mathematical models base don polynomic equations have been setted for the prediction of particle size and monodispersity (PDI) according with the methodological parameters values.

  Additionally, studies of colloidal stability carried out by mmeassuring Zeta potential (ζ) and backscattering profiles, as well as encapsulation efficiency of bioactive compounds, have demonstrated their potential use for biotechnological applications, such as the distribution and controlled release of bioactive compounds, analytical signal amplification systems, and development of biomimetic elements.

- Conventional and high-resolution 3D printing have been evaluated for manufacturing the thermostatic and microfluidic device respectively. This technique has allowed the production of functional and low-cost devices, although the morphology and dimensions of the chip microchannels differed from those proposed in the computer-assisted design. These differences could

be attributed to the operational parameters of the printers and should be further studied in future works.

The results of this study have demonstrated the suitability of these devices for the preparation of nanovesicles. The development of a temperature control system adapted to the microfluidic device has allowed the use of non-ionic surfactants with a high transition temperature (T_m). Those have been demonstrated as suitables for the formulation of niosomes.

On the other hand, the device design and its coupling to an inverted microscope have allowed obtaining information on key processes in the formation of these particles such as molecular diffusion in parallel flow. The role of temperature on this diffusion and on the principle on which the microfluidic device is based, the hydrodynamic flow focusing, has also been reported. In a similar way to the previous study, it has been possible to establish the importance of the methodological parameters, being the flow rate ratio of organic:aqueous streams the fundamental parameter to control the mixing efficiency and the morphological properties of the particles.

On the other hand, the concentration of the membrane components in the organic phase determined the final sizes and the PDI values. However, the total volumetric rate had reduced effect, but it has an important influence on the extent of mixing, as well as on the production rate. The temperature can improve the properties of the particles, such as reduce size and PDI values.

- The encapsulation of hydrophilic compounds in vesicular systems represents a challenge, and it is not adequate to be carried out by means of solvent injection methods. Therefore, a study of the influence of the composition of the hydration solution was carried out during the method called *thin film hydration*. It has been possible to verify how the encapsulation efficiency (EE) can be improved with the composition of this solution, and also it was observed a significant influence over particle size.

  On the other hand, particular effects of the molecular weight of the compounds to be encapsulated have been described over the size and EE values for the vesicles.

Using calorimetric techniques such as DSC, it has been possible to verify how the composition of the hydration medium alters the order and packaging of the bilayers, which may be responsible for the observations on size and EE in the study.

Aditional, it has been possible to verify the suitability of dialysis and gel filtration for the purification of these vesicular systems formulated in viscous media. A discrepancy between them has been observed for this type of suspensions, and it has been concluded that very viscous media prevent a correct chromatographic separation and introduce a size bias in the population of vesicles.

- Finally, the information obtained from the models for the ethanol injection method has been used to improve the characteristics of the niosomes formulated with Span® 60: Cholesterol (1: 0.5 molar ratio). Specifically, the organic:aqueous phase volume ratio has set high while the concentration of the membrane components has been reduced. This has allowed obtaining niosomes with a similar size to that of natural exosomes, with acceptable PDI values, and all these avoiding sonication processes, since it has been observed that the aging of the probe introduces uncontrollable variability in the process.

  These particles have been surface-functionalized with *streptavidin* molecules after optimization of the process, and have allowed subsequent functionalization with biotinylated recombinant tetraspanins, specifically CD9 and CD63. Mono- and double-functionalized particles have been obtained with sizes similar to natural exosomes, although with slightly different size distributions, probably due to the purification process by size exclusion chromatography used in final steps for its preparation. These fully artificial exosomes produced by bio-nanotechnological techniques based on supramolecular chemistry have been recognized and differentiated based on surface tetraspanins by sandwich ELISA type immunoassays. In fact, the analytical signal is concentration-dependant, which makes them suitable candidates to be used as analytical standards in this type of detection methods based on molecular recognition.

However, the design of these particles determines the selection of antibodies that can be used for their detection and makes necessary the evaluation of whether such configurations are suitable for biological samples. In addition, these exosomes must be characterized in depth to know the surface density of proteins, as well as the real molar ratio between them when they are doubly functionalized. This parameter is important to explain the difference in concentration of natural exosomes in a sample that has been obtained by using a calibration obtained with artificial exosomes and the value obtained by NTA (*Nanoparticle Tracking Analysis*). This information will help to improve the design of this type of biomaterial for analytical purposes, and its adaptation to the type of natural exosomes that want to mimic since it is known the huge phenotypic diversity that exists.

ANEXO I. Publicaciones derivadas de la Tesis Doctoral

I&EC research
Industrial & Engineering Chemistry Research

Article

pubs.acs.org/IECR

Using Factorial Experimental Design To Prepare Size-Tuned Nanovesicles

Pablo García-Manrique,[†,‡] María Matos,[†] Gemma Gutiérrez,[†] Oscar R. Estupiñán,[†,‡] María Carmen Blanco-López,[‡] and Carmen Pazos*[,†]

[†]Department of Chemical and Environmental Engineering and [‡]Department of Physical and Analytical Chemistry, University of Oviedo, Julián Clavería 8, 33006 Oviedo, Spain

Supporting Information

ABSTRACT: The aim of this work was to prepare size-tuned nanovesicles using a modified ethanol injection method (EIM) by applying factorial experimental design. Stable size-tuned nanovesicles (liposomes and niosomes) with controlled sizes and high EE values for hydrophobic compounds (Sudan Red 7B and vitamin D_3) were achieved. Equations that were able to predict the mean particle sizes, in the ranges of 55−156 nm for liposomes and 224−362 nm for niosomes with PDI values between 0.032 and 0.378, were obtained. These customized soft nanoparticles could be suitable in food, cosmetic, pharmaceutical, or medical applications, such as diagnosis or therapy.

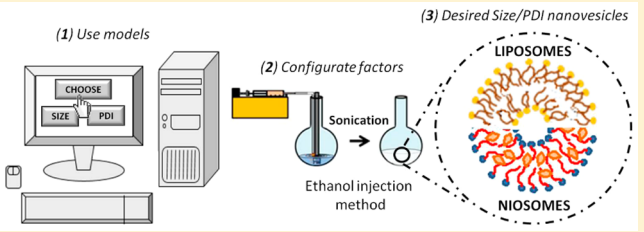

1. INTRODUCTION

Controlled preparation of nanoparticles has attracted great interest in recent years.[1] Nanovesicles are an important family of organic nanoparticles, produced by bottom-up nanotechnology, with relevant applications in biomedicine,[2] food science,[3] analytical chemistry,[4,5] and biosensors.[6] They are considered soft nanoparticles because interactions among their molecular components are similar to those arising from biological systems.[7] Most of the work describing their preparation for specific uses has focused on the optimization of their composition with the aim of maximizing encapsulation efficiency, delivery, or delivery control.

However, size is one of the most critical properties (together with shape and surface chemistry) for understanding cell-uptake processes and, therefore, bioavailability and targetability.[7] Several studies have focused on the optimization of the drug encapsulation efficiency while considering size as just a property for controlling administration parameters, such as penetration kinetics in topical formulations. For example, Padamwar et al.[8] studied the encapsulation of vitamin E in liposomes and found that the amount of lipids yielded a positive correlation with size, which was, in turn, negatively correlated with penetration efficiency into the skin. Sometimes, size has been found to increase with higher amounts of membrane components, such as cholesterol, whereas it decreased with higher amounts of surfactants (e.g., Tween 80). Simultaneously, cholesterol or surfactants can affect encapsulation efficiency (EE). Optimal situations can be reached as a compromise at intermediate levels of both factors. In that case, Taha[9] also reported an interaction between membrane-component concentration and size reduction by ultrasound, making factor optimization an essential task. In other cases, an opposite effect was observed, and higher concentrations of membrane components (such as Span 60 and cholesterol) produced larger sizes and increased EEs. It is useful to deliver efficient amounts of a selected drug into superficial skin layers without systemic absorption.[10] On this basis, the goal of our work was to set up a bulk method for producing nanovesicles of controlled size that could be subsequently modified for specific applications.

Vesicles are colloidal particles in which a concentric bilayer made up of amphiphilic molecules surrounds an aqueous compartment. These vesicles are commonly used to encapsulate both hydrophilic and lipophilic compounds, for food, cosmetic, pharmaceutical, or medical applications, such as diagnosis or therapy.[11] Hydrophilic compounds are entrapped into the aqueous compartments between bilayers, whereas lipophilic compounds are preferentially located inside the bilayers.[12,13] The most common types of vesicles are liposomes and niosomes.

Liposomes were first described by Bangham et al. in 1965,[14] and they are basically spherical bilayer vesicles formed by the self-assembly of phospholipids. This self-assembly process is based on the interactions occurring between phospholipids and water molecules, where the polar head groups of phospholipids are exposed to the aqueous phases (inner and outer) and the hydrophobic hydrocarbon tails are forced to face each other in a bilayer.[15] Because of the presence of both lipid and aqueous phases in liposome structures, they can be used for the encapsulation, delivery, and controlled release of hydrophilic, lipophilic, and amphiphilic compounds.[15,16]

On the other hand, niosomes are vesicles formed by the self-assembly of nonionic surfactants in aqueous media resulting in

Received: April 21, 2016
Revised: July 28, 2016
Accepted: August 10, 2016
Published: August 10, 2016

DOI: 10.1021/acs.iecr.6b01552
Ind. Eng. Chem. Res. 2016, 55, 9164−9175

Table 1. Plackett–Burman Fractional Factorial Design: Responses, Levels, and Factors

response code	meaning
Y_1	*Z*-average size of PC liposomes
Y_2	PDI of PC liposomes

	factors											
	formulation			injection			evaporation		sonication			
level	O/A (X_1)	C (X_2) (g/L)	I (X_3) (mM)	Q_V (X_4) (mL/h)	T_I (X_5) (°C)	N_S (X_6) (rpm)	T_E (X_7) (°C)	N_R (X_8) (rpm)	A (X_9) (%)	t (X_{10}) (min)		
−1	5:50	2.5	10	50	30	350	35	30	25	15		
1	20:50	6.0	150	215	60	900	60	120	42	30		
batch	X_1	X_2	X_3	X_4	X_5	X_6	X_7	X_8	X_9	X_{10}	Y_1	Y_2
PB1	1	1	−1	−1	−1	−1	1	−1	1	1	90	0.254
PB2	1	−1	−1	1	−1	1	1	1	1	−1	93	0.129
PB3	−1	−1	−1	−1	−1	−1	1	1	−1	−1	97	0.152
PB4	1	−1	1	−1	1	0	1	−1	1	−1	72	0.205
PB5	−1	1	−1	1	−1	−1	1	−1	−1	1	258	0.413
PB6	1	1	1	1	−1	−1	−1	1	−1	−1	102	0.176
PB7	−1	−1	1	1	−1	−1	−1	−1	1	1	84	0.218
PB8	1	−1	−1	1	1	1	−1	1	−1	1	106	0.240
PB9	−1	−1	−1	−1	1	1	−1	1	1	1	71	0.229
PB10	1	−1	1	−1	−1	−1	−1	−1	−1	1	81	0.141
PB11	−1	1	1	−1	1	−1	1	1	−1	1	152	0.316
PB12	1	1	1	1	1	1	1	1	1	1	65	0.260
PB13	−1	−1	1	1	1	1	1	−1	−1	−1	87	0.189
PB14	−1	1	1	−1	−1	1	−1	1	1	−1	115	0.273
PB15	1	1	−1	−1	1	1	−1	−1	−1	−1	113	0.199
PB16	−1	1	−1	1	1	−1	−1	−1	1	−1	74	0.271

closed bilayer structures.[13,17,18] As liposomes, their formation process is a consequence of unfavorable interactions between surfactants and water molecules, and they can also entrap hydrophilic, lipophilic, and amphiphilic compounds.[19,20]

Niosomes exhibit a number of advantages over liposomes, such as higher stability, easy access to raw materials, lower toxicity, high compatibility with biological systems, non-immunogenicity, and versatility for surface modification.[20]

Cholesterol is commonly used as a membrane additive for nanovesicle preparation to improve vesicle stability, entrapment efficiency, and release under storage.[20] It increases vesicle size and rigidity, improving encapsulation efficiency, but at high concentrations, it can adversely affect the encapsulation rate.[21,22] Cholesterol also plays a fundamental role in niosome formation when hydrophilic surfactants are used (hydrophilic/lipophilic balance of ∼10).[20]

More than 20 different methods have been identified for nanovesicle preparation, and these methods were recently reviewed.[23,24] In this work, a modified ethanol injection method (EIM) is used, because it offers some advantages over other methods, such as simplicity, absence of potentially harmful chemicals, and suitability for scaleup.[25]

The conventional EIM was first described in 1973.[26] In this technique, lipids/surfactants and additives are first dissolved in an organic solvent, such as diethyl ether or ethanol, and then injected slowly through a syringe into an aqueous phase containing the compound of interest. Then, the organic solvent is removed using a vacuum rotary evaporator. When ethanol is used as the organic solvent, the spontaneous formation of vesicles occurs as soon as the organic solution is in contact with the aqueous phase,[27] but vigorous agitation is needed to obtain narrow size distributions. For this purpose, a final sonication stage was applied in this study after organic-phase removal by vacuum evaporation.

However, a large number of variables are involved in this modified EIM, and selection of the most important of them (screening) is a crucial step in rationally preparing vesicles by this versatile method. In this work, the *Z*-average size and polydispersity index (PDI) were selected as the dependent variables. They are considered to be of great importance in nanovesicle design because most of the final applications of these vesicular systems are directly related to these two parameters. Factorial experimental design and the analysis of variance (ANOVA) methodology are appropriate and efficient statistical tools that permit the effects of several factors that influence responses to be studied by varying the factors simultaneously in a limited number of experiments.

In the recent past, design of experiments (DoE) has been extensively used for the study and optimization of vesicles and other similar organic materials. Different designs can be applied to reduce the number of factors involved in the preparation techniques[28] and, therefore, to minimize the number of experiments without losing valuable information. Plackett–Burman design is a type of fractional design involving relatively few runs,[29] commonly used for the screening of variables.

Another important role of DoE is in the optimization of nanovesicle composition for the enhancement of intended purposes. For instance, it has been applied to the formulation of liposomes (phospholipid and cholesterol ratio) for the topical delivery of vitamin E,[8] hybrid liposomes (with both low- and high-transition-temperature phospholipids) to improve the encapsulation and delivery of silymarin,[30] and niosomes for topical delivery applications.[10,31] DoE has also been used to enhance the transdermal flux of raloxifene hydrochloride[32] and diclofenac diethylamine[33] loaded transfersomes and of other polymeric nanoparticles encapsulating an anticancer drug.[34] Moreover, the interactions between vesicles and proteins, such as pectin, to improve drug-delivery properties has been studied by

DOI: 10.1021/acs.iecr.6b01552
Ind. Eng. Chem. Res. 2016, 55, 9164–9175

DoE.[35] Nanostructured lipid carriers (NLCs) loaded with flurbiprofen were also produced under optimal conditions using full factorial design.[36]

In this work, an initial fractional factorial design with two levels (Plackett−Burman) was used to screen the most important factors in vesicle preparation by the EIM. Then, a 2^3 two-level full factorial design using center-point replicates was applied to study the influence of the main factors and their interactions on the *Z*-average size and PDI. Once the appropriate operating conditions were determined, vesicle stability was studied by using multiple light scattering technology and by measuring the encapsulation efficiencies (EEs) of different compounds.

2. MATERIALS AND METHODS

2.1. Materials. Phosphatidylcholine (PC) (predominant species $C_{42}H_{80}NO_8P$, MW = 775.04 g/mol) from soybean (Phospholipon 90G) was a kind gift from Lipoid (Ludwigshafen, Germany). Sorbitan monostearate (Span 60, S60) ($C_{24}H_{46}O_6$, MW = 430.62 g/mol) and cholesterol (Cho) ($C_{27}H_{46}O$, MW = 386.65 g/mol) were purchased from Sigma-Aldrich (St. Louis, MO). All membrane components were dissolved in absolute ethanol (Sigma-Aldrich, St. Louis, MO).

Methanol, acetonitrile, 2-propanol, and acetic acid of high-performance liquid chromatography (HPLC) grade were supplied by Sigma-Aldrich (St. Louis, MO).

A phosphate buffer (PB) solution (10 mM, pH 7.4) was used in all experiments as the aqueous phase. The buffer solution was prepared in Milli-Q water by dissolving proper amounts of sodium dihydrogen phosphate and sodium hydrogen phosphate, supplied by Panreac (Barcelona, Spain). Sodium chloride from Panreac (Barcelona, Spain) was added to increase the ionic strength when required according to the experiments listed in Table 1. For the encapsulation experiments, Fat Red Bluish or Sudan Red 7B dye ($C_{24}H_{21}N_5$, MW = 379.46 g/mol) and cholecalciferol or vitamin D_3 ($C_{27}H_{44}O$, MW = 384.64 g/mol) were purchased from Sigma-Aldrich (St. Louis, MO).

2.2. Factorial Design of Experiments. Factors that could potentially affect the size of vesicles produced by the EIM were classified in four groups, according to the different steps involved in this preparation method: formulation (organic/aqueous phase volume ratio, phospholipid concentration, and ionic strength), injection (injection flow rate, temperature, and stirring speed), evaporation (temperature and rotation speed), and sonication (amplitude and time of sonication).

To identify the relative effects of variables on the response, a two-level fractional factorial design was used. A Plackett−Burman (P−B) resolution III design with $n = 16$ runs was proposed for screening of the initial factors. Two levels were selected for each variable.

Table 1 lists the factors and levels involved in the P−B fractional factorial design used, where O/A is the organic/aqueous phase volume ratio, C is the concentration of phospholipid, I is the ionic strength, Q_V is the injection flow rate, T_I is the injection temperature, N_S is the stirring speed during injection, T_E is the evaporation temperature, N_E is the evaporator rotation speed, A is the sonication amplitude, and t is the sonication time.

In a second step, a 2^3 full factorial design with center-point repetitions ($n = 5$) was carried out to study the main effects and interactions between factors previously selected by the screening design (Table 2). All other factors were fixed at certain values.

In both designs, mean diameter (*Z*-average size) and PDI were selected as response variables. Minitab statistical software (version 17) was used for all data analysis. Analysis of variance (ANOVA) was used for this purpose.

Once the models were obtained taking into account significant factors and interactions, a set of selected size-tuned vesicles were prepared and characterized.

Table 2. Full Factorial Design (2^3) with Center-Point Repetitions ($n = 5$): Factors, Levels, and Responses

response code	meaning
Y_1	*Z*-average size of PC liposomes
Y_2	PDI of PC liposomes
Y_3	*Z*-average size of S60:Cho niosomes
Y_4	PDI of S60:Cho niosomes

	factors		
level	O/A (X_1)	C (X_2) (g/L)	A (X_3) (%)
−1 (low)	5:50	2	30.0
0 (medium)	12.5:50	5	42.5
1 (high)	20:50	8	55.0

batch	X_1	X_2	X_3	Y_1	Y_2	Y_3	Y_4
FF1	1	−1	1	65	0.299	305	0.075
FF2	1	1	−1	97	0.249	362	0.136
FF3	−1	1	−1	149	0.296	294	0.206
FF4	−1	1	1	88	0.307	262	0.291
FF5	−1	−1	1	64	0.342	242	0.120
FF6	1	1	−1	100	0.257	360	0.143
FF7	1	1	1	64	0.272	241	0.182
FF8	−1	−1	−1	90	0.196	235	0.078
FF9	0	0	0	82	0.219	301	0.195
FF10	1	−1	−1	84	0.205	253	0.032
FF11	−1	1	1	107	0.297	276	0.235
FF12	−1	1	−1	156	0.308	275	0.145
FF13	1	−1	1	65	0.378	248	0.066
FF14	1	−1	−1	97	0.246	268	0.045
FF15	−1	−1	−1	84	0.173	239	0.094
FF16	0	0	0	75	0.224	305	0.253
FF17	0	0	0	84	0.250	317	0.118
FF18	1	1	1	55	0.307	224	0.203
FF19	0	0	−1	77	0.242	308	0.241
FF20	0	0	0	84	0.251	337	0.171
FF21	−1	−1	1	69	0.343	233	0.124

2.3. Vesicle Preparation. For liposome preparation, appropriate weighed amounts of PC were dissolved in different volumes of absolute ethanol (5−20 mL range). The same procedure was applied to niosome preparation by weighing and dissolving S60 and Cho in a 1:0.5 weight ratio. Then, the organic solution was injected, with a syringe pump (KD Scientific, Holliston, MA) at a flow rate of 120 mL/h, into Milli-Q water that was kept at 60 °C and stirred at 500 rpm. Once vesicles formed, ethanol was removed at 40 °C under reduced pressure (90 kPa) in a rotary evaporator. The resulting vesicular systems were further sonicated for 15 min (CY-500 sonicator, Optic Ivymen System, Biotech SL, Barcelona, Spain), using and amplitude of 30−55%, a power of 500 W, and a frequency of 20 kHz. The sonication probe was placed in a 100 mL glass beaker at a constant depth, 1.5 cm above the container bottom.

2.4. Vesicle Characterization. *2.4.1. Vesicle Size.* The *Z*-average size and PDI of vesicles were determined by dynamic light scattering (DSL) using a Zetasizer Nano ZS system (Malvern Instruments Ltd., Malvern, U.K.). Three independent samples were taken from each formulation, and measurements

DOI: 10.1021/acs.iecr.6b01552
Ind. Eng. Chem. Res. 2016, 55, 9164−9175

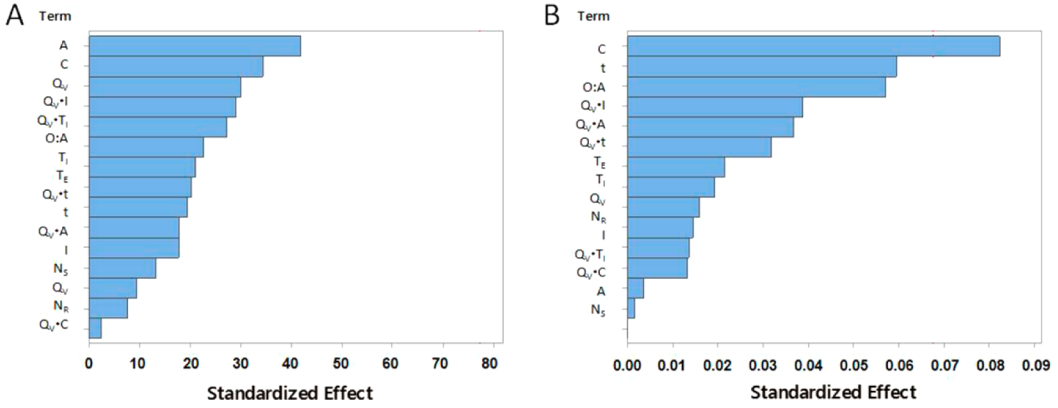

Figure 1. Pareto chart of the standardized effects of independent variables (factors) on the (A) *Z*-average size and (B) PDI of PC liposomes for the Plackett−Burman fractional factorial design.

were performed three times at room temperature without dilution.

2.4.2. Vesicle Morphology. Morphological analysis of vesicles was carried out by negative staining transmission electron microscopy (NS-TEM), using a JEOL-2000 Ex II transmission electron microscope (Tokyo, Japan). A sample drop was placed on a carbon-coated copper grid, and excess sample was removed with filter paper. Then, a drop of 2% (w/v) phosphotungstic acid (PTA) solution was applied to the carbon grid and allowed to stand for 1 min. Once the excess staining agent had been removed with filter paper, the sample was air-dried, and the thin film of stained and fixed vesicles was observed with the transmission electron microscope.

2.4.3. Vesicle Stability. Vesicle stability was determined by measuring backscattering (BS) profiles in a Turbiscan Lab Expert apparatus (Formulaction, L'Union, France) provided with an aging station (Formulaction, L'Union, France).

Samples were placed in cylindrical glass test cells, and backscattered light was monitored at 30 °C as a function of time and cell height every 2 h for 7 days.

The optical reading head scans the sample in the cell, providing BS data every 40 μm in percentages relative to standards as a function of the sample height (in millimeters). These profiles build up a macroscopic fingerprint of the sample at a given time, providing useful information about changes in the size distribution or appearance of a creaming layer or a clarification front with time.[3,37,38]

2.4.4. Encapsulation Efficiency (EE). EE also provides useful information related to the stability of the vesicle membrane. Hydrophilic compounds are entrapped in aqueous compartments between bilayers, whereas lipophilic compounds are preferentially located within the surfactant or lipid bilayer.[39] Substances such as drugs, bioactive compounds, dyes, and nanomaterials incorporated into vesicles can also affect the morphology and stability of the final dispersion.

For the purpose of determining EEs, Sudan Red 7B and vitamin D_3 (hydrophobic compounds) were encapsulated in the two different formulations.

Each compound was analyzed by reverse-phase high-performance liquid chromatography (RP-HPLC) (HP series 1100 chromatograph, Hewlett-Packard, Palo Alto, CA). Before RP-HPLC analysis could be performed, the nonencapsulated compound had to be removed by passing the sample through a Sephadex G-25 column (GE Healthcare Life Sciences, Wauwatosa, WI). Then, both filtered and nonfiltered samples were diluted 1:10 (v/v) with methanol to facilitate vesicle rupture and to extract the encapsulated compound. EE was calculated according to the equation

$$\text{EE}\ (\%) = \frac{\text{peak area of filtered sample}}{\text{peak area of unfiltered sample}} \times 100 \quad (1)$$

The RP-HPLC system was equipped with an HP G1315A UV/vis absorbance detector (Agilent Technologies, Palo Alto, CA). The column was a Zorbax Eclipse Plus C18 column with a particle size of 5 μm, 4.6 mm × 150 mm (Agilent Technologies, Palo Alto, CA). The mobile phase consisted of a mixture of (A) 100% Milli-Q-water and (B) 100% methanol with gradient elution at 0.8 mL/min. The step gradient started with a mobile phase of 80% A, running 100% mobile phase B starting in minute 5 for 10 min. Mobile phase B was fed for 2 min after each injection to prepare the column for the next sample. The separation was carried out at 30 °C. Different wavelengths were used for the UV/vis detector, namely, 533 nm for Sudan Red 7B and 270 nm for vitamin D_3.

3. RESULTS AND DISCUSSION

3.1. Effects of Variables on Morphological Characteristics. The responses (*Z*-average size and PDI) of each batch from P−B design were measured by dynamic light scattering (DLS). The relative importance of the main effects on the *Z*-average size and PDI of PC liposomes are shown in the Pareto chart given in Figure 1.

Researchers must be aware of the confusion of main effects with two-factor interactions in this type of design (resolution III), where the alias structure is too complex. However, we decided to use the initial Plackett−Burman design only for screening purposes and selection of the main factors from the Pareto chart, as is usually accepted. Effects were selected by applying the hierarchical ordering principle, known sometimes as the sparsity-of-effects principle, where higher-order effects (three- or four-way interactions) are sacrificed to study lower-order effects (main effects first and two-way interactions next). This principle suggests that priority should be given to the estimation of lower-order effects, especially when resources (time and money) are scarce. This postulate is an empirical principle whose validity has been confirmed by the analysis of many real experiments.

According to these data, the most important variables for both responses are the organic/aqueous phase volume ratio, the (final aqueous-phase) phospholipid concentration, and the sonication amplitude. These results are in good agreement with previous studies carried out by Kremer et al.,[40] who evaluated the effects of

DOI: 10.1021/acs.iecr.6b01552
Ind. Eng. Chem. Res. 2016, 55, 9164−9175

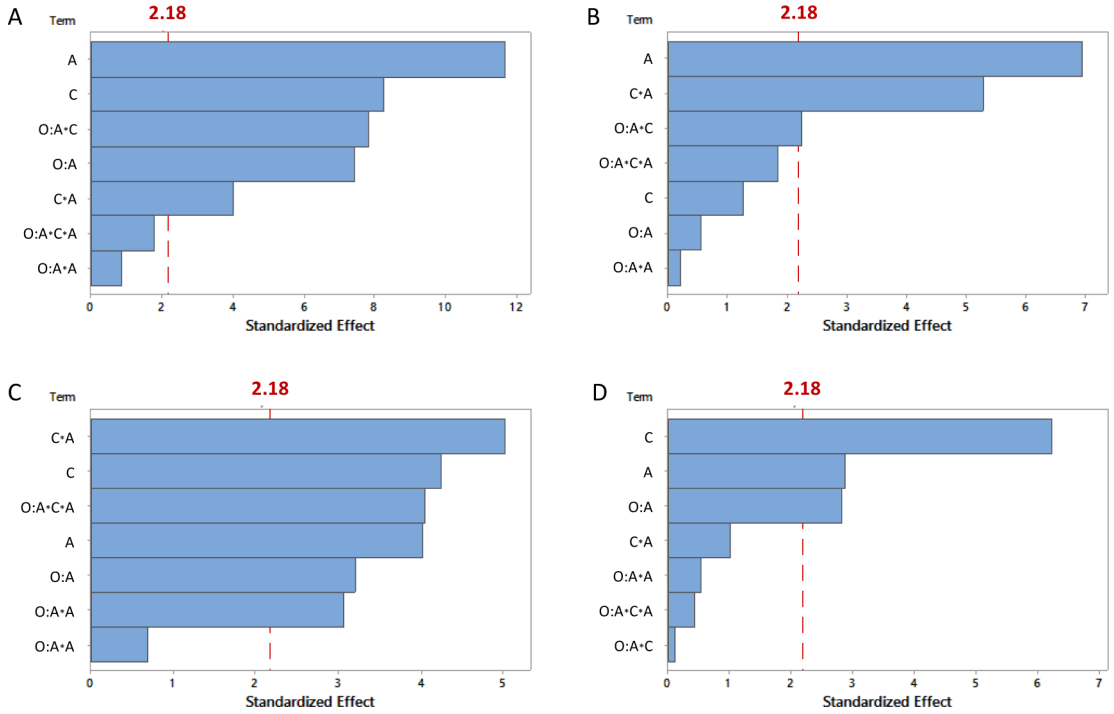

Figure 2. Pareto chart of the standardized effects of independent variables (factors) on the (A,C) *Z*-average size and (B,D) PDI of (A,B) PC liposomes and (C,D) S60:Cho niosomes (1:0.5, w/w) for the 2^3 full factorial design.

some preparation variables on the size and polydispersity of liposomes made from two different natural phosphatidylcholines. Their experimental results showed that the most important factor in the final size of the liposomes was the lipid concentration in the alcohol injected into the buffer solution. This factor corresponds to the interaction of the lipid amount and the flow rate of organic solvent injected, two factors present in the Pareto chart in Figure 1. The same explanation was postulated by other authors,[8,41,42] confirming that the lipid concentration clearly affects the liposome size. This factor was found to be the most relevant one for controlling morphological characteristics of phosphatidylcholine liposomes. Szoka[43] found that stirring, ionic strength, and temperature of the aqueous phase could also contribute to the final size, but the effects of these factors were smaller than those observed for lipid concentration, organic/aqueous phase ratio, and chemical nature of the organic solvent (a parameter not included in our study). Therefore, the experimental results in Figure 1 confirm the previously reported observations.[43]

The ethanol injection method is usually chosen because it avoids the sonication step, which is needed in several other methods of liposome preparation, such as the thin-film hydration method. Preliminary experiments (data not shown) indicated that sonication is a crucial step for reducing the size of both liposomes and niosomes. Alternatively, small vesicles can be produced without sonication by using low concentrations of lipids/surfactants, but with low yield. This is why we decided to include this step as a factor in the present study.

3.2. PC Liposomes. The first three main effects from the Pareto chart obtained for the P−B design were selected for the 2^3 full factorial design. The ANOVA results for *Z*-average size and PDI values are listed in Tables S1 and S2 (Supporting Information), respectively, whereas the corresponding Pareto chart is shown in Figure 2. Mean sizes in the range of 55−156 nm with PDI values between 0.173 and 0.378 were obtained for PC liposomes (with standard deviations ranging from 0.304 to 4.40 nm for size and from 0.003 to 0.053 for PDI). Similar size ranges were also obtained using the EIM in other previously reported studies.[22,27,41,43,44]

The normality, variance homogeneity, and randomness assumptions were tested with a normal probability plot, frequency histogram, and residuals versus fits and residuals versus order plots, respectively (Supporting Information, Figure S2).

No clear aberrant tendencies were observed, because the residuals tended to form a line, no typical cornet pattern was observed, and no time-based pattern was detected. Only some outlier values were detected (Cook's distance and DFITS values are given in Table S3 of the Supporting Information).

The ANOVA results allowed for an analysis of the contributions of the effects of the independent variables on the response function (mean size of PC liposomes). In this case, significant two-way interactions were identified: (O/A) × *C* and *C* × *A* (see Figure 3). Larger sizes are reached when the organic solution has a higher lipid concentration (more than 20 g/L). On the other hand, the *C* × *A* interaction reveals that the degree of size reduction upon application of a higher amplitude depends on the total lipid concentration present in the medium (referred to the final volume of the dispersion).

All of the main effects are significant ($p < 0.05$), with a positive effect on the mean size (a higher response value with an increase in the factor level) for the total lipid concentration and a negative effect (a lower response value with a decrease in factor level) for the organic/aqueous phase volume ratio and the sonication amplitude.

These effects can be explained according to a previously reported vesicle formation model.[45−47] This model relies on the formation of vesicles through intermediate structures, such as phospholipid bilayer fragments and sheet-like micelles. These

DOI: 10.1021/acs.iecr.6b01552
Ind. Eng. Chem. Res. 2016, 55, 9164−9175

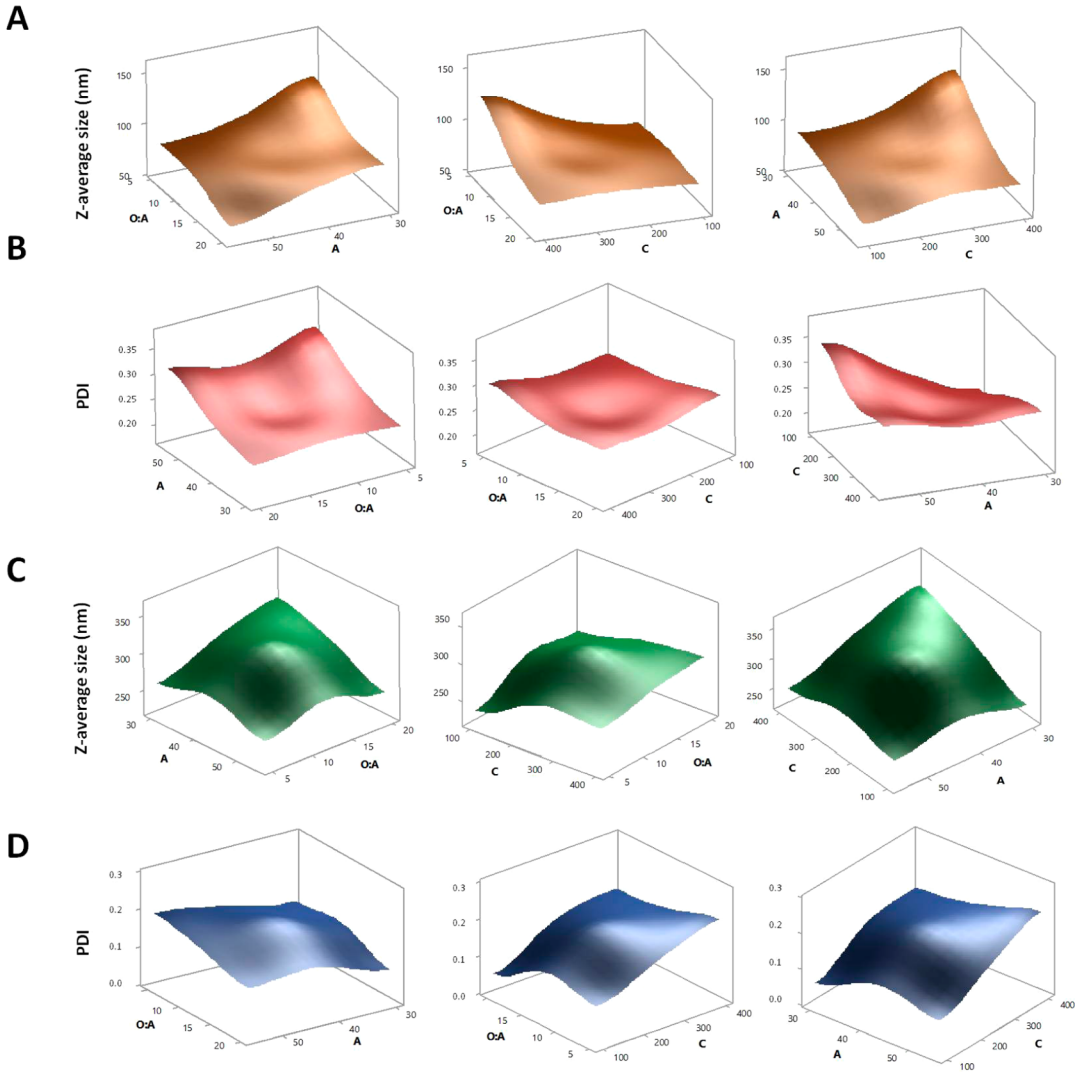

Figure 3. Three-dimensional (3D) response surface plots for the factors O/A (organic/aqueous phase volume ratio), C (lipid or surfactant/stabilizer concentration, g/L), and A (sonication amplitude, %) for the (A,C) *Z*-average size and (B,D) PDI of (A,B) PC liposomes and (C,D) S60:Cho niosomes (1:0.5, w/w).

intermediates are the result of amphiphilic self-assembly because of their characteristic physicochemical properties.[48]

During the injection of ethanol droplets into the aqueous phase, lipid reorganization inside these dispersed droplets to form bilayers is favored by the fact that lipids energetically prefer a parallel molecular arrangement.[45] These planar structures give rise to closed vesicles when their size induces enough surface tension to close the structure and minimize the bending energy.

The sizes of these intermediates depend directly on the number of lipid molecules (concentration) and the dispersion degree (solubilization) in the organic phase. It is obvious from the previous assessment that higher concentrations of lipids in the droplets will form higher membrane fragments, as our experimental results and previous observations confirm.[8,40−42]

It is also important to know how easily lipid droplets are dispersed, as well as their size and homogeneity. Lipids of higher solubility will then form smaller lipid droplets and, consequently, shorter membrane fragments (and ultimately tiny vesicles).[40] This explains, in a simplified way, why higher organic/aqueous phase ratios yield smaller liposomes.

The negative effect of the sonication amplitude is explained by vesicle rupture, which takes place when an excess of energy is applied to vesicles during the sonication process as a result of the effect of induced cavitation.[49,50] The final effect of ultrasounds can be controlled by varying the input power, ultrasound frequency, sonication time, and probe depth into the container. As frequency increases, liposomes of smaller size are produced as a result of stronger acoustic cavitation events. This assumption was confirmed by our results, in accordance with previous studies.[49,50] It is important to point out that, to minimize the effects of variations in the probe depth, this factor was kept constant at 1.5 cm above the container bottom.

Another aspect to be taken into consideration is the effect of sonication time. It was reported by Silva et al.[49] that sonication time plays an important role in decreasing vesicle size, although they observed that this effect reached a plateau at about 21 min. Our P−B design revealed a positive effect of sonication time on the *Z*-average size (from 15 to 30 min), although it was weaker than the effects of the other variables selected for the 2^3 full factorial design (especially sonication amplitude). A similar influence was observed for the PDI response, but with a stronger effect. We preferred to select sonication amplitude instead of sonication time because one of the goals of controlling factors is to obtain a narrow size distribution.

DOI: 10.1021/acs.iecr.6b01552
Ind. Eng. Chem. Res. 2016, 55, 9164−9175

Table 3. Estimated Coded Coefficients for the Considered Effects on the *Z*-Average Size and PDI of PC Liposomes and S60:Cho Niosomes (1:0.5, w/w)

	coefficients[a]								
response	constant	X_1	X_2	X_3	X_1X_2	X_1X_3	X_2X_3	$X_1X_2X_3$	R^2
				Z-Average Size					
liposome (Y_1)	89.68	−11.14	12.40	−17.50	−11.75	–	−5.97	–	96.69
niosome (Y_3)	269.82	12.72	16.87	−15.94	–	−12.15	−19.92	−16.04	91.27
				PDI					
liposome (Y_2)	0.280	–	–	0.038	−0.012	–	−0.029	–	89.35
niosome (Y_4)	0.136	−0.026	0.057	0.026	–	–	–	–	84.73

[a] X_1, organic/aqueous phase volume ratio; X_2, PC or S60:Cho concentration (g/L); X_3, sonication amplitude (%).

As the design included a center point with several repetitions ($n = 5$), the presence of curvature in the response variables could be tested (Figure 3). Because curvature seemed to be significant ($p < 0.05$), a term involving center point (Ct Pt) was included in the equations for its estimation.

With all of this information about the effects and their estimated coefficients, the following equation ($R^2 = 96.69\%$) for the *Z*-average size value of PC liposomes (Y_1) was generated

$$Y_1 = 62.8 + 2.55(\mathrm{O/A}) + 0.449C - 0.185A - 0.0185(\mathrm{O/A}) \times C - 0.00555C \times A - 9.26(\mathrm{Ct\,Pt}) \quad (2)$$

Different behavior was observed regarding PDI, which was strongly affected by the sonication amplitude as the only significant main effect and its interaction with the total lipid amount. The O/A × C interaction was also detected, but with a lower effect on the PDI response.

To understand the $C \times A$ interaction, it is important to take into account the effect of the sonication amplitude as the main effect. An increase in this factor leads to a less monodisperse size distribution, that is, higher PDI values. However, according to the interaction, this response depends highly on the total amount of lipids present in the sample. At a low level of the lipid amount, the reduction in size is more effective (as previously mentioned), but the size distribution is large. However, at a high level of the lipid amount, this enlargement of the size distribution is significantly lower.

Curvature in the response was also tested, again revealing a significant presence ($p < 0.05$). For the PDI response (Y_2), the following equation with an R^2 value of 89.35% was obtained

$$Y_2 = -0.160 + 0.00939A - 0.0000420(\mathrm{O/A}) \times C - 0.0000250C \times A - 0.0425(\mathrm{Ct\,Pt}) \quad (3)$$

These equations were formulated with uncoded coefficients, making it easier to use them to predict selected target size and PDI values.

3.3. S60:Cho Niosomes. To investigate whether the selected factors in the P−B design for PC liposomes (a reference model for vesicular systems) produced similar effects with other different formulations, the same 2^3 full factorial design using center-point replicates was performed for a typical niosome formulation, in this particular case, S60:Cho niosomes (1:0.5, w/w). The main variables were the organic/aqueous phase volume ratio (O/A), the total concentration of surfactant and stabilizer (C), and the sonication amplitude (A).

The ANOVA results for *Z*-average size and PDI values are listed in Table S1 (Supporting Information), and the corresponding Pareto chart and three-dimensional surface plot are shown in Figures 2 and 3, respectively. Mean sizes in the range of 224−362 nm with PDI values between 0.032 and 0.291 were obtained for S60:Cho niosomes (with standard deviations ranging from 1.05 to 7.28 nm for size and from 0.009 to 0.052 for PDI). Similar size and PDI ranges were reported for niosomes prepared by the EIM using Span 60 as the membrane component.[17]

Two-way interactions (O/A × A, $C \times A$) and a three-way interaction (O/A × $C \times A$) were detected, with sonication amplitude (A) as the common factor in these interactions (see Figure 2C). Therefore, it can be postulated that sonication amplitude is the key factor in the niosome size response. The response depends on both the O/A and C factor levels, with a higher interaction between the sonication amplitude and the total amount of membrane components. Differences in the magnitude of the coefficient of this factor between liposomes and niosomes can be attributed to the initial size before sonication (smaller for liposomes) and vesicle stability.[50]

The three main effects are significant, but in contrast to the case for liposomes, the organic/aqueous phase volume ratio (O/A) shows a positive effect on niosome size. This behavior could be due to different molecular features of the surfactant and stabilizer that result in different interactions with the organic phase and, therefore, poor or insufficient solubility.

The other two variables (C, A) have effects similar to those described above for liposomes. Therefore, the same explanation regarding surfactant concentration and sonication amplitude can be applied here to justify their effects on niosome size. In this case, the stronger effect of C is explained by the influence of cholesterol on the final size of vesicles, as reported by Padamwar and Pokharkar.[8]

Once again, curvature was detected for the *Z*-average size response. The following equation was obtained to model this case, with an adjusted correlation coefficient (R^2) of 91.27%

$$Y_3 = 236.9 - 4.31(\mathrm{O/A}) - 0.012C - 0.56A + 0.0461(\mathrm{O/A}) \times C + 0.00363C \times A - 0.00114(\mathrm{O/A}) \times C \times A + 44.00(\mathrm{Ct\,Pt}) \quad (4)$$

On the other hand, a completely different behavior was observed regarding the PDI response. Only the three main effects (O/A, C, A) were found to be significant, and no interactions were found. Two positive effects on the niosome PDI were detected: surfactant/stabilizer concentration and sonication amplitude. In this case, the total concentration of membrane components seemed to have an important role in the vesicle size distribution, as can be seen in the correspondent Pareto chart (Figure 2). This observation once again can be attributed to the solubilization of membrane components in the organic phase. Higher concen-

DOI: 10.1021/acs.iecr.6b01552
Ind. Eng. Chem. Res. 2016, 55, 9164−9175

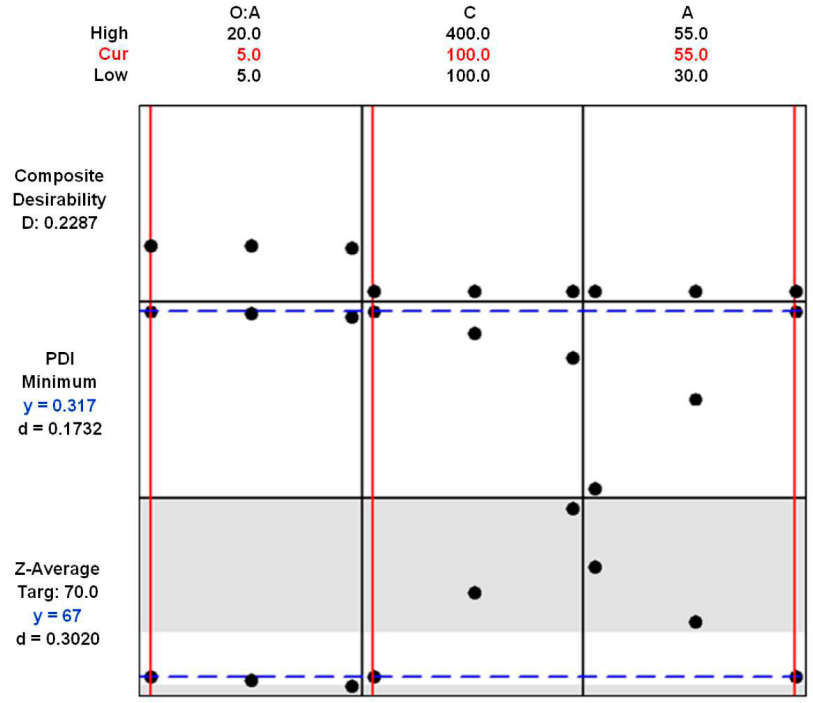

Parameters

Response	Goal	Lower	Target	Upper	Weight	Importance
Z-Average PC-Liposomes	Target	65	70.000	75.000	1	1
PDI PC-Liposomes	Minimum		0.173	0.378	1	1

Solution

Solution	O:A	C	A	Z-Average PC-Liposomes Fit	PDI PC-Liposomes Fit	Composite Desirability
1	5	100	55	67	0.317	0.2287

Response	Fit	SE Fit	95% CI	95% PI
Z-Average PC-Liposomes	67	4	(57, 76)	(51, 83)
PDI PC-Liposomes	0.317	0.013	(0.308, 0.377)	(0.284, 0.402)

Figure 4. Optimization plot and values of individual (d) and composite (D) desirability provided by the response optimizer (Minitab, version 17) for an example of size-tuned PC liposome (desired size = 70 nm, with a minimum PDI value).

trations of these components require better solubilization in dispersed droplets to reach small membrane fragments.

It is important to note that some combinations of factors yielded narrow size distributions, namely, PDI $\leq$ 0.100, a value frequently obtained by other preparation methods, such as microfluidic hydrodynamic focusing[51] also using S60:Cho as the formulation.

A negative effect was detected for the organic/aqueous phase volume ratio (O/A). As the final concentration of ethanol increased during the injection process, a smaller size distribution was obtained. As previously mentioned, no interaction between this factor and the total concentration of membrane components was observed.

The following equation with an R^2 value of 84.73% was obtained for the niosome PDI model response (Y_4)

$$Y_4 = 0.053 - 0.00392(\mathrm{O/A}) + 0.000039C + 0.00067A + 0.0597(\mathrm{Ct\ Pt}) \quad (5)$$

The estimated coded coefficients for the considered effects on the Z-average sizes and PDIs of PC liposomes and S60:Cho niosomes are listed in Table 3, as a summary of the factors' influence. Coded coefficients were used to maintain the orthogonality of the designs and to allow for a direct comparison between coefficients.

3.4. Vesicle Characterization. Size-tuned vesicles were prepared under selected operating conditions by applying the models obtained from the experimental design (eqs 2−5) and the assistance of the response optimizer and response predictor in Minitab statistical software (version 17). These tools can be applied to the simultaneous optimization of several responses only when the same set of factors are studied separately, because a common experimental region is needed.

The operating conditions were selected to prepare PC liposomes with a mean size of 70 nm and the minimum PDI value (predicted values of $Y_1 = 67 \pm 4$ and $Y_2 = 0.317 \pm 0.013$) and S60-Cho niosomes with a mean size of 240 nm and the

DOI: 10.1021/acs.iecr.6b01552
Ind. Eng. Chem. Res. 2016, 55, 9164−9175

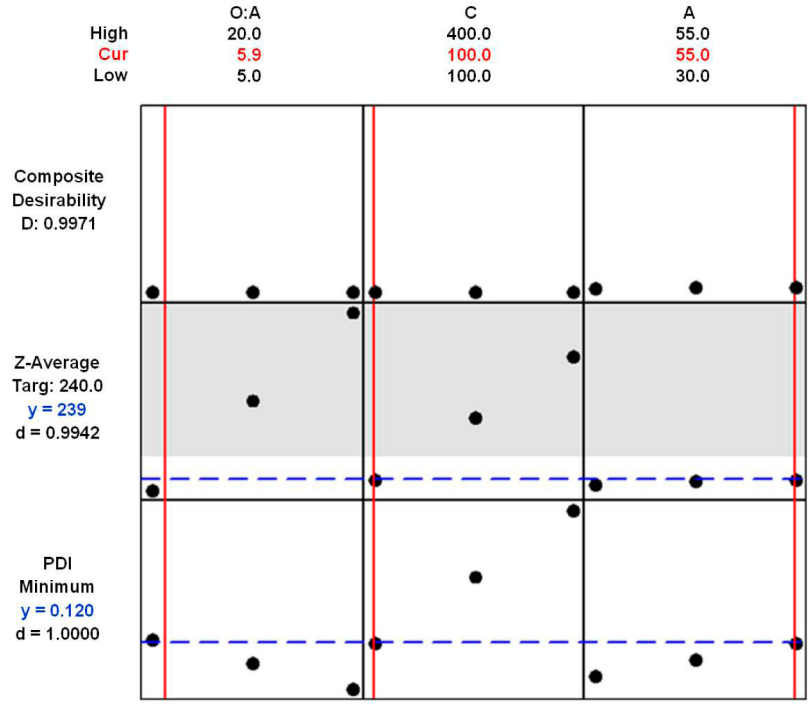

Parameters

Response	Goal	Lower	Target	Upper	Weight	Importance
Z-Average S60:Cho Niosomes	Target	235	240.000	245.000	1	1
PDI S60:Cho Niosomes	Minimum		0.120	0.291	1	1

Solutions

Solution	O:A	C	A	PDI S60:Cho Niosomes Fit	Z-Average S60:Cho Niosomes Fit	Composite Desirability
1	5.9	100	55	0.120	239	0.9971

Response	Fit	SE Fit	95% CI	95% PI
Z-Average S60:Cho Niosomes	239	11	(217, 263)	(198, 281)
PDI S60:Cho Niosomes	0.120	0.025	(0.066, 0.172)	(0.024, 0.214)

Figure 5. Optimization plot and values of individual (d) and composite (D) desirability provided by the response optimizer (Minitab, version 17) for an example of size-tuned S60:Cho niosome (1:0.5 w/w) (desired size = 240 nm, with a minimum PDI).

minimum PDI value (predicted values of $Y_3 = 239 \pm 11$ and $Y_4 = 0.120 \pm 0.025$). These sizes and PDI values were selected only as an example. The factor output values were O/A = 5:50, C = 2 g/L, and A = 55% for the liposomes and O/A = 5.9:50, C = 2 g/L, and A = 55% for the niosomes. Figures 4 and 5 show optimization plots and values of individual and composite desirability for size-tuned liposomes and size-tuned niosomes, respectively.

The experimental results showed that the models obtained with the experimental design were accurate, because mean sizes of 69 ± 0.5 nm (PDI = 0.245 ± 0.005) and 233 ± 3 nm (PDI = 0.112 ± 0.004) were obtained for the PC liposomes and S60:Cho niosomes, respectively. The relative error was low for the experimental results regarding mean size (3% for Y_1 and Y_3) but higher for the size distributions (22% for Y_2 and 7% for Y_4).

The sizes and morphologies of the vesicles were investigated by TEM, using a negative contrast. Figure 6 shows black-stained vesicles, as a result of the interactions of the electron beam with PTA, which produces a selective deposit of metal ions that enhances morphological details. The micrographs show spherical structures of approximately 80 nm for the liposomes (Figure 6C) and about 250 nm for the niosomes (Figure 6D). These values agree with the DLS measurements.

Figure 6D shows clusters of niosomes that are all similar in size. Aggregation arose during the drying step prior to TEM measurements, because no flocculation phenomena were monitored with the Turbiscan apparatus.

Slight differences were noticed in the zeta potential measurements, exhibiting low values for both types of vesicles. Niosomes had values of about -16.8 ± 0.7 mV, whereas the liposomes had values of -6.9 ± 0.3 mV. This small value for the liposomes could be due to neutralization of the negative charge from the

DOI: 10.1021/acs.iecr.6b01552
Ind. Eng. Chem. Res. 2016, 55, 9164−9175

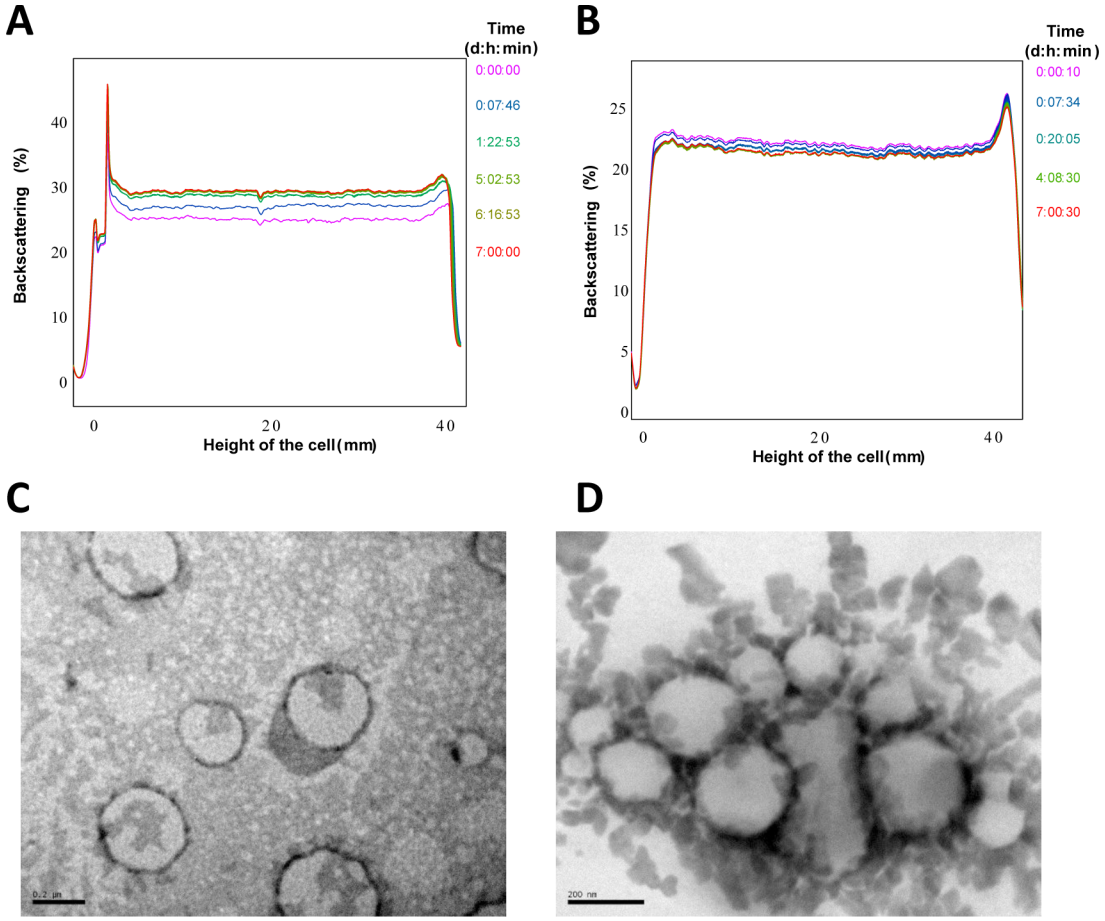

Figure 6. (A,B) BS profiles and (C,D) TEM micrographs of empty vesicles designed with a controlled size and PDI values by applying the models obtained from experimental design: (A,C) PC liposomes and (B,D) S60:Cho niosomes (1:0.5, w/w).

phosphate groups by sodium cations present in the medium (from sodium chloride in the PB solution).

The formulated vesicles exhibited a high stability after 1 week of monitoring time. BS profiles obtained for the PC liposomes are given in Figure 6, where a variation of 4.5% in the middle part of the cell (from 10 to 30 mm) is noticed. A simultaneous slight clarification process was observed in the middle and top parts of the cell in the corresponding transmission profile (results not shown). This was promoted by some movement of the PC liposomes toward the bottom of the cell, resulting in a slight increase in BS (sedimentation). However, this was a reversible process, caused by differences in concentration, with the sample remaining stable and maintaining its initial properties (size and PDI). The vesicles were again characterized after gentle agitation of the cell at the end of the monitoring time with analogous results.

For the S60:Cho niosomes (Figure 6B), the BS profile remained nearly constant (variations of approximately 0.5%) with time, showing high stability. Some variation was also observed in the transmission profile all along the cell height, because the sample was not translucent.

3.4.1. Encapsulation Efficiency (EE). Vesicles containing Sudan Red 7B and vitamin D_3 as model compounds (both lipophilic) were also prepared and characterized. No differences were observed regarding mean size and PDI values or TEM, zeta potential, or Turbiscan measurements, meaning that the entrapped compounds did not affect the vesicle's behavior.

High EE values were obtained for both Sudan Red 7B and vitamin D_3, as expected taking into account their hydrophobic character. EE values up to 90.1% and 88.0% were obtained for Sudan Red 7B encapsulated in PC liposomes and S60:Cho niosomes, respectively. Experiments carried out with vitamin D_3 led to EE values of 99.2% for PC liposomes and 73.9% for S60:Cho niosomes. These results are in good agreement with those of previous studies, where compounds with similar chemical properties were encapsulated.[12,13,27]

4. CONCLUSIONS

In this work, an adequate approximation using DoE was applied to study the influence of experimental factors of the EIM on the mean size and size distribution of PC liposomes and S60:Cho niosomes (1:0.5, w/w).

An initial screening design enabled a reduction of the number of variables. This was a necessary step before carrying out a full factorial design. Finally, response models were applied to prepare selected size-tuned nanovesicles, which were characterized from a stability point of view.

This was achieved with a low number of experiments (58 runs). This methodology enabled two different formulations (liposomes and niosomes, the most common types of nanovesicles) to be studied in a comparative way. Stable liposomes and niosomes of the targeted sizes were successfully prepared with the model equations obtained, with encapsulation efficiencies higher than 73.9% in all cases for selected hydrophobic compounds.

DOI: 10.1021/acs.iecr.6b01552
Ind. Eng. Chem. Res. 2016, 55, 9164−9175

The most important variables identified by ANOVA were the organic/aqueous phase volume ratio, the (final aqueous-phase) phospholipid concentration, and the sonication amplitude.

These results offer new insights into the mechanism and effects of the factors involved in nanovesicle preparation by the EIM, one of the most easily scaled-up methods for preparing vesicles for several fields of interest.

■ ASSOCIATED CONTENT

Supporting Information

The Supporting Information is available free of charge on the ACS Publications website at DOI: 10.1021/acs.iecr.6b01552.

ANOVA results for *Z*-average size and PDI of PC liposomes for the 2^3 full factorial design; Cook's distances and DFITS values for each response in the full factorial designs; optimization contour plot for the factors studied in the full factorial design for both responses; testing for normality, variance homogeneity, and randomness assumptions of ANOVA for the full factorial design (PDF)

■ AUTHOR INFORMATION

Corresponding Author

*Tel.: +34 985103509. E-mail: cpazos@uniovi.es.

Notes

The authors declare no competing financial interest.

■ ACKNOWLEDGMENTS

This work was supported by the Ministerio de Economía y Competitividad (MINECO, Spain), under Grant MINECO-13-CTQ2013-47396-R. This study was also cofinanced by the Consejería de Educación y Ciencia del Principado de Asturias (ref FC-04-COF-50-MEC, PCTI Asturias 2006-2009, ref EQP06-024, and FC15-GRUPIN14-022). We especially thank Prof. Antonia Salas (University of Oviedo) for her advice with the statistical work.

■ REFERENCES

(1) Capretto, L.; Carugo, D.; Mazzitelli, S.; Nastruzzi, C.; Zhang, X. Microfluidic and lab-on-a-chip preparation routes for organic nanoparticles and vesicular systems for nanomedicine applications. *Adv. Drug Delivery Rev.* **2013**, *65*, 1496−1532.

(2) Rongen, H. A. H.; Bult, A.; van Bennekom, W. P. Liposomes and immunoassays. *J. Immunol. Methods* **1997**, *204*, 105−133.

(3) Pando, D.; Gutiérrez, G.; Coca, J.; Pazos, C. Preparation and characterization of niosomes containing resveratrol. *J. Food Eng.* **2013**, *117*, 227−234.

(4) Gómez-Hens, A.; Fernández-Romero, J. M. The role of liposomes in analytical processes. *TrAC, Trends Anal. Chem.* **2005**, *24*, 9−19.

(5) Edwards, K. A.; Bolduc, O. R.; Baeumner, A. J. Miniaturized bioanalytical systems: enhanced performance through liposomes. *Curr. Opin. Chem. Biol.* **2012**, *16*, 444−452.

(6) Liu, Q.; Boyd, B. J. Liposomes in biosensors. *Analyst* **2013**, *138*, 391−409.

(7) Canton, I.; Battaglia, G. Endocytosis at the nanoscale. *Chem. Soc. Rev.* **2012**, *41*, 2718−39.

(8) Padamwar, M. N.; Pokharkar, V. B. Development of vitamin loaded topical liposomal formulation using factorial design approach: Drug deposition and stability. *Int. J. Pharm.* **2006**, *320*, 37−44.

(9) Taha, E. I. Lipid vesicular systems: formulation optimization and ex vivo comparative study. *J. Mol. Liq.* **2014**, *196*, 211−216.

(10) Abdelbary, A. A.; AbouGhaly, M. H. H. Design and optimization of topical methotrexate loaded niosomes for enhanced management of psoriasis: Application of Box−Behnken design, in-vitro evaluation and in-vivo skin deposition study. *Int. J. Pharm.* **2015**, *485*, 235−243.

(11) Jadhav, S. M.; Morey, P.; Karpe, M.; Kadam, V. Novel vesicular system: An overview. *J. Appl. Pharm. Sci.* **2012**, *02*, 193−202.

(12) Rajera, R.; Nagpal, K.; Singh, S. K.; Mishra, D. N. Niosomes: a controlled and novel drug delivery system. *Biol. Pharm. Bull.* **2011**, *34*, 945−53.

(13) Uchegbu, I. F.; Vyas, S. P. Non-ionic surfactant based vesicles (niosomes) in drug delivery. *Int. J. Pharm.* **1998**, *172*, 33−70.

(14) Bangham, A. D.; Standish, M. M.; Watkins, J. C. Diffusion of univalent ions across the lamellae of swollen phospholipids. *J. Mol. Biol.* **1965**, *13*, 238−252.

(15) da Silva Malheiros, P.; Daroit, D. J.; Brandelli, A. Food applications of liposome-encapsulated antimicrobial peptides. *Trends Food Sci. Technol.* **2010**, *21*, 284−292.

(16) du Plessis, J.; Weiner, N.; Müller, D. G. The influence of in vivo treatment of skin with liposomes on the topical absorption of a hydrophilic and a hydrophobic drug in vitro. *Int. J. Pharm.* **1994**, *103*, R1−R5.

(17) Manconi, M.; Sinico, C.; Valenti, D.; Loy, G.; Fadda, A. M. Niosomes as carriers for tretinoin I: Preparation and properties. *Int. J. Pharm.* **2002**, *234*, 237−248.

(18) Manca, M. L.; Manconi, M.; Nacher, A.; Carbone, C.; Valenti, D.; Maccioni, A. M.; Sinico, C.; Fadda, A. M. Development of novel diolein−niosomes for cutaneous delivery of tretinoin: Influence of formulation and in vitro assessment. *Int. J. Pharm.* **2014**, *477*, 176−186.

(19) Mahale, N. B.; Thakkar, P. D.; Mali, R. G.; Walunj, D. R.; Chaudhari, S. R. Niosomes: Novel sustained release nonionic stable vesicular systems — An overview. *Adv. Colloid Interface Sci.* **2012**, *183*−*184*, 46−54.

(20) Moghassemi, S.; Hadjizadeh, A. Nano-niosomes as nanoscale drug delivery systems: An illustrated review. *J. Controlled Release* **2014**, *185*, 22−36.

(21) Mali, N.; Darandale, S.; Vavia, P. Niosomes as a vesicular carrier for topical administration of minoxidil: formulation and in vitro assessment. *Drug Delivery Transl. Res.* **2013**, *3*, 587−592.

(22) Fan, M.; Xu, S.; Xia, S.; Zhang, X. Preparation of salidroside nanoliposomes by ethanol injection method and in vitro release study. *Eur. Food Res. Technol.* **2008**, *227*, 167−174.

(23) Marianecci, C.; Di Marzio, L.; Rinaldi, F.; Celia, C.; Paolino, D.; Alhaique, F.; Esposito, S.; Carafa, M. Niosomes from 80s to present: The state of the art. *Adv. Colloid Interface Sci.* **2014**, *205*, 187−206.

(24) Akbarzadeh, A.; Rezaei-Sadabady, R.; Davaran, S.; Joo, S. W.; Zarghami, N.; Hanifehpour, Y.; Samiei, M.; Kouhi, M.; Nejati-Koshki, K. Liposome: classification, preparation, and applications. *Nanoscale Res. Lett.* **2013**, *8*, 102.

(25) Justo, O. R.; Moraes, Â. M. Analysis of process parameters on the characteristics of liposomes prepared by ethanol injection with a view to process scale-up: Effect of temperature and batch volume. *Chem. Eng. Res. Des.* **2011**, *89*, 785−792.

(26) Batzri, S.; Korn, E. D. Single bilayer liposomes prepared without sonication. *Biochim. Biophys. Acta, Biomembr.* **1973**, *298*, 1015−1019.

(27) Pham, T. T.; Jaafar-Maalej, C.; Charcosset, C.; Fessi, H. Liposome and niosome preparation using a membrane contactor for scale-up. Colloid. *Colloids Surf., B* **2012**, *94*, 15−21.

(28) Loukas, Y. L. Experimental studies for screening the factors that influence the effectiveness of new multicomponent and protective liposomes. *Anal. Chim. Acta* **1998**, *361*, 241−251.

(29) Shah, S. R.; Parikh, R. H.; Chavda, J. R.; Sheth, N. R. Application of Plackett−Burman screening design for preparing glibenclamide nanoparticles for dissolution enhancement. *Powder Technol.* **2013**, *235*, 405−411.

(30) El-Samaligy, M. S.; Afifi, N. N.; Mahmoud, E. A. Increasing bioavailability of silymarin using a buccal liposomal delivery system: Preparation and experimental design investigation. *Int. J. Pharm.* **2006**, *308*, 140−148.

(31) Shaikh, K. S.; Chellampillai, B.; Pawar, A. P. Studies on nonionic surfactant bilayer vesicles of ciclopirox olamine. *Drug Dev. Ind. Pharm.* **2010**, *36*, 946−53.

DOI: 10.1021/acs.iecr.6b01552
Ind. Eng. Chem. Res. 2016, 55, 9164−9175

(32) Mahmood, S.; Taher, M.; Mandal, U. K. Experimental design and optimization of raloxifene hydrochloride loaded nanotransfersomes for transdermal application. *Int. J. Nanomed.* **2014**, *9*, 4331−4346.
(33) Chaudhary, H.; Kohli, K.; Kumar, V. Nano-transfersomes as a novel carrier for transdermal delivery. *Int. J. Pharm.* **2013**, *454*, 367−380.
(34) Derakhshandeh, K.; Erfan, M.; Dadashzadeh, S. Encapsulation of 9-nitrocamptothecin, a novel anticancer drug, in biodegradable nanoparticles: Factorial design, characterization and release kinetics. *Eur. J. Pharm. Biopharm.* **2007**, *66*, 34−41.
(35) Alund, S. J.; Smistad, G.; Hiorth, M. A. A multivariate analysis investigating different factors important for the interaction between liposomes and pectin. *Colloids Surf., A* **2013**, *420*, 1−9.
(36) Gonzalez-Mira, E.; Egea, M. A.; Garcia, M. L.; Souto, E. B. Design and ocular tolerance of flurbiprofen loaded ultrasound-engineered NLC. *Colloids Surf., B* **2010**, *81*, 412−421.
(37) Pando, D.; Caddeo, C.; Manconi, M.; Fadda, A. M.; Pazos, C. Nanodesign of olein vesicles for the topical delivery of the antioxidant resveratrol. *J. Pharm. Pharmacol.* **2013**, *65*, 1158−1167.
(38) Pando, D.; Matos, M.; Gutiérrez, G.; Pazos, C. Formulation of resveratrol entrapped niosomes for topical use. *Colloids Surf., B* **2015**, *128*, 398−404.
(39) Devaraj, G. N.; Parakh, S. R.; Devraj, R.; Apte, S. S.; Rao, B. R.; Rambhau, D. Release Studies on Niosomes Containing Fatty Alcohols as Bilayer Stabilizers Instead of Cholesterol. *J. Colloid Interface Sci.* **2002**, *251*, 360−365.
(40) Kremer, J. M. H.; Van der Esker, M. W.; Pathmamanoharan, C.; Wiersema, P. H. Vesicles of variable diameter prepared by a modified injection method. *Biochemistry* **1977**, *16*, 3932−3935.
(41) Pons, M.; Foradada, M.; Estelrich, J. Liposomes obtained by the ethanol injection method. *Int. J. Pharm.* **1993**, *95*, 51−56.
(42) Justo, O. R.; Moraes, A. M. Kanamycin incorporation in lipid vesicles prepared by ethanol injection designed for tuberculosis treatment. *J. Pharm. Pharmacol.* **2005**, *57*, 23−30.
(43) Szoka, F. C., Jr. Preparation of liposome and lipid complex compositions. U.S. Patent 5,549,910, 1996.
(44) Ghanbarzadeh, S.; Arami, S. Enhanced Transdermal Delivery of Diclofenac sodium via conventional liposomes, ethosomes, and transfersomes. *BioMed Res. Int.* **2013**, *2013*, 1−7.
(45) Antonietti, M.; Förster, S. Vesicles and liposomes: a self-assembly principle beyond lipids. *Adv. Mater.* **2003**, *15*, 1323−1333.
(46) Wang, Z.; He, X. Dynamics of vesicle formation from lipid droplets: Mechanism and controllability. *J. Chem. Phys.* **2009**, *130*, 094905.
(47) Lasic, D. D. The mechanism of vesicle formation. *Biochem. J.* **1988**, *256*, 1−11.
(48) Janmey, P. A.; Kinnunen, P. K. J. Biophysical properties of lipids and dynamic membranes. *Trends Cell Biol.* **2006**, *16*, 538−546.
(49) Silva, R.; Ferreira, H.; Little, C.; Cavaco-Paulo, A. Effect of ultrasound parameters for unilamellar liposome preparation. *Ultrason. Sonochem.* **2010**, *17*, 628−632.
(50) Yamaguchi, T.; Nomura, M.; Matsuoka, T.; Koda, S. Effects of frequency and power of ultrasound on the size reduction of liposome. *Chem. Phys. Lipids* **2009**, *160*, 58−62.
(51) Lo, C. T.; Jahn, A.; Locascio, L. E.; Vreeland, W. N. Controlled self-assembly of monodisperse niosomes by microfluidic hydrodynamic focusing. *Langmuir* **2010**, *26*, 8559−8566.

DOI: 10.1021/acs.iecr.6b01552
Ind. Eng. Chem. Res. 2016, 55, 9164−9175

Supporting Information

Using factorial experimental design to prepare size-tuned nanovesicles

Pablo García-Manrique[1,2], María Matos[1], Gemma Gutiérrez[1], Oscar R. Estupiñán[1,2], María Carmen Blanco-Lopez[2] and Carmen Pazos[1]*

[1]Department of Chemical and Environmental Engineering, University of Oviedo, Julián Clavería 8, 33006 Oviedo, Spain.

[2]Department of Physical and Analytical Chemistry, University of Oviedo, Julián Clavería 8, 33006 Oviedo, Spain.

*Corresponding author. Tel: +34 985103509

E-mail address: cpazos@uniovi.es (Carmen Pazos)

Table S1. *ANOVA results (coded units) for Z-average size of PC-liposomes for the 2^3 full factorial design; results for S60:Cho niosomes are also given (cursive numbers)*

Source	DF	Seq SS	Adj SS	Adj MS	F	P
Main effects	3	9349.7	9349.7	3116.6	86.7	0.000
		11209.8	*11209.8*	*3736.6*	*14.9*	*0.000*
2-Way Interactions	3	2805.3	2805.3	935.1	26.0	0.000
		8828.3	*8828.3*	*2942.8*	*11.7*	*0.001*
3-Way Interactions	1	113.2	113.2	113.2	3.2	0.101
		4116.8	*4116.8*	*4116.8*	*16.4*	*0.002*
Curvature	1	326.9	326.9	326.9	9.1	0.011
		7370.0	*7370.0*	*7370.0*	*29.3*	*0.000*
Residual Error	12	431.2	431.2	35.9		
		3015.0	*3015.0*	*251.3*		
Pure Error	12	431.2	431.2	35.9		
		3015.0	*3015.0*	*251.3*		
Total	20	13026.3				
		34539.9				

ANOVA indicates analysis of variance; DF, degrees of freedom; SS, sum of squares; MS, mean of squares; F, Fischer's ratio; P, p-value.

Table S2. *ANOVA results (coded units) for PDI of PC-liposomes for the 2^3 full factorial design; results for S60:Cho niosomes are also given (cursive numbers)*

Source	DF	Seq SS	Adj SS	Adj MS	F	P
Main effects	3	0.0256	0.0256	0.0082	16.72	0.0000
		0.0728	*0.0728*	*0.0243*	*18.30*	*0.0000*
2-Way Interactions	3	0.0162	0.0162	0.0054	11.02	0.0010
		0.0017	*0.0017*	*0.0006*	*0.43*	*0.7370*
3-Way Interactions	1	0.0017	0.0017	0.0017	3.39	0.0900
		0.0002	*0.0002*	*0.0002*	*0.18*	*0.6830*
Curvature	1	0.0069	0.0069	0.0069	14.05	0.0030
		0.0136	*0.0136*	*0.0136*	*10.22*	*0.0080*
Residual Error	12	0.0059	0.0059	0.0005		
		0.0159	*0.0159*	*0.0013*		
Pure Error	12	0.0059	0.0059	0.0005		
		0.0159	*0.0159*	*0.0013*		
Total	20	0.0550				
		0.1042				

ANOVA indicates analysis of variance; DF, degrees of freedom; SS, sum of squares; MS, mean of squares; F, Fischer's ratio; P, p-value.

Table S3. *COOK's distance and DFITS values obtained for each response in the full factorial designs*

BATCH	COOK Y_1	DFIT Y_1	COOK Y_2	DFIT Y_2	COOK Y_3	DFIT Y_3	COOK Y_4	DFIT Y_4
FF1	0.000	-0.019	0.708	-3.530	0.706	3.518	0.003	0.168
FF2	0.015	-0.358	0.007	-0.245	0.001	0.073	0.002	-0.130
FF3	0.089	-0.889	0.016	-0.369	0.077	0.823	0.156	1.207
FF4	0.530	-2.693	0.011	0.307	0.046	-0.626	0.131	1.096
FF5	0.028	-0.486	0.000	-0.031	0.020	0.413	0.001	-0.074
FF6	0.015	0.358	0.007	0.245	0.001	-0.073	0.002	0.130
FF7	0.116	1.024	0.139	-1.131	0.063	0.740	0.018	-0.393
FF8	0.058	0.705	0.060	0.720	0.004	-0.173	0.011	-0.299
FF9	0.001	0.103	0.023	-0.457	0.022	-0.440	0.000	-0.009
FF10	0.255	-1.614	0.191	-1.355	0.046	-0.626	0.007	-0.242
FF11	0.530	2.693	0.011	-0.307	0.046	0.626	0.131	-1.096
FF12	0.089	0.889	0.016	0.369	0.077	-0.823	0.156	-1.207
FF13	0.000	0.019	0.708	3.530	0.706	-3.518	0.003	-0.168
FF14	0.255	1.614	0.191	1.355	0.046	0.626	0.007	0.242
FF15	0.058	-0.705	0.060	-0.720	0.004	0.173	0.011	0.299
FF16	0.033	-0.554	0.012	-0.325	0.010	-0.291	0.086	0.980
FF17	0.016	0.368	0.012	0.315	0.002	0.122	0.158	-1.571
FF18	0.116	-1.024	0.139	1.131	0.063	-0.740	0.018	0.393
FF19	0.010	-0.294	0.002	0.116	0.005	-0.208	0.054	0.729
FF20	0.015	0.361	0.014	0.341	0.077	0.909	0.016	-0.370
FF21	0.028	0.486	0.000	0.031	0.020	-0.413	0.001	0.074

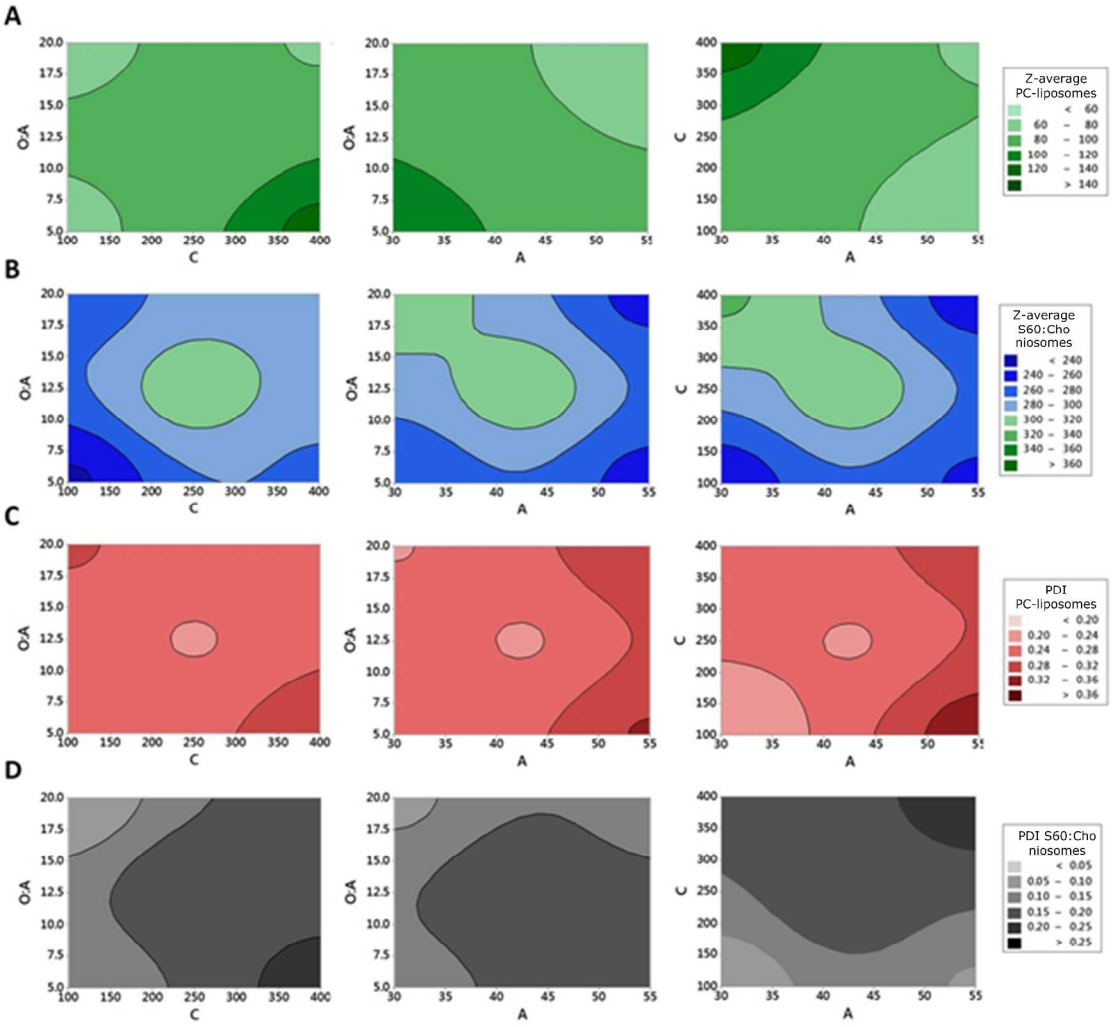

Figure S1. *Contour Plot for the factors O:A (organic:aqueous phase volume ratio), C (lipid or surfactant/stabilizer concentration, g/L) and A (sonication amplitude, %) on Z-average size, nm (A) and PDI (C) of PC-liposomes, and Z-average size, nm (B) and PDI (D) of S60:Cho niosomes (1:0.5, w/w).*

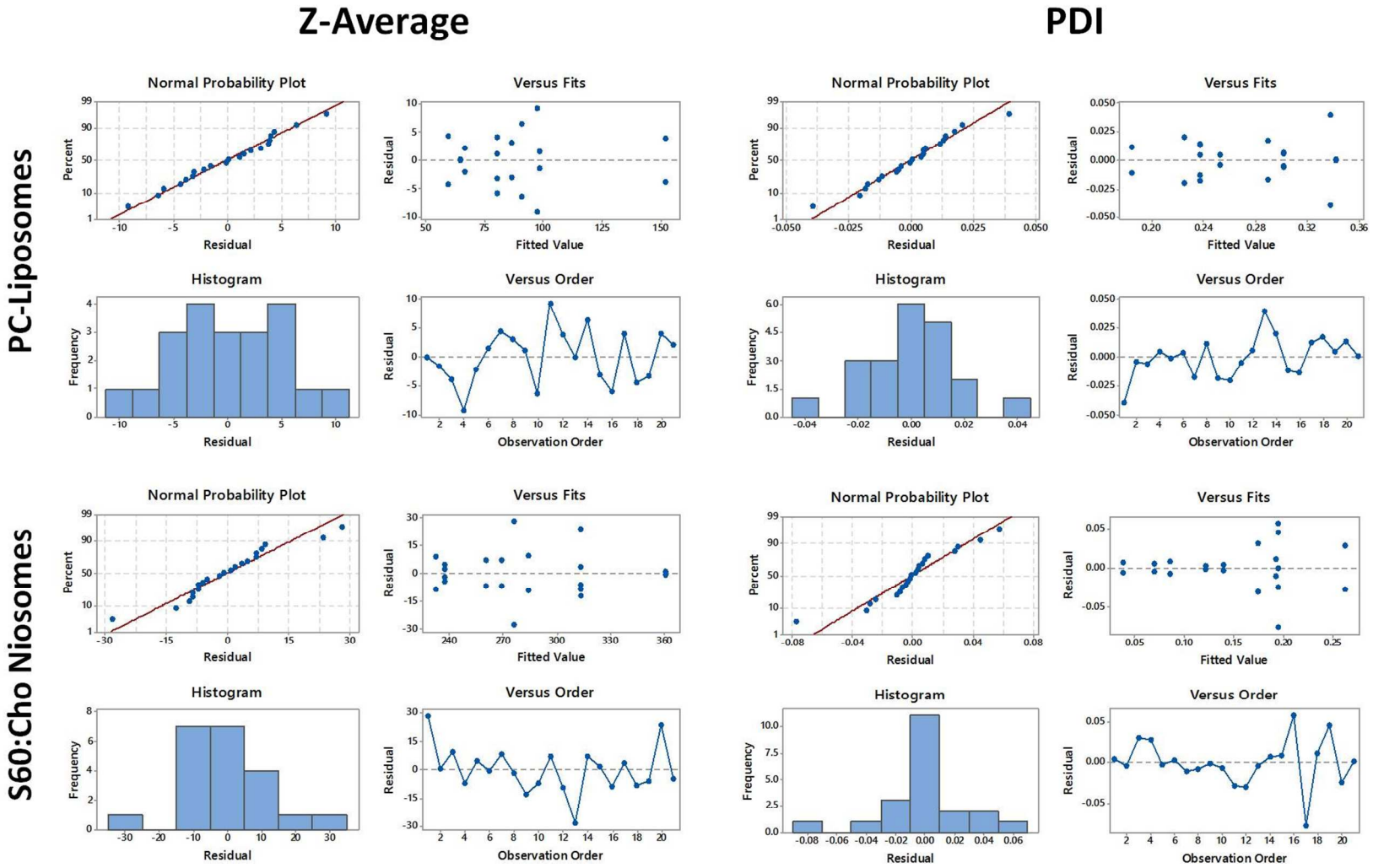

Figure S2. *Testing for normality, variance homogeneity and randomness assumptions of ANOVA for the full factorial design of PC-liposomes and S60:Cho niosomes (1:0.5 w/w).*

responsive plant cultivars and most efficient light spectra for production of high-quality products. A potential risk related to the use of light spectra deviating substantially from the daylight spectrum is enrichment of nontarget phytochemicals, for example, alkaloids, which may give pungent tastes or act as toxins or allergens. Therefore, composition of nontarget phytochemicals should also be monitored when plants are grown under modified light spectra. The new methodologies may also face difficulties if public opinion questions the use of photonics to modify the chemical quality of edible plants. These aspects will need open discussion before plant production becomes more extensively dependent on narrow-bandwidth LED lighting.

Acknowledgements

This work was supported by UEF spearhead project CABI (JKH, RJ-T) and the European Social Fund (ESF) grant no. S12530 (JKH, MK).

[1]Department of Environmental and Biological Sciences, University of Eastern Finland, P.O. Box 1627, FI-70211 Kuopio, Finland
[2]Department of Environmental and Biological Sciences, University of Eastern Finland, P.O. Box 111, FI-80101, Joensuu, Finland

*Correspondence:
jarmo.holopainen@uef.fi (J.K. Holopainen).

http://dx.doi.org/10.1016/j.tibtech.2017.08.009

References

1. Ballare, C.L. (2014) Light regulation of plant defense. *Annu. Rev. Plant Biol.* 65, 335–363
2. Junker, R.R. *et al.* (2017) Covariation and phenotypic integration in chemical communication displays: biosynthetic constraints and eco-evolutionary implications. *New Phytol.* Published online March 3, 2017. http://dx.doi.org/10.1111/nph.14505
3. Carvalho, S.D. *et al.* (2016) Light quality dependent changes in morphology, antioxidant capacity, and volatile production in sweet basil (*Ocimum basilicum*). *Front. Plant Sci.* 7, 1328
4. Tholl, D. (2015) Biosynthesis and biological functions of terpenoids in plants. *Adv. Biochem. Eng. Biotechnol.* 148, 63–106
5. Kadomura-Ishikawa, Y. *et al.* (2013) Phototropin 2 is involved in blue light-induced anthocyanin accumulation in *Fragaria x ananassa* fruits. *J. Plant Res.* 126, 847–857
6. Han, T. *et al.* (2017) Improving "color rendering" of LED lighting for the growth of lettuce. *Sci. Rep.* 7, 45944
7. Colquhoun, T.A. *et al.* (2013) Light modulation of volatile organic compounds from petunia flowers and select fruits. *Postharvest Biol. Technol.* 86, 37–44
8. Christie, J.M. *et al.* (2012) Plant UVR8 photoreceptor senses UV-B by tryptophan-mediated disruption of cross-dimer salt bridges. *Science* 335, 1492–1496
9. Olle, M. and Virsile, A. (2013) The effects of light-emitting diode lighting on greenhouse plant growth and quality. *Agric. Food Sci.* 22, 223–234
10. Taulavuori, K. *et al.* (2013) Blue mood for superfood. *Nat. Prod. Commun.* 8, 791–794
11. Kopsell, D.A. and Sams, C.E. (2013) Increases in shoot tissue pigments, glucosinolates, and mineral elements in sprouting broccoli after exposure to short-duration blue light from light emitting diodes. *J. Am. Soc. Hort. Sci.* 138, 31–37
12. Sabzalian, M.R. *et al.* (2014) High performance of vegetables, flowers, and medicinal plants in a red-blue LED incubator for indoor plant production. *Agron. Sustain. Dev.* 34, 879–886
13. Amoozgar, A. *et al.* (2017) Impact of light-emitting diode irradiation on photosynthesis, phytochemical composition and mineral element content of lettuce cv. Grizzly. *Photosynthetica* 55, 85–95
14. Arena, C. *et al.* (2016) The effect of light quality on growth, photosynthesis, leaf anatomy and volatile isoprenoids of a monoterpene-emitting herbaceous species (*Solanum lycopersicum* L.) and an isoprene-emitting tree (*Platanus orientalis* L.). *Environ. Exp. Bot.* 130, 122–132
15. Crozier, A. *et al.*, eds (2007) *Plant Secondary Metabolites: Occurrence, Structure and Role in the Human Diet*, Blackwell

Forum

Fully Artificial Exosomes: Towards New Theranostic Biomaterials

Pablo García-Manrique,[1,2] Gemma Gutiérrez,[1] and Maria Carmen Blanco-López[2,*]

Bionanotechnology routes have been recently developed to produce fully artificial exosomes: biomimetic particles designed to overcome certain limitations in extracellular vesicle (EV) biology and applications. These particles could soon become true therapeutic biomaterials. Here, we outline their current preparation techniques, their explored and future possibilities, and their present limits.

Biology and Applications of Extracellular Vesicles

The past decade has witnessed a revolution in our understanding of human body homeostasis based on cellular communication. Advances in our comprehension of the development and expansion of several pathologies are largely due to our increased understanding of the biological roles of EVs, with a particular focus on exosomes [1].

The increasing amount of data on the composition, biogenesis, and roles of exosomes in physiology and pathology has created new possibilities in diagnosis and therapy [2]. Exosomes have unique characteristics that result from their cellular origin which make them valuable as new biomarkers for diagnosis, stratification and planning, and for treatment efficacy evaluation. Their molecular composition, in terms of both their membrane and cargo, includes lipids, proteins, and nucleic acids, providing information about their cells of origin and their status. Our ability to now acquire this valuable cellular information and the fact that it also comes from hard-to reach tissues, has resulted in the term 'liquid biopsy', a new frontier in the clinical field.

In addition, exosomes combine the advantages of nanocarriers (i.e., particles used to efficiently deliver molecules) and therapeutic agents. Exosomes are currently considered among the most promising drug delivery systems, especially for gene therapy in different disorders (such as genetic deficiencies or antitumor progression) [3]. Several studies have been published during the past 5 years regarding the modification of targeting moieties and/or the encapsulation of endogenous and exogenous material in exosomes, pre or post isolation from cell cultures [4]. These studies represent the development of so-called 'exosome-based semisynthetic nanovesicles (NVs)', a subtype of artificial exosomes that includes all exosomes with modifications for specific purposes. They have even been tested for autologous therapy, using the patient's own immune cells (cultured and expanded outside the body) as a source of exosomes.

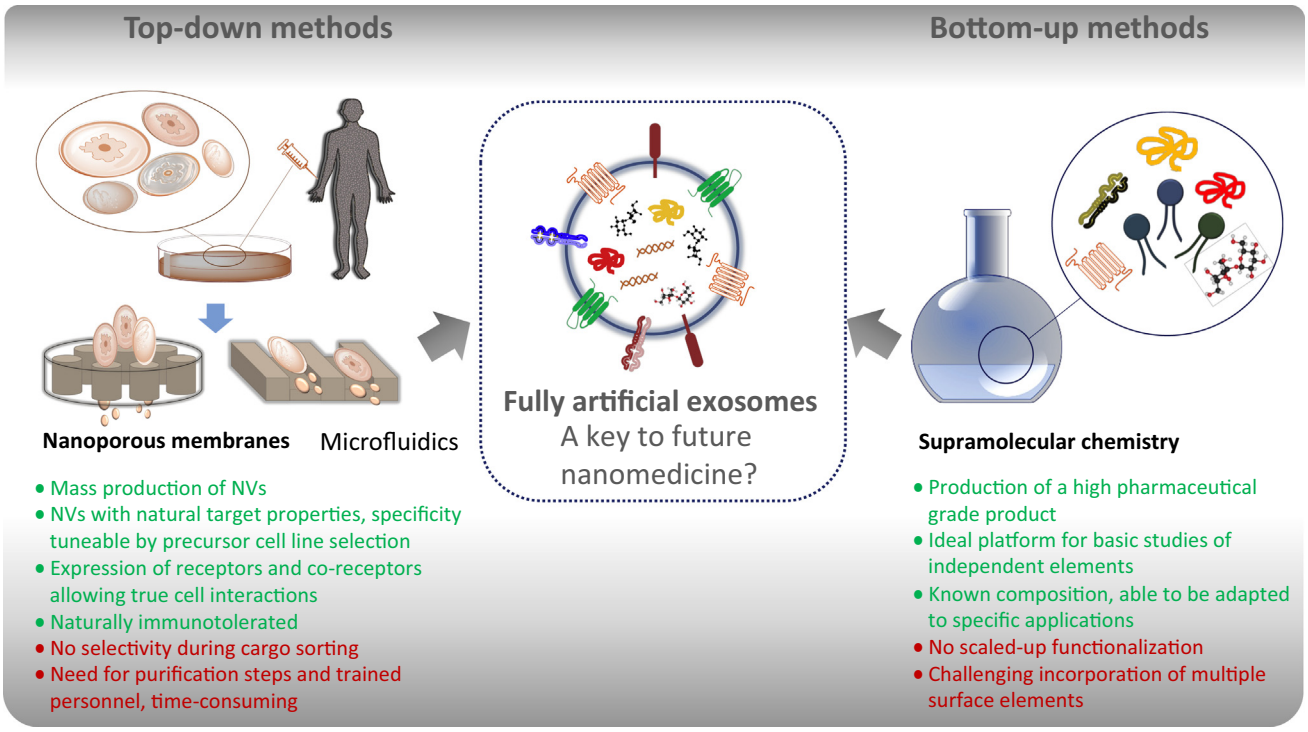

Figure 1. Advantages (Green) and Disadvantages (Red) of Two Approaches for the Bionanotechnological Development of Fully Artificial Exosomes as Theranostic Agents. Abbreviation: NV, nanovesicles.

Despite the great expansion of techniques for developing semisynthetic exosomes, the main drawbacks concerning their clinical application include production, isolation, modification, and purification on a large scale and at a suitable clinical grade. However, these drawbacks have resulted in the design and manufacture of fully synthetic exosome-mimetic particles using bionanotechnology. Here, we provide an overview of these techniques, organized according to two trends in nanofabrication: top-down and bottom-up approaches (Figure 1).

Top-Down Methodologies: Bioengineering Cells as Membrane Fragment Precursors

Top-down methodologies rely on the production of nanosized materials by breaking bigger and more complex units into smaller parts. In this case, the production of artificial exosomes begins with cultured cells that are then used to produce membrane fragments that will be used to form the vesicles. Different methodologies based on this approach have been developed, mainly for drug delivery, but also for enhancing cell proliferation and for generating exosome-mimetic models for biodistribution analyses (i.e., monitoring exosomes after exogenous administration) (Table 1). Two of the most relevant strategies involve: (i) extrusion over polycarbonate membrane filters. This is a common way to reduce the mean size and homogenize the size distribution of colloidal systems. By applying this technique to cultured cells, NVs have been produced with a simple commercial liposome extruder and diminishing pore size filters [5,6]; they have been used to treat tumors by targeted encapsulated chemotherapeutics. A scaled-up version was also developed with a device designed to be used with conventional laboratory centrifuges [7]. This device was used to mass-produce NVs in a study of cell proliferation enhancement [8]; and (ii) specific microfluidic devices. Simple pressurization over a device based on an array of parallel hydrophilic microchannels has been described for the production of NVs for the delivery of endogenous RNA to targeted cell cultures [9]. The fabrication of microchannels on microblades (fabricated in silicon nitride) resulted in a device able to slice living cells as they flowed through the channels [10]. The incorporation of exogenous material in the cell suspension enhanced their encapsulation by plasma membrane fragments during reassembly and suggested a method for *in vitro* exogenous material delivery.

Both of these methods are suitable for the production of larger amounts (by a factor of more than 250) of biologically active particles compared with natural exosome release yields. Sizing and biochemical profiling showed that these NVs were

Table 1. Fully Artificial Exosomes based on Top-Down and Bottom-Up Bionanotechnology.[a]

Mechanism of membrane fragmentation	Precursor cell lines	Type and example of material incorporated	Application	Refs
Studies based on top-down approaches				
Manual extrusion over polycarbonate membrane filters with a device for liposome preparation	Human monocytes (U937) and murine mouse macrophages (Raw 264.7)	Exogenous, chemotherapeutic drugs (doxorubicin, 5-FU, gemcitabine, and carboplatin)	Targeted delivery of chemotherapeutics to an *in vitro* model (TNFα-treated HUVECs) and *in vivo*-induced malignant tumors (CT26 mouse colon adenocarcinoma cells)	[5]
	Murine mouse macrophages (Raw 264.7)	Exogenous, radiolabeling agent ^{99m}Tc-HMPAO	*In vivo* biodistribution of exosomes and artificial counterparts	[6]
Centrifugal-induced extrusion over membrane filters in a device designed to be used in lab centrifuges	Murine mouse embryonic stem cell line (D3)	Endogenous, precursor cell characteristic RNA (mOct 3/4 and mNanog)	Gene delivery to NIH-3T3 fibroblast cells	[7]
		No intention to encapsulate any specific compounds	Enhanced *in vitro* cell proliferation for regenerative medicine (murine skin fibroblasts)	[8]
Pressurization over hydrophilic microchannels array on a microfluidic device	Murine mouse embryonic stem cell line (D3)	Endogenous, precursor cell characteristic RNA (mOct 3/4 and mNanog)	Gene delivery to NIH-3T3 fibroblast cells	[9]
Living cells sliced with silicon nitride blades in a microfluidic device	Murine mouse embryonic stem cell line (D3)	Exogenous, polystyrene beads as representative exogenous material	Material delivery to mouse embryonic fibroblasts	[10]
Type of formulation	NV preparation strategy	Proteins for NV functionalization	Application	Refs
Studies based on bottom-up approaches				
Classical liposome, PC:Chol	Thin film hydration method (TFHM) and maleimide-based bioconjugation strategy	MHC class I peptide complexes and FAB regions against T cell receptors for adhesion, early and late activation, and survival	*Ex vivo* and *in vivo* T cell expansion for immunotherapies	[12]
Mimicking exosome lipid composition, PC:Chol:SM	TFHM and Ni^{2+}/His-Tag protein coordination as bioconjugation strategy	APO2L/TRIAL-His_{10} recombinant proteins	Downregulation of T cell activation in an autoimmune disease animal model (antigen-induced arthritis); immunotherapy for apoptosis induction in hematological tumors	[13,14]
Innovative liposomes, PC: CpEL:DOPE	Microemulsion and micelle-assembling method for vesicle formation	Monoclonal antibody against DEC205 dendritic cell antigen	Proof of concept of artificial antigen presentation to dendritic cells	[15]

[a]Abbreviations: ^{99m}Tc-HMPAO, ^{99m}Tc-hexamethylpropyleneamineoxime; Chol, cholesterol; CpEL, chemopor EL; DOPE, dioleoyl-phosphoethanolamine; HUVECs, human umbilical vein endothelial cells; MHC, major histocompatibility complex; PC, phosphatidylcholine; SM, sphingomyelin; TFHM, thin film hydration method.

substantially similar to natural exosomes [4–9]. Their ability to exhibit receptors and co-receptors, which is essential to target and effectively interact with receptor cell populations, is of special relevance. In addition, their natural origin from cells renders them immunotolerant [4–9].

However, these methods have some drawbacks. Cargo sorting lacks selectivity due to the passive encapsulation of the surrounding medium during membrane fragment self-assembly. Another relevant issue regarding the production of these mimetic particles is the need for final purification steps identical to those used for exosome isolation, which require trained personnel and are time-consuming.

Bottom-Up Techniques: Mimicking the Plasma Membrane by Preparing Artificial Bilayers

By contrast, bottom-up techniques create complex structures from molecular building blocks by using their physical and chemical properties. These methods include those used in the cosmetic and drug-delivery industries for the preparation of liposomes, which are particles formed by a lipid bilayer that resembles the plasma membrane. These materials are a promising starting point to design and manufacture artificial exosomes. The self-assembled synthetic bilayer can be then functionalized with selected proteins to mimic the desired exosomal functions. With this purpose in mind, special lipids can be incorporated into the liposome formulation. These can be modified with

chemical groups (such as carboxylic, amine, or metal chelating agents) with the capacity to create covalent bonds with the selected biomolecules through known bioconjugation techniques [11].

Among the many methods for preparing liposomes, one of the most often used to develop mimetic NVs is the thin film hydration method. This is a two-step process where a dried film of lipids is hydrated by an aqueous medium containing the compounds to be encapsulated. Artificial exosomes have been produced with a classical liposome formulation [12] and a lipid formulation simulating the composition of exosomes [13]. Using chemical bioconjugation procedures, certain protein and/or peptide complexes and ligands involved in T cell receptor interactions and activation have been attached to vesicles for immunotherapy (*ex vivo* and *in vivo* cell expansion, Table 1). In addition, the incorporation of certain ligands was reported to induce apoptosis and downregulate T cell activation in autoimmune diseases, such as antigen-induced arthritis, [13]. These NVs have also been evaluated for the treatment of hematological tumor cells [14].

More recently, a method based on microemulsification and micelle assembly was described for encapsulating BSA as an artificial exosome mimicking antigen presentation to dendritic cells (DCs) [15]. To specifically target DCs, a monoclonal antibody against a highly expressed receptor on the surface of DCs that facilitate endocytosis was selected.

The main advantage of this strategy relies on the production of a high-grade pharmaceutical product because the final composition is fixed by the selected formulation. However, publications on this topic are scarce. Additionally, because these are methods adapted from conventional liposome production routes, expensive high-purity lipids are required (especially if the artificial exosomes are to be functionalized with proteins). The attachment of multiple molecules to NVs is also challenging because conjugation procedures require stable and specific conditions [14].

On the other side, another advantage of this method is that it can be adapted to the encapsulation of nucleic acids, which is challenging due to the unstable nature of the molecules. The best encapsulation efficiencies are obtained with cationic lipids, which are more immunogenic than their uncharged counterparts [15].

Concluding Remarks and Future Perspectives

New therapies with fully artificial exosomes could be a basis for future personalized nanomedicine. However, whereas clinical trials of natural EVs have just begun, biomimetic materials produced by the synthetic routes discussed here have not yet reached clinical translation. Current challenges include the establishment of regulatory protocols, mode of actions, and clarification of safety aspects. Commercialization also requires scaling-up procedures. Automatization of purification steps would also be highly desirable. A multidisciplinary approach, with contributions from molecular biology, engineering, biotechnology, and chemistry, will be essential to overcome these limitations. Research to improve the manufacturing methods could include the combination of both approaches: semi- and fully synthetic artificial exosomes.

Techniques for modifying cells before exosome isolation could be easily coupled to any top-down method to tailor artificial exosomes with complementary elements to those naturally present in selected donor cells. These could also be used to enhance the physical stability of generated products, a property that has not yet been fully studied.

Regarding bottom-up techniques, microfluidics represents a promising versatile platform for particle production and drug encapsulation. This strategy can rapidly test multiple formulations thanks to the fast product generation and also consumes a significantly smaller amount of chemicals.

In terms of the composition of NVs, alternatives to lipids are being explored. Current research is testing the possibilities of niosomes (vesicles formulated with non-ionic surfactants) as a sustainable alternative to lipid-based particles in the development of artificial exosomes. The main advantages of these vesicles are their wide array of starting compounds, lower price, better physical and chemical stability, and higher biocompatibility.

As new production routes are improved, novel NVs closer to real exosomes will become available, making personal nanomedicine and theranostic agents adapted to particular needs possible.

Acknowledgments

This work was financed by the Consejería de Economía y Empleo del Principado de Asturias (Plan de Ciencia, Tecnología e Innovación 2013-2017), under the Grant GRUPIN14-022. Support from the European Regional Development Fund (ERDF) is gratefully acknowledged.

[1]Department of Chemical and Environmental Engineering, University of Oviedo, Julián Clavería 8, 33006 Oviedo, Spain
[2]Department of Physical and Analytical Chemistry, University of Oviedo, Julián Clavería 8, 33006 Oviedo, Spain

*Correspondence:
cblanco@uniovi.es (M.C. Blanco-López).

http://dx.doi.org/10.1016/j.tibtech.2017.10.005

References

1. Yáñez-Mó, M. *et al.* (2015) Biological properties of extracellular vesicles and their physiological functions. *J. Extracell. Vesicles* 4, 1–60
2. Fuhrmann, G. *et al.* (2015) Cell-derived vesicles for drug therapy and diagnostics: opportunities and challenges. *Nano Today* 10, 397–409
3. Van der Meel, R. *et al.* (2014) Extracellular vesicles as drug delivery systems: lessons from the liposome field. *J. Control. Release* 195, 72–85
4. Johnsen, K.B. *et al.* (2014) A comprehensive overview of exosomes as drug delivery vehicles – endogenous nanocarriers for targeted cancer therapy. *Biochim. Biophys. Acta* 1846, 75–87

5. Jang, S.C. *et al.* (2013) Bioinspired exosome-mimetic nanovesicles for targeted delivery of chemotherapeutics to malignant tumors. *ACS Nano* 7, 7698–7710
6. Hwang, D.W. *et al.* (2015) Noninvasive imaging of radiolabelled exosome-mimetic nanovesicles using ^{99m}Tc-HMPAO. *Sci. Rep.* 5, 15636
7. Jo, W. *et al.* (2014) Large-scale generation of cell-derived nanovesicles. *Nanoscale* 6, 12056–12064
8. Jeong, D. *et al.* (2014) Nanovesicles engineered from ES cells for enhanced cell proliferation. *Biomaterials* 35, 9302–9310
9. Jo, W. *et al.* (2014) Microfluidic fabrication of cell-derived nanovesicles as endogenous RNA carriers. *Lab Chip* 14, 1261–1269
10. Yoon, J. *et al.* (2015) Generation of nanovesicles with sliced cellular membrane fragments for exogenous material delivery. *Biomaterials* 59, 12–20
11. Hermanson, G.T. (2008) Preparation of liposome conjugates and derivatives. In *Bioconjugate Techniques* (2nd edn) (Hermanson, G.T., ed.), pp. 858–899, Academic Press
12. De La Peña, H. *et al.* (2009) Artificial exosomes as tools for basic and clinical immunology. *J. Immunol. Methods* 344, 121–132
13. Martinez-Lostao, L. *et al.* (2010) Liposome-bound APO2L/TRAIL is an effective treatment in a rabbit model of rheumatoid arthritis. *Arthritis Rheum.* 62, 2272–2282
14. De Miguel, D. *et al.* (2013) Liposomes decorated with APO2L/TRAIL overcome chemoresistance of human hematologic tumor cells. *Mol. Pharm.* 10, 893–904
15. Li, K. *et al.* (2015) A novel micro-emulsion and micelle assembling method to prepare DEC205 monoclonal antibody coupled cationic nanoliposomes for simulating exosomes to target dendritic cells. *Int. J. Pharm.* 491, 105–112

Journal of Extracellular Vesicles

ISSN: (Print) 2001-3078 (Online) Journal homepage: https://www.tandfonline.com/loi/zjev20

Therapeutic biomaterials based on extracellular vesicles: classification of bio-engineering and mimetic preparation routes

Pablo García-Manrique, María Matos, Gemma Gutiérrez, Carmen Pazos & María Carmen Blanco-López

To cite this article: Pablo García-Manrique, María Matos, Gemma Gutiérrez, Carmen Pazos & María Carmen Blanco-López (2018) Therapeutic biomaterials based on extracellular vesicles: classification of bio-engineering and mimetic preparation routes, Journal of Extracellular Vesicles, 7:1, 1422676, DOI: 10.1080/20013078.2017.1422676

To link to this article: https://doi.org/10.1080/20013078.2017.1422676

Published online: 17 Jan 2018.

JOURNAL OF EXTRACELLULAR VESICLES
2018, VOL. 7, 1422676
https://doi.org/10.1080/20013078.2017.1422676

Taylor & Francis
Taylor & Francis Group

REVIEW ARTICLE

OPEN ACCESS Check for updates

Therapeutic biomaterials based on extracellular vesicles: classification of bio-engineering and mimetic preparation routes

Pablo García-Manrique [a,b], María Matos [b], Gemma Gutiérrez [b], Carmen Pazos [b] and María Carmen Blanco-López [a]

[a]Department of Physical and Analytical Chemistry, University of Oviedo, Oviedo, Spain; [b]Department of Chemical and Environmental Engineering, University of Oviedo, Oviedo, Spain

ABSTRACT

Extracellular vesicles (EVs) are emerging as novel theranostic tools. Limitations related to clinical uses are leading to a new research area on design and manufacture of artificial EVs. Several strategies have been reported in order to produce artificial EVs, but there has not yet been a clear criterion by which to differentiate these novel biomaterials. In this paper, we suggest for the first time a systematic classification of the terms used to build up the artificial EV landscape, based on the preparation method. This could be useful to guide the derivation to clinical trial routes and to clarify the literature. According to our classification, we have reviewed the main strategies reported to date for their preparation, including key points such as: cargo loading, surface targeting strategies, purification steps, generation of membrane fragments for the construction of biomimetic materials, preparation of synthetic membranes inspired in EV composition and subsequent surface decoration.

ARTICLE HISTORY
Received 24 July 2017
Accepted 22 December 2017

KEYWORDS
artificial extracellular vesicles; biomimetic materials; nanomedicine; drug-delivery nanocarrier

Extracellular vesicles in nanomedicine: possibilities and limitations

Extracellular vesicles (EVs) represent an important portion of the secretome. An overview of their functions in physiological conditions of EVs was compiled by a recent position paper from the International Society of Extracellular Vesicles (ISEV) [1]. Some of the described properties can be used for therapeutic uses, and their testing has been transformed sometimes into several registered clinical trials [2]. Exosomes are being applied in antitumour immunotherapy [3], as therapeutic agents against infectious diseases [4], unmodified exosomes for immune-modulatory [5] and regenerative therapies [6], and modified ones for targeted drug delivery [7], especially in gene therapy [8]. Although some of the mechanisms behind their properties remain undescribed, some general characteristics of EVs make them advantageous over other therapeutic strategies.

Both the structure of the membrane and the formation route are the origin of the following advantageous aspects: (1) high selective targetability and minimum off-target effect, thanks to a set of molecules involved in targeting, signalling and receptor-mediated uptake, complete with all the co-receptors needed for the internalization process; (2) capacity of extravasation due to a gel-state core derived from the presence of hydrated macromolecules (proteins and nucleic acids) combined with a minimum cytoskeleton that allows deformability while keeping the whole integrity of the vesicle. (3) size distribution; (4) great stability in the blood due to the evasion of the innate immune system; (5) adaptative responses that cause clearance from the blood, with the corresponding decrease in bioavailability.

EVs can be used as a therapeutic agent by themselves or as delivery systems. The great potential of EVs as drug-delivery vehicles has been acknowledged in the literature [7–12]. In most cases, the encapsulated drug acts in collaboration with elements naturally present in the EVs, creating a synergetic effect. In other cases, EVs serve only as vehicles to reach a specific target population, sometimes highly protected from conventional administration routes.

Nevertheless, limitations of EVs as therapeutic agents have also been reported, including the absence of a good definition from a pharmaceutical point of view [13], an incomplete understanding of their role in the development and spread of pathology, the absence of methods for the isolation of homogeneous populations and subpopulations of EVs, and cost-ineffective technology for the availability of sufficient quantities for clinical trials with constant characteristics. Moreover, it has been acknowledged that there is little understanding on how biological barriers are crossed by EVs, and a need for

CONTACT María Carmen Blanco-López cblanco@uniovi.es

loading methods with scalable properties in clinical translation has been identified [14].

Bio-engineered and mimetic EVs for nanomedicine: classification of artificial EVs

EVs have been modified in the search for broader therapeutic capability. Sometimes, this included the incorporation of new elements for targeted puporses, *in vitro* or *in vivo* traceability, or the material to be delivered. In other cases, modification was aimed at the enhancement of colloidal stability, or change in surface charge to increase their uptake rate. These new approaches have generated new terms such as bio-engineered exosomes, artificial exosomes [15], exosome-mimetic nanovesicles [16], exosome-like nanovesicles [17,18] and exosome-based semi-synthetic vesicles [19]. These expressions have been used with different meanings in the literature, but to date, there has not yet been a clear criterion for their classification. One example is the term "exosome-like nanovesicles". In some works, this concept is used to name artificial vesicles made from cells through different techniques to mimic exosomes [17,18]. However, cell-derived vesicles with morphological and biochemical characteristics similar to exosomes were also named exosome-like nanovesicles by other authors [19,20]. Other authors working with non-animal research models used this term to refer to vesicles with size and flotation density values similar to those of exosomes. For example, Regente et al. [21] described the presence of exosome-like vesicles in sunflower plant fluids, and Prado et al. [22] showed evidence of vesicles quite similar to exosomes during pollen germination.

In order to provide a systematic classification to move around in this new emerging field, we suggest the nomenclature given in Figure 1. This artificial EVs landscape is based on the concept behind the term. In this way, "artificial EVs" will be used as a general concept to designate all vesicles, modified or manufactured (from natural or synthetic sources), with the aim to mimic EVs (mainly exosomes) for therapeutic uses. Behind this term, two categories of artificial EVs can be discerned: "semi-synthetic EVs" and "fully synthetic" or "EVs mimetic vesicles", corresponding to modified natural EVs (pre- or post-isolation) and artificial structures, lab-made or generated from cultured cells.

The former generate semi-synthetic products, as they start from a natural substrate, which can be subsequently modified before or after their isolation. The modification affects the structures of the outer surface of the vesicles, the membrane or the cargo that travels within, and could also include hydrophobic molecules at the membrane.

The term *fully synthetic*, on the other hand, stresses the artificiality of the product. We have recently briefly commented their potential in therapeutics [23]. These techniques can be classified on the basis of their manufacturing route: those starting from larger substrates (cells) that are reduced to units for the creation of small size vesicles (top-down nanotechnology) or those taking individual molecules (lipids, proteins, etc.) that self-assemble in higher-order structures with tunable composition (bottom-up nanotechnology). Top-down products differ from natural EVs in terms of micro-structure and biochemical composition, since they are formed from cell fragments: the characteristic membrane microdomains [24] (lipid rafts) and

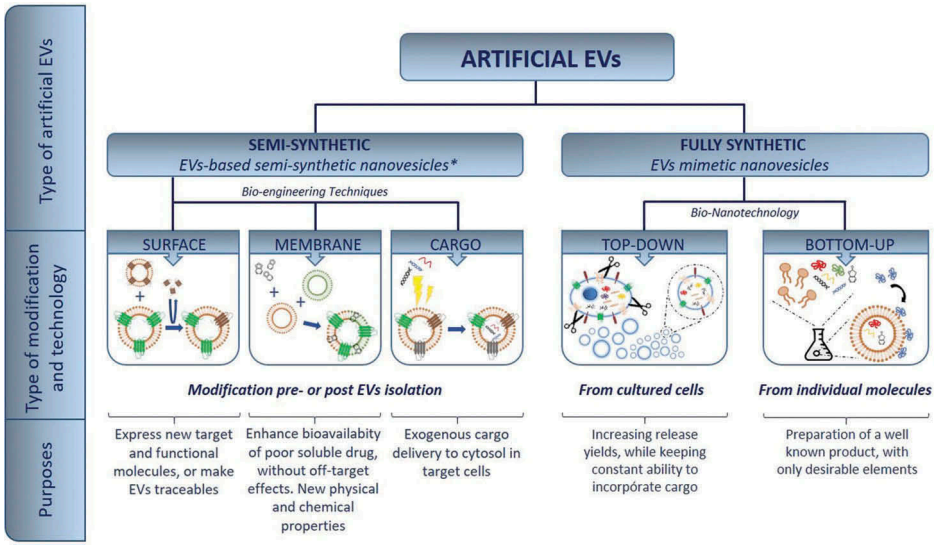

Figure 1. Artificial EV landscape: explored routes to date for the preparation of artificial EVs for specific purposes. *EBSSNs [19].

associated pools of surface markers (especially tetraspanins) are absent, and the minimal cytoskeleton is not present.

Impact of the artificial EV classification in the design of new therapeutic agents based on EVs

The preparation route chosen is important for the final purpose of artificial EVs, but it could be critical for the clinical trials and subsequent commercialization. The extensive manipulation of EVs during the bio-engineering methods is the reason for their classification as advanced therapy medicinal products (ATMPs) [2], with a particular regulatory framewok. Following the same criteria, fully artificial EVs produced from cultured cells (top-down) should also be incorporated into this category.

On the other hand, bottom-up artificial mimetic EVs are more difficult to assign to one or another category. To date, a set of proteins have been fixed on lipidic vesicles with an undefined purpose. While there is some evidence that the EV membrane is important for the uptake process [1], the role of the artificial membranes is not yet clear. Comparative studies of the effects over target cell lines with conventional liposomes and exosome-mimetic nanovesicles would be very useful to clarify this. The work in this field is reviewed in the section "Bottom-up methodologies: artificial membranes decorated with functional proteins to mimic EVs functions."

A critical evaluation of the *fully synthetic EVs* concept would imply providing an answer to questions such as: "What we are trying to mimic from EVs?"; "Is the biochemical composition, the morphology or the whole entity?"; "Is it worth mimicking a specific function?" This is still a challenge in the field, since some of these questions are being answered at the same time for natural EVs. The best approach would involve an extensive biochemical characterization of natural EVs and a detailed description of their functions. Regarding functionality, other populations and not only the target cell lines should be assayed. This could provide information about possible side effects. In the same way, multiple parameters should be registered as output factors, not just the process targetted by the EV-based treatment. Proteins, nucleic acids and lipid composition from specific types of exosomes are registered in specialized databases such as ExoCarta [25], EVpedia [26] and Vesiclepedia [27]. But this is not enough: a database with assays performed with EVs reporting treated cell lines, EV type as therapeutical agents, type of assay (*in vitro* or *in vivo*) and experimental conditions could be of great interest to the scientific community. The combination of both sources of information would be the perfect scenario for the design of future artificial EV-based therapies.

In any case, both types of artificial EVs should meet product specifications related to "purity, identity, quantity, potency and sterility" in concordance with the pharmaceutical market regulations [28]. Once more, there are several important differences in the definition of these parameters depending on the semi- or fully synthetic character of EVs. These key points will be considered and discussed in the following sections.

Semi-synthetic exosomes: biotechnological modification of naturally released exosomes

The simplest idea to manufacture EVs would be to use the natural mechanisms for the formation of vesicles, that is, the cellular machinery itself. It is known that the composition of the EVs at all levels responds to a high degree of control at very selective cellular mechanisms [29]. Therefore, the composition of the EVs could be controlled by intentional alteration of the cellular environment.

This method would lead to the creation of EVs with a composition profile adapted to a specific purpose. The technological methods used for bioengineering EVs are explained in the following sections. Two key aspects are the selection of producer cells (and their *in vitro* harvesting conditions) and the EV isolation/enrichment procedures. Both choices will condition subsequent uses.

Selection of EV cellular origin

Cell lines could potentially release EVs vesicles, but there are great differences in release rate and biochemical composition and their susceptibility to modifications [30]. It is also accepted that before translation to clinical use of EVs, limitations regarding biocompatibility, economic viability, harvesting methods and immunotolerance must be overcome. A summary of cell lines used for the production of EVs for clinical purposes, especially drug delivery, can be found in the literature [31]. Dendritic cells and cancer cell lines, such as melanoma, are the most commonly used lines for EV production.

Mesenchymal stem cells (MSCs) are one of the most promising sources of EVs, especially exosomes [32]. Yeo et al. [33]. defended their use for mass production of exosomes with future therapeutic purposes based on some important facts related to their advantages over other cell lines. Mainly, MSCs are easy to obtain from

all human tissues (even those considered as medical waste), and they have a high *ex vivo* expansion capacity compatible with immortalization without compromising their therapeutic efficacy. These two facts are essential to establish a scalable and long-term source of well-characterized EVs, particularly exosomes [14,28]. In addition, their immunomodulatory effect gives them and their derived EVs important features in autologous and allogenic therapeutic applications.

Dendritic cells (DCs) have important roles in immunity (both innate and adaptative). Some authors have paid attention to this cell line in order to enhance the production of clinical grade DC-derived exosomes for immunotherapy [33]. Properties of DCs have even been enhanced with different nanoparticles [34]. Exosomes from DCs modified to express indoleamine 2,3-dioxygenase (IDO), a tryptophan-degrading enzyme that is important for immune regulation and tolerance maintenance, have been used in the treatment of rheumatoid arthritis [35]. In another study, DC-derived exosomes modified to express FasL on the surface (ligand involved in apoptosis induction) were tested as inflammatory and autoimmune therapy [36]. Other recent works are related to the role of tumour-released exosomes to load antigens into DCs for the therapy of malignant mesothelioma [37].

To overcome the problem of low release rate, some authors lowered the micro-environmental pH, mimicking the natural cancer mechanism [38]. By culturing HEK293 cell lines at different pHs, these authors found that low pH values were best to isolate high amounts of exosomes. In spite of the impact of these results, it would be necessary to test similar effects in non-cancerous cell lines and to determine how the change in the harvesting conditions affects EV composition (membrane components and cargo).

Not only human cells have been explored as a source of EVs: exosomes isolated from bovine milk and loaded with different drugs were a promising strategy for mass production of therapeutic EVs [39]. They can be easily isolated by differential centrifugation. The biocompatibility of milk-derived exosomes was checked by clinical biochemical analysis in an animal model by oral gavage during 6 h (short-term toxicity) and 15 days (medium-term toxicity).

In recent years, some attention has been drawn to non-animal (especially plant) EVs and their potential use in therapy [40]. In particular, fruit-derived exosomes (lemon [41] and grapes [42]) have been isolated, characterized and tested as beneficial products. Perhaps this new source of EVs could be used in the near future for the development of EBSSNs following modifications to express the desired targeting molecules against specific cell lines. Evidence about immunotolerance should also be provided in order to avoid any interference in the results.

In any case, studies involving the encapsulation of the same drug into different cell lines-derived EVs would be desirable in order to clarify whether the beneficial effect is due to the drug or the combination of drug/type of carrier.

Obtaining a good substrate for modification: isolation procedures

Since the final destination of artificial EVs would be the administration for therapeutic purposes, the highest level of standards would be required in order to preserve patient safety [27,43]. A key point in artificial EVs development is the enrichment from different biological samples, from cell-culture supernatants to several body fluids. There are different reviews [43–45] and technique-comparative papers [46–49] about isolation procedures. They involve ultracentrifugation, filtration, immunoaffinity isolation, polymeric precipitation and microfluidics techniques, with different degrees of purity for the final product [50]. In this review, we have focussed on scalability, reproducibility and synthetic EV potential damage or physical modification.

Since the efficient function of EVs depends on their *size distribution*, aggregation and size changes after isolation are important. Lane et al. [47] studied these parameters in four isolation methods: two aggregation kits, a density-based method and ultracentrifugation. These authors found that some methods kept a constant vesicle size, but large differences were observed regarding yield of isolation (the two sedimentation methods gave recovery values two orders of magnitude higher than the other methods). Another reported obstacle is the co-purification of material with similar physical characteristics to EVs [42,51,52].

Scalability is also important, since the batch size is correlated with the homogeneity of the final product; sometimes small batches are more prone to being susceptible to *bias* during the process, but on other occasions, higher batches yield more heterogeneous populations due to microenvironments during procedures.

The scale-up step with ultracentrifugation (UC) is limited by the number of rotor positions and the maximum sample volume. On the other hand, methods such as size exclusion chromatography (SEC) are easy to scale up by using large columns, but with the associated longer separation time. Pressure application to reduce processing time can disturb EVs [43]. Other

methods, such as immunoaffinity isolations, are only used for small amounts of original sample because of the high price of the reagents required. Finally, microfluidic methods [45,53] are promising, with the possibility of being coupled to online analysis [54].

Reproducibility is crucial when the product is going to be used in the clinical field. Comparative results of UC are difficult to obtain due to the high number of models available in the market, and this could affect the quality of the isolated product [43]. The use of a fixed instrument would keep low variability between batches [47].

Welton et al. [55] reported that ready-to-use SEC columns could overcome some problems related to homemade poured columns [52], thereby avoiding variations from column to column, and facilitating robust protocols to be used routinely. The main problem associated with this method is dilution of EVs in the final sample and the subsequent need for concentration using precipitating agents or UC. This increases retention time and the possibilities of co-precipitation of other molecules with the same size and physical properties.

Considerable effort has been made in the field of EV isolation methods, which are still limiting the expansion of this field. There is not yet a perfect and universal method, and it is also accepted that selection of the isolation method could impact downstream steps [56].

Table 1. Classification of techniques for the production of artificial EVs, mainly exosomes, according to type of final product (semi- or fully synthetic) and the principle of the obtention mechanism.

Semi-synthetic exosome production: modification of vesicles naturally produced by cells	
Pre-isolation modification	
Class I	Co-localization of cargo and exosomal carrier moiety thanks to the natural tropism of the second
Class II	Use of sequences (i.e. nucleic acid-based sequences) for the exosomal biogenesis pathway signalling
Class III	Take advantage of passive loading via increments of their presence, by genetic overexpression or active loading of producer cells
Post-isolation modification	
Class IV or passive methods	Methods that use passive adsorption of molecules into external surface of EVs, owing to their hydrophobicity nature
Class V or active methods	V.a (Physical methods), based on the creation of transitional alteration in the integrity of EVs that allows cargo to enter the vesicles by concentration gradient or by passive incorporation during subsequent restoring of initial status post-stimuli
	V.b (Chemical methods), based on induced chemical reactions between EVs and cargo with or without previous introduction of functionalization agents into vesicles
Creation of artificial mimetic structures of the natural exosomes	
Type I or top-down bio-nanotechnology	Starting from larger substrates (cells) that are reduced to units for the creation of vesicles with reduced size
Type II or bottom-up bio-nanotechnology	Starting with individual molecules (lipids, proteins, etc.) that are assembled in a controlled way for generating complex structures of higher order

Strategies for biochemical modification

Pre-isolation modification using own cellular machinery

The advantages and disadvantages of the methods applied to incorporate proteins of nucleic acids are shown in Tables 2 and 3. Based on the study of exosome biogenesis-related mechanisms, several methods have been developed [50,57–62]. The following criteria have been identified for their classification (see Table 1):

(I) location of exosomal functional entities, such as transmembrane proteins and the use of their natural tropism to co-localized the exogenous element;
(II) strategies using molecular mechanisms for the introduction of exogenous molecules into EVs for cytosolic delivery;
(III) increasing the amount of molecules into the cellular plasma to be encapsulated by passive mechanism during MVB formation.

Class I methods (Table 2) involve the design of chimeric constructions of proteins by genetic engineering. In this case, the fusion between the gene of a protein to be incorporated and the gene of an exosomal-localized protein can be used for the expression of the former on the outer surface of exosomes. This has been referred to in the literature as *Exosome Display* technology [63], and it enables the manipulation of the protein content of exosomes and the subsequent tailoring of activities. The potential of the method was successfully demonstrated by the production of specific antibodies against human leukocyte antigen (HLA), a low immunogenic antigen [64].

Lactadherin C1C2 domain was also used for similar purposes by Zeelemberg et al. [65] and Hartman et al. [66] to induce expression of chicken egg ovalbumin (OVA) peptide and the human epidermal growth factor receptor 2 antigen (HER2), respectively. Álvarez-Erviti et al. [67] described a method of inducing surface expression of the central nervous system-specific rabies viral glycoprotein (RVG) peptide on exosomes isolated from immature dendritic cells derived from mice. Complementarily, these brain-targeted exosomes were loaded with siRNA for the first time by electroporation. The delivery of

Table 2. Pre-isolation methods for cargo incorporation into EVs.

Cargo incorporation previous to the release of exosomes					
Method	EV modified component	Category of modification (according with Table 1)	Advantages	Disadvantages	Molecules incorporated
Genetic fusion of cargo gene with an exosomal protein gene	Surface	Class I	Efficient exposure of targeting moiety on the surface of EVs By selecting the EVs protein to be fusioned with, different expression rate can be achieved	Only successfully explored with exosomal membrane proteins	Peptides, small proteins such as GE11 peptide [69], HLA [63], OVA [65], HER2 [66], and RVG [67]
Exosome surface display technology	Surface	Class I	Suitable to induce expression of protein in both, extravesicular and intravesicular sides at the same time	Not tested with high-molecular-weight proteins	Fluorescent proteins [62] such as GFP and RFP
RNA zipcodes	Cargo	Class II	Alternative to electroporation of miRNA	Applicable only to mRNA and miRNA Influence of mRNA size not tested	mRNA [70] and miRNA [71] modified with zipcodes
EXPLORE platform	Cargo	Class II	Excellent platform to load proteins to be delivered to the cytosol of the target cell Expected better results than commercial solutions available	Limited loading capacity due to the presence of fluorescence reporter proteins in future work, this protein can be omitted	mCherry, Bax, SrIκB and Cre recombinase proteins [61]
TAMEL platform	Cargo	Class II	By selection of one component of the platform, the EV-enriched protein loading efficiency can be controlled	Highly cost-effective method Required highly experimented personal EE values depending on RNA molecule size	RNA [59] with variable length
Overexpression of RNA cargo into producing cells	Cargo	Class III	Used in all types of exosomes Applicable to all types of RNA	Nonspecific loading mechanism Low efficiency, especially for mRNA	RNA and proteins by expression of RNA into cell producer cytosol
Fusion with liposomes	Surface and/or cargo	Class III	High efficiency Both hydrophilic and hydrophobic compounds can be loaded	Cellular uptake rate can be decreased Better efficiencies for hydrophobic molecules	Hydrophobic and hydrophilic compounds, such as DiI and calcein respectively [72] Photosensitizer drugs, such as ZnPc [72]

GAPDH-siRNA specifically to neurons, microglia and oligodendrocytes in the brain resulted in a specific gene knockdown. This was considered the first example of EV-based genetic therapy. One of the most important facts of this work was the successful treatment of a highly protected tissue, the brain, in spite of the existence of brain–blood-barrier selectivity.

Tian et al. [68] used lysosome-associated membrane glycoprotein 2b to target electroporated doxorubicin-loaded exosomes (20% of loading efficacy) produced in dendritic cells. Ohno et al. [69] used platelet-derived growth factor receptor transmembrane domain to anchor GE11 peptide, a ligand of the epidermal growth factor receptor (EGFR). This construction was transfected to Human Embryonic Kidney cell line 293 (HEK293) using pDisplay vector and FuGENE HD transfection reagent. As a model cargo, siRNA let-7 was selected for its ability to alter cell-cycle progression and reduce cell division in cancer cells. This siRNA was introduced into EV producer cells by the lipofection method. Modified exosomes (15–21% of total released exosomes) were isolated by centrifugation and intravenously injected into an animal model with induced breast cancer. GE11 peptide as the targeting moiety was selected by the elevated expression of his receptor (EGFR) in tumours of epithelial origin.

More recently, Stickney et al. [62] developed another genetic engineering method for surface expression of proteins in human cells, called *surface display technology*. In this case, tetraspanin CD63 was used as a scaffold for the presentation in both extravesicular and intravesicular orientations.

Class II methods include a heterogeneous group of strategies that have in common the use of specific molecular interactions between two elements and can be used to transport the complex into the exosomes.

One example of this strategy is the interaction between specific sequences in RNA molecules and proteins that are present in the route of exosomes formation [16]. Highly observed sequence motifs into RNA types studied in EVs, called EXOmotifs, were found in mRNA [70] and miRNA [71]. Exosomes for Protein Loading via Optically Reversible protein–protein interactions (EXPLORs) and Targeted and Molecular EV Loading (TAMEL) are technologies based on the molecular interaction between certain types of proteins or between RNA special structures and specific proteins. Proteins of interest can also be loaded into the inner compartment of exosomes for their direct

Table 3. Post-isolation methods for cargo incorporation into EVs.

Cargo incorporation after the release of exosomes					
Method	EVs Modified component	Category of modification (according with Table 1)	Advantages	Disadvantages	Molecules incorporated
Co-incubation with exosomes	Cargo	Class IV	The simplest method Inexpensive Compatible with the addition of a small amount of organic solvent for the enhancement of hydrophobic drug dissolution	More suitable for hydrophobic molecules	Low- and medium-molecular-weight hydrophobic molecules such as curcumin [74], placlitaxel [95], cucurbitacin I [75], celastrol [76] and different porphyrins [58] Enzymes, such as catalase [80]
Electroporation	Cargo	Class Va	Used in all types of exosomes Able to incorporate large compounds, such as 5 nm NPs	Applicable only for hydrophilic compounds RNA type-dependence effectiveness Slight differences in EE depending on the cellular origin (cell line) of the exosomes Induce aggregation of siRNA, with valuable reduction in EE. Exosome aggregation trend during electroporation process	RNA, especially siRNA [67] Different drugs such as placlitaxel [60], porphyrins [58] SPIONs [79]
Extrusion	Cargo	Class Va	Simple method	Induces changes in EVs which reduce delivery efficiency	Small molecules such as Porphyrins with different hydrophobicity [58] Enzymes, such as catalase [80]
Saponin-assisted loading	Cargo	Class Va	Similar loading efficiency to electroporation, but without the associated problems Saponin can enhance in some cases the efficiency of co-incubation	Low efficiency for some large molecules, but better than simple incubation	
Hypotonic dialysis	Cargo	Class Va		Not tested with large molecules	
Sonication	Cargo	Class Va	Enhance simple incubation through decreasing bilayer rigidity	Not tested with hydrophilic molecules Not tested with different EV populations	Small molecules such as placlitaxel [95] or Doxorubicin Enzymes, such as Catalase [80]
Click chemistry	Surface	Class Vb	Keep constant morphology or functionality of EV properties Applicable to any molecule previously modified	A two-step procedure with subsequent purification steps to remove unbound molecules and activate agents	Fluorescent dyes such as azide-Flour 545 [81] Potentiality to any type of molecule susceptible to being modified by azide groups
Fusion with liposomes	Surface and/or membrane				Lipids with different chemical nature [85] (zwitterionic, cationic, anionic, PEGliated, etc.)

delivery to the cytosol of the target cell as an alternative for therapeutic target locations. EXPLORs [61] has recently presented for that purpose. The system integrates two elements: one is produced by the genetic fusion of the photoreceptor cryptochrome 2 (CRY2) to the protein to be loaded, and the other is made by the fusion of a truncated version of the CRY-interacting basic-helix-loop-helix 1 (CIBN) to tetraspanin CD9. Both elements can be transitorily attached by exposure to blue light, which induces the interaction between CRY and CIBN, and the interaction can be stopped once the blue light is not present.

TAMEL is another genetic engineering tool that has recently been published [59] for the active cargo of RNA. This platform is a fusion between an engineered EV-loading protein and the RNA to be loaded. Engineered EV-loading protein is also a fused product between an EV-enriched protein and an RNA-binding domain. This construction is transfected into EV producer cells to make his function. Different loading degrees can be obtained by selecting the EV-enriched protein. This is related to the natural expression of different proteins into EVs.

Class III methods includes the simplest method: passive loading into vesicles through their biogenesis. There can be two different approximations to this objective. First, the overexpression of RNA cargo in the producer cells. The major disadvantage of this method is the lack of selectivity in the loading process, since it is gradient-driven (the higher the concentration in the cytoplasm, the higher its possibility of being trapped into exosomes during invagination of MVB formation). On the other

hand, the great advantage of the method is that by translation of mRNA into receptor cell cytoplasm, codified proteins can also be passively loaded into EVs.

The second approximation explores the active loading of the producer cells, i.e. by nanocarriers such as fusogenic liposomes. This strategy is based on physico-chemical properties that govern the type of mechanism (the fusiogenic properties of the two elements that take place in the method, cells and liposomes). Second, they modify the whole cell and not only the exosomes.

As an alternative method for the incorporation of exogenous molecules (specially designed for hydrophobic compound) into EVs, Lee et al. [72] presented the use of membrane fusogenic liposomes (MFLs). By the treatment of cells with MFLs loaded with a hydrophobic compound (DiI) and a hydrophilic molecule (calcein), these authors obtained EVs modified with both molecules. Only slight differences in the efficiency of incorporation into EVs were found, since a hydrophobic compound would remain in the plasma membrane after liposome fusion and in the subsequent formation of EVs membrane through their routes of biogenesis. In contrast, a hydrophilic molecule would be released into the cytosol. Intercellular transport of both molecules mediated by EVs was successfully observed *in vitro* in a multicellular tumour spheroid model.

A similar method was used to modify the composition of EVs, with a special focus on the modification of the properties of the EV membrane [57]. Dyes, fluorescent lipids with different lengths and saturation grade of acyl chains, and chemotherapeutics were loaded into cells by means of EVs.

These authors also carried out a membrane surface modification, with the possibility of conjugation with molecules for targeting purposes. They first prepared MFLs containing azide-modified lipids which were fused with cells. By simple incubation with dibenzocyclooctyne (DBCO)-modified peptides, a covalent bond was created due to the fast and selective reaction between DBCO and the azide group [73]. This strategy will allow new possibilities of surface ligand decoration on EVs for targeting purposes (such as peptides, aptens or antibodies) or for the introduction of molecules with therapeutic properties via interaction with selective receptors. By the combination of a different headgroup modified lipids, several different ligands could be incorporated into EV outer membranes, including receptors and co-receptors.

Physical and chemical post-isolation modifications

These are the methods that require an external force (chemical or physical) to incorporate new molecules on previously isolated exosomes (Table 3).

Passive methods. Incubation of EVs and cargo. The simplest way to incorporate any cargo into cell culture or body fluid isolated EVs is the co-incubation of both elements. This strategy was explored by Sun et al. [74], who found that curcumin exosome-loaded exhibited a better stability and higher bioavailability in serum in an animal model. For these therapeutic-modified exosomes, an improvement in *in vivo* anti-inflammatory and septic shock was observed.

In another study [75], two anti-inflammatory compounds were loaded into exosomes and microparticles, and they were administrated intranasally, opening up new therapeutic possibilities. The effects of solvents and drug release kinetics from loaded exosomes by dialysis have been studied [39,76].

Active methods. Physical methods: electroporation and other temporary membrane disruptive methods. The most commonly used method for cargo incorporation into EVs after their release is electroporation [77]. This technique involves the temporary permeabilization of membranes through the creation of pores due to the application of high-voltage electricity. Some authors have pointed out that this method is not suitable for siRNA cargo into EVs due to technical problems, and an overestimated encapsulation into EVs could be observed. It has been reported that electroporation induces siRNA aggregation and co-pelletization with EVs during purification by ultracentrifugation, without any dependence on electroporation buffer composition [78]. They also postulated that slight differences could be found between different EVs regarding their cellular origin (e.g. primary cells).

Another relevant problem concerning electroporation is exosome aggregation and subsequent decrease in functionality. To avoid these problems, Hood et al. [79] electroporated exosomes from mouse B16-F10 melanoma cells by incorporating 5 nm superparamagnetic iron oxide nanoparticles (SPIONs) as model exogenous cargo. Other authors compared the loading efficiency of different porphyrins with different hydrophobicities into EVs with various origins by passive loading (co-incubation), and by active loading, such as electroporation, extrusion, saponin-assisted drug loading and hypotonic dialysis [58]. The best results were obtained for hydrophobic compounds and for electroporation. Interestingly, zeta potential (ζ) related to the chemical composition of EV membranes seems to play a role in loading efficiency, since higher ζ values led to higher EE. The chemical properties of cargo are

also relevant, since their charge will condition the final outcome. Electroporation did not induce drug precipitation.

In contrast, extrusion over polycarbonate membranes altered the morphology of vesicles and, subsequently, their delivery efficacy. Other authors used the sonication of EVs in the presence of drug solutions [60].The loading efficacy was found to follow the order: incubation at RT < electroporation ≪ mild sonication. A similar trend was observed for size changes after the loading procedure. On the other hand, surface charge and protein profile were similar after loading, evidencing no alteration in exosome stability. These authors explained the results concerning sonication as a decrease in bilayer rigidity after sonication, which allowed a better incorporation of the hydrophobic drug. Therefore, mild sonication should be considered as an enhancement of co-incubation. Additionally, loaded exosomes were stable over large periods of time at different temperatures.

A similar comparative study was carried out with the enzyme catalase [80]. For the preparation of exosomes modified with this oxidative stress-protecting agent used for the treatment of Parkinson's disease, these authors selected four methods: incubation at RT in the presence/absence of saponin, freeze/thaw, sonication and extrusion. Sonication yielded the higher EE (26.1%) and the more stable product. In contrast, this method also produced the higher increment in size, from 105 nm naïve exosomes to 183.7 nm in catalase-loaded exosomes. Associated with size increment, AFM observation also revealed a change in morphology, with a final non-spherical shape.

Despite these promising results regarding the encapsulation of different molecules into exosomes, standardization in systematic conditions followed by the study of several cell lines is still necessary to strongly support the use of these methods as routine practice in the clinical field.

Chemical methods: click chemistry mediated functionalization and other targeted drug-delivery strategies. The chemical copper-catalysed reaction between an alkyne and an azide that forms a triazole linkage (*click chemistry*) has been used for the surface functionalization of exosomes [81]. These were first chemically modified by the incorporation of alkyne groups into amine groups from proteins by carbodiimide chemistry [82]. These authors conjugated azide-Fluor 545 (a fluorescent compound) to activated EVs. Since no differences in morphological and functional properties were found, it was concluded that modification by *click chemistry* does not alter exosome characteristics and allows the incorporation of exogenous molecules to the surface of EVs.

Finally, there is another type of cargo modification that has been applied into artificial vesicular systems (liposomes) with potential applicability to EVs. This method is based on the ability of some peptides to be incorporated into lipidic membranes causing disruption [83,84]. By fusion of the peptide D1-7 to an adhesion molecule expressed in cells, targeted lipidic carriers with therapeutic cargo were produced and successfully tested *in vitro* and *in vivo*. Another interesting application of this strategy is its ability to insert peptidic cargo into live cell membranes, giving possibilities of imaging live cells and modifying cell surfaces. This last property could be explored for the modification of plasma membrane in EV producer cells.

The modification of EV membranes results in changes in surface charge, fusiogenic properties, immunogenicity decrease and colloidal stability [85]. Engineered hybrid exosomes were prepared by membrane fusion with liposomes formulated with different types of lipids (i.e. zwitterionic, anionic, cationic and PEGlilated). Fusion properties with cell-culture-derived exosomes were studied according to the chemical nature of liposome lipids [86]. It was found that zwitterioninc and anionic lipids did not alter the uptake rate, while the introduction of cationic lipid greatly decreased the phenomena, and PEGilated lipid increased it by twofold. Therefore, it can be concluded that functional properties could be tuned by modifying the membrane composition.

Top-down and bottom-up methods for the development of full synthetic EVs

Production of artificial EVs by generation of plasma membrane fragments: a top-down-inspired methodology

Different approaches based on top-down nanotechnology have been developed for the production of EVs mimetic nanovesicles using cells as precursors of plasma membrane fragments. Those strategies rely on the principle of self-assembly of lipids and lipid membranes into spherical structures and the encapsulation of surrounding material into the aqueous cavity of generated nanovesicles. Current methods include extrusion over membrane filters [16,17,87], hydrophilic microchannels [88] or cell slicing by Si_xN_y blades [18] (see Table 4).

Extrusion over polycarbonate membrane filters

Jang et al. [16] used a serial extrusion through polycarbonate membrane filters with decreasing pore sizes

Table 4. Summary of the published work about the generation of mimetic EVs nanovesicles by top-down bio-nanotechnology (cell source and type of cargo are encapsulated, and main characteristics are given).

Generation technique	Precursor cell type	Type of material encapsulated	Nanovesicles characteristics	Reference
Manual extrusion over polycarbonate membrane filters	Monocytes and macrophages	Exogenous, chemotherapeutic drugs	Mean size and distribution similar to that of exosomes Exosomal protein profile similar to that of natural exosomes EE of chemotherapeutics dependent on the original amount used during extrusion High rate of drug release 100 times more that of nanovesicles than exosomes from the same number of cells Results reproducible with different cell types	[16]
Pressurization and extrusion over hydrophilic parallel microchannels in a microfluidic device	Murine embryonic stem cells	Endogenous, proteins and RNA	Average size in the exosome range Similar intracellular and membrane protein and total RNA profile to the original cells and exosomes Same ability to deliver RNA content as exosomes	[88]
Centrifugal force and extrusion over a filter with micro-size pores into a polycarbonate holder structure	Murine embryonic stem cells	Endogenous, proteins and RNA	NVs size and morphology similar to exosomes Cargo of RNA, intracellular proteins and plasma membrane proteins similar in types to exosomes Small RNA profile differs in quantity, especially in miRNA with respect to exosomes Intravesicle contain twice the concentration of natural exosomes 250 times more vesicles than naturally secreted exosomes	[87]
Slicing living cell membrane with silicon nitride blades in a microfluidic device	Murine embryonic stem cells	Exogenous, polystyrene latex beads	Generated NVs in the size range of exosomes Nanovesicle production 100 times more productive than natural exosome 30% of EE for 22 nm nanoparticles as model of exogenous material encapsulation NVs can deliver exogenous encapsulated material	[18]

(10 μm, 5 μm and 1 μm) in a mini-extruder, similar to those commonly used for the preparation of liposomes. Human monocytes were chosen as precursors for membrane fragments. The yield production of NVs was 100-fold in comparison with the production of exosomes by using the same number of cells. Morphological studies of these NVs by crio-TEM and NTA showed many similarities with the exosomes, round shape and a peak diameter around 130 nm. Even the exosomal protein marker profile (CD63, Tsg101, moesin and beta-actin) checked by Western blot was identical for the NVs and exosomes. The chemotherapeutic drugs, doxorubicin, 5-FU, gemcitabine and carboplatin were added to the buffer where cells were resuspended. The encapsulation efficiency in the final purified NVs was found to be dependent on the initial amount of added drug.

Looking for a scaled-up process using extrusion as the generation procedure of NVs, Jo et al. [87] developed a device that uses centrifugal force to extrude cells over polycarbonate filters (10 μm and 5 μm pore sizes). The device has a central piece where filters are located and connected to two syringes where the sample is dispensed by the centrifugal force. Uniformly sized 100 nm NVs with a yield 250-fold higher than that of exosomes from the same number of cells was achieved. Analysis of the filters by TEM showed that many cells remained trapped in the structure.

The same device previously cited was employed by Jeon et al. [17] to produce exosome-mimetic NVs from murine embryonic stem cells for the treatment of mice isolated skin fibroblasts. These authors wanted to explore the potential of mimetic exosomes to induce proliferation and recovery after injury in an *in vitro* model. Genomic and proteical profiles similar to original cells were assessed by PCR and Western blotting of specific markers, and it was confirmed that successful delivery of genetic material by NVs was reached.

Pressurization, extrusion and slicing over hydrophilic parallel microchannels in a microfluidic device

Jo et al. [87] produced exosome-mimetic nanovesicles by extruding cells over hydrophilic microchannels, with the aim of delivering endogenous RNA across the plasma membrane with high efficiency and low toxicity. These authors developed a microfluidic device made of PDMS by soft lithography. This device had an array of 37 parallel microchannels, with a common inlet and outlet connection for the pumping with a syringe pump and the collection of NVs, respectively. The higher amount of nanovesicles generated by extrusion over hydrophilic channels with a similar size to exosomes was obtained with a length of 200 μm and a width of 5 μm. These results showed that an appropriate total shear force induced by the channel has to be reached in order to produce NVs with acceptable results. This force is responsible for NV generation due to elongation of the plasma membrane on the microchannel surface. When the elongated membrane reaches a certain value, it breaks into small portions

that directly form nanovesicles, thanks to the self-assembly property of lipids in aqueous media.

With the appropriate channel morphology, these authors produced 100 nm nanovesicles similar in composition (proteinical and nucleic acid profile) to naturally produced exosomes. The analysis of these NVs [88] revealed that the formation of exosome-like NVs through hydrophilic channels produced a delivery system of endogenous material with identical results to those with exosomes.

More recently, Yoon et al. [18] reported the production of exosome-mimetic nanovesicles by the slicing of cells through Si_xN_y blades aligned to the flow direction over hydrophilic microchannels. These authors combined the induced shear stress formation on NVs with the fragmentation of plasma membrane by the blades to obtain fragments for the generation of exosome-like nanovesicles and the co-encapsulation of exogenous material (polystyrene latex beads as a model substance). It was found that NV diameter increased as the width channel increased. This is because channel morphology is proportional to the Reynolds number (*Re*). In this particular case, *Re* is proportional to the hydraulic diameter and, therefore, to the inertial force, which directly increases with the channel width. In other words, NVs travelling through wide channels have a higher inertial force when they reach the blades, generating larger sliced fragments that produce larger NVs. These have a similar composition to that of parental cells and naturally released exosomes by those cell lines.

One of the most interesting works in the literature [18] describes the encapsulation of 22 nm fluorescent polystyrene latex beads as an exogenous simulated material, adding these nanoparticles to the media where cells were diluted before slicing. With a final corrected EE of 30%, these NVs containing exogenous material were given to fibroblasts in an *in vitro* experiment. After a period of time, red dots corresponding to fluorescent beads were detected in the cytoplasm of fibroblast by confocal microscopy. The delivery efficiency of encapsulated beads into exosome-like NVs was higher than that of bead-aggregated NVs, revealing that exogenous material delivery with these NVs was possible, but the efficiency was still lower than that achieved with parental cell-component generated NVs.

Bottom-up methodologies: artificial membranes decorated with functional proteins to mimic EV functions

The third option for obtaining artificial EVs is their construction in a fully synthetic way by assembling individual molecules (lipids, proteins and cargo) into complex structures, such as a bilayer structure resembling EV membranes functionalized with proteins for mimicking EV functions. This could be achieved by assuming that not all components in natural exosomes are essential for specific and efficient delivery [13], including the transport of a message through direct contact with target cell receptors. Another assumption that encourages researchers to explore this route is that, from a structural and biochemical point of view, exosomes are liposomes with attached proteins. Therefore, this type of vesicular system could be an ideal substrate to develop exosome-mimetic structures. The main functional components of exosomes to be incorporated in mimetic materials have been reviewed [13]. The three main components of exosomes reported were lipids, membrane proteins and therapeutic cargo.

One of the main advantages of fully artificial EVs over previous strategies is the production of pure and well-defined biomaterial. In addition, production strategies of artificial EVs based on liposomes are more sustainble and easier to scale up [11,89]. This fact is quite important for preclinical and clinical studies and in order to manufacture products ready to be sent to the market [2].

Liposome preparation techniques have been extensively reviewed [89–101], but not all the methods yield vesicles suitable for becoming an artificial exosome. It could be considered that only small unilamellar vesicles (SUVs) are ideal precursors due to their similarities to natural exosomes (size range and membrane disposition).

Methodologies for SUV preparation (Table 5) can be classified according to different criteria [92]. For example, number of steps to reach SUV. Another classification is based on the physical principle applied to prepare vesicles: mechanical processes, organic solvent replacement, detergent removal and other techniques as microfluidic-based methods. Reverse-phase evaporation, ethanol injection method, ether injection method (EtIM), thin-film hydration method (TFH), homogenization techniques, French press cell extrusion, microfluidization, extrusion over membranes, ultrasound and membrane contactors are some of the techniques developed for SUV preparation.

All these techniques rely on the self-assembly of amphiphilic molecules, such as lipids, in ordered structures due to their physicochemical behaviour in aqueous media [93,94]. This principle is the basis of bottom-up nanotechnology. Vesicles with a size range similar to that of natural EVs could be obtained [95]

Table 5. Advantages and disadvantage of most frequently used methods for small unilamellar vesicles (SUVs) preparation.

Method	One-step method for SUVs preparation	Physical method applied for preparation	Advantages	Disadvantages
Ether injection method	Yes	Organic solvent replacement	Scale-up adapted High hydrophobic compound encapsulation No mechanical degradation of compounds	Not suitable for thermosensitive compounds Solvent not suitable for some biocompounds
Ethanol injection method	Yes	Organic solvent replacement	Scale-up adapted Non-dangerous substances are handled High hydrophobic compound encapsulation No mechanical degradation of compounds	Ultrasounds are needed when concentrated samples are produced Low encapsulation efficacies of low-molecular-weight hydrophilic compounds Not suitable for thermosensitive compounds
Reverse-phase evaporation	No	Emulsification/organic solvent replacement	Widely used Suitable for mass production	Frequently used solvents are not suitable for some biocompounds
Thin-film hydration method	No	Mechanical processes	Applied for any type of amphiphilic molecules High encapsulation of Hydrophilic compounds compared to other methods	Difficult to scale up production Timely and cost-ineffective due to necessary downsizing techniques
Downsizing Techniques French press cell extrusion Microfluidization Extrusion over membranes	/	Mechanical processes	Good reproducibility Adapted to scale-up requirements	Product loss associated with clogging of membrane by concentrated samples
Ultrasounds	Yes	Mechanical processes	Simple methodology Possibility of being scaled up	Degradation of biological compounds Scale-up unadapted

when operational variables were oprtimized by design of experiments. In addition, a wide spectrum of molecules with biological activity, independently of their physicochemical nature (hydrophilic or hydrophobic, low molecular weight or macromolecules), can be incorporated into liposomes, during or after their formation [96].

Functionalization of liposomes with biomolecules is possible, owing to the different headgroup-modified lipids that are available [97]. Headgroup modification usually includes a molecule of polyethylene glycol as a spacer between the functional group and the polar region of the lipid. This avoids the sterical hindrance caused by the proximity of biomolecules and liposome surface. The chemical modification includes the introduction of different types of functional groups, such as biotin, amine, maleimide, carboxylic acid, folate, cyanur, DBCO, azide and succinyl groups. These groups determine the crosslinking strategy [98–101] which should not compromise the biological function. Bioconjugation should ideally be carried out under mild conditions, aqueous media and chemoselectivity, and with a high yield.

Successful conjugation of peptides/proteins with liposomes can be checked using conventional molecular biology techniques such as dot-blot [15], SDS-PAGE [102] or even flow cytometry [102]. A preliminary purification step is required in order to remove unconjugated biomolecules. For this purpose, the authors have used classical separation methods, such as ultracentrifugation [102] or gel filtration [15,103] (SEC) with high exclusion limit resins (Sepharose CL-2B, 4B mainly). Dialysis, however, is not used due to the high molecular weight of biomolecules selected for mimicking exosomes.

Undecorated liposomes have also been used in the EV research field as EV models for comparing isolation efficacy and physical integrity [47], detection by flow cytometry [104] and EV refractive index study [105]. However, their use as a scaffold for artificial EV development could offer new possibilities in basic research about EVs and theranostic applications. To date, there have been few examples of this approximation for the development of mimetic exosomes, and no comparative results are available owing to the great differences between the methods used. A summary of the main experimental work on mimicking exosomes by bottom-up nanotechnology is given in Table 6 and briefly commented on below.

The most frequent preparation technique for SUVs as templates for EVs mimicking is the TFH method combined with extrusion over polycarbonate membranes and with [102] or without [15] previous freeze–thaw cycles. Martínez-Lostao et al. [102] had a formulation that included lipids and stoichiometry inspired in natural exosomes. The introduction of only 5% (w/w) of an iminodiacetic acid derivative or DOGS-NTA allowed the binding of APO2L/TRAIL-

Table 6. Summary of published work about the development of mimetic EVs nanovesicles by bottom-up bio-nanotechnology, showing formulation of the vesicles, molecules for the surface functionalization and main physical characteristic (size).

Formulation	Preparation method	Conjugation strategy	Size	Protein for functionalization	Reference
PC:SM:Cho:DOGS-NTA (55:30:10:5) weight ratio For fluorescent labelling, 0.25% mole/mole DSPE-RhodB	Thin-film hydration method (KCl 100 mM, HEPES 10 mM pH 7.0, EDTA 0.1 mM; KHE buffer) Filtered and degassed + extrusion over 200 nm membranes	Ni^{2+}-NTA headgroup functionalized lipid + histidine-tagged recombinant peptides 37°C, 30 min	150–200 nm	APO2L/TRAIL-His_{10}	[102]
PC:Cho:DSPE-PEG:DSPE-PEG-MAL (1:0.5:0.04:0.01) Molar ratio For fluorescent labelling, 1% of PC amount of DSPE-RhodB	Thin-film hydration method (Hepes 25mM, NaCl 140mM; pH 7.4) Filtered and degassed + extrusion over 100 nm membranes	Maleimide headgroup functionalized lipid + Traut's reagent protein activation 1h RT 20/1 ratio	100 nm	MHC class I peptide complexes and FAB regions against T-cell receptors (adhesion, early and late activation and survival)	[15]
Micro-emulsion phase PC:CpEL (7:3, w/w) Micelle phase In 10:1 v/v DE:A DOPE:DC-Cho (4:1, w/w) In 1:2 v/v EtOH:DW	Micro-emulsion and micelle combining method + sonication step for 3min	Carboxilic group from ChoS and amine group from protein EDC/NHS 4°C for 12 h	82 nm	Monoclonal antibody against DEC205 antigen expressed on dendritic cells	[103]

His_{10} to liposomes in a single step. Its bioactivity was a higher activity than that of the soluble ligand. Moreover, a treatment based on these synthetic exosomes achieved 60% of disease improvement in a rheumatoid arthritis-induced animal model. In another study, liposome-bound Apo2L/TRAIL overcame the resistance to the soluble ligand exhibited by chemorresistive tumour cell mutants [106]. The mechanism of action of LUV-TRAIL in haematologic cells [107] was also studied using mimetic structures of exosomes.

Another approximation to artificial EVs (exosomes) for therapeutic purposes was carried out by De la Peña et al. [15] using a reported formulation [108,109]. The main components were phosphatidylcholine and cholesterol, and headgroup-modified lipids such as DSPE-PEG DSPE-PEG-MAL. In order to make traceable NVs, both *in vivo* and *in vitro*, a fluorescent lipid was included in the formulation, and magnetic nanoparticles (SPIONs) were encapsulated during a thin-film hydration step. After optimization of chemical-activated ligands binding, mimetic SNVs simulating DCs derived exosomes were successfully tested as new tools in basic and clinical immunology. A T-cell expansion rate higher than that with previously reported experiments using conventional methods was achieved.

An innovative methodology for the production of protein encapsulated nanoliposomes was also reported [103]. This produced 82 ± 4 nm antibody-coated liposomes with approximately 93% EE of BSA. The preparation route that combined a micro-emulsion contained the protein to be encapsulated, with micelles, in order to create a lipid bilayer formed through layer-by-layer assembly. In this work, the authors selected a Box–Behnken experimental design to optimize (maximize) the EE by adjusting some formulation parameters. The final optimized formulation is summarized in Table 6. In this particular case, researchers selected mimetic exosomes for the potential transmission of antigen to DCs by a controlled target delivery using a conjugated monoclonal antibody anti-DEC205, a highly expressed receptor on the surface of DCs. The introduction of cholesterol succinate in the outer layer of the liposomes allowed the bioconjugation of the Ab by EDC/NHS chemistry.

Despite the promising results and the advantages of these methods for the development of liposome-based artificial EVs, there are several limiting aspects that hinder the transfer to the clinical field. While technological progress has allowed the design, development and production of nanomedicines with high pharmaceutical grade, their clinical impact has been smaller than expected due to a lack of sufficient information about *in vivo* interactions and fates inside the human body [11]. Specific challenges [13] are related to the functionalization of vesicle surface with a combination of functional proteins at the same time because actual methodologies are time-consuming and because of the incorporation of nucleic acids with acceptable efficiencies. The dependence of vesicle formulation on parameters such as fusion properties and stability could be another limit of special relevance to immunotolerance. Finally, the knowledge about key components in exosomes is not yet complete, since they may vary from one cell line to another. They could even be health-state-dependent and sensitive to harvesting conditions.

Despite attempts to mimic the exosome natural lipid composition, there is a need for actually checking whether the formulation is active and involved in the expected functions or is just a passive element involved only in the scaffolding of true functional elements. Comparison of the efficiency of the intended integrated component in differently formulated vesicles could be an interesting experiment to elucidate the role of membrane components. Parameters of uptake route and incorporation efficiency could also be measured with different cell lines, in order to assess the role of the target cell. Other compounds as an alternative to lipids, with a high grade of biocompatibility, could also be used for the formulation of artificial exosome bilayers. One option is to use non-ionic surfactants [110] for the preparation of niosome-based artificial exosomes. These compounds offer several advantages [111] over lipids, such as price, versatility and sustainability. On the other hand, their chemical structure offers enhanced stability from both a chemical and physical point of view. Niosomes with a size range close to that of EVs can also be produced [95].

In recent years, microfluidics has been playing an important role in the development of enhanced vesicular systems, enabling robust and highly controlled preparation routes of vesicles [112] and allowing rapid characterization of products [113]. Another important aspect in the development of exosome-based therapy, regarding any preparation route, is the creation of reduced systems for the study of traffic and delivery into in vivo microenvironments [19]. Again, microfluidic-based systems are opening up new possibilities by the development of organ-on-a-chip platforms that enable the study of these processes in an innovative and highly efficient way [114].

It is expected that microfluidic synthesis of nanovesicles will open the path for new artificial EV routes, with the required control of size and EE, and minimal consumption of reagents.

Other recently explored drug-delivery systems have developed platelet-mimetic nanoparticles by also using bottom-up technology. These authors have produced unilamellar polymeric nanoparticles functionalized with immunomodulatory and adhesion antigens, and they have tested them as another approach to disease-targeted delivery [115].

Conclusions and future perspectives

Knowledge about all the biological aspects related with EVs, especially exosomes, has opened up new frontiers in the clinical field. After an explosion of publications in recent years about the role of EVs in physiological and pathological conditions, novel opportunities for the development of enhanced therapeutic biomaterials have arisen. These observations could help in the production of new materials inspired by natural vesicles, without the classical inconveniences associated with up-to-date synthetic alternatives (liposomes, polymersomes, inorganic nanoparticles, etc.). EV-based therapies include tissue regeneration or immunomodulation, but drug delivery is one of the most promising applications. Production, isolation, modification and purification at a large-scale clinical grade are the main limitations of EVs becoming a true clinically settled therapeutic agent.

These limitations have promoted the development of mimetic materials inspired by EVs, the so-called artificial EVs. In this article, we have introduced a systematic classification of the types of artificial EVs according to their preparation routes. Two well-defined strategies have been developed: semi-synthetic or fully synthetic products. The first strategy uses natural exosomes as precursors that are modified at the moment of their biogenesis (pre-isolation modifications), whereas the second strategy modifies the vesicles after their release by cells and their isolation from cultured media or biological fluids. Genetic engineering-based modifications, active loading platforms, specific signalling sequences for selective sorting or precursor cell modifications with nanomaterials are some of the methods developed for exosome-based semi-synthetic nanovesicle production.

Fully synthetic vesicles with EVs mimetic properties can be produced by bio-nanotechnology. Top-down techniques that produce vesicles made of membrane fragments obtained from the extrusion or slicing of cells, or bottom-up techniques that take advantage of supra-molecular chemistry (mainly self-assembly) to produce vesicles from individual molecules, represent the technology developed for that purpose.

Despite the great potential of artificial EVs, some limitations to their development as therapeutic tools have been identified. There is no perfect technique, and, depending on the final purpose of artificial EVs, combinations of procedures could offer new insights in the field. Systematic studies with different cellular origins and target cell lines would expand and consolidate the applications of artificial exosomes. Comparative work including the encapsulation into different artificial vesicles would be interesting in order to identify effects due to the carrier.

Multidisciplinary teams with complementary actions in the fields of applied biology, pharmacology, chemical engineering, material sciences and medicine would allow the definitive consolidation of these therapeutic biomaterials in clinical routines.

Highlights

- A new systematic classification of artificial EVs is provided.
- Bio-engineering modification of naturally released exosomes is summarized.
- Relevant examples in pre- or post-released modifications are presented.
- Bio-nanotechnological methods for fully artificial EVs generation are compelled.

Acknowledgements

This work was supported by the Ministerio de Economía y Competitividad (MINECO, Spain), under the Grant CTQ2013-47396-R. This study was also financed by the Consejería de Economía y Empleo del Principado de Asturias (Plan de Ciencia, Tecnología e Innovación 2013-2017), under the Grant GRUPIN14-022. Support from the European Regional Development Fund is gratefully acknowledged.

Disclosure statement

No potential conflict of interest was reported by the authors.

Funding

This work was supported by the Consejería de Economía y Empleo del Principado de Asturias [GRUPIN14-022]; Ministerio de Economía y Competitividad (MINECO, Spain) [CTQ2013-47396-R].

ORCID

Pablo García-Manrique http://orcid.org/0000-0003-2489-5753
María Matos http://orcid.org/0000-0002-6980-0554
Gemma Gutiérrez http://orcid.org/0000-0003-2700-4944
Carmen Pazos http://orcid.org/0000-0002-6894-7693
María Carmen Blanco-López http://orcid.org/0000-0002-9776-9013

References

[1] Yáñez-Mó M, Siljander PRM, Andreu Z, et al. Biological properties of extracellular vesicles and their physiological functions. J Extracell Vesicles. 2015;4:27066.
[2] Lener T, Gimona M, Aigner L, et al. Applying extracellular vesicles based therapeutics in clinical trials – an ISEV position paper. J Extracell Vesicles. 2015;4:30087.
[3] Tran TH, Mattheolabakis G, Aldawsari H, et al. Exosomes as nanocarriers for immunotherapy of cancer and inflammatory diseases. Clin Immunol. 2015;160:46–58.
[4] Aline F, Bout D, Amigorena S, et al. *Toxoplasma gondii* antigen-pulsed-dendritic cell-derived exosomes induce a protective immune response against *T. gondii* infection. Infect Immun. 2004;74:4127–4137.
[5] Dalal J, Gandy K, Domen J. Role of mesenchymal stem cell therapy in Crohn's disease. Pediatr Res. 2012;71:445–451.
[6] Lamichhane TN, Sokic S, Schardt JS, et al. Emerging roles for extracellular vesicles in tissue engineering and regenerative medicine. Tissue Eng Part B Rev. 2015;21:45–54.
[7] Batrakova EV, Kim MS. Using exosomes, naturally-equipped nanocarriers, for drug delivery. J Control Release. 2015;219:396–405.
[8] Tan A, Rajadas J, Seifalian AM. Exosomes as nano-theranostic delivery platforms for gene therapy. Adv Drug Deliv Rev. 2013;65:357–367.
[9] van Dommelen SM, Vader P, Lakhal S, et al. Microvesicles and exosomes: opportunities for cell-derived membrane vesicles in drug delivery. J Control Release. 2012;161:635–644.
[10] Ha D, Yang N, Nadithe V. Exosomes as therapeutic drug carriers and delivery vehicles across biological membranes: current perspectives and future challenges. Acta Pharm Sin B. 2016;6:287–296.
[11] van der Meel R, Fens MHAM, Vader P, et al. Extracellular vesicles as drug delivery systems: lessons from the liposome field. J Control Release. 2014;195:72–85.
[12] El Andaloussi S, Lakhal S, Mäger I, et al. Exosomes for targeted siRNA delivery across biological barriers. Adv Drug Deliv Rev. 2013;65:391–397.
[13] Kooijmans SAA, Vader P, van Dommelen SM, et al. Exosome mimetics: A novel class of drug delivery systems. Int J Nanomed. 2012;7:1525–1541.
[14] Lakhal S, Wood MJA. Exosome nanotechnology: an emerging paradigm shift in drug delivery. Bioessays. 2011;33:737–741.
[15] De La Peña H, Madrigal JA, Rusakiewicz S, et al. Artificial exosomes as tools for basic and clinical immunology. J Immunol Methods. 2009;344:121–132.
[16] Jang SC, Kim OY, Yoon CM, et al. Bioinspired exosome-mimetic nanovesicles for targeted delivery of chemotherapeutics to malignant tumors. ACS Nano. 2013;7:7698–7710.
[17] Jeong D, Jo W, Yoon J, et al. Nanovesicles engineered from ES cells for enhanced cell proliferation. Biomaterials. 2014;35:9302–9310.
[18] Yoon J, Jo W, Jeong D, et al. Generation of nanovesicles with sliced cellular membrane fragments for exogenous material delivery. Biomaterials. 2015;59:12–20.
[19] Forterre A, Jalabert A, Berger E, et al. Proteomic analysis of C2C12 myoblast and myotube exosome-like vesicles: A new paradigm for myoblast-myotube cross talk? PLoS One. 2014;9:e84153.
[20] Bryniarski K, Ptak W, Jayakumar A, et al. Antigen-specific, antibody-coated, exosome-like nanovesicles deliver suppressor T-cell microRNA-150 to effector T cells to inhibit contact sensitivity. J Allergy Clin Immunol. 2013;132:170–181.
[21] Regente M, Corti-Monzón G, Maldonado AM, et al. Vesicular fractions of sunflower apoplastic fluids are

associated with potential exosome marker proteins. FEBS Lett. 2009;583:3363–3366.
[22] Prado N, de Dios Alché J, Casado-Vela J, et al. Nanovesicles are secreted during pollen germination and pollen tube growth: A possible role in fertilization. Mol Plant. 2014;7:573–577.
[23] García-Manrique P, Gutiérrez G, Blanco-López MC. Fully Artificial Exosomes: towards New Theranostic Biomaterials. Trends Biotechnol. Forthcoming.
[24] Laulagnier K, Motta C, Hamdi S, et al. Mast cell- and dendritic cell-derived exosomes display a specific lipid composition and an unusual membrane organization. Biochem J. 2004;380:161–171.
[25] Simpson RJ, Kalra H, Mathivanan S. ExoCarta as a resource for exosomal research. J Extracell Vesicles. 2012;1:18374.
[26] Kim DK, Lee J, Simpson RJ, et al. EVpedia: A community web resource for prokaryotic and eukaryotic extracellular vesicles research. Semin Cell Dev Biol. 2015;40:4–7.
[27] Kalra H, Simpson RJ, Ji H, et al. Vesiclepedia: A compendium for extracellular vesicles with continuous community annotation. PLoS Biol. 2012;10:e1001450.
[28] Gimona M, Pachler K, Laner-Plamberger S, et al. Manufacturing of human extracellular vesicle-based therapeutics for clinical use. Int J Mol Sci. 2017;18:1190.
[29] Villarroya-Beltri C, Baixauli F, Gutiérrez-Vázquez C, et al. Sorting it out: regulation of exosome loading. Sem Cancer Biol. 2014;28:3–13.
[30] Yeo RWY, Lai RC, Zhang B, et al. Mesenchymal stem cell: an efficient mass producer of exosomes for drug delivery. Adv Drug Deliv Rev. 2013;65:336–341.
[31] Johnsen KB, Gudbergsson JM, Skov MN, et al. A comprehensive overview of exosomes as drug delivery vehicles—endogenous nanocarriers for targeted cancer therapy. Biochim Biophys Acta Reviews Cancer. 2014;1846:75–87.
[32] Lai RC, Yeo RWY, Tan KH, et al. Exosomes for drug delivery—a novel application for the mesenchymal stem cell. Biotechnol Adv. 2013;31:543–551.
[33] Lamparski HG, Metha-Damani A, Yao JY, et al. Production and characterization of clinical grade exosomes derived from dendritic cells. J Immunol Methods. 2002;270:211–226.
[34] Klippstein R, Pozo D. Nanotechnology-based manipulation of dendritic cells for enhanced immunotherapy strategies. Nanomed Nanotechnol Biol Med. 2010;6:523–529.
[35] Bianco NR, Kim SH, Ruffner MA, et al. Therapeutic effect of exosomes from indoleamine 2,3-dioxygenase–positive dendritic cells in collagen-induced arthritis and delayed-type hypersensitivity disease models. Arthritis Rheumatol. 2009;60:380–389.
[36] Hee Kim S, Bianco N, Menon R, et al. Exosomes derived from genetically modified DC expressing FasL are anti-inflammatory and immunosuppressive. Mol Ther. 2006;13:289–300.
[37] Mahaweni N, Lambers M, Dekkers J, et al. Tumour-derived exosomes as antigen delivery carriers in dendritic cell-based immunotherapy for malignant mesothelioma. J Extracell Vesicles. 2013;2:22492.
[38] Ban JJ, Lee M, Im W, et al. Low pH increases the yield of exosome isolation. Biochem Biophys Res Commun. 2015;461:76–79.
[39] Munagala R, Aqil F, Jeyabalan J, et al. Bovine milk-derived exosomes for drug delivery. Cancer Lett. 2016;371:48–61.
[40] Zhang M, Viennois E, Xu C, et al. Plant derived edible nanoparticles as a new therapeutic approach against diseases. Tissue Barriers. 2016;4(2):e1134415.
[41] Raimondo S, Naselli F, Fontana S, et al. Citrus limon-derived nanovesicles inhibit cancer cell proliferation and suppress CML xenograft growth by inducing TRAIL-mediated cell death. Oncotarget. 2015;6:19514–19527.
[42] Pérez-Bermúdez P, Blesa J, Soriano JM, et al. Extracellular vesicles in food: experimental evidence of their secretion in grape fruits. Eur J Pharm Sci. 2017;98:40–50.
[43] Witwer KW, Buzás EI, Bemis LT, et al. Standardization of sample collection, isolation and analysis methods in extracellular vesicle research. J Extracell Vesicles. 2013;2:20360.
[44] Sunkara V, Woo HK, Cho YK. Emerging techniques in the isolation and characterization of extracellular vesicles and their roles in cancer diagnostics and prognostics. Analyst. 2016;141:371–381.
[45] Liga A, Vliegenthart ADB, Oosthuyzen W, et al. Exosome isolation: A microfluidic road-map. Lab Chip. 2015;15:2388–2394.
[46] Andreu Z, Rivas E, Sanguino-Pascual A, et al. Comparative analysis of EV isolation procedures for miRNAs detection in serum samples. J Extracell Vesicles. 2016;5:31655.
[47] Lane RE, Korbie D, Anderson W, et al. Analysis of exosome purification methods using a model liposome system and tunable-resistive pulse sensing. Sci Rep. 2015;5:1–7.
[48] Tauro BJ, Greening DW, Mathias RA, et al. Comparison of ultracentrifugation, density gradient separation, and immunoaffinity capture methods for isolating human colon cancer cell line LIM1863-derived exosomes. Methods. 2012;56:293–304.
[49] Greening DW, Xu R, Ji H, et al. A protocol for exosome isolation and characterization: evaluation of ultracentrifugation, density-gradient separation, and immunoaffinity capture methods. In: Posch A, editor. Proteomic profiling: methods and protocols. New York: Springer; 2015. p. 179–209.
[50] Marcus ME, Leonard JN. FedExosomes: engineering therapeutic biological nanoparticles that truly deliver. Pharmaceuticals. 2013;6:659–680.
[51] Yamada T, Inoshima Y, Matsuda T, et al. Comparison of methods for isolating exosomes from bovine milk. J Vet Med Sci. 2012;74:1523–1525.
[52] Böing AN, van der Pol E, Grootemaat AE, et al. Single-step isolation of extracellular vesicles by size-exclusion chromatography. J Extracell Vesicles. 2014;3:23430.
[53] Davies RT, Kim J, Jang SC, et al. Microfluidic filtration system to isolate extracellular vesicles from blood. Lab Chip. 2012;12:5202–5210.
[54] He M, Crow J, Roth M, et al. Integrated immunoisolation and protein analysis of circulating exosomes using microfluidic technology. Lab Chip. 2014;14:3773–3780.

[55] Welton JL, Webber JP, Botos LA, et al. Ready-made chromatography columns for extracellular vesicle isolation from plasma. J Extracell Vesicles. 2015;4:27269.
[56] Taylor DD, Shah S. Methods of isolating extracellular vesicles impact down-stream analyses of their cargoes. Methods. 2015;87:3–10.
[57] Lee J, Lee H, Goh U, et al. Cellular engineering with membrane fusogenic liposomes to produce functionalized extracellular vesicles. ACS Appl Mat Interfaces. 2016;8:6790–6795.
[58] Fuhrmann G, Serio A, Mazo M, et al. Active loading into extracellular vesicles significantly improves the cellular uptake and photodynamic effect of porphyrins. J Control Release. 2015;205:35–44.
[59] Hung ME, Leonard JN. A platform for actively loading cargo RNA to elucidate limiting steps in EV-mediated delivery. J Extracell Vesicles. 2016;5:31027.
[60] Kim MS, Haney MJ, Zhao Y, et al. Development of exosome-encapsulated paclitaxel to overcome MDR in cancer cells. Nanomed Nanotechnol Biol Med. 2016;12(3):655–664.
[61] Yim N, Ryu SW, Choi K, et al. Exosome engineering for efficient intracellular delivery of soluble proteins using optically reversible protein–protein interaction module. Nat Commun. 2016;7:1–9.
[62] Stickney Z, Losacco J, McDevitt S, et al. Development of exosome surface display technology in living human cells. Biochem Biophys Res Commun. 2016;472(1):53–59.
[63] Delcayre A, Estelles A, Sperinde J, et al. Exosome display technology: applications to the development of new diagnostics and therapeutics. Blood Cells, Mol Dis. 2005;35:158–168.
[64] Delcayre A inventor, Le PJB inventor; Methods and compounds for the targeting of protein to exosomes. European patent WO2003016522 A2. 2003.
[65] Zeelenberg IS, Ostrowski M, Krumeich S, et al. Targeting tumor antigens to secreted membrane vesicles in vivo induces efficient antitumor immune responses. Cancer Res. 2008;68:1228–1235.
[66] Hartman ZC, Wei J, Glass OK, et al. Increasing vaccine potency through exosome antigen targeting. Vaccine. 2011;29:9361–9367.
[67] Alvarez-Erviti L, Seow Y, Yin H, et al. Delivery of siRNA to the mouse brain by systemic injection of targeted exosomes. Nat Biotechnol. 2011;29:341–345.
[68] Tian Y, Li S, Song J, et al. A doxorubicin delivery platform using engineered natural membrane vesicle exosomes for targeted tumor therapy. Biomaterials. 2014;35:2383–2390.
[69] Ohno SI, Takanashi M, Sudo K, et al. Systemically injected exosomes targeted to EGFR deliver antitumor microRNA to breast cancer cells. Mol Ther. 2013;21:185–191.
[70] Bolukbasi MF, Mizrak A, Ozdener GB, et al. miR-1289 and "Zipcode"-like sequence enrich mRNAs in microvesicles. Mol Ther Nucleic Acids. 2012;1:1–10.
[71] Villarroya-Beltri C, Gutiérrez-Vázquez C, Sánchez-Cabo F, et al. Sumoylated hnRNPA2B1 controls the sorting of miRNAs into exosomes through binding to specific motifs. Nat Commun. 2013;4:1–10.
[72] Lee J, Kim J, Jeong M, et al. Liposome-based engineering of cells to package hydrophobic compounds in membrane vesicles for tumor penetration. Nano Lett. 2015;15:2938–2944.
[73] Chang PV, Prescher JA, Sletten EM, et al. Copper-free click chemistry in living animals. Proc Natl Acad Sci USA. 2010;107:1821–1826.
[74] Sun D, Zhuang X, Xiang X, et al. A novel nanoparticle drug delivery system: the anti-inflammatory activity of curcumin is enhanced when encapsulated in exosomes. Mol Ther. 2010;18:1606–1614.
[75] Zhuang X, Xiang X, Grizzle W, et al. Treatment of brain inflammatory diseases by delivering exosome encapsulated anti-inflammatory drugs from the nasal region to the brain. Mol Ther. 2011;19:1769–1779.
[76] Aqil F, Kausar H, Agrawal AK, et al. Exosomal formulation enhances therapeutic response of celastrol against lung cancer. Exp Mol Pathol. 2016;101:12–21.
[77] Weaver JC. Electroporation: A general phenomenon for manipulating cells and tissues. J Cell Biochem. 1993;51:426–435.
[78] Kooijmans SAA, Stremersch S, Braeckmans K, et al. Electroporation-induced siRNA precipitation obscures the efficiency of siRNA loading into extracellular vesicles. J Control Release. 2013;172:229–238.
[79] Hood JL, Scott MJ, Wickline SA. Maximizing exosome colloidal stability following electroporation. Anal Biochem. 2014;448:41–49.
[80] Haney MJ, Klyachko NL, Zhao Y, et al. Exosomes as drug delivery vehicles for Parkinson's disease therapy. J Control Release. 2015;207:18–30.
[81] Smyth T, Petrova K, Payton NM, et al. Surface functionalization of exosomes using click chemistry. Bioconjug Chem. 2014;25:1777–1784.
[82] Hermanson GT. Zero-length crosslinkers. In: Hermanson GT, editor. Bioconjugate Techniques. 3rd ed. Boston: Academic Press; 2013. p. 259–273.
[83] Sessa G, Freer JH, Colacicco G, et al. Interaction of a lytic polypeptide, melittin, with lipid membrane systems. J Biol Chem. 1969;244:3575–3582.
[84] Pan H, Myerson JW, Ivashyna O, et al. Lipid membrane editing with peptide cargo linkers in cells and synthetic nanostructures. Faseb J. 2010;24:2928–2937.
[85] Sato YT, Umezaki K, Sawada S, et al. Engineering hybrid exosomes by membrane fusion with liposomes. Sci Rep. 2016;6:1–11.
[86] Morris GJ, McGrath JJ. The response of multilamellar liposomes to freezing and thawing. Cryobiology. 1981;18:390–398.
[87] Jo W, Kim J, Yoon J, et al. Large-scale generation of cell-derived nanovesicles. Nanoscale. 2014;6:12056–12064.
[88] Jo W, Jeong D, Kim J, et al. Microfluidic fabrication of cell-derived nanovesicles as endogenous RNA carriers. Lab Chip. 2014;14:1261–1269.
[89] Wagner A, Vorauer-Uhl K. Liposome technology for industrial purposes. J Drug Deliv. 2011;2011:1–9.
[90] Mozafari MR. Liposomes: an overview of manufacturing techniques. Cell Mol Biol Lett. 2015;10:711–719.
[91] Szoka JF, Papahadjopoulos D. Comparative properties and methods of preparation of lipid vesicles (liposomes). Annu Rev Biophys Bioeng. 1980;9(1):467–508.

[92] Abdus S, Sultana Y, Aqil M. Liposomal drug delivery systems: an update review. Curr Drug Deliv. 2007;4:297–305.
[93] Antonietti M, Förster S. Vesicles and liposomes: A self-assembly principle beyond lipids. Adv Mat. 2003;15:1323–1333.
[94] Lasic DD. The mechanism of vesicle formation. Biochem J. 1988;256:1–11.
[95] García-Manrique P, Matos M, Gutiérrez G, et al. Using factorial experimental design to prepare size-tuned nanovesicles. Ind Eng Chem Res. 2016;55:9164–9175.
[96] Gregoriadis G, editor. Entrapment of drugs and other materials into liposomes.Volume II, Liposome Technology. Boca Ratonn: CRC Press; 2007.
[97] Avanti Polar Lipids products. Available from: http://www.avantilipids.com
[98] Sullivan SM, Connor J, Huang L. Immunoliposomes: preparation, properties, and applications. Med Res Rev. 1986;6:171–195.
[99] Hermanson GT. The reactions of bioconjugation. In: Hermanson GT, editor. Bioconjugate techniques. 3rd ed. Boston: Academic Press; 2013. p. 229–258.
[100] Nobs L, Buchegger F, Gurny R, et al. Current methods for attaching targeting ligands to liposomes and nanoparticles. J Pharm Sci. 2004;93:1980–1992.
[101] Schuber F. Chemistry of ligand-coupling to liposomes. In: Schuber F, Philippot JR, editors. Liposomes as tools in basic research and industry. Boca Raton: CRC Press; 1995. p. 21–39.
[102] Martinez-Lostao L, García-Alvarez FC, Basáñez G, et al. Liposome-bound APO2L/TRAIL is an effective treatment in a rabbit model of rheumatoid arthritis. Arthritis Rheum. 2010;62:2272–2282.
[103] Li K, Chang S, Wang Z, et al. A novel micro-emulsion and micelle assembling method to prepare DEC205 monoclonal antibody coupled cationic nanoliposomes for simulating exosomes to target dendritic cells. Int J Pharm. 2015;491:105–112.
[104] Chandler WL, Yeung W, Tait JF. A new microparticle size calibration standard for use in measuring smaller microparticles using a new flow cytometer. J Throm Haemost. 2011;9:1216–1224.
[105] Gardiner C, Shaw M, Hole P, et al. Measurement of refractive index by nanoparticle tracking analysis reveals heterogeneity in extracellular vesicles. J Extracell Vesicles. 2014;3:25361.
[106] De Miguel D, Basáñez G, Sánchez D, et al. Liposomes decorated with Apo2L/TRAIL overcome chemoresistance of human hematologic tumor cells. Mol Pharm. 2013;10:893–904.
[107] de Miguel D, Gallego-Lleyda A, Galan-Malo P, et al. Immunotherapy with liposome-bound TRAIL overcomes partial protection to soluble TRAIL-induced apoptosis offered by down-regulation of Bim in leukemic cells. Clin Trans Oncol. 2015;17:657–667.
[108] Pagnan G, Stuart DD, Pastorino F, et al. Delivery of c-myb antisense oligodeoxynucleotides to human neuroblastoma cells via disialoganglioside GD2-Targeted immunoliposomes: antitumor effects. J Natl Cancer Inst. 2000;92:253–261.
[109] Pastorino F, Brignole C, Marimpietri D, et al. Doxorubicin-loaded Fab′ fragments of anti-disialoganglioside immunoliposomes selectively inhibit the growth and dissemination of human neuroblastoma in nude mice. Cancer Res. 2003;63:86–92.
[110] Marianecci C, Di Marzio L, Rinaldi F, et al. Niosomes from 80s to present: the state of the art. Adv Colloid Interface Sci. 2014;205:187–206.
[111] Moghassemi S, Hadjizadeh A. Nano-niosomes as nanoscale drug delivery systems: an illustrated review. J.Control Release. 2014;185:22–36.
[112] Capretto L, Carugo D, Mazzitelli S, et al. Microfluidic and lab-on-a-chip preparation routes for organic nanoparticles and vesicular systems for nanomedicine applications. Adv Drug Deliv Rev. 2013;65:1496–1532.
[113] Birnbaumer G, Kupcu S, Jungreuthmayer C, et al. Rapid liposome quality assessment using a lab-on-a-chip. Lab Chip. 2011;11:2753–2762.
[114] Bhise NS, Ribas J, Manoharan V, et al. Organ-on-a-chip platforms for studying drug delivery systems. J Control Release. 2014;190:82–93.
[115] Hu CMJ, Fang RH, Wang KC, et al. Nanoparticle biointerfacing by platelet membrane cloaking. Nature. 2015;526:118–121.

Colloids and Surfaces B: Biointerfaces 182 (2019) 110378

Contents lists available at ScienceDirect

Colloids and Surfaces B: Biointerfaces

journal homepage: www.elsevier.com/locate/colsurfb

Continuous flow production of size-controllable niosomes using a thermostatic microreactor

Pablo García-Manrique[a,b], Gemma Gutiérrez[b], María Matos[b], Andrea Cristaldi[c], Ali Mosayyebi[c], Dario Carugo[d], Xunli Zhang[c,*], María Carmen Blanco-López[a,*]

[a] Department of Physical and Analytical Chemistry, University of Oviedo, Spain
[b] Department of Chemical Engineering and Environmental Technology, University of Oviedo, Spain
[c] Bioengineering Sciences Group, School of Engineering, Institute for Life Sciences (IfLS), University of Southampton, United Kingdom
[d] Mechanotronics and Bioengineering Sciences Research Groups, School of Engineering, Institute for Life Sciences (IfLS), University of Southampton, United Kingdom

ARTICLE INFO

Keywords:
Organic colloids
Niosomes
Size control
Hydrodynamic flow-focussing
Microreactor
3D-printing

ABSTRACT

The new roles of vesicular systems in advanced biomedical, analytical and food science applications demand novel preparation processes designed to reach the new standards. Particle size and monodispersity have become essential properties to control. In this work, key parameters, involved in a microfluidic reactor with hydrodynamic flow focusing, were investigated in order to quantify their effects on niosomes morphology. Particular attention was given to temperature, which is both a requirement to handle non-ionic surfactants with phase transition temperature above RT, and a tailoring variable for size and monodispersity control. With this aim, niosomes with two different sorbitan esters and cholesterol as stabilizer were formulated. High resolution and conventional 3D-printing technologies were employed for the fabrication of microfluidic reactor and thermostatic systems, since this additive technology has been essential for microfluidics development in terms of cost-effective and rapid prototyping. A customised device to control temperature and facilitate visualization of the process was developed, which can be easily coupled with commercial inverted microscopes. The results demonstrated the capability of microfluidic production of niosomes within the full range of non-ionic surfactants and membrane stabilizers.

1. Introduction

A precise control over local environment during production of colloids is essential to minimise perturbations in chemical characteristics that could lead to heterogeneous populations, and then, differences in particle properties. To achieve such homogeneity and uniform properties, a strict control of particle size is necessary [1,2].

Nanovesicles (organic colloids) are particles formed by self-assembled amphiphilic molecules into closed bilayered structures with an inner aqueous core. Depending on the chemical nature of bilayer constituents, these particles are categorised into liposomes (lipids), niosomes (non-ionic surfactants) or polymersomes (block copolymers), as most frequently found in the literature [3–5].

Niosomes exhibit unique advantages over the other types of vesicular systems due to their inherent characteristics of non-ionic surfactants [6,7]. These advantages include; (i) better chemical and physical stability of suspensions due to the absence of oxidation-related degradation, (ii) easy derivatization to introduce different functional groups for stability enhancement or bioconjugation, (iii) wide range of surfactant types available (with single or double acyl chain, with different length or saturation), (iv) high immunological tolerance, and (v) cost effectiveness. Firstly introduced in the cosmetic industry by L'Oreal [8] for dermal bioactive compounds delivery, over the last 15 years their applications have expanded to many fields. Food fortification [9], diagnostic agents [10], analytical chemistry [11], nanomaterial synthesis [12], and drug delivery [13] are just some of examples. For all of these applications, a product with specific characteristics, homogeneity and reproducibility is desired, and in particular, controlled size and monodispersity are essential.

Effort has been made to the production of niosomes by traditional methods with tight control over size and size distribution [14] for some specific applications [15]. For example, in our previous work [16], we have used experimental design to study the influence of variables in the ethanol injection process, in order to improve particle size tunability.

One of the most popular chemical families for niosome production involves sorbitan esters (commercially available as Span®). Span family

* Corresponding authors.
E-mail addresses: XL.Zhang@soton.ac.uk (X. Zhang), cblanco@uniovi.es (M.C. Blanco-López).

https://doi.org/10.1016/j.colsurfb.2019.110378
Received 14 March 2019; Received in revised form 16 June 2019; Accepted 17 July 2019
Available online 18 July 2019
0927-7765/

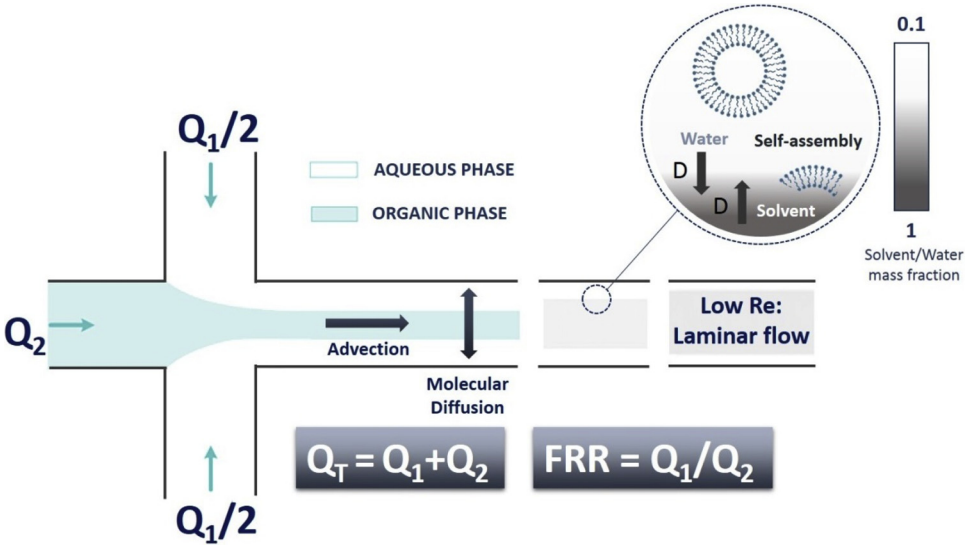

Fig. 1. Schematic diagram of a continuous flow microreactor based on hydrodynamic flow focusing for vesicular systems production. The reduction of focused stream width under laminar flow conditions makes possible the mixing of chemical species by molecular diffusion, since time for mixing decreases with the square root of distance. By changing flow rates, the kinetics and extension of mixing can be modified, and then, the size of particles. Amphiphilic molecules are self-assembled into bilayers once critical concentration of solvent is reached, and molecules acquired an ordered state to minimize the interaction with water molecules. At a certain size bending modulus induce planar bilayer to be closed into vesicles.

members differ in terms of acyl chain length and saturation, with a big range of hydrophilic-lipophilic balance values (HLB), where HLB is an important parameter with implications in drug encapsulation efficiency and morphological characteristics of particles. This parameter is also related to the physical state at room temperature (RT), and influences the minimum temperature (together with *gel-to-liquid* transition temperature, or T_c) that is required at the very stage of the particle formation. On the other hand, some of the compounds used in formulations with great loading capacity, low release rate and stability in solution are solid at RT. For these reasons, a higher and controlled temperature level is mandatory for this process.

Microfluidics technology is very promising for precise control over input variables when mixing chemical species [17]. Other advantages include low consumption of chemicals (relevant in formulation optimization), scale-up possibilities for industrial production, on-line coupling to other processes (such as purification steps), and efficient control over temperature if required [18]. Jahn et al. [19] reported for the first time the hydrodynamic flow focussing (HFF) technique (Fig. 1) for liposomes production. Following that, other researchers have used this method to examine various liposomes formulations and for encapsulating either hydrophobic or hydrophilic molecules [20,21]. Under laminar flow conditions within the HFF configuration, a stream of lipids in organic phase is focussed between two aqueous streams in microchannels, allowing the mixing of chemical species by molecular diffusion. At the two organic/aqueous interfaces, bilayers can be formed and self-assembled into liposomes once a critical concentration is reached. By controlling the flow, the extension of mixing and hence the size of liposomes, could also be controlled. However, the production of niosomes through microfluidic routes remains less explored, and limited attention has been paid to using HFF technique [22–24].

At present, the high temperature required for the preparation of niosomes has not been well taken into account in microfluidics routes. For example, the previous work that firstly explored microfluidics assembly of niosomes faced such temperature related challenge, thus only included Span® 20 and Span® 80 (T_m = 25 °C and -30 °C, respectively) in the study. [22]

Along with the wide application of continuous flow microreactors for organic colloids preparation [18] is the development of microreactor itself, including design and manufacturing of such microdevices, with simpler and more affordable production methods [25]. As a result, some traditional fabrications methods which stem from the photo-electronics field, such as photolithography [26], are being substituted by new processes that require less expensive equipment and can be performed in common labs with no need for clean rooms facilities [27]. Among the techniques explored, additive manufacturing, especially 3D-printing, has emerged as a promising method for microfluidic device manufacturing [28]. The rapid development of 3D-printing technology and the commercialization of desk printers have enabled researchers to explore its utility in microfluidic prototyping and manufacturing [29–31], that generally use low cost raw materials and can print objects with desired resolution.

The aim of the present work was to develop a thermostatic microreactor platform for the continuous flow production of niosomes in a size-controllable manner. The microfluidic reactor was designed with a hydrodynamic flow focusing configuration, and fabricated in order to allow visualization of the dynamic process including molecular diffusion, with the aid of an inverted microscope and a digital image acquisition system. 3D-printing technology was used for fabricating the microfluidic device (positive mould) and thermostatic system. The effect of operational parameters was investigated on the final morphological characteristic of niosomes. Niosomes were formulated with non-ionic surfactants with different transition temperatures (T_m) with controlled temperature as a tailoring parameter to tune the size and homogeneity of particles.

2. Materials and methods

2.1. Materials

Sorbitan monostearate or Span® 60 (Sigma-Aldrich), sorbitan monolaureate or Span® 20 (Sigma-Aldrich), cholesterol from lamb wool (Akros Organics), Phosphate Buffer Saline (10 mM, pH 7.4) prepared from tablets according to manufacture instructions (Sigma-Aldrich), Bromoxylenol blue (Sigma-Aldrich), and technical grade solvents such as ethanol absolute, 2-propanol (or isopropyl alcohol, IPA), and acetone (all from J.T. Baker, Avantor, USA) were used in this work. Ultrapure water was used for all experiments. Poly(dimethylsiloxane) monomer Sylgard® 184 or PDMS was purchased from Dow Corning Corporation (Auburn, AL, USA). Other materials used for devices fabrication are specified in the following respective sections.

2.2. Thermostatic system fabrication

Thermostatic chamber was design in Autodesk® Inventor® and 3D-printed with PLA filaments using a special printer for fused deposition modelling (Ultimaker 2 + 3D printer, Ultimaker B.V., The Netherlands). Main chamber and cap of the device were produced separately. A microscope glass slide of 50 x 70 mm (Corning® microscope

slides, Sigma-Aldrich, Gillingham, UK) was sealed to the chamber with a 2-phase adhesive glue special for plastic materials, bought in a local store. A transparent piece of plastic was glued to the cap aperture with the same adhesive used with the other piece. Teflon tape was used to enhance the closure of both elements in a removable way. Holes for the inlets and outlet pipes of the microfluidic device were manually prepared with a sharp tool.

The previously described chamber was connected to a temperature-controllable recirculation system (F12-MC, Julabo GmbH, Germany) through the inlet, and a peristaltic pump (MasterFlex®, Cole-Parmer Instruments Company, USA) through the outlet. The plastic pipes were those from the recirculator, and connections to the chamber were made with common plastic adapters (see supplementary material).

External supply of the recirculator was set approximately at a flow rate of 55% of the total volume, while peristaltic pump revolution rate was adjusted to remove water from the chamber at a rate that allowed a continuous and constant flow through it. Temperature inside the chamber was monitored with a digital temperature probe (Testo 110, Testo SE & Co., Germany). The sensor probe was introduced into the chamber through a hole placed in one side of plastic window of the cap (see Fig. S2).

2.3. Microfluidic devices manufacturing and channel characterization

Master mould of devices was designed in Solidworks® CAD 2016 software and 3D-printed onto VeroClear™ resin with the HR-3D printer Objet350 Connex™ (Stratasys Ltd., USA). A post-printing process was also needed. First, mould was flushed with (I) IPA, (II) deionized water, (III) acetone, and finally compressed air. Then, it was cured overnight at 60 °C, and on the following day a treatment of the inner surface was carried out with Aquapeel® (to avoid interference of the resin with PDMS curing process). Three individual moulds were printed.

Once the positive mould was ready, a mixture of degassed PDMS curing agent (1:10 w/w) was poured into it, and left overnight in an oven at 40 °C. For degassing the PDMS mixture, a bench centrifuge was used at 3000 rpm for 10 min. It should be noted that pouring into master mould must be done slowly to minimise bubble formation. On the following day, the replica of the mould was carefully peeled off from the mould, and inlets and outlet holes were prepared with a 1.5 mm biopsy punch with plunger (Miltex®, Fischer Scientific, UK).

Oxygen plasma (PVA-TePla 300 plasma cleaner, Wettenberg, Germany) treatment was applied to bond a microscope glass slide (50 x 70 mm; Corning® microscope slides, Sigma-Aldrich, Gillingham, UK) to the PDMS replica to complete the microfluidic channel. Four pieces of thermic resistant plastic (Ø 8 mm and 3 mm height) were glued in each corner at the bottom of the glass slide, to elevate the device allowing a flow of hot water under the channels.

Polytetrafluoroethylene (PFTE, 0.5 mm I.D.) pipes (Cole-Parmer, UK) were inserted into the holes, and the other end was attached to a syringe needle to create a connection for introduction of the fluids from syringe pumps (NE-300, NEW ERA Pump Systems Inc., USA). Luer lock syringes (Becton, Dickinson and Company, UK) of 1, 10 or 20 mL were used depending on the selected Flow Rate Ratio (FRR), *i.e.* volumetric flow rate of total aqueous phase/volumetric flow rate of organic phase.

The mixing channel (23 mm long) on the 3D-printed positive mould was characterized in terms of morphology, accuracy and reproducibility by mechanical profilometry (Talysurf-120 L, Taylor-Hobson, United Kingdom). Three equidistance measurements were taken (2 mm across the channel, perpendicular to it), and data were processed with OriginPro 18 (OriginLab Corporation, USA) software.

The whole setup (microfluidic device inside the thermostatic chamber with respective inlets and outlets) was placed over the stage of an inverted microscope (IN200TAB series, AmScope, USA) with a digital imaging system to capture images (5 M.P USB CCD camera, AmScope, USA) supported with the software supplied by the camera manufacturer. The entire experimental setup is illustrated in Fig. S2.

2.4. Niosomes production and morphological characterization

Working solutions of 5 and 20 mM of Span® 60:cholesterol and Span® 20:cholesterol (1:0.5 molar ratio) were prepared by dilution from a 50 mM stock solution. Ethanol absolute was used as organic solvent, since it is miscible in aqueous buffer (PBS, 10 mM pH 7.4). Aqueous and organic phases were pumped into microfluidic device once appropriate temperature was reached. Three different total flow rates (Q_T) were studied (50, 100 and 200 μL/min), and aqueous:organic flow rates were adjusted to five different flow rates ratios (FRR) (5, 15, 25, 35 and 50). Span® 20:cholesterol formulation was injected at 30, 40, 50 and 60 °C; while Span® 60: cholesterol was only injected at 50 °C. All the combination of membrane components concentration, Q_T, FRR, and temperature was conducted by duplicate.

A total volume of 2.5 mL was collected from the outlet of the device for each experimental condition in a glass vial. Size (z-average or peak value, depending on the number of peaks in the size distribution) and homogeneity (PDI) of particles were measured by Dynamic Light Scattering (DLS) in a Zetasizer NANO-ZS equipment (Malvern Instruments Ltd, Malvern, UK). Samples were measured undiluted by triplicate, with the 173° backscatter detector in disposable low volume cuvettes (Malvern Instruments Ltd, Malvern, UK).

2.5. Mixing efficiency visualization

Solvent and no-solvent diffusion by hydrodynamic flow focusing was monitored by an adaption of a previous published methodology [32]. Briefly, a change in colour of a pH indicator dye (bromoxylenol blue) was used, since this dye exhibits a strong yellowish colour at pH below 6.0 and blue at pH above 7.6. A saturated solution of dye in absolute ethanol acidified with acetic acid was focused by PBS adjusted to pH 10.0 with 2 M NaOH solution. Once focused, a change in colour of the stream from yellow to blue indicated a molar fraction of aqueous phase close to one, and then, completes mixing by diffusion.

3. Results and discussion

With the microreactor platform developed, systematic characterisation and operation were conducted in terms of 3D printing outcomes and nanoproduction, as detailed below. (The performance and optimization of the thermostatic system are described in the Supplementary material, Fig. S1).

3.1. High resolution 3D-printing of master moulds for microfluidic devices fabrication

As a key element of the device, mixing channel morphology was characterized by mechanical profilometry onto 3D-printed positive moulds. A considerable difference in nominal dimensions between Computer Aided Design (CAD) and printed object was observed (Table S1). With an original squared cross sectional geometry of 100 μm width and 100 μm height, printed features onto VeroClear® resin showed a curved morphology five times wider and approximately half of the height. At the same time, variations in width and height of the mixing channel were found between the three 3D-printed positive moulds (see Table S1) even following the same fabrication procedure. However, these dimensions were reasonably constant along the mixing channel length, especially for channel height.

A possible explanation for these variations in channel dimensions could be related to printer operational parameters. Objet350 Connex3 printer used Polyjet™ inkjet-head patented technology for a layer-by-layer process based on Stereolithography [33]. The jetting head dispensed a proper amount of a photopolymer resin onto a build tray and instantly cured them with UV light. The process took place in XY-axes to create a 2D sheet (down to 16 microns thickness), and by lowering the build tray, another layer was created over the previous one. The

cycle was repeated until the whole design was completed. With a resolution of 600 × 600 × 1600 dpi (X-Y-Z-axes respectively) and an accuracy of 20–85 microns for features below 50 mm (up to 200 microns for full model size), the final features depended on geometry (proximity between elements), build parameters (exposure time, printing speed) and model orientation [29]. Comina et al. [29] reported the successful printing of positive moulds for microfluidics devices with elements from 50 µm to 2 mm, however, some artefacts were described between close elements with 50 µm in dimension differences, though working with optimized parameters. Unfortunately, no details about cross section geometry were given for these channels. Some other authors [34] have reported differences between CAD and printed designs with efforts in resin formulation optimization.

In our recent work [31], we found that 3D printed channels with the Objet350 Connex3 printer were smoother than channels printed with a conventional desk 3D printer (Ultimaker 2+). However, for the same dimensions and aspect ratio, accuracy in cross sectional shape was lower for the HR-3D printer even at large dimensions (1 mm squared channels). It suggested that further studies are needed to understand this effect with the scale and for different materials in order to inform printing parameters optimization in terms of element dimensions, geometry, and printing materials. Apart from the difference between CAD and 3D-PMs, the cross sectional area of Mould 3 was similar to that previously used by Lo et al. [22], on which the selected operational parameters of the present work were based.

3.2. Production of nanoparticles with temperature control for formulations with high T_m non-ionic surfactants

The use of non-ionic surfactants for the formulation of organic colloids, especially for NVs preparation, exhibits numerous advantages [4,6]. However, a strict control of the temperature is necessary if Span® 60 (T_m = 45 °C), one of the most commonly used surfactant in niosome formulation) is involved. Fig. 2 shows its precipitation at RT in microchannels once reaching the focusing region, highlighting the significance of temperature effect.

In Fig. 2 surfactant precipitation was observed at the focussing region and persists along the channel length when Span® 60 is used at 25 °C. However, at 50 °C a complete mix of both phases were produced without the presence of any surfactant precipitation. Moreover, the production of niosomes at this temperature conditions were observed using Transmission Electron Microspcopy (TEM) and negative staining protocol.

This technique has been less explored than traditional bulk preparation routes [18], and with important advantages such as better control over particle preparation and the subsequent final characteristics (size and monodispersity, *i.e.*). This is important for biomedical [1], food [35] and analytical chemistry [2] applications. In this regard, the influence of operational conditions over particles physical properties was tested by analysing the results of 3 total flow rates (Q_T), two different concentrations of bilayer components, for 5 different FRR. Particle size (nm) and size distribution (PDI) were measured by DLS as output variables. All the combinations were conducted at 50 °C, a temperature over surfactant T_m.

In general terms, smaller particles were produced as the FRR increased (Fig. 3A and B) for both concentrations (5 and 20 mM), and for all the Q_T levels. At a concentration of 5 mM (Fig. 3A), the particle size decreased from 278, 298 and 358 nm (when FRR = 5) to 155, 129 and 143 nm (when FRR = 50), where Q_T = 50, 100 and 200 µL/min, respectively. At a concentration of 20 mM (Fig. 3B), similarly, the particle size reduced from 342, 361 and 386 nm (when FRR = 5) to 164, 147 and 151 nm (when FRR = 50) at the three Q_T levels of 50, 100 and 200 µL/min, respectively. Size reduction was rapidly reached with an increment in FRR from 5 to 15, and this reduction became less pronounced from FRR 15 to 50. It is important to take into account that when FRR increased the total amount of bilayer components decreased, not only producing vesicle with smaller size, since particle concentration was also reduced.

No significant effect of different Q_T was observed, while only some differences were noticed in some particular combinations of parameters at low surfactant concentration (5 mM), as seen in Fig. 3A. These observations were in accordance with previous studies [22] carried out with identical chip configuration for the production of niosomes formulated with other sorbitan esters (Span® 20 and 80), and also for the production of liposomes [19,20,36,37]. At lower Q_T, also the linear velocity was lower (hence larger residence time) what can counteract the effect of the bilayer components concentration.

The increase in FRR, and the subsequent decrease in initial focused width (W_f), reduced the time needed for a complete mixing between solvent and no-solvent (t_{mix}), thus the critical concentration to induce molecules self-assembly was reached faster. This led to smaller vesicles since the total amount of bilayer components was reduced [38]. On the other hand, the reduction of solvent introduced in the mixing channel also decreased the possibility of particle fusion into bigger unities by Ostwald-ripening phenomena [20,39]. A reduced t_{mix} also led to complete mixing in limited length channels. In other cases, no diffused solvent containing amphiphilic molecules self-assembled out of the channel under entirely different conditions (outlet pipes, with no

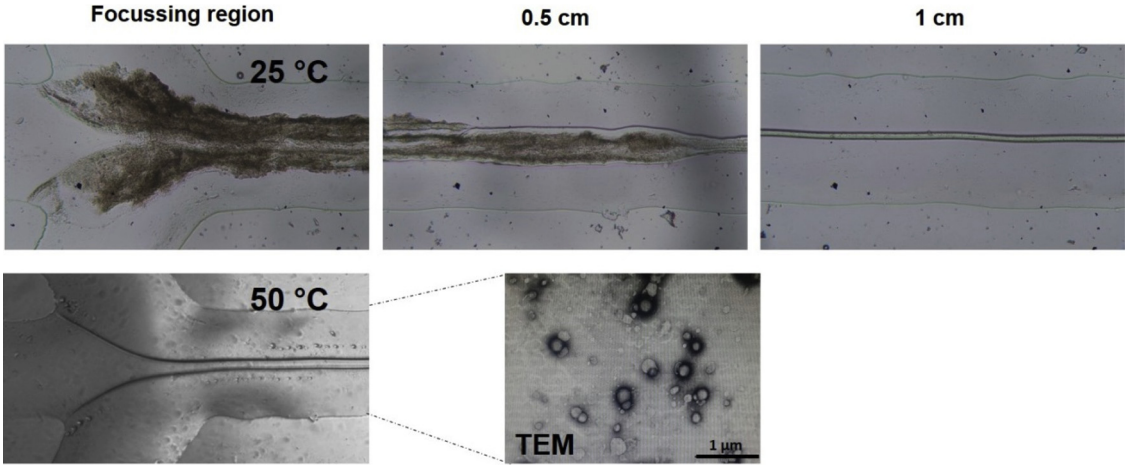

Fig. 2. Precipitation of Span® 60 (T_m = 45 °C) at room temperature (upper arrow) at the focusing region (left), 0.5 and 1.0 cm downstream (centre and right). At a temperature above surfactant Tm, focusing is complete and vesicles formation could be checked by negative staining (Phosphotungstic acid 2%) and Transmission Electron Microscopy (TEM).

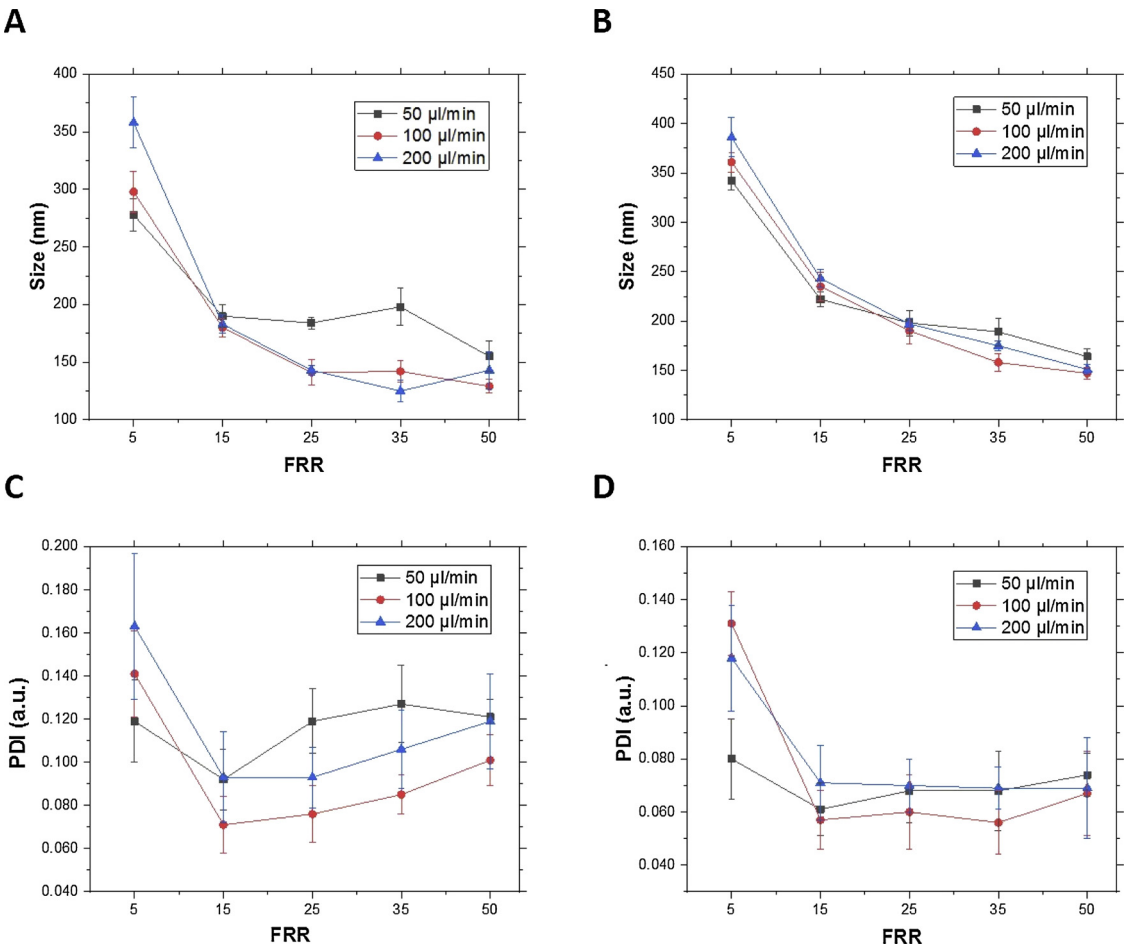

Fig. 3. Size (nm) and size distribution (PDI, a.u.) measured by DLS in undiluted samples from niosomes formulated with Span® 60:Cholesterol (1:0.5 molar ratio) at 5 mM (A,C) and 20 mM (B,D) in a continuous flow microreactor based on hydrodynamic flow focusing at controlled temperature (50 °C). Each condition was tested twice, and each batch was measured by triplicate.

laminar flow characteristics).

Regarding size distribution of particles (Fig. 3C and D), PDI value reduced as FRR increased from 5 to 15, (for 5 mM: from 0.119, 0.141 and 0.163 at FRR = 5 to 0.092, 0.071 and 0.093 at FRR = 15; for 20 mM: from 0.080, 0.131 and 0.118 at FRR = 5 to 0.061, 0.057 and 0.071 at FRR = 15; for both concentration values are indicated for Q_T = 50, 100 and 200 µL/min respectively). and remained without significant changes at higher FRR for both concentrations. Some authors [19,20,32] reported a significantly increase in PDI with the increment of FRR for an identical chip configuration, but for liposomes production instead. However, our observation was in line with that of Bottaro et al. [32] in a "Y"-shaped device, while Joshi et al. [21] described also a reduction in PDI as FRR increase during liposome formation. No significant differences on PDI were observed for all Q_T levels applied.

The use of microreactors with different channel configurations, and the use of static mixing enhancers [40], could be the reason of different results among published works. Some of them have highlighted the influence of channel dimensions and configurations over mixing efficiency and particle properties [19,22,38]. The preparation of solvent mixture containing bilayer precursors can also influence the extension and homogeneity of solubilisation, and in consequence, nanoprecipitation process. In the present work, ethanol was used as solvent for microfluidic-based preparation of niosomes for the first time, and this limited the possibility for comparison with other studies.

We have noticed that at high FRRs some transitory perturbations of the focused fluid were recorded, especially at 50 µL/min. The focused stream exhibited a "beating pulse" like effect that was likely produced by the syringe pump due to its own pumping mechanism. These pulses created really short increments in the width of the focused fluid that introduced alteration in solvent exchange kinetics and the subsequent changes in the local concentration of bilayer precursors and solvent concentration.

Surprisingly, lower PDI values were obtained at 20 mM for all FRRs at the three different Q_T. Indeed, these differences were higher at 50 µL/min. At low concentration, those mentioned instabilities can induce more pronounced local changes in bilayer precursor's abundances, with the corresponding effect in particle monodispersity. To gain insights into these observations further studies are needed.

On the other hand, larger particles were obtained when a higher concentrated ethanolic solution of bilayer components was used (20 mM *vs.* 5 mM). This was observed at all Q_T and FRR levels (see Supplementary material, Fig. S4). The same observation was also reported by other authors when producing liposome using microchannels [38], and in agreement with the mechanism of vesicle formation under microfluidic flow dynamic mixing.

The efficiency of mixing under the assayed working conditions was studied following a published methodology [32]. With this method, mixing efficiency was measured through the change in colour of a pH indicator dye (bromoxylenol blue), that changed from yellow (acidic ethanolic solution containing bilayer precursors) to blue (basic aqueous phase, PBS pH = 10). A shift in focused fluid colour from yellow to blue indicated that molar fraction of water into the stream was close to 1 and the subsequent molar fraction of EtOH became close to 0, evidencing a

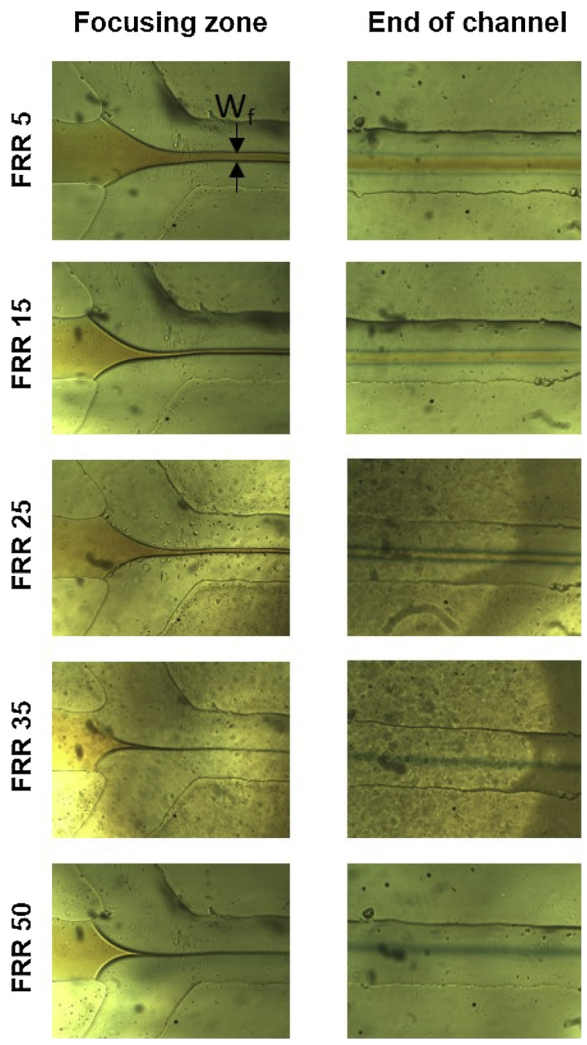

Fig. 4. Images (4X) of focusing region and end of the mixing channel evidencing hydrodynamic flow focussing of a central ethanol stream at different FRR values for Q_T = 100 µL/min and 50 °C. Yellow colour indicates acid pH (pure EtOH, no mixing), while blue colour indicates basic pH (complete mixing by co-diffusion of solvent and no solvent). Bromoxylenol blue dye was dissolved in EtOH (acidified with acetic acid), and PBS was adjusted with NaOH to pH 10 (For interpretation of the references to colour in this figure legend, the reader is referred to the web version of this article).

complete mixing by solvent and aqueous effluents. This change in colour was easily detected in the inverted microscope, and recorded with the digital camera. As an example, results for Q_T = 100 µl/min at several FRRs are shown in Fig. 4.

Complete mixing was only reached at high values of FRR (35 and 50) for Q_T = 50 µl/min and Q_T = 100 µl/min, and only at the high FRR (50) for Q_T = 200 µl/min. As Q_T increased, residence time of the fluid inside mixing channel reduced (from 0.5 s at 50 µl/min to 0.13 s at 200 µl/min), preventing to stay the necessary time to reach complete mixing. Only at high FRR value, t_{mix} was short enough to be compatible with low values of residence time for our channel dimension (t_{mix} = 17 ms and 8 ms for FRR = 35 and 50, respectively) predicted according to a theoretical model (Eq. (1), [41]). In this model W_f represents the width of focused stream, where w is the channel width and D is solvent diffusion coefficient.

$$t_{mix} \sim \frac{W_f^2}{4D} \approx \frac{w^2}{9D\,(1+FRR)^2} \quad (1)$$

As seen in Fig. 4, W_f decreased as FRR increased, and a dependence of W_f with Q_T was observed at lower FRR values (Fig. 5A). It was also observed that a lower Q_T generated wider focused streams probably due to the lower pressure exercised by the lateral aqueous flows to the middle solvent flow, but these differences became less pronounced at higher FRRs. A similar trend was observed by Bottaro et al. [32] in an identic channels configuration, but contrary to Jahn et al. [19] who reported a non-variation in W_f with modifications in Q_T.

Moreover, an intense inverse correlation (potential) between FRR and W_f was observed at all the Q_T levels (Table S2). However, a strong negative correlation (linear) between particle size and W_f was observed at the two different concentrations studied. These correlations reflect that particle size is governed by focusing parameters. It is clear that niosomes size can be tuned with the selection of the appropriate FRR and Q_T values, which are key parameters for W_f and residence time.

3.3. Production of niosomes at different temperatures to study potential tailoring effect over particle morphology

In this part of work Q_T of 100 µL/min and 5 mM of components concentration were selected, since these have been the best operating conditions in terms of smaller particles with narrower size distributions.

The effect of temperature was examined in a rage of 30 °C and 60 °C as another operating parameter on size-tuned niosomes formation through flow-focused based microfluidics. For this purpose, a non-ionic surfactant with low T_m was needed that allowed to test a wide range of working temperatures. Sorbitan monolaureate or Span® 20 (T_m = 25 °C and HLB 8.6) was selected, another common surfactant used for niosomal formulations [42], and surfactant:cholesterol molar ratio was kept in 1:0.5 as for Span® 60 in order to allow formulations comparisons.

Fig. 6 depicts the results of particle size at the same FRRs previously used for Span® 60 niosomes at different working temperatures: 30, 40, 50 and 60 °C. At 30 °C, a reduction in particle size from FRR = 5 to FRR = 15 was observed. As FRR increased size became also larger (even higher that those particles produced at FRR = 5). This phenomenon could be related to the observation of cholesterol precipitates inside the mixing channel that were formed immediately after focusing region. The low solubility of cholesterol in water at nearly room temperature induced its precipitation as crystals. Those precipitates modified the flow properties and introduced turbulences that induced micro domains in the fluid with different concentrations of bilayer components, and particles with different morphologies. Also the depletion of cholesterol could generate different particles than those produced in their presence. These perturbations were magnified at higher FRR, since as seen in Fig. 5B the width of focused fluid became smaller with the increment of FRR, and this stream was relatively smaller than the formed crystals (around 100 µm structures).

For the rest of temperatures, a similar behaviour as for Span® 60 niosomes was observed. Particles size became smaller with an inverse correlation with FRR. At higher temperatures, focused ethanol stream was wider, and these differences were reduced with the increment in FRR. Only slight differences in particle size could be detected (Fig. 6A).

Regarding temperature effect some authors reported an increase in particle size as temperature increased [24] which were attributed to the bilayer expansion at higher temperature [43]. In our case, such increase in particle size was not observed. It is know that collapse pressure and surface compressional moduli decrease with temperature for all surfactants, and this implies that Span monolayers are more expanded with increments in temperature. However, as temperature increases planar bilayer precursors are less rigid, which could be easily bended to closed structures, and this effect could lead then to smaller particles [39].

Regarding size distribution and temperature, it was observed that the increment of temperature yielded more monodisperse particles, especially at 50 °C. Complete mixing can be reached at FRR = 35 and FRR = 50 at any temperature. Only at 50 and 60 °C PDI values remained nearly constant (after a first reduction from FRR = 5 to 15)

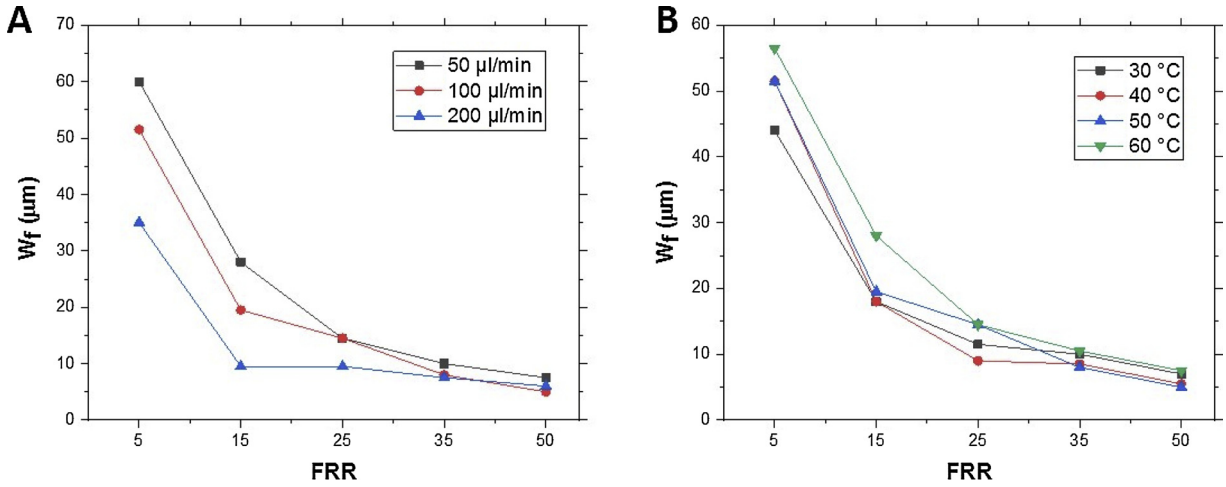

Fig. 5. Values of ethanol focused stream (W_f, µm) as flow rate ratio (FRR) increased for different values of volumetric rates (Q_T) at constant temperature (50 °C), and different temperatures at constant Q_T (100 µL/min). Values represent the average of two independent measurements, taken at approx. at 100 µm from the end of focussed region.

with the increment in FRR.

3.4. Effect of surfactant acyl chain length over particles size and monodispersity

Another interesting finding resulted from the comparison between niosomes formulated with different non-ionic surfactants under identical preparation conditions. In this work niosomes with sorbitan esters with different saturated acyl chain lengths (C12 and C18 for Span® 20 and 60 respectively) were prepared. As seen in Fig. 7, shorter chains generally yielded larger niosomes. That was contrary to what would be expected; it is generally understood that shorter chains increase the curvature radius of the bilayer, according to the critical packing parameter (cpp) of the molecules [6], allowing smaller particles. However, if was taken into account the higher hydrophilic character of Span® 20 compared to Span® 60 (higher HLB value) the higher hydrophilicity could enhance water soak into the inner core of the vesicle, resulting in larger vesicles size. Similar results were reported by Gutierrez et al. [44] when niosomes were prepared by mechanical agitation. Regarding niosome size distributions, no differences between both types of surfactants were observed.

4. Conclusions

Novel prototyping and additive manufacturing techniques such as (HR)3D-printing have been applied for the fabrication of a microfluidic continuous flow reactor for hydrodynamic flow focusing at controlled temperature compatible with commercial inverted microscopes. Despite some alteration in cross sectional dimensions and morphology accuracy with respect to the original CAD design, high resolution 3D-printed positive moulds allow us to create functional microreactors for organic colloid production under different working conditions, and to study their effect on aqueous/solvent mixing efficiency through molecular diffusion, and its relationship with particles morphology.

This work shows that temperature is an essential parameter that must be taken into consideration when formulating niosomes with surfactants with T_m over RT. Also it can be used to modify the properties of particles (size and dispersity) produced with non-ionic surfactants with T_m above RT.

We have found that flow focussing at controlled temperature follows the same patterns as for RT, with the ratio between aqueous and solvent streams being the main parameter to control focused stream width and hence, mixing efficiency and kinetics. However, total flow rate only has insignificant effect when FRRs are set to low values, whilst it can influence residence time, and subsequently, mixing efficiency. In

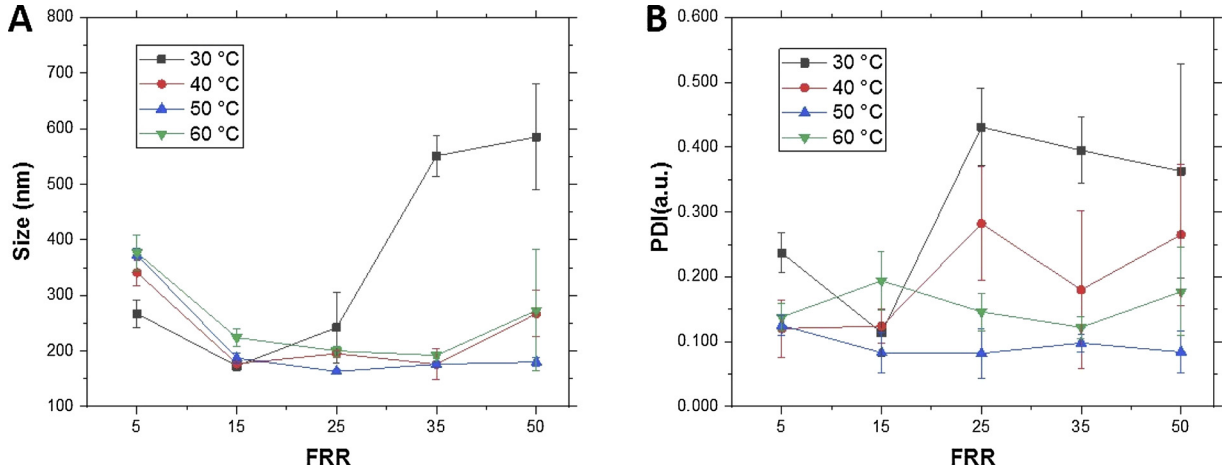

Fig. 6. Size (nm) (left) and size distribution (PDI, a.u.) (right) measured by DLS in undiluted samples from niosomes formulated with Span® 20:Cholesterol (1:0.5 molar ratio) at 5 mM in a continuous flow microreactor based on hydrodynamic flow focusing at different controlled temperatures (30, 40, 50, and 60 °C). Each condition was tested twice, and each batch was measured by triplicate.

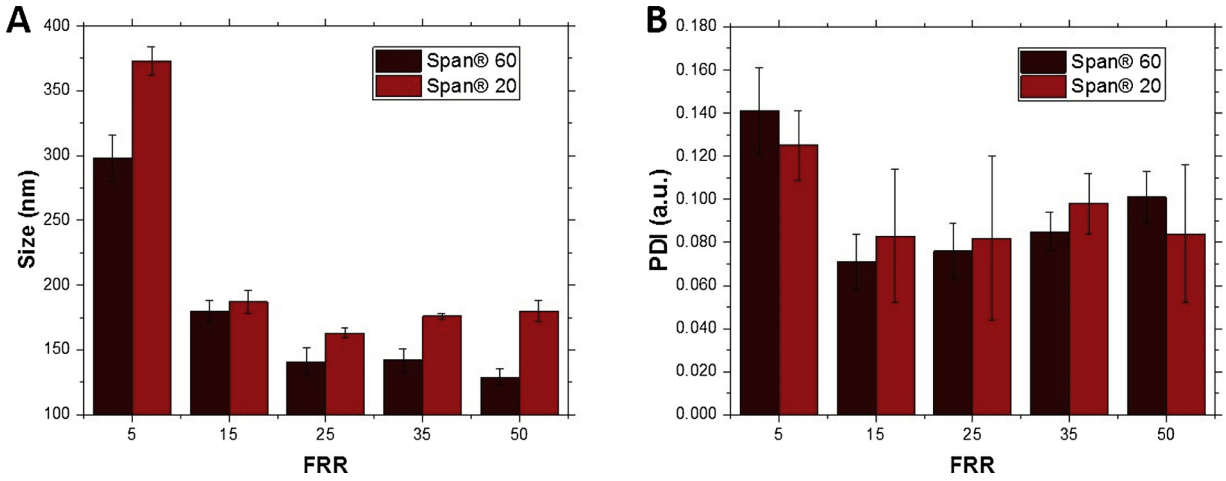

Fig. 7. Influence of acyl chain length (C12 and C18 for Span® 20 and Span® 60 respectively) of two different sorbitan sters used in niosomes formulation (surfactant:cholesterol 1:0.5 molar ratio, 5 mM), and produced under different conditions by hydrodynamic flow focusing at controlled temperature (50 °C) and a flow rate Q_T = 100 µl/min.

general terms, an increase in FRR yields a focused stream being narrower, and then, smaller particles due to the reduction in residual solvent and the introduction of less amount of bilayer components. This reduction allows complete mixing, even at high total flow rate, resulting in the size distribution of generated particles being more homogeneous. The counterpart is that production yield is reduced, since particles are generated in a less concentrated suspension. Another variable found to be relevant is the component concentration in ethanol feeding solution, with a direct effect on particle size and monodispersity. A more concentrated solution induces an increment in particle size at any total flow rate, but surprisingly, better size distribution. Complementary, we have checked the influence of acyl chain length over particles morphology, and the versatility that introduces this parameter into the properties and functionalities of this type of biomaterial.

The effect of ethanol stratification due to differences in density was not taken into account, which need further investigation in for future work, in particular in its relationship with focusing temperature.

The findings in this works provide valuable information about microfluidics-based production of niosomes at different operational conditions, and are expected to support the expansion of this technique for the preparation of a wider range of organic colloids with important characteristics for related industries with growing interest in different application fields.

Declaration of Competing Interest

The authors declare no conflicts of interest in this work.

Acknowledgements

This work was supported by the Ministerio de Economía y Competitividad (MINECO, Spain), under the Grant CTQ2013-47396-R and MAT2017-84959-C2-1-R. This study was also financed by the Consejería de Economía y Empleo del Principado de Asturias (Plan de Ciencia, Tecnología e Innovación 2013-2017), under the Grant GRUPIN14-022 and IDI/2018/000185. Support from the European Regional Development Fund (ERDF) is gratefully acknowledged. Pablo García-Manrique is especially grateful to Campus de Excelencia de la Universidad de Oviedo and Banco Santander for his mobility fellowship for the stay at University of Southampton.

Appendix A. Supplementary data

Supplementary material related to this article can be found, in the online version, at doi:https://doi.org/10.1016/j.colsurfb.2019.110378.

References

[1] A. Albanese, P.S. Tang, W.C. Chan, The effect of nanoparticle size, shape, and surface chemistry on biological systems, Annu. Rev. Biomed. Eng. 14 (2012) 1–16.
[2] K.L. Kelly, E. Coronado, L.L. Zhao, G. Schatz, The optical properties of metal nanoparticles: the influence of size, shape, and dielectric environment, J. Phys. Chem. B 107 (3) (2003) 668–677.
[3] G. Tarun, K.G. Amit, Liposomes: targeted and controlled delivery system, Durg Deliv. Lett. 4 (1) (2014) 62–71.
[4] H. Abdelkader, A.W.G. Alani, R.G. Alany, Recent advances in non-ionic surfactant vesicles (niosomes): self-assembly, fabrication, characterization, drug delivery applications and limitations, Drug Deliv. 21 (2) (2013) 87–100.
[5] J.S. Lee, J. Feijen, Polymersomes for drug delivery: design, formation and characterization, J. Control. Release 161 (2) (2012) 473–483.
[6] C. Marianecci, L. Di Marzio, F. Rinaldi, C. Celia, D. Paolino, F. Alhaique, S. Esposito, M. Carafa, Niosomes from 80 s to present: the state of the art, Adv. Colloid Interface Sci. 205 (2014) 187–206.
[7] S. De, M.R. Prasad, Self-assembled cell-mimicking vesicles composed of amphiphilic molecules: structure and applications, first edition, in: Hiroyuki Ohshima (Ed.), Encyclopedia of Biocolloids and Biointerface Science, vol. 1, John Wiley & Sons, 2016.
[8] R. Handjani-Vila, A. Ribier, B.A. Rondot, G. Vanlerberghie, Dispersions of lamellar phases of non-ionic lipids in cosmetic products, Int. J. Cosmet. Sci. 1 (5) (1979) 303–314.
[9] G. Gutiérrez, M. Matos, P. Barrero, D. Pando, O. Iglesias, C. Pazos, Iron-entrapped niosomes and their potential application for yogurt fortification, Food Sci. Technol. 74 (2016) 550–556.
[10] B. Demir, B.F. Baris, G.Z. Pinar, P. Unak, S. Timur, Theranostic niosomes as a promising tool for combined therapy and diagnosis: “all-in-one” approach, Appl. Nano Mater. 1 (6) (2018) 2827–2835.
[11] P. García-Manrique, E. Lozano-Andrés, O.R. Estupiñán-Sánchez, G. Gutiérrez, M. Matos, C. Pazos, M. Yañez-Mo, C. Blanco-López, Biomimetic small extracelular vesicles, 3rd GEIVEX Simposium, San Sebastian, Spain, 29-30 September, (2016) Poster communication.
[12] S. De, R. Kundu, A. Biswas, Synthesis of gold nanoparticles in niosomes, J. Colloid Interface Sci. 386 (2012) 9–15.
[13] R. Bartelds, N.M. Hadi, T. Pols, M.C.A. Stuart, A. Pardakhty, G. Asadikaram, B. Poolman, Niosomes, an alternative for liposomal delivery, PLoS One 13 (4) (2018) e0194179.
[14] O.R. Justo, A.M. Moraes, Analysis of process parameters on the characteristics of liposomes prepared by ethanol injection with a view to process scale-up: effect of temperature and batch volume, Chem. Eng. Res. Des. 89 (2011) 785–792.
[15] M. Danaei, M. Dehghankhold, S. Ataei, F. Davarani Hasanzadeh, R. Javanmard, A. Dokhani, S. Khorasani, M.R. Mozafari, Impact of particle size and polydispersity index on the clinical applications of lipidic nanocarrier systems, Pharmaceutics 57 (10) (2018) 1–17.
[16] P. García-Manrique, M. Matos, G. Gutierrez, O.R. Estupiñán, M.C. Blanco-López, C. Pazos, Using factorial experimental design to prepare size-tuned nanovesicles, Ind. Eng. Chem. Res. 55 (34) (2016) 9164–9175.
[17] D. van Swaay, A. deMello, Microfluidic methods for forming liposomes, Lab Chip 13 (2013) 752–767.

[18] L. Capretto, D. Carugo, S. Mazzitelli, C. Nastruzzi, X. Zhang, Microfluidic and lab-on-a-chip preparation routes for organic nanoparticles and vesicular systems for nanomedicine applications, Adv. Drug Deliv. Rev. 65 (2013) 1496–1532.
[19] A. Jahn, W.N. Vreeland, D.L. DeVoe, L.E. Locascio, G. Michael, Microfluidic directed formation of liposomes of controlled size, Langmuir 23 (11) (2007) 6289–6293.
[20] E. Kastner, V. Verma, D. Lowry, Y. Perrie, Microfluidic-controlled manufacture of liposomes for the solubilisation of a poorly water soluble drug, Int. J. Pharm. 485 (2015) 122–130.
[21] S. Joshi, M.T. Hussain, B.R. Carla, G. Anderluzzi, E. Kastner, S. Salmaso, D.J. Kirby, Y. Perrie, Microfluidics based manufacture of liposomes simultaneously entrapping hydrophilic and lipophilic drugs, Int. J. Pharm. 514 (2016) 160–168.
[22] C.T. Lo, A. Jahn, L.E. Locascio, W.N. Vreeland, Controlled self-assembly of monodisperse niosomes by microfluidic hydrodynamic focusing, Langmuir 26 (11) (2010) 8559–8566.
[23] M.A. Obeid, I. Khadra, A.B. Mullen, R.J. Tate, V.A. Ferro, The effects of hydration media on the characteristic of non-ionic surfactant vesicles (NISV) prepared by microfluidics, Int. J. Pharm. 56 (2017) 52–60.
[24] S. García-Salinas, E. Himawan, M. Gracia, M. Arruebo, V. Sebastian, Rapid on-Chip assembly of niosomes: batch versus continuous flow reactors, Appl. Mater. Interfaces 10 (2018) 19197–19207.
[25] B.C. Gross, J.L. Erkal, S.Y. Lockwood, C. Chen, D.M. Spence, Evaluation of 3D printing and its potential impact on biotechnology and the chemical sciences, Anal. Chem. 86 (2014) 3240–3253.
[26] J. Dong, J. Liu, G. Kang, J. Xie, Y. Wang, Pushing the resolution of photolithography down to 15 nm by surface plasmon interference, Sci. Rep. 4 (2014) 5618.
[27] D. Carugo, J.Y. Lee, A. Pora, R.J. Browning, Capretto Lorenzo, C. Nastruzzi, E. Stride, Facile and cost effective production of microscale PDMS architecture using a combined micromilling-replica moulding (μMI-REM) technique, Biomed. Microdevices 18 (2016) 1–10.
[28] A.K. Au, W. Huynh, L.F. Horowitz, A. Folch, 3D-prinded microfluidics, Angew. Chem. Int. Ed. 55 (2016) 3862–3881.
[29] G. Comina, A. Suska, D. Filippini, PDMS lab-on-a-chip fabrication using 3D printed templates, Lab Chip 14 (2014) 424–430.
[30] Y. Hwang, O.H. Paydar, R.N. Candler, 3D Printed molds for non-planar PDMS microfluidic channels, Sens. Actuators A 226 (2015) 137–142.
[31] D.A. Cristaldi, F. Yanar, A. Mosayyebi, P. García-Manrique, E. Stulz, D. Carugo, X. Zhang, Easy-to-perform and cost-effective fabrication of continuous-flow reactors for their application for nanomaterials synthesis, N. Biotechnol. 47 (2018) 1–7.
[32] E. Bottaro, A. Mosayyebi, D. Carugo, C. Nastruzzi, Analysis of the diffusion process by pH indicator in microfluidic chips for liposomes production, Micromachines 8 (2017) 209.
[33] Chee Kai Chua, Kah Fai Leong (Eds.), 3D Printing and Additive Manufacturing-Fifth Edition, Principles and Applications, World Scientific Publishing Co. Pte. Ltd., Singapore, 2017.
[34] G. Gaal, M. Mendesa, T.P. de Almeideb, M.H.O. Piazzettad, Â.L. Gobbi, A. Riul Jr, V. Rodrigues, Simplified fabrication of integrated microfluidic devices using fused deposition modeling 3D printing, Sens. Actuators B Chem. 242 (2017) 35–40.
[35] P.N. Ezhilarasi, P. Karthik, N. Chhanwal, C. Anandharamakrishnan, Nanoencapsulation techniques for food bioactive components: a review, Food Bioprocess Technol. 6 (2013) 628–647.
[36] D. Carugo, E. Bottaro, J. Owen, E. Stride, C. Nastruzzi, Liposome production by microfluidics: potential and limiting factors, Sci. Rep. 19 (6) (2016) 25876.
[37] R.R. Hood, D.L. DeVoe, High-throughput continuous flow production of nanoscale liposomes by microfluidic vertical flow focusing, Small 11 (2015) 5790–5799.
[38] M. Antonietti, S. Förster, Vesicles and liposomes: a self-assembly principle beyond lipids, Adv. Mater. 15 (2003) 1323–1333.
[39] I.V. Zhigaltsev, N. Belliveau, I. Hafez, A.K.K. Leung, J. Huft, C. Hansen, P.R. Cullis, Bottom-up design and synthesis of limit size lipid nanoparticle systems with aqueous and triglyceride cores using millisecond microfluidic mixing, Langmuir 28 (2012) 3633–3640.
[40] E. Kastner, R. Kaur, D. Lowry, B. Moghaddam, A. Wilkinson, Y. Perrie, High-throughput manufacturing of size-tuned liposomes by a new microfluidics method using enhanced statistical tools for characterization, Int. J. Pharm. 477 (2015) 361–368.
[41] R. Karnik, F. Gu, P. Basto, C. Cannizzaro, L. Dean, Kyei-Manu, R. Langer, O.C. Farokhzad, Microfluidic platform for controlled synthesis of polymeric nanoparticles, Nano Lett. 8 (9) (2018) 2906–2912.
[42] A. Manosroi, P. Wongtrakul, J. Mnosroim, H. Sakai, F. Sugawara, M. Yuasa, M. Abe, Characterization of vesicles prepared with various non-ionic surfactants mixed with cholesterol, Colloids Surf. B Biointerfaces 30 (2003) 129–138.
[43] L. Peltonen, J. Hirvonen, J. Yliruusi, The effect of temperature on sorbitan surfactant monolayers, J. Colloid Interface Sci. 239 (2001) 134–138.
[44] G. Gutiérrez, J.M. Benito, C. Pazos, J. Coca, Evaporation of aqueous dispersed systems and concentrated emulsions formulated with non-ionic surfactants, Int. J. Head Mass Transf. 69 (2014) 117–128.

Supplementary Material-

Controlled size niosome production using a thermostatic microfluidic device

Pablo García-Manrique[1,2], Gemma Gutiérrez[2], María Matos[2], Andrea Cristaldi[3], Ali Mosayyebi[3], Dario Carugo[4], Xunli Zhang[3]*, Mª Carmen Blanco[1]*

[1] *Department of Physical and Analytical Chemistry, University of Oviedo; Spain*
[2] *Department of Chemical Engineering and Environmental Technology, University of Oviedo; Spain*
[3]*Bioengineering Sciences group, Faculty of Engineering and the Environment, Institute for Life Sciences (IfLS), University of Southampton; United Kingdom*
[4]Mechanotronics and Bioengineering sciences research groups, *Faculty of Engineering and the Environment, Institute for Life Sciences (IfLS), University of Southampton; United Kingdom*

***Corresponding authors; *E-mail address*:** cblanco@uniovi.es, XL.Zhang@soton.ac.uk

Table S1. Morphological characteristics of mixing channel for original Solidworks® CAD 2016 design and 3D-Printed positive moulds (3D-PM) onto VeroClear™ resin with the 3D printer Objet350 Connex™ (Stratsys). Average and standard deviation values are given for the parameters.

Mould	Width (µm)	Height (µm)	Cross sectional area (µm)
CAD	100	100	10000
3D-PM1	535 ± 40	47 ± 2	13090 ± 485
3D-PM2	423 ± 14	51 ± 1	11605 ± 262
3D-PM3	507 ± 28	68 ± 3	18007 ± 1092

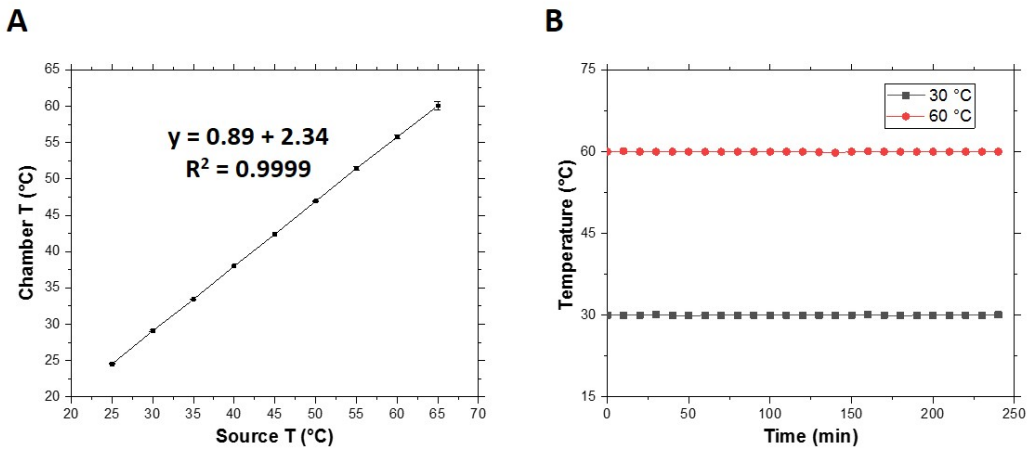

Figure S1. Calibration plot (**A**) and temperature stability (**B**) of the *in-house* designed thermostatic chamber for microfluidics chips, fabricated by 3D-printing technology with PLA filaments. Values represented are the average of three independents measurements.

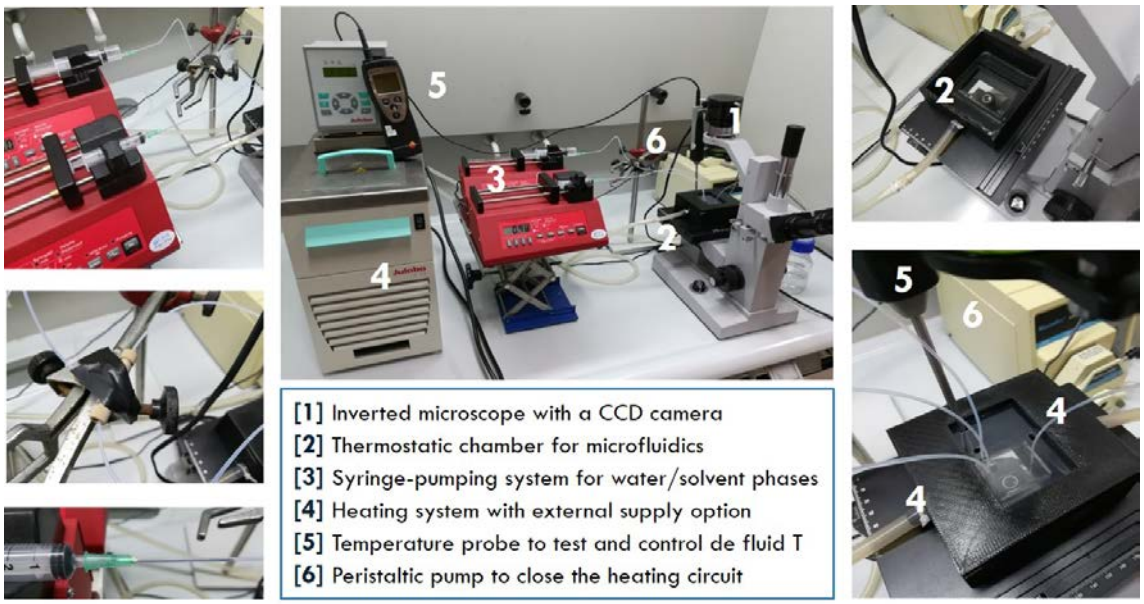

Figure S2. Pictures composition showing the whole setup (central) and detailed components (sides) used in this work for niosomes production by Hydrodynamic Flow Focusing with controlled temperature.

Table S2. Correlation factor between flow focusing parameters (FRR and W_f) and particle size at different concentration of bilayer components and variable Q_T (**A**), and at fixed concentration and Q_T for different working temperatures (**B**).

(A)

R^2 *(T = 50 °C)*	50 µl/min	100 µl/min	200 µl/min
(*) **FRR *vs* W_f**	0.99	0.97	0.92
(**) **W_f *vs* Particle size**	0.86 *(5 mM)*	0.98 *(5 mM)*	0.97 *(5 mM)*
	0.98 *(20 mM)*	0.99 *(20 mM)*	0.93 *(20 mM)*

FRR, Flow Rate Ratio; **Q_T**, Total volumetric rate; **W_f**, initial width of focused stream; (*) potential correlation; (**) linear correlation

(B)

R^2 *(Q_T = 100 µl/min)*	30 °C	40 °C	50 °C	60 °C
(*) **FRR *vs* W_f**	1.00	0.99	0.97	0.98
(**) **FRR *vs* Particle size**	0.24	0.56	0.91	0.65

FRR, Flow Rate Ratio; **Q_T**, Total volumetric rate; **W_f**, initial width of focused stream; (*) potential correlation; (**) linear correlation

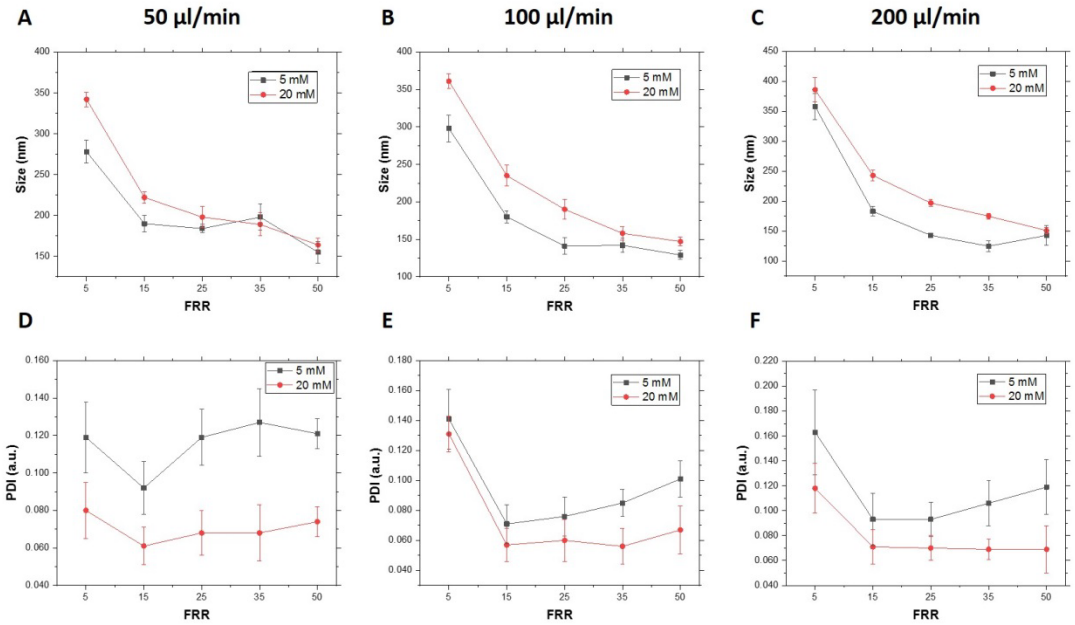

Figure S3. Effect of bilayer components concentration for niosomes formulated with Span® 60:Cholesterol (1:0.5 molar ratio) and produced under the same flow conditions (Q_T and FRR) for size (upper row) and size distribution (lower row).

ANEXO II. Publicaciones relacionadas con la Tesis Doctoral

New BIOTECHNOLOGY 47 (2018) 1–7

Contents lists available at ScienceDirect

New BIOTECHNOLOGY

journal homepage: www.elsevier.com/locate/nbt

Easy-to-perform and cost-effective fabrication of continuous-flow reactors and their application for nanomaterials synthesis

Domenico Andrea Cristaldi[a,c], Fatih Yanar[a], Ali Mosayyebi[a], Pablo García-Manrique[b], Eugen Stulz[c,**], Dario Carugo[d,*], Xunli Zhang[a,**]

[a] Bioengineering Group, Faculty of Engineering and the Environment, Institute for Life Sciences (IfLS), University of Southampton, UK
[b] Departments of Physical and Analytical Chemistry, and Chemical Engineering and Environmental Technology, University of Oviedo, Spain
[c] School of Chemistry & Institute for Life Sciences, University of Southampton, Highfield, Southampton, UK
[d] Mechatronics and Bioengineering Science Research Groups, Faculty of Engineering and the Environment, Institute for Life Sciences (IfLS), University of Southampton, UK

ARTICLE INFO

Keywords:
3D printing
Lab-on-a-chip
Soft lithography
Nanoparticles
Liposomes
Continuous-flow reactors.

ABSTRACT

The translation of continuous-flow microreactor technology to the industrial environment has been limited by cost and complexity of the fabrication procedures and the requirement for specialised infrastructure. In the present study, we have developed a significantly more cost-effective and easy-to-perform fabrication method for the generation of optically transparent, continuous-flow reactors. The method combines 3D printing of master moulds with sealing of the PDMS channels' replica using a pressure-sensitive adhesive tape. Morphological characterisation of the 3D printed moulds was performed and reactors were fabricated with an approximately square-shaped cross-section of 1 mm^2. Notably, they were tested for operation over a wide range of volumetric flow rates, up to 20 ml/min. Moreover, the fabrication time (i.e., from design to the finished product) was < 1 day, at an average material cost of ~£5. The flow reactors have been applied to the production of both inorganic nanoparticles (silver nanospheres) and organic vesicular systems (liposomes), and their performance compared with reactors produced using more laborious fabrication methods. Numerical simulations were performed to characterise the transport of fluids and chemical species within the devices. The developed fabrication method is suitable for scaled-up fabrication of continuous-flow reactors, with potential for application in biotechnology and nanomedicine.

Introduction

Photolithography has been widely used to manufacture continuous-flow reactors at high spatial resolution, in terms of both size and shape of the channels' architecture [1]. However, this process involves numerous steps and generally requires specialised cleanroom facilities, and expensive materials or instrumentation. In addition, the whole process (i.e., from the design of the device architecture to the end product) is highly time-consuming. The combination of these factors has hindered the widespread adoption of this technology by industries and researchers, particularly in the non-specialised or less resourced laboratories.

In the last decade, efforts have been made to develop more cost-effective and user friendly manufacturing approaches [2]. For instance, the micromilling-replica moulding (μMi-REM) technique recently developed by Carugo et al. [3] involves the fabrication of positive epoxy masters obtained from negative micromilled moulds (made of polymethyl methacrylate, PMMA). This procedure does not require the fabrication of photomasks *via* photolithography, which is typically performed in a cleanroom environment. However, the method requires the use of micromilling machines, as well as oxygen plasma bonding for the sealing of the polydimethylsiloxane (PDMS) channels onto a glass layer. Alternatively, positive moulds can be fabricated in a single step using high-resolution 3D printing (with channel width down to 50 μm), as demonstrated by Comina et al. [4]. Similarly, three-dimensional (3D) PDMS microfluidic reactors can be fabricated via UV-activated 3D printing, as described by Chan et al. [5]. Although 3D printing of resin moulds may be less complex to perform compared to μMi-REM, it requires specific treatments of the moulds prior to PDMS casting, due to the inhibition effect of the resin on the PDMS cross-linker [6,4]. In addition, both methods rely on the use of oxygen plasma during the bonding process. On the other hand, microfluidic devices could be entirely 3D printed, as demonstrated by Kitson et al. [7]. This method is cost-effective and easy-to-perform; however, devices are not optically

* Corresponding author.
** Co-corresponding authors.
E-mail addresses: est@soton.ac.uk (E. Stulz), d.carugo@soton.ac.uk (D. Carugo), XL.Zhang@soton.ac.uk (X. Zhang).

https://doi.org/10.1016/j.nbt.2018.02.002
Received 25 July 2017; Received in revised form 2 February 2018; Accepted 4 February 2018
Available online 06 February 2018
1871-6784/

transparent, thus limiting the ability to optically monitor flow and mixing processes. The optical transparency of 3D printed channels was recently improved by Gaal et al. [8], using a custom built 3D printer to create polylactic acid/polydimethylsiloxane (PLA/PDMS) architectures. However, careful adjustments of the 3D printer settings were needed during the fabrication process, and the cross-section of the produced channels differed significantly from the original computer-aided design (CAD).

Developments have also been made in terms of the microchannel dimensions obtainable using 3D printing, with recent studies researching novel resin formulations for stereolithgraphy (SL) and 3D printing with Digital Light Processing (DLP) [9]. With this technique, Gong et al. demonstrated the generation of remarkably small microchannels (i.e., with cross section as small as 18 × 20 μm) [10]. Significant efforts have also been devoted to development of simple bonding techniques for microfluidic devices. For example, Serra et al. [11] recently demonstrated the use of a commercially available sealing tape (Thermalseal RTS™) for bonding of various substrates. The PDMS channel architectures in this study were fabricated from micromilled brass masters.

In the present study, we developed a fast, cost-effective and facile manufacturing process to fabricate optically transparent flow reactors, with milli- or sub-millimetre scale flow channels (i.e., with 0.5–1.0 mm channel width). A combination of techniques was employed including 3D printing of positive moulds followed by PDMS casting (3D printed mould casting, 3DPM-C), and direct sealing of the PDMS layer using a pressure-sensitive adhesive tape. The 3D printed moulds were characterized in terms of surface roughness and cross-sectional shape, and reactors were tested over a wide range of operational conditions. To demonstrate the usability of the developed fabrication technique, reactors were applied to the production of silver nanospheres (SNSs) and liposomes, as examples of inorganic and organic synthesis, respectively.

Silver nanospheres (SNSs) have been employed in many research fields ranging from photocatalysis [12] to optoelectronics [13], as well as for biological applications due to their antibacterial properties [14]. SNSs synthesis typically needs a carefully balanced stoichiometry, in order to obtain the desired particle size and/or shape [15]. Recently, Barber et al. demonstrated a coaxial glass reactor for continuous-flow production of SNSs [16], with superior control over the fluidic environment and properties of the produced SNSs, when compared to bulk methods. Liposomes, spherical vesicles comprising an aqueous core surrounded by a lipid bilayer, are employed as vehicles for transporting and administering pharmaceutical actives [17]. Production of liposomes *via* solvent exchange mechanism in continuous-flow reactors has emerged as a promising technique, offering a higher degree of control over the physical and dimensional properties of the end product, compared to batch methods.

In this study, we demonstrate continuous-flow production of both types of nanoscale particles using cost-effective and easy-to-operate reactors.

Materials and methods

Design, fabrication and morphological characterization of flow reactors

Fabrication of the 3D printed mould casting (3DPM-C) channels is illustrated in Scheme 1. Solidworks® CAD 2016 software was used for designing the master mould. The flow reactor architecture has two semi-circular inlet channels of 0.50 mm × 1.00 mm (width × height) and 1.50 mm radius. Inlets converge in to a straight channel of 1.00 mm × 1.00 mm × 60.00 mm (width × height × length). The channel architecture was positioned at the bottom surface of a box structure having a 7.00 mm high edge, which acted as a container for uncured PDMS (see Step 1 in Scheme 1). The Ultimaker 2+ 3D printer, loaded with PLA filaments, was employed as a representative fused deposition modelling (FDM) tool for the production of the master moulds. The following printing settings were adopted: bottom/top thickness = 0.5 mm, fill density = 100%, print speed = 50 mm/s, and nozzle size = 0.4 mm. PDMS replicas were prepared by pouring a 10.2/0.8 (w/w) ratio of degassed PDMS precursor and curing agent mixture (Sylgard® 184, Dow Corning Corporation, Michigan, USA) over the mould (Scheme 1, Step 2). Degassing was carried out by prior centrifugation at 3000 rpm for 15 min, using the Eppendorf Centrifuge 5804 and Corning Centristar™ tubes (50 ml). After pouring, the liquid PDMS was left at room temperature for 4 h and any formed gas bubble removed using a sharp tool (every 1 h). This step could be significantly accelerated by placing the mould under vacuum. PDMS curing was performed in the oven at 40 °C overnight. The cured PDMS replica channel was peeled off from the master mould, and a 1.5 mm diameter biopsy punch with plunger (Miltex®, Fischer Scientific, UK) was used for creating inlets/outlets. Sealing of the PDMS layer was performed on ThermalSeal RT™ tape purchased from Excel Scientific (USA) (Scheme 1, Step 3). To characterise the morphology of the 3D printed moulds, a non-contact Alicona Infinite Focus 3D optical profilometer was employed (5 × magnification lens, vertical resolution: 410 nm, lateral resolution: 6.59 μm). In order to evaluate the method's repeatability, three identical devices were printed and two-dimensional (2D) images (at 2.5 × magnification) were acquired to measure (i) the width of the mixing channel at five equidistant locations along the channel (separation distance between measurements = 2 mm) starting from the junction, and (ii) the radius of curvature of both inlet channels. Measurements were performed using Image-J software (NIH, USA).

The manufacture of μMi-REM devices was performed following a protocol previously reported [3]. The PVA-TePla 300 plasma cleaner was employed to assist the bonding of the PDMS layer with a 50 × 70 mm glass sheet (Corning® microscope slides, Sigma Aldrich, Gillingham, UK).

The two fabrication methods employed in this study are herein defined as 3DPM-C/Tape and μMi-REM*Glass, where '/' and '*' indicate adhesive tape and plasma bonding procedures, respectively.

Synthesis of inorganic and organic nanoparticles

The same experimental set-up was used for the production of both silver nanospheres and liposomes. Syringe pumps (AL-1010) were purchased from World Precision Instruments (UK). Luer Lock syringes (20 ml) (BD Plastipak) were purchased from BD (Becton, Dickinson and Company, UK). Polytetrafluoroethylene (PTFE) tubing and connectors (Cole-Palmer, UK) were employed for interfacing the device inlets and outlet with syringes and collection vials, respectively. The length of the tube from the outlet to the collection vial was 26.70 cm.

Silver nanoparticles were synthesized using silver nitrate 99.9999% ($AgNO_3$), tri sodium citrate dihydrate ≥ 99.0% (TSCD), polyvinylpyrrolidone (PVP), and sodium borohydride 99% ($NaBH_4$), which were purchased from Sigma Aldrich UK (Gillingham, UK). Propan-2-ol (or isopropyl alcohol, IPA) laboratory reagent grade was purchased from Fisher Chemical (UK). Milli-Q water was collected using the Q-Gard purification filter, connected to the Milli-Q Gradient A10 system (Merck Millipore, USA).

Scheme 2 shows the experimental set-up employed for the synthesis of both silver nanoparticles and liposomes. Syringes were spatially arranged in a way that allowed performing the same experiment for both 3DPM-C/Tape and μMi-REM*Glass devices, by simply changing the reactor.

For SNSs production, a 20 ml syringe was primed with a Milli-Q water solution containing $AgNO_3$ (1.02 mM), TSCD (15.02 mM), and PVP (0.45 M). The second syringe was primed with 15 ml of an IPA/Milli-Q solution (9:1 v/v) of $NaBH_4$ (5.28 mM). The total flow rate ($TFR = FR_A + FR_B$) was kept at the constant value of 1 ml/min, whereas the flow rate ratio ($FRR = FR_A/FR_B$) was varied (5, 7, 9 and 11). Each sample was separately collected in a 1.5 ml Eppendorf tube, and 1.5 ml were collected in a waste vial in between each experimental

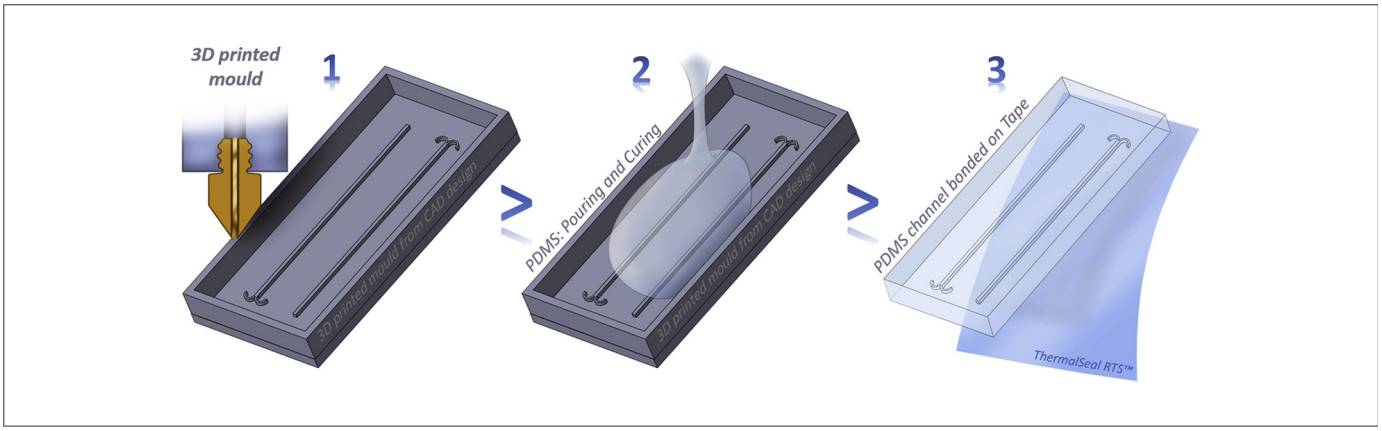

Scheme 1. Graphical representation of the manufacturing steps for the 3DPM-C/Tape reactor: 1) Low-cost 3D printing of the positive mould; 2) PDMS casting; and 3) sealing of the cured PDMS layer onto adhesive tape.

run. In order to evaluate the robustness of the reaction, experiments were repeated in triplicate at selected TFR and FRR values.

For the synthesis of liposomes, Phospholipon® 90G (lipids) and purified phosphatidylcholine from soybean lecithin, were kindly provided by Lipoid GmbH (Germany). Pure ethanol (99.9%) was purchased from Sigma-Aldrich Company Ltd. (UK). A 100 mM lipid solution in ethanol was prepared, and the lipid concentration selected to produce liposomes of a clinically relevant size and mass [18–20]. Milli-Q water was injected into one inlet (Syringe A) and ethanol-containing lipids was injected into a second inlet (Syringe B), for each reactor (Scheme 2).

Experiments were carried out maintaining a constant FRR of 25, at varying TFRs of 1, 3 and 6 ml/min to demonstrate devices' usability for producing liposomes at high-throughput. Three samples were collected, at each TFR and for each device tested.

Characterisation of nanoparticles

The UV–vis characterization of silver nanospheres (SNSs) was carried out using a Varian Cary300Bio UV–vis Spectrophotometer. All measurements were performed in the 200–800 nm range, with an increment step of 0.5 nm. SNS analytical samples (1 ml) were collected from the flow reactors, and diluted to 3 ml with Milli-Q water into a quartz cuvette for the spectrophotometric characterization. The baseline was subtracted from each experimental condition (i.e., considering the specific Milli-Q/IPA volume ratio).

Transmission electron microscopy (TEM) characterization of SNSs was also performed. Images were acquired using the TEM Hitachi HT7700. Silver nanoparticles were prepared by drop-casting of the colloidal synthesis solution (5 µl), on carbon and Formvar coated Cu/Pd 200 mesh grids, and left to dry under atmospheric conditions at room temperature.

A dynamic light scattering (DLS) technique was used instead to measure the mean diameter (z-average), the polydispersity index (PDI), and zeta potential of all liposomal formulations, produced with both 3DPM-C/Tape and µMi-REM*Glass reactors. Liposome dimensional stability was assessed by measuring the mean diameter of samples stored at both 4 °C and 25 °C, every 5 days for a total 30 days. All measurements were performed using the Zetasizer Nano ZS Malvern, UK.

Results and discussion

Characterisation of the 3D printed moulds and PDMS channels

The morphology and roughness of the flat base of the 3D printed master are important characteristics affecting spatial uniformity and durability of the sealing. From the morphological examination, diagonal grooves can be observed due to the oblique motion of the nozzle in the *x-y* plane during printing (see Fig. 1a). The average roughness (*Ra*) value of the master mould is 6.56 µm (Fig. 1a), and a maximum peak-to-valley (*Rz*) value of 85.13 µm is detected in proximity to the diagonal features over the base surface (representative cross sectional profiles are shown in Figure SI-1a). Notably, we observed that grooves could promote fluid leakage at flow rates greater than 5 ml/min.

In order to overcome this limitation, the PDMS mixture (monomer/curing agent) was prepared using 8% curing agent (instead of the commonly used 10% by mass), to reduce PDMS stiffness. Notably, a softer PDMS could be deformed more easily by applying external pressure during sealing. Manual compression using a plastic spatula was initially performed (at an estimated pressure of 1 bar), followed by compression at ~0.5 bar for 1 h. In this way, no leakages were observed even at a total flow rate of 20 ml/min (see Supporting information video, at https://youtu.be/EpmnLZDXtBo), confirming the effectiveness of the sealing procedure for continuous-flow synthesis at high-throughput.

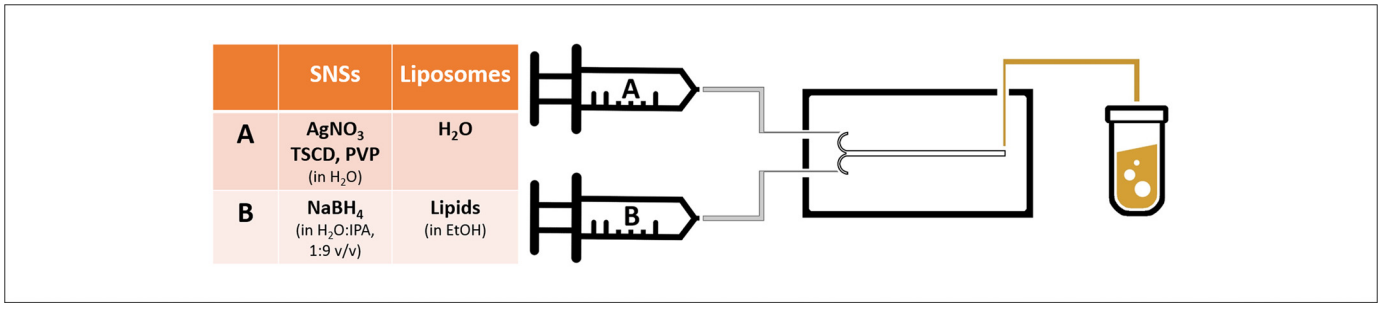

Scheme 2. Schematic of the experimental set-up and list of chemicals injected through syringes A and B for the production of SNSs and liposomes, respectively.

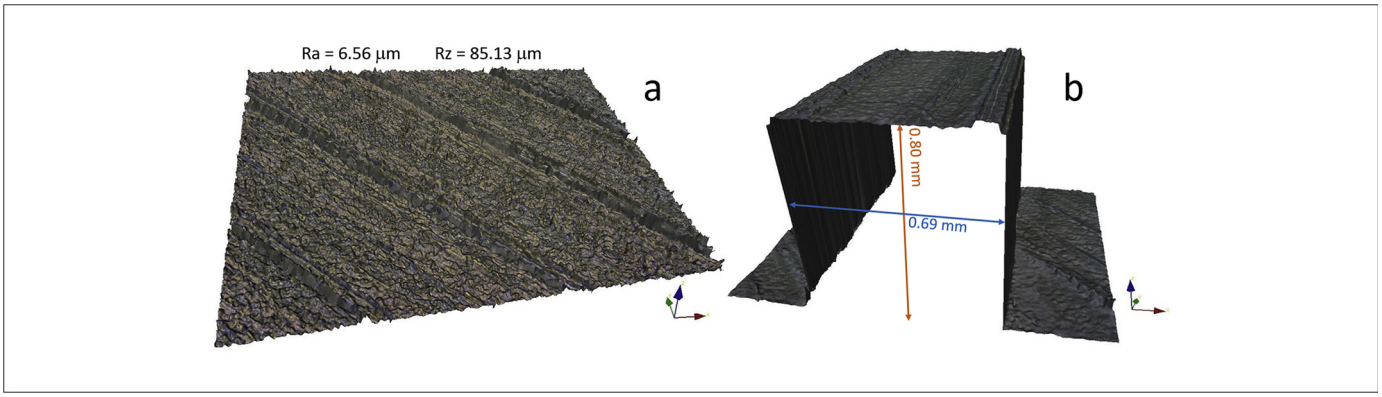

Fig. 1. Morphology and cross-sectional shape of the 3D printed moulds. a) Morphological characterisation of the 3D printed base, including average roughness (Ra) and maximum peak-to-valley value (Rz). b) Cross section of a representative channel design of 0.60 × 0.80 mm (width × height), obtained from optical profilometry.

Accurate reproduction of the designed (i.e., nominal) channel size and shape should ideally be achieved by the 3D printing process. In this respect, the high resolution (HR) resin 3D printer (Object Connex 350) was tested against the Ultimaker 2+ by printing channels of different cross-sectional dimension, as illustrated in Figure SI-1b. The HR 3D printer was able to create smaller and smoother channels; however, reproduction of the cross sectional shape was less accurate, even for the relatively large channel dimension of 1.00 × 1.00 mm (see cross section in Figure SI-1c obtained from profilometry). Thus, the Ultimaker 2+ was selected to generate the master moulds in the remaining experiments.

Two additional test channels were printed having different size but the same aspect ratio of 1.33, using the Ultimaker 2+. The mean experimental values obtained with the optical profilometer (representative test Channel 1 in Fig. 1b) are compared with the nominal dimensions of both channels in Table 1. The channel height is accurately reproduced, whereas the width is affected by a 0.09 mm difference for both test channels 1 and 2 (a 3D cross section of test Channel 2 is shown in Figure SI-1c). This is due to the orientation angle (90°) of the side walls of the channels with respect to the light source of the profilometer. This effect is clearly visible in Fig. 1b in which the side walls of the channel are represented as the projection of the edge of the channel roof towards the base, causing overestimation of the measured width.

Nonetheless, in order to assess repeatability of the reactor's fabrication method, three replicas of the 3D printed moulds were manufactured using the Ultimaker 2+ (Fig. 2). The width of the mixing channel (measured at five separate and equidistant locations along the channel) and the radius of curvature of the inlet channels were measured, and results are shown in Fig. 2a and b respectively. Insets illustrate the positions at which measurements were taken.

The width of the mixing channel is comparable between the three different moulds, as illustrated in Fig. 2a. The maximum difference is at 6 mm from the junction, between mould n.1 and n.3, and is equal to 0.0011 mm only. All moulds had a slightly larger channel width in proximity to the junction, which gradually reduced along the channel and reached a plateau value at about 8–10 mm from the junction (see Fig. 2a). The radius of curvature of the inlet channels was also very comparable between different moulds (mean value = 1.770 ± 0.012 mm), and only slightly differed from the nominal value of 1.75 mm (see Fig. 2b).

Table 1
Size comparison between the CAD design and the 3D printed channels.

Design-Morphology Comparisons	Width × Height (mm) Test Channel 1	Width × Height (mm) Test Channel 2
CAD Design	0.60 × 0.80	0.80 × 1.33
3D Printed mould profile (mean values)	0.69 × 0.80	0.89 × 1.33

*Synthesis of silver nanospheres and liposomes via 3DPM-C/Tape & µMi-REM*Glass reactors*

Nanoparticle synthesis via 3DPM-C/Tape reactor was performed in parallel with the already established µMi-REM*Glass technique. In order to compare the performance of the two fabrication methods, the physical properties of the produced nanomaterials were measured and evaluated at varying fluid dynamic boundary conditions.

Synthesis of silver nanospheres

Silver nanospheres (SNSs) were synthetized using the chemical reduction method [15], which was adapted for usage in a continuous-flow reactor. Specifically, $NaBH_4$ solution was prepared initially by dissolving the solid in 1.5 ml of Milli-Q water, followed by dilution to 15 ml with IPA. The use of IPA was to minimise the generation of H_2, produced from the degradation of $NaBH_4$ in water [21]. This drastically reduces the formation of gas bubbles within the channels, which may significantly alter the flow field or cause clogging. This effect may however be less problematic in millimetre-scale channels. An alternative approach may involve the generation of a strong basic condition (NaOH, 14 M) in water, as described by Barber et al. [16]. However, with the protocol described in this study, we were able to produce SNSs at all FRRs investigated, obtaining the maximum absorbance (A_{max}) of 2.9 ± 0.2 nm after 1:3 dilution with Milli-Q water. Nevertheless, the stoichiometry played a critical role in SNSs synthesis, and although the numerical results (see Figure SI-2b) show a marginal increase in mixing efficiency at FRR = 11, the SNSs production performance was more effective at FRR = 7.

Fig. 3a reports the UV–vis spectra of SNSs prepared using the 3DPM-C/Tape and the µMi-REM*Glass reactors, applying the same operational conditions in both devices (TFR = 1 ml/min; FRR = 7). In order to assess the reproducibility of the reaction, samples were produced in triplicate under the same conditions for both devices.

The typical absorption spectra, due to SNSs surface plasmon resonance (SPR) [22], are observed. Notably, the SNSs spectra obtained using the two different fabrication methods are almost overlapping across the whole wavelength spectrum. The mean value of maximum absorbance (A_{max}) is equal to 3.252 ± 0.050 and 3.236 ± 0.068 for the Tape and Glass reactors, respectively (see Fig. 3a and inset). More importantly, in both types of reactor the maximum absorption value of 398.0 nm is obtained, further indicating a comparable performance between them. The absorbance value is also related to the particle size

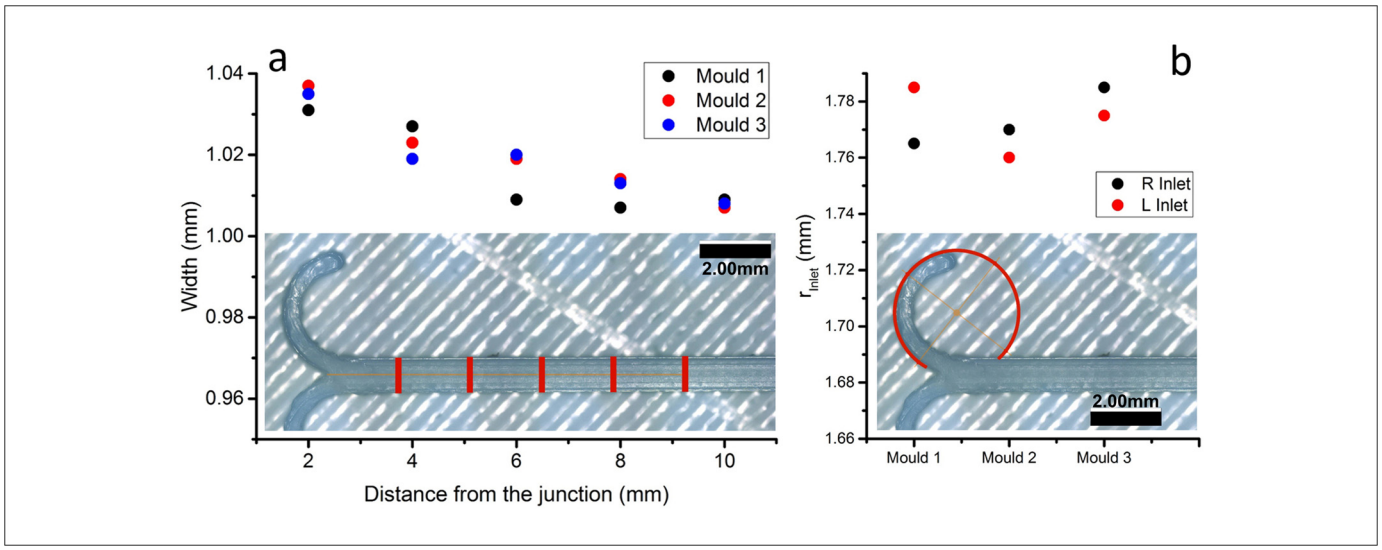

Fig. 2. a) Width of the mixing channel at 2, 4, 6, 8, and 10 mm from the junction between inlets, for three different 3D printed moulds. An image of a representative channel (at 2.5 × magnification) showing the measurement lines (red lines) is reported in the inset. b) Radius of curvature of both right (R) and left (L) inlet channels, for three different 3D printed moulds. A graphical representation of the measurement method is reported in the inset, for the right inlet channel.

[23], which ranged from 10 to 20 nm as shown in the TEM images (Fig. 3b).

Synthesis of liposomes

Having demonstrated that flow reactors fabricated with different methods have comparable performance when employed to produce silver nanoparticles, they were also tested for continuous-flow synthesis of liposomes. Devices were operated at total flow rates which were significantly higher than those typically used in microfluidic reactors [20], to demonstrate their potential utility for scaled-up synthesis.

Fig. 4 shows the size (z-average) and polydispersity index (PDI) of liposomes produced at varying TFR values (1, 3, 6 ml/min) and a fixed FRR of 25. A representative intensity-based liposome size distribution (at TFR = 1 ml/min and FRR = 25) is also shown in Figure SI-3a, for the μMi-REM*Glass reactor. Notably, liposome size and dispersity are not significantly different across different devices, for all the hydrodynamic conditions investigated. For instance, liposomes produced with the 3DPM-C/Tape and μMi-REM*Glass reactors at TFR = 1 ml/min and FRR = 25, have a diameter of 188.61 ± 1.62 nm and 191.37 ± 3.19 nm, respectively. Moreover, by increasing the TFR from 1 to 6 ml/min caused only a slight increase in liposome diameter in both devices, which is consistent with the numerical simulations showing a relatively small difference in the mixing index at the different flow regimes investigated (see Figure SI-2b). Fig. 4b shows that liposomes have a relatively small dispersity, and that PDI slightly increased with increasing the TFR from 1 to 6 ml/min.

Liposomes produced by the 3DPM-C/Tape reactor had a larger mean dispersity at the higher flow rates investigated, which could be potentially attributed to the surface roughness of the PDMS channels. Further investigations will be performed to better understand the effect of surface properties on the transport of fluids and chemical species in these devices.

In addition, the diameter of liposomes produced by 3DPM-C/Tape reactor (at FRR of 25 and TFR of 1 ml/min) was measured up to 30 days from production, at two different storage temperatures (4 °C and 25 °C), as shown in Fig. 4c. The size of liposomes stored at 4 °C increased over time, and reached a maximum% increase of approximately 15% after

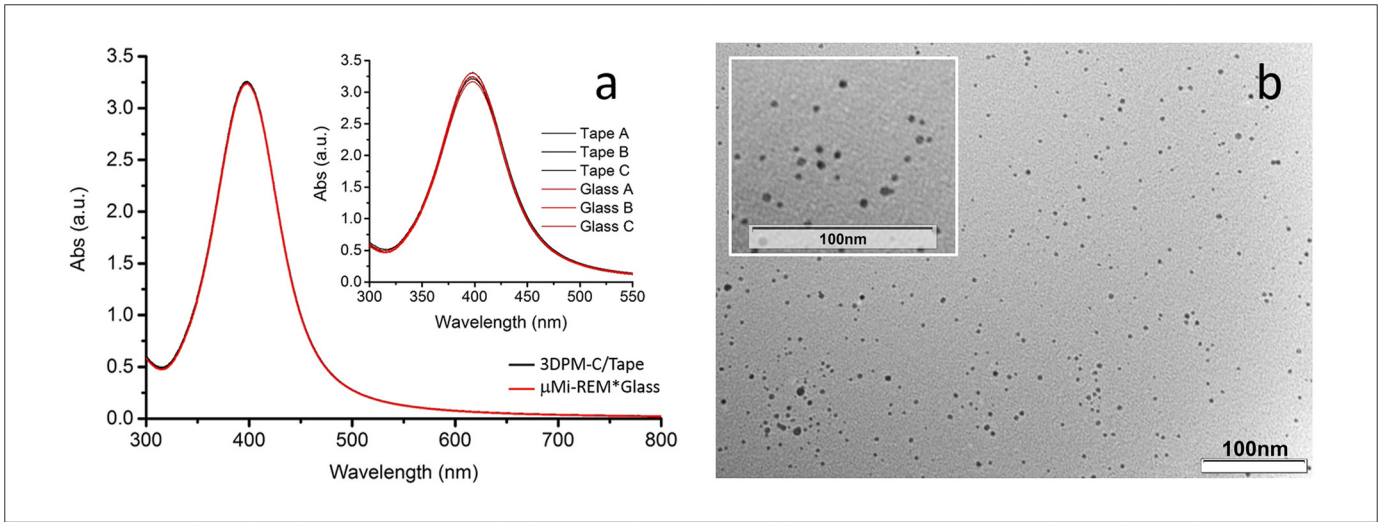

Fig. 3. a) UV–vis characterization of SNSs prepared using the 3DPM-C/Tape (black) and the μMi-REM*Glass (red) reactors. Spectra are shown as the mean of triplicate samples prepared using both types of reactor, at the same operating conditions (TFR = 1 ml/min; FRR = 7) (individual spectra are shown in the inset). b) Representative TEM image of the SNSs prepared with the 3DPM-C/Tape (TFR = 1 ml/min; FRR = 7); with a magnified view shown in the inset.

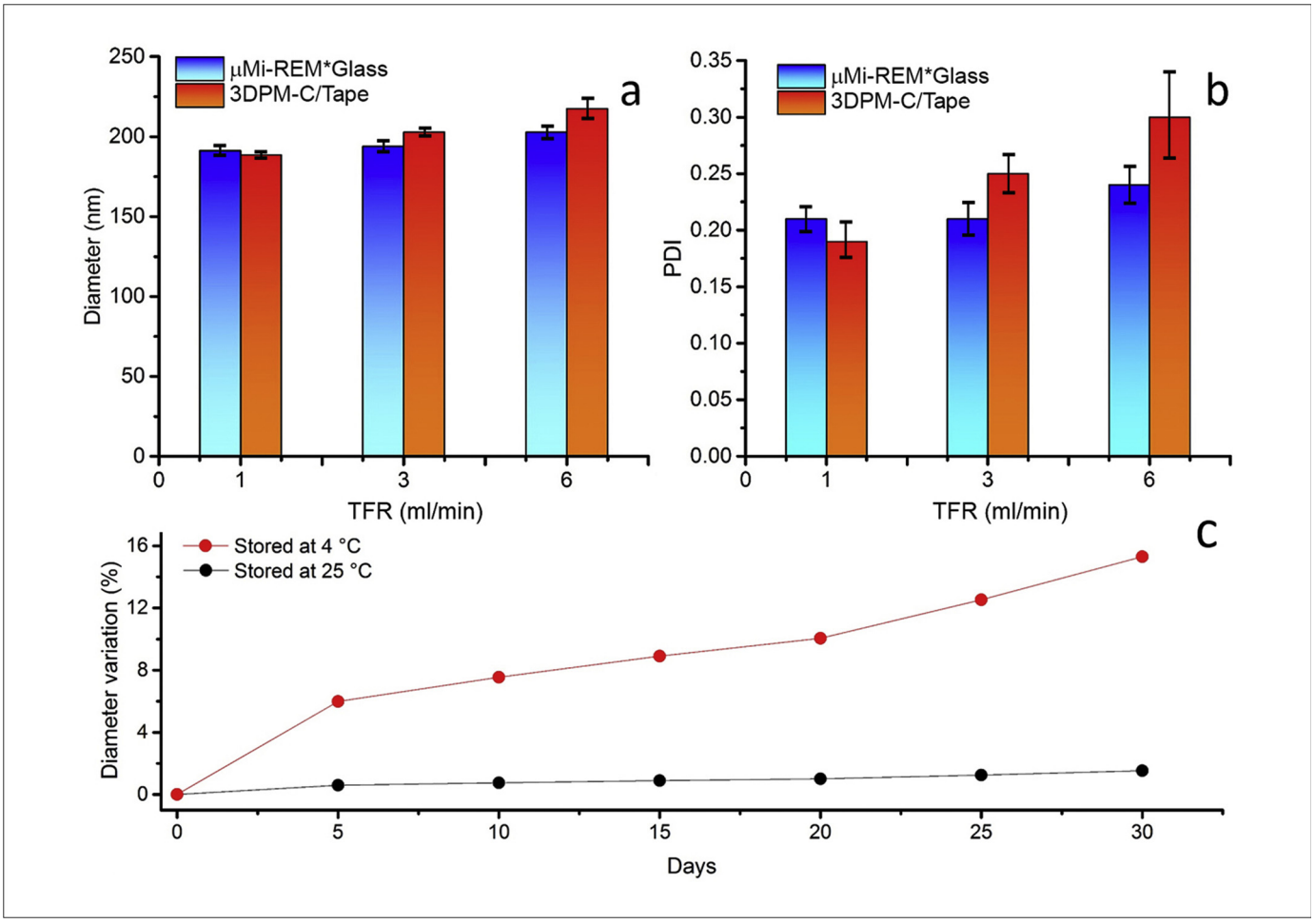

Fig. 4. Comparison of liposome size and dispersity. Size (z-average) (a) and dispersity (PDI) (b) of liposomal formulations produced by μMi-REM*Glass and 3DPM-C/Tape reactors. Each experiment was performed at TFR of 1 ml/min, 3 ml/min and 6 ml/min, at a fixed FRR of 25. Data are reported as the mean of three independent samples, with the corresponding standard deviation. c) Size stability of liposomal formulations produced by 3DPM-C/Tape reactor, at FRR of 25 and TFR of 1 ml/min. Liposome size was measured every 5 days and up to 30 days, at storage temperatures of both 4 °C and 25 °C.

30 days. These results are comparable with the ones previously reported in the literature [24], although they refer to different Phospholipon90G-based liposomal formulations. The increase in vesicle diameter could be attributed to sterical hindrance of bilayer stability [25] or aggregation, which may result in liposome coalescence [26]. Conversely, the size of liposomes stored at 25 °C was almost unchanged over time. Moreover, the zeta potential of liposomes produced using the 3DPM-C/Tape rector (at FRR of 25 and TFR of 1 ml/min) was −15.06 mV, which is coherent with the literature [27].

Conclusions

We have developed an easy-to-perform and cost-effective method for the fabrication of PDMS based continuous-flow reactors, through 3D printed mould casting (3DPM-C). In this method, the positive mould was "printed" using a desktop 3D printer, followed by PDMS casting to produce replica channels of millimetre or sub-millimetre width and height. Channels on the PDMS replica were then sealed using a commercially available pressure-sensitive adhesive tape. It was also demonstrated that the whole fabrication process can be completed within 24 h from the CAD design of the channel architecture, at an average cost of £5 per reactor. Simple modifications to the conventional PDMS curing process were also implemented, in order to overcome limitations associated with the use of a relatively low-cost 3D printer. The fabricated reactors were further applied to the production of both inorganic nanoparticles (silver nanospheres) and organic vesicular systems (liposomes). They exhibited comparable performance to reactors fabricated using more laborious and expensive fabrication methods. The manufacturing technique presented in this study is therefore potentially suitable for scaling-up, as devices can be fabricated at low-cost, and without resorting to sophisticated instrumentation and time-consuming multistep procedures. Moreover, devices produced with this technique can be operated at relatively high total flow rates (> 20 ml/min), which is a desirable characteristic for application in continuous-flow chemical synthesis.

Acknowledgment

Authors would like to thank the University of Southampton for supporting the research through a PhD studentship.

Appendix A. Supplementary data

Supplementary data associated with this article can be found, in the online version, at https://doi.org/10.1016/j.nbt.2018.02.002.

References

[1] Dong J, Liu J, Kang G, Xie J, Wang Y. Pushing the resolution of photolithography down to 15 nm by surface plasmon interference. Sci Rep 2014;4:5618.
[2] Hood RR, Wyderko T, DeVoe DL. Programmable digital droplet microfluidics using a multibarrel capillary bundle. Sens Actuators B Chem 2015;220:992–9.
[3] D. Carugo, J.Y. Lee, A. Pora, R.J. Browning, L. Capretto, et al., Facile and cost-

effective production of microscale PDMS architectures using a combined micro-milling-replica moulding (μMi-REM) technique, 18 (2016) 1–10.
[4] Comina G, Suska A, Filippini D. PDMS lab-on-a-chip fabrication using 3D printed templates. Lab Chip 2014;14:424–30.
[5] Chan HN, Chen Y, Shu Y, Chen Y, Tian Q, Wu H. Direct, one-step molding of 3D-printed structures for convenient fabrication of truly 3D PDMS microfluidic chips. Microfluid Nanofluid 2015;19:9–18.
[6] Hassan S-U, Nightingale AM, Niu X. Continuous measurement of enzymatic kinetics in droplet flow for point-of-care monitoring. Analyst 2016;141:3266–73.
[7] Kitson PJ, Rosnes MH, Sans V, Dragone V, Cronin L. Configurable 3D-printed millifluidic and microfluidic 'lab on a chip' reactionware devices. Lab Chip 2012;12:3267.
[8] Gaal G, Mendesa M, de Almeidab TP, Piazzettad MHO, Gobbi ÂL, et al. Simplified fabrication of integrated microfluidic devices using fused deposition modeling 3D printing. Sens. Actuators B Chem. 2017;242:35–40.
[9] Gong H, Beauchamp M, Perry S, Woolley AT, Nordin GP. Optical approach to resin formulation for 3D printed microfluidics. RSC Adv 2015;5:3627–37.
[10] Gong H, Bickham B, Woolley AT, Nordin GP. Custom 3D printer and resin for 18 μm × 20 μm microfluidic flow channels. Lab Chip 2017;12:3267–71. http://dx.doi.org/10.1039/C7LC00644F.
[11] Serra M, Pereiro I, Yamada A, Viovy J-L, Descroix S, Ferraro D. A simple and low-cost chip bonding solution for high pressure, high temperature and biological applications. Lab Chip 2017;17:629–34.
[12] Navjot Tovstolytkin A, Lotey GS. Plasmonic enhanced photocatalytic activity of Ag nanospheres decorated BiFeO3 nanoparticles. Catal Lett 2017;147:1640–5.
[13] Wang L, Chen R, Ren Z-F, Ge C-W, Liu Z-X, et al. Plasmonic silver nanosphere enhanced ZnSe nanoribbon/Si heterojunction optoelectronic devices. Nanotechnology 2016;27:215202.
[14] Le Ouay B, Stellacci F. Antibacterial activity of silver nanoparticles: a surface science insight. Nano Today 2015;10:339–54.
[15] Griffith M, Udekwu KI, Gkotzis S, Mah T, Alarcon EI. Silver Nanoparticle Applications. 2015. http://dx.doi.org/10.1007/978-3-319-11262-6.
[16] Baber R, Mazzei L, Thanh NTK, Gavriilidis A. Synthesis of silver nanoparticles in a microfluidic coaxial flow reactor. RSC Adv 2015;5:95585–91.
[17] Akbarzadeh A, Rezaei-sadabady R, Davaran S, Joo SW, Zarghami N. Liposome: classification, preparation, and applications. Nanoscale Res Lett 2013;1–9. http://dx.doi.org/10.1186/1556-276X-8-102.
[18] van Swaay D, deMello A. Microfluidic methods for forming liposomes. Lab Chip 2013;13:752–67.
[19] Jahn A, Vreeland WN, Gaitan M, Locascio LE. Controlled vesicle self-assembly in microfluidic channels with hydrodynamic focusing. J Am Chem Soc 2004;126:2674–5.
[20] Carugo D, Bottaro E, Owen J, Stride E, Nastruzzi C. Liposome production by microfluidics: potential and limiting factors. Sci Rep 2016;6:25876.
[21] Carboni M, Capretto L, Carugo D, Stulz E, Zhang X. Microfluidics-based continuous flow formation of triangular silver nanoprisms with tuneable surface plasmon resonance. J Mater Chem C 2013;1:7540.
[22] Amendola V, Bakr OM, Stellacci F. A study of the surface plasmon resonance of silver nanoparticles by the discrete dipole approximation method: effect of shape, size, structure, and assembly. Plasmonics 2010;5:85–97.
[23] Paramelle D, Sadovoy A, Gorelik S, Free P, Hobley J, Fernig DG. A rapid method to estimate the concentration of citrate capped silver nanoparticles from UV-visible light spectra. Analyst 2014;139:4855–61.
[24] Briuglia M-L, Rotella C, McFarlane A, Lamprou DA. Influence of cholesterol on liposome stability and on in vitro drug release. Drug Deliv Transl Res 2015;5:231–42.
[25] Thoma K, Jocham UE. Liposome Dermatics. Berlin, Heidelberg: Springer; 1992. p. 150–66. http://dx.doi.org/10.1007/978-3-642-48391-2_15.
[26] Takeuchi H, Yamamoto H, Toyoda T, Toyobuku H, Hino T, Kawashima Y. Physical stability of size controlled small unilameller liposomes coated with a modified polyvinyl alcohol. Int J Pharm 1998;164:103–11.
[27] Mahmud M, Piwoni A, Filiczak N, Janicka M, Gubernator J. Long-circulating curcumin-loaded liposome formulations with high incorporation efficiency, stability and anticancer activity towards pancreatic adenocarcinoma cell lines in vitro. PLoS One 2016;11:e0167787.

Glossary

3DPM-C/Tape: 3D printed mould casting bonded on tape (the symbol "/" is used for the simple adhesion on tape)
A_{max}: Maximum absorbance
CFD: Computational fluid dynamics
Phospholipon® 90G: Lipids, purified phosphatidylcholine from soybean lecithin, 3,4-dihydro-2,5,7,8-tetramethyl-2-4,8,12-trimethyltridecyl-2Hbenzopyran-6-ol
Ra: Average roughness
Rz: Maximum peak-to-valley value (refers to the *z*-axis)
z-average: Average diameter or radius, intensity-based overall average size
μMi-REM: Micromilling-replica moulding technique
*μMi-REM*Glass:* Micromilled replica moulding bonded on glass by oxygen plasma (the symbol " * " refers to the oxygen plasma treatment)

Supporting information

SI-1. Morphological characterisation of the 3D printed moulds

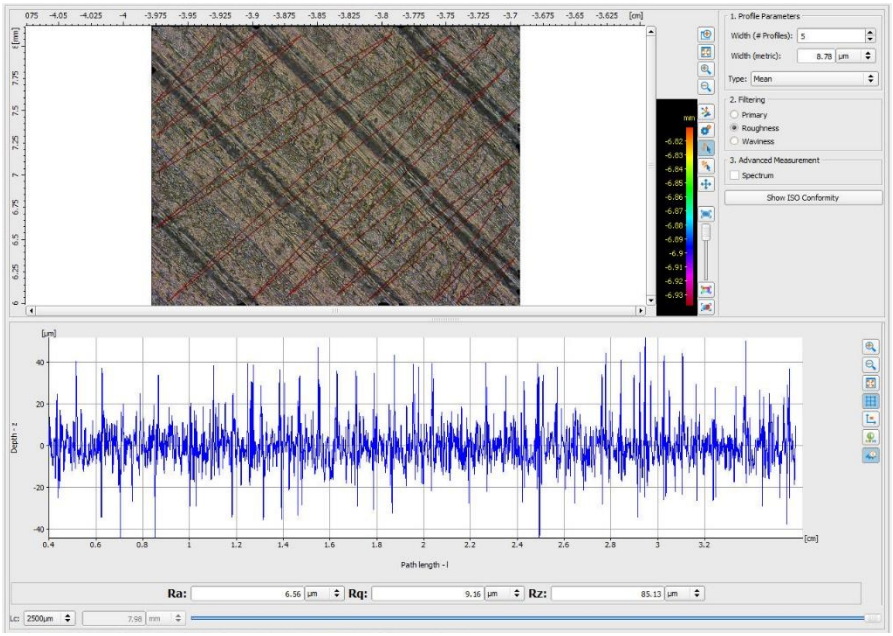

Figure SI-1a: *Cross sectional profile of the 3D printed mould base, showing the presence of diagonal grooves.*

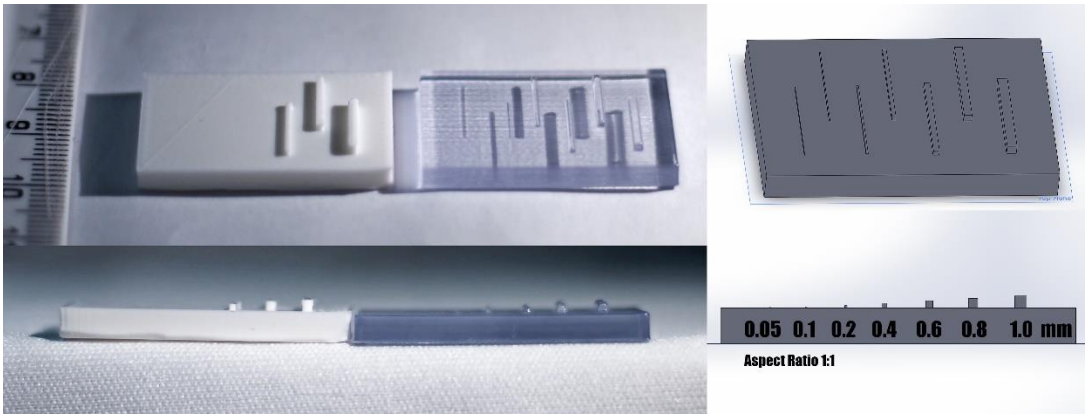

Figure SI-1b: Comparison between the Ultimaker 2+ 3D printer (white PLA material) and the High Resolution 3D printer Object Connex 350 (Veroclean® resin material). Although in this test the 0.4 mm channel was not printed by the Ultimaker 2+, channels of 0.5 mm could be generated (these correspond to the inlet channels of the reactor). The HR can reach smaller dimensions but the designed (i.e. nominal) cross sectional shape could not be accurately reproduced (see SI-1c).

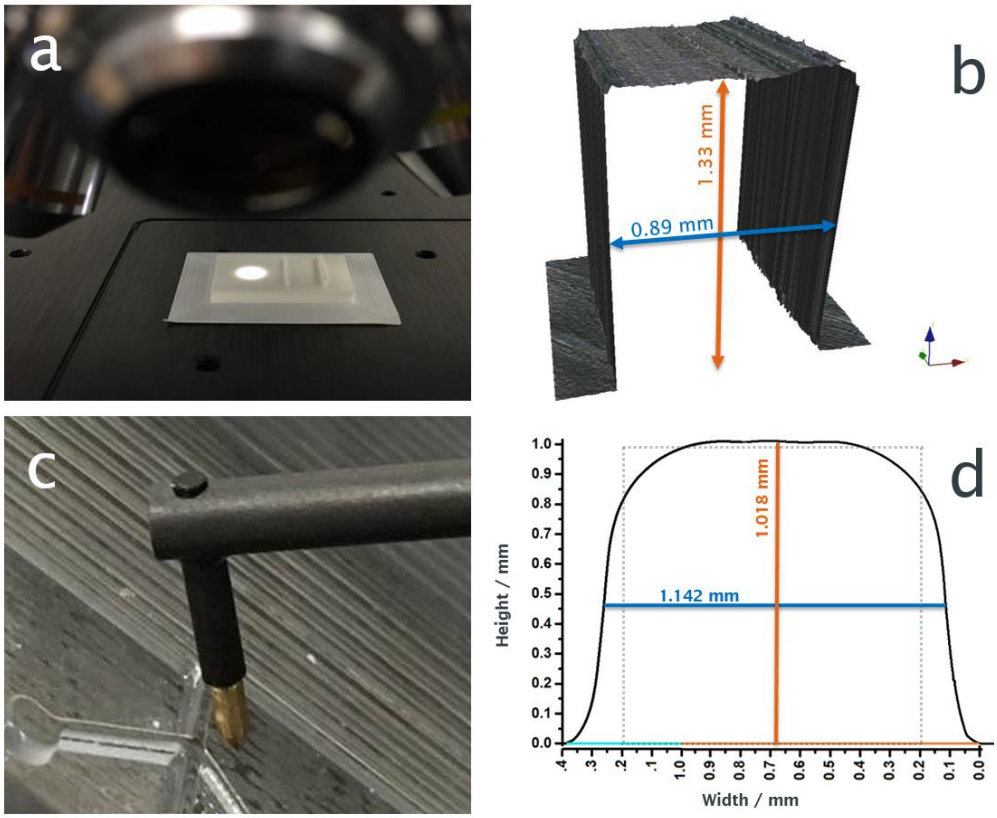

Figure SI-1c: a) Ultimaker 2+ mould test using the Alicona microscope. b) 3D morphological reproduction of the designed 0.80 mm × 1.33 mm (width × height) channel. c) Object Connex 350 mould test under the Taylor-Hobson profilometer. d) Profile graph of the actual channel (solid black line) compared with the designed (nominal) 1.00 mm × 1.00 mm (width × height) channel (dotted line). The reproduction error for the HR 3D printed channels is greater for smaller channel sizes.

SI-2. Computational fluid dynamic (CFD) simulations

SI-2a. *Simulation methods*

The transport of fluids and chemical species within the reactors was characterised numerically via computational fluid dynamic (CFD) simulations. The process comprised the following steps: (i) design of the flow reactor geometry using Inventor Pro 2016 (Autodesk Inc., San Rafael, CA, USA); (ii) meshing of the fluidic domain in ICEM CFD 17.0 (Ansys Inc., Concord, MA, USA) using finite volumes of tetrahedral shape. The mesh element edge length was equal to 0.05 mm, and was identified from a mesh dependence study as the optimal compromise between solution accuracy and computational cost (Figure SI-2a).

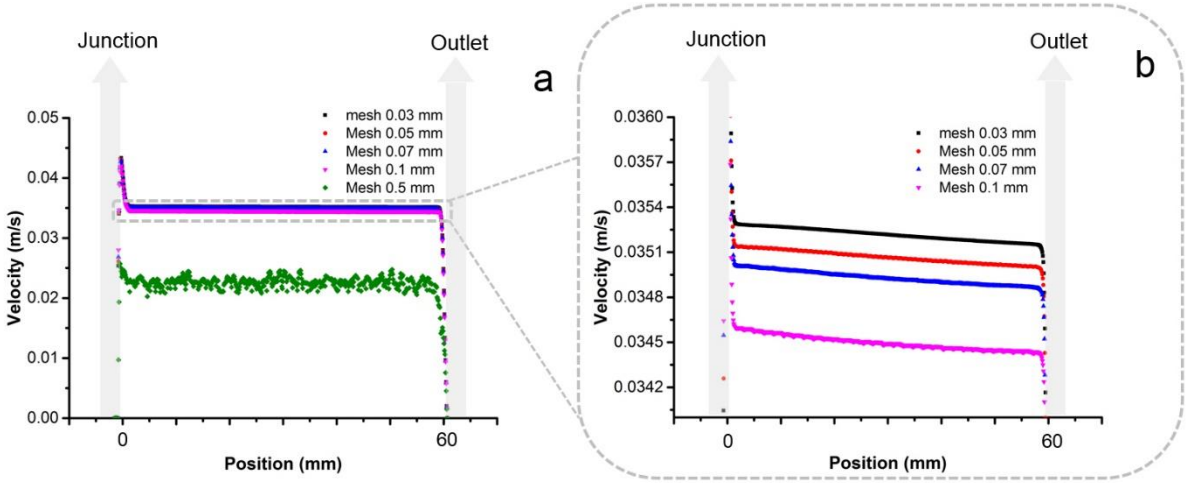

Figure SI-2a: mesh dependence study performed at mesh volume sizes of 0.5, 0.1, 0.07, 0.05 and 0.03 mm. a) velocity magnitude (in m/s) along the channel midline and b) inset of velocity (in m/s) for the mesh sizes of 0.1, 0.07, 0.05 and 0.03 mm. 48-64 processors were used for running the simulations at the TFR of 1 ml/min and FRR of 11. Simulations at the mesh size of 0.05 mm took 3 hours and about 3500 iteration to converge, whereas simulations at the mesh size of 0.03 mm took about 12 hours and 10,000 iteration to converge. Therefore, a mesh size of 0.05 mm was selected as the best compromise between solution accuracy and computational cost.

The total number of mesh volumes was equal to 8'123'298; (iii) solving for steady state mass and momentum conservation equations (i.e., Navier-Stokes equations at laminar flow regime, see Equations 1 & 2 below), and species transport (i.e., advection-diffusion) equations (see Equations 3 & 4 below), using Ansys® Fluent 17.0 (Ansys Inc., Concord, MA, USA).

$$\nabla \cdot (\boldsymbol{v}) = 0 \qquad \text{(Eq. 1)}$$

$$\rho \boldsymbol{v} \cdot \nabla \boldsymbol{v} = -\nabla P + \mu \nabla^2 \boldsymbol{v} \qquad \text{(Eq. 2)}$$

$$\nabla \cdot \left(\rho \boldsymbol{v} M_{f,i}\right) = -\nabla \cdot J \qquad \text{(Eq. 3)}$$

$$J = -\rho D_i \nabla M_{f,i} \qquad \text{(Eq. 4)}$$

Where $\boldsymbol{v}$, ρ, μ and P represent fluid velocity, density, dynamic viscosity and pressure, respectively. $M_{f,i}$ is the mass fraction of species *i*. J is the diffusion flux, and D_i is the mass diffusion coefficient for species *i*.

To reproduce the experimental conditions, the following boundary conditions were imposed: (i) mass flow boundary condition at the inlets, (ii) atmospheric pressure at the outlet, and (iii) no-slip at the channel walls. The experimental values of TFR and FRR were replicated numerically.

Fluids were assumed incompressible and Newtonian, and the IPA/ethanol-water diffusion coefficient was set to 1×10^{-9} m^2/s [1,2]. The effect of solvents' mixing on fluid density and viscosity was taken into consideration in the simulations. The mass fraction of IPA or ethanol was calculated in a cross sectional plane located in the vicinity of the outlet, and the mixing index in this specific location was determined for each TFR and FRR investigated.

SI-2b. *Numerical analysis of fluids and species transport*

CFD simulations were performed in order to gain insights into the flow field and the transport of chemical species within the reactor (Figure SI-2b(a)), to aid the interpretation of the experimental findings.

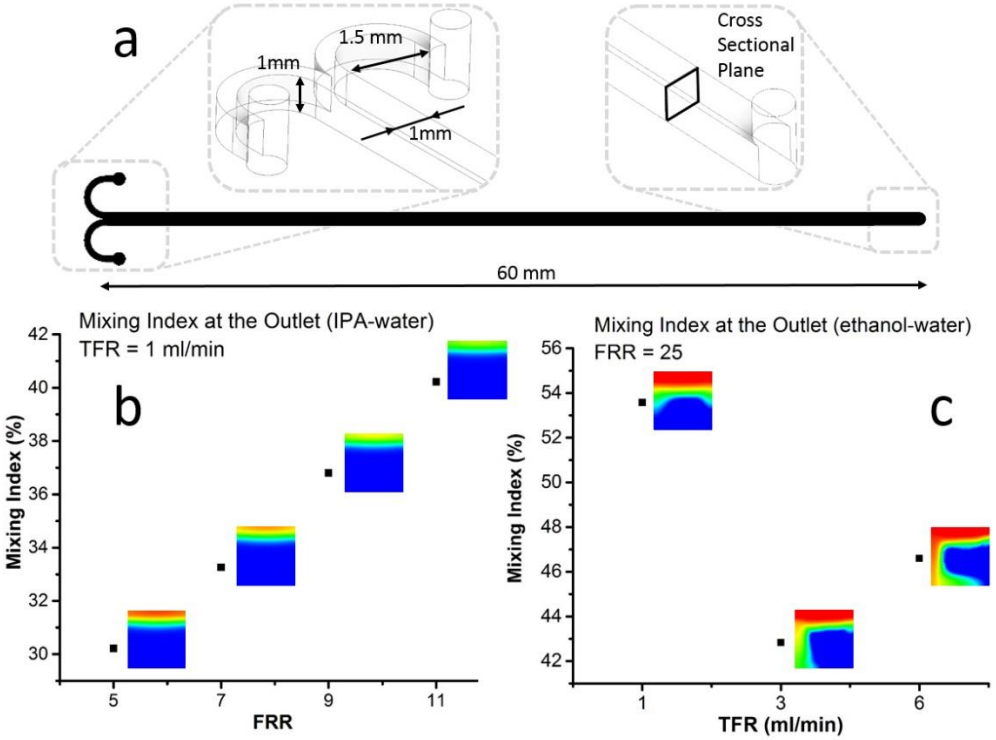

Figure SI-2b: Mixing index calculated over a cross sectional plane in the vicinity of the outlet surface, as shown in a). Results refer to b) IPA-water at TFR of 1 ml/min and FRRs of 5, 7, 9 and 11; and c) ethanol-water at TFRs of 1, 3 and 6 ml/min and FRR of 25. Contours of IPA or ethanol mass fraction are reported next to each data point.

The extent of mixing was quantified *via* the mixing index [3], which is defined as a measure of the homogeneity of chemical species (in this case water and ethanol/IPA), over a selected surface in the reactor. Figure SI-2b shows the mixing index calculated at different fluidic

conditions, which correspond to those employed in the production of SNSs and liposomes, (b & c respectively). Figure SI-2b(b) demonstrates that increasing the FRR from 5 to 11, while keeping the TFR constant at 1 ml/min, resulted in increased mixing efficiency between water and IPA. However, complete mixing was not achieved within the reactor, suggesting that the production of SNSs continued within the collection tube at these flow regimes. Stratification of different chemical species due to differences in density could also be observed.

Figure SI-2b(c) shows that increasing the TFR from 1 ml/min to 6 ml/min, at a fixed FRR of 25, resulted in a reduction of the mixing efficiency between ethanol and water. This could be attributed to interfacial instabilities or vortical flow occurring at the higher flow rates, and merits further investigations. It should however be noted that variations in the mixing index are within a 10% range, for the different flow rates investigated.

SI-3. Liposome size distribution

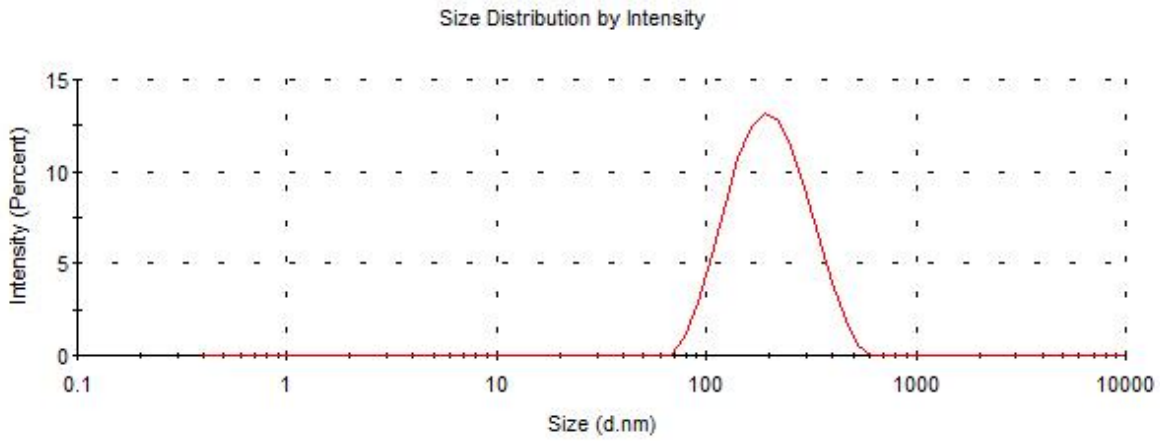

Figure SI-3a: Representative liposome size distribution obtained by DLS, at TFR of 1 ml/min and FRR of 25. All liposomes have mean hydrodynamic radius between 63 and 615 nm. The mean diameter is of 190 nm, with a PDI of 0.180.

Bibliography

1. Bottaro, E., Mosayyebi, A., Carugo, D. & Nastruzzi, C. Analysis of the diffusion process by pH indicator in microfluidic chips for liposome production. *Micromachines* **8,** 1–16 (2017).

2. Hills, E. E., Abraham, M. H., Hersey, A. & Bevan, C. D. Diffusion coefficients in ethanol and in water at 298K: Linear free energy relationships. *Fluid Phase Equilib.* **303,** 45–55 (2011).

3. Hashmi, A. & Xu, J. On the quantification of mixing in microfluidics. *J. Lab. Autom.* **19,** 488–91 (2014).